A THEORY OF SPATIAL ACUITY

by

Brian Charles Madden

Submitted in partial fulfillment

of the requirements for the degree

Doctor of Philosophy

Supervised by Dr. Christopher M. Brown

Department of Computer Science

University of Rochester

Rochester, New York

1985

Abstract

A theory is proposed that explains the substantial differences among the various measures of spatial acuity. According to this theory, the visual system can localize stimuli only to within regions that are several minutes of arc wide. Other measures of spatial acuity have limits that are one (two-line resolution) and two (localization) orders of magnitude finer because they allow the coarse positional labeling to be supplemented by detection of changes in contrast within limited bands of spatial frequency. It is argued here that the use of an intensive dimension (contrast), as a supplement to location, taps visual abilities that are not part of the position sense. The failure of the traditional theories to reconcile the disparate measures of spatial acuity may be traced to differences in the observers' ability to discriminate changes in contrast in the presence of the different acuity targets. Discrimination sensitivity in an array of contrast-sensitive filters varies with acuity targets and thus precludes a fixed transformation between contrast and position.

Support for the theory is obtained both from experimental data and from simulations. Positional labeling was measured by testing the ability of observers to correctly identify the location of a single line. Both resolution and localization thresholds were measured under a range of contrasts. In addition, sinewave masks at a variety of spatial frequencies and phases caused the changes in perceived offset required by the theory.

The model, made up of an array of spatial filters, each with a one octave bandpass, accounts for both the absolute sensitivity to positional offset and the variation of threshold with stimulus configuration. The parameters in a vector magnitude formulation of probability summation are derived from sinewave contrast sensitivity data. The detection model is extended to discrimination by the addition of a Weber response compression mechanism.

Table of Contents

Title i

Abstract ii

Table of Contents iv

Acknowledgments vi

List of Tables vii

List of Figures viii

Chapter 1: Onset 1

Chapter 2: The Stimulus as Frequencies and Features 6

Detection of a sinewave 6

Detection of a single line 38

Detection of four lines 45

Density of labeled positions 63

Chapter 3: Offsets and Contrast 70

Two line resolution 71

Two line interval judgment 103

Three line interval judgment 114

Four line interval judgment 118

Chapter 4: An Offset by Another Name 126

Sinewave masks 126

Sinewave cancellation of offset 128

Effect of contrast on cancellation of offset 142

Cancellation in asymmetric stimuli 149

Chapter 5: What's in an Offset? 153

Rationale 153

Analysis of interactions 163

Comments on the model 191

What is the observer doing? 210

Conclusions 230

Appendix A: Localization Performance 234

Appendix B: Theories of Localization 294

Appendix C: Aggregate Response Measures 324

References 361

To my father, who has been supportive through all the turns my path has taken.

Acknowledgments

I would like to thank my committee for their helpful comments:

Christopher Brown	Computer Science
James Hamerly	Xerox Corporation
Patrick Hayes	Cognitive Science
Peter Lennie	Psychology
Walter Makous	Psychology

My tenure at the University of Rochester was made possible by the financial support of the Center for Visual Science, Xerox Corporation and Eastman Kodak.

I am especially indebted to Bruce Henning, placed here by good fortune in 1980 as the R. T. French visiting professor from Oxford University. Resolution of the issues raised in his critique of my first draft clarified both theoretical and syntactic opacities.

Graduate school is not easy even if you conform to all the rules. And if you don't, it is essential to find and advisor like Chris Brown. AI is in large part the study of flexibility and understanding; it is no wonder to me why Chris is an expert in AI.

List of Tables

2.1 CELT: Summary of model parameters 15

5.1 CELT: Summary of model performance 194

B.1 Summary of localization theories 316

List of Figures

2.1 Spatial sinewave contrast sensitivity 13

2.2 Attenuation by the optics of the eye 16

2.3 One octave gaussian filter 20

2.4 Range of filters 23

2.5 Number of filters 26

2.6 Decline in sensitivity with eccentricity 28

2.7 The effect of filter distribution on the aggregate response 29

2.8 Neural transfer function 30

2.9 Comparison of model responses to the NTF 32

2.10 Individual filter gains 33

2.11 Filter responses to single sinewaves 36

2.12 Filter response to narrow- and broadband stimuli 43

2.13 Filter response to localized and spatially extensive stimuli 46

2.14 A one octave filter at 6 cpd 47

2.15 Four line detection threshold 50

2.16 Four line amplitude spectra 54

2.17 Filter responses to 4 lines 58

2.18 Distribution of labeled position 68

3.1 Resolution criteria 72

3.2 Diffraction pattern of a point source 74

3.3 Diffraction pattern for a white line and the human line spread function 75

3.4 Variation in two line resolution with contrast 78

3.5 Retinal flux distribution at threshold separations 81

3.6 Maximum flux change at resolution 84

3.7 Two line resolution spectra 87

3.8 Contrast discrimination functions 91

3.9 Aggregate discrimination responses for two line resolution 98

3.10 Filter responses to two line resolution stimuli at threshold 99

3.11 Response differences for two line resolution threshold offsets 100

3.12 Two line localization spectra 105

3.13 Correspondence between two line criterion and difference spectra 107

3.14 Model responses for two line localization 109

3.15 Two line critical interval: observer and model thresholds 113

3.16 Correspondence of three line criterion and offset spectra 115

3.17 Three line critical interval: observer and model thresholds 117

3.18 A decomposition of the four line spectrum 119

3.19 Correspondence of four line criterion and offset spectra 121

3.20 Variation of four line offset threshold with criterion separation and contrast 122

4.1 Psychometric functions for the detection of offset in the presence of a nonoptimal sinewave 131

4.2 Psychometric functions for the detection of offset in the presence of an optimal sinewave 133

4.3 Perceived zero offset (160" arc criterion separation) 136

4.4 Perceived zero offset (80" arc criterion separation) 140

4.5 Perceived zero offset (320" arc criterion separation) 141

4.6 Perceived zero offset (640" arc criterion separation) 143

4.7 Psychometric function for the detection of offset obtained at a large criterion separation 144

4.8 Effect of sinewave contrast on offset cancellation 146

4.9 Psychometric functions for the detection of offset in the presence of a threshold sinewave 147

4.10 Relative retinal flux distribution of offset and criterion. 148

4.11 Perceived zero offset, three line stimuli (160" arc criterion separation) 151

5.1 Spatial frequency spectra at different line widths 158

5.2 Fourier spectrum of an edge 160

5.3 Fourier spectra for coincidence stimuli (separation = 3' arc) 169

5.4 Fourier spectra for coincidence stimuli (separation = 30" arc) 171

5.5 Fourier difference spectra for coincidence stimuli (separation = 3' arc) 175

5.6 Fourier difference spectra for coincidence stimuli (separation = 30" arc) 177

5.7 Fourier spectra of flanking lines 181

A.1 Vernier measurement 236

A.2 Coincidence stimulus 238

A.3 Interaction of length, width and vertical separation 239

A.4 Dot stimuli used in alignment tasks 242

A.5 Effect of vertical separation on threshold for different line lengths 244

A.6 Positioning tasks requiring feedback 246

A.7 Adjustment of the separation between two bars 248

A.8 Spatial interval judgments 249

A.9 The effect of flanking lines on a coincidence task 250

A.10 Orientation discrimination stimulus 252

A.11 Variation of orientation threshold 253

A.12 Coincidence thresholds as a function of line length 254

A.13 Periodic lateral displacement 256

A.14 Coincidence threshold as a function of the orientation of a masking

grating 259

A.15 Interference of orientation judgments by a flanking line 260

A.16 The effect of luminance level on vernier threshold 262

A.17 The effect of luminance level on the threshold of stationary and moving coincidence targets 263

A.18 Double coincidence stimulus 267

A.19 The effect of blur on coincidence thresholds 268

A.20 "Center of gravity" stimuli 269

A.21 Degradation of acuity as a function of separation 271

A.22 Monocular and binocular vernier acuity as a function of separation 279

A.23 The effects of practice on vernier threshold 282

A.24 Vernier threshold as a function of the number of trials 283

A.25 Improvement in contrast sensitivity 284

B.1 Detection of vernier offset by means of local signs 297

B.2 Localization model of Helmholtz 299

B.3 Retinal flux distribution of a luminous edge 301

B.4 Mean retinal local sign theory 303

B.5 Cortical local sign theory 306

B.6 Sinusoidal masking of a coincidence task 312

C.1 Noise distribution implicit in Weibull/Quick psychometric function 329

C.2 Single linear filter aggregate response model (constant octave bandwidth) 336

C.3 Single linear filter aggregate response model (fixed bandwidth) 342

C.4 Rms aggregate response model 345

C.5 Higher power aggregate response models 347

C.6 Effect of exponent (B) on filter sensitivity 348

C.7 Aggregate response model with probability summation across space 351

C.8 Linear systems solution for CELT 354

C.9 Logarithmic separation of medium bandwidth filters 356

C.10 Logarithmic separation of narrow bandwidth filters 358

Chapter 1

ONSET

From the time of Helmholtz there has been a concordance among almost all measures of spatial acuity. The detection of thin dark and light lines, the resolution of gratings and line pairs, the recognition of features in Snellen Es or Landolt Cs - all have been found to be in general agreement with a theory of spatial acuity in which a threshold percept occurs when the image, after passing through the optics of the eye, contains a change in flux over the extent of at least one photoreceptor that is commensurate with brightness discrimination (Riggs, 1965). In this view, limitations of the spatial sense are derivative of the integration within and the labeling of individual photoreceptors. The one major exception has been localization, the ability to detect small displacements within an image.

For over 100 years localization has remained one of the most tenaciously intractable problems in vision. This vexation stems from the lack of a unifying theory to explain the exceptional performance obtained in a variety of discrimination tasks involving the alignment of contours or the equation of spatial intervals between contours. Observers' abilities (appendix A) go beyond the acuity limits consistent with the properties of the mechanisms traditionally thought to subserve spatial vision. Theories of localization (appendix B) have attempted to relate these fine positional offsets to differential responses between adjacent

receptors; however, vernier displacement thresholds are typically a factor of five finer than the closest interreceptor spacing. In order to augment the limitations imposed by retinal resolution, mechanisms of averaging or interpolation have been proposed. These attempts have proven inadequate because the problem posed by localization involves more than seconds of arc resolution; it also evinces a collection of interactions among spatial parameters. A model of localization must not only allow for seconds of arc thresholds, but it must allow optimal thresholds to be obtained only under a restricted set of conditions. Under this criterion, the theories all fail to explain localization performance in at least one of its forms.

The major tenet of the theory proposed here is that localization performance is not exceptional, rather, seconds of arc thresholds may be reconciled entirely with the response of mechanisms normally proposed to subserve spatial vision. Based on this view, mechanisms that process spatial contrast are used to supplement a relatively coarse positional labeling. The notion of supplementation is a major departure from previous theories that explain localization performance by appeal to mechanisms that use averaging or interpolation to improve the labeling of features within a stimulus. Changes in the pattern of activity in a collection of bandpass spatial filters, whose individual responses may be localized to minutes of arc, are used to discriminate stimuli containing offsets much smaller than can be resolved into distinct labeled positions. Optimal performance is always accompanied by a particular pattern of contrast amplitudes that strongly activate some contrast filters while leaving others essentially unstimulated.

Positional offsets produce changes in the stimulus spectrum that are greatest in the region of unstimulated detectors, allowing them to operate near their point of maximum sensitivity. A simple model based on patterns of activity in the population of contrast filters accounts for all the spatial interactions associated with vernier-like performance, including critical intervals, masking by flanking lines, discrimination of offsets about a non-zero offset, changes in threshold with length and separation, and effects of blurring and contrast.

Enhancement of performance is not limited to localization tasks. The responses of filters sensitive to limited frequencies of spatial contrast but only coarsely resolving spatial position also contribute to the resolution of line pairs. Spatial acuity in the two line resolution task is less than in localization because the amplitude spectra of the closely spaced line pairs do not create nulls in the pattern of filter responses. The resulting contrast discrimination is based on the response of filters that are at less than optimal sensitivity.

Support for the theory is developed by first establishing an appropriate description of the stimuli and then simulating performance with a model based on psychophysical data. A multiple filter model of contrast sensitivity (CELT: Contrast Enhanced Localization Theory) is specified with parameters derived from the Observers' sinewave thresholds (chapter 2). The model is then shown to be consistent with the detection of broadband stimuli (1 and 4 line targets). Detection of the 4 line stimuli is shown, in turn, to be consistent with sinewave

contrast sensitivity for lines at small separations and independent detection of the lines with larger spacing. The independent detection of the lines occur at spacings that exceed the minimum separation required for the absolute localization of the lines. This analysis establishes that the spatial extent of filters that are sensitive to contrast is sufficiently large to allow changes in contrast to be detected in multiple line stimuli while the lines are still individually labeled.

Changes in the detectability of small positional offsets as a function of target contrast are shown (chapter 3) to be consistent with the detection and discrimination of responses in contrast sensitive filters for both the two line resolution task and the interval judgment task. The small thresholds observed in the interval judgment task are shown to be related to the presence of spectrum nulls. The probability summation detection model is extended to encompass the gain changes associated with discrimination performance.

The relation between the critical filters and the detection of offset is further strengthened (chapter 4) through the demonstration that sinewaves masquerade as offsets when they stimulate the critical filters located at the spectrum nulls. Of particular importance is the finding that the contrast necessary to detect a sinewave at the critical spatial frequency is close to that required to produce a shift in the perceived offset equal to the offset threshold.

In the discussion (chapter 5) these new findings are combined with the results in the literature to form a unified theory of absolute position judgments, spatial resolution tasks and localization performance, describing both the exceptional

resolution abilities and the spatial interactions. In addition, the approximations, limitations and interactions within CELT are described. Enhancements of the model are proposed that should improve its simulation of the human visual system. Finally, the implications that the proposed sensory substrate has on perception and performance are discussed.

Chapter 2

THE STIMULUS AS FREQUENCIES AND FEATURES

The goal of this dissertation is to reconcile the major metrics of spatial vision. To achieve a unified description, the demands of Observer performance are used to constrain the sensitivity and diversity of the spatial filters in a model (CELT). The unification will be a success if the model parameters do not exceed current estimates of psychophysical, physiological and anatomical bounds and can be defined with a small number of degrees of freedom. The model is derived primarily from psychophysical data. In this chapter many of the model parameters are derived from the results of detection tasks. Although there is a clear bias toward the spatial frequency description because of computational ease and quantitative accuracy, feature (spatial) descriptions are accommodated as well; indeed, the reconciliation of sinewave and line sensitivity is the first step in unifying measures of acuity.

Detection of a sinewave

background

Schade (1956) was one of the first to produce a measure of the human visual system's sensitivity to sinusoids as a function of spatial frequency. The spatial contrast sensitivity function (CSF's) found by Schade had a three octave

bandwidth and a unimodal profile that reflected the insensitivity of the human visual system to both low and high spatial frequencies. The shape of the CSF, however, is not constant. The CSF varies considerably with temporal duration and luminance (e.g., Kelly and Burbeck, 1980) and among subjects.

methods

Stimuli were created on an X-Y display monitor (Tektronix model 606) with a green phosphor (P31) that decayed to less than 1% of its initial value in well under 1 msec. Each frame was composed of a 1024 element vertical raster and had a refresh rate of 100 Hz. The luminance of each raster element could be set independently and was adjusted to compensate for the nonlinear voltage to luminance relation of the monitor. At the mean luminance used in these experiments (6 cd/m^2) the contrast of the individual raster elements could be set in 1/8% steps. Individual frames were stored in a computer (DEC PDP11/60) as integer arrays and could be transmitted in real time to the display. This procedure allowed the spatial and/or luminance properties of the stimuli to be altered at 10 msec intervals.

The MTF of the display was measured by drifting sinusoidal gratings past a thin slit and imaging the slit on a photosensor. The amplitude of modulation of the sensor output voltage was obtained over a range of spatial frequencies. This measure of the display attenuation was incorporated in the model and used to transform the spectrum of the theoretical stimulus into the spectrum of the

stimulus that was displayed.

The display was reflected off of a trapezoidal first surface mirror that was deposited on a larger piece of clear glass and placed at 45° to both the monitor screen and the line of sight. At a viewing distance of 1.3 m this arrangement resulted in a perceived rectangular aperture 4.4° wide and 2.2° high. Behind the mirror, 1.3 m down the line of sight, was a 17.6 by 8.8° uniform field that closely matched the luminance and chromaticity of the display. The contiguity of this uniform region eliminated the distracting afterimages produced by the display when viewed sans surround. Beyond the surround the room was dimly illuminated by the display and surround projector. Observations were made binocularly and with natural pupils (5 to 6 mm). Although variations in pupil diameter undoubtedly occurred during a session, changes in the 5 to 6 mm range do not alter the shape of the line spread function appreciably (q.v., figure 3.3). The results of the model would not be qualitatively different in this range. Changes in accommodation, however, might have a greater effect. The ability to acquire and maintain the conjugacy of the retina and the display can be severely degraded due to fatigue in long sessions. The concomitant blur attenuates moderate and high spatial frequencies, significantly so for some tasks. To avoid fatigue, sessions were kept short (15 to 25 minutes). In addition, a fixation cross was placed on the rear wall 3m distant and slightly above the display. Fixating the cross counteracted the proximal focussing error brought on by fatigue. A portion of the data were checked to see if the later trials differed from the early ones. An

analysis of the pattern of responses in a portion of the sessions indicated that there were no statistically significant decreases in sensitivity near the end of a session.

The 1024 line image displayed in a 4.4° aperture resulted in a 16" arc raster separation. The aperture size was derived from a compromise among several factors: the extent of spectrum broadening of continuous functions brought on by truncation with narrow apertures, the data transmission rate of the computer, the spatial resolution of the monitor and the sensitivity of the Observer. Although continuous functions could be shifted in phase by any amount, the 16" arc resolution limit was markedly coarse with respect to Observer performance for discrete stimuli. To obtain increased positional resolution for discrete patterns, additional lines were superimposed on the raster, interdigitated in zero to three 4" arc offsets. Additionally, the extra lines were superimposed upon one another to obtain line luminances not available with the raster alone.

Two experimental procedures were used. The first was a temporal two interval two alternative forced choice (2TAFC) paradigm. The Observer's task was to select which of two intervals contained a stimulus with the desired property. For detection tasks the target stimulus was paired with a uniform field; for discrimination tasks the alternative stimulus was the criterion (e.g., 4 equally spaced lines). A bright fixation dot centered in the rectangular display aperture served both to locate the stimulus and as an aid to accommodation. The dot was displayed continuously between trials. At the beginning of a trial the fixation dot was turned off, leaving a uniform field that lasted 500 msec. A high frequency

tone was presented coextensively with the first test interval (200 msec). The short test duration, although not optimal for most tasks, was selected to reduce the effects of eye movements. The minimization of image motion allowed the spatial phase of the masks relative to the acuity targets to be maintained. Following a one second delay during which a uniform field was displayed, the second test interval (200 msec) occurred and was similarly marked with a tone. A uniform field was displayed again at the end of this sequence and the reappearance of the fixation dot signaled the end of the trial. The control program waited for the Observer's response before initiating the next trial. With this procedure a trial occurred approximately every seven seconds.

The data were collected in blocks of 100 or 200 trials. Prior to each block the Observer was adapted to the mean luminance and then was presented a series of trials which increased in task difficulty. This initial run continued until the Observer's first error, serving both to locate the stimulus level near threshold and as a short practice session. Following the initial error, the block of data trials began. Depending on condition, 1, 2 or 4 independent staircases (each with up to 12 stimulus levels) were employed. The magnitude of the independent variable (e.g., spatial offset, contrast) was decreased one level after each correct response and increased three levels after each error. When provided, feedback took the form of a short tone burst that followed each incorrect response. Both the selection of the interval for the target stimulus and the intermixing of the staircases was randomized, with no attempt to counterbalance conditions.

The 12 stimulus levels in each staircase spanned the region between chance and certainty. The 1:3 rule acted to concentrate the trials near threshold (75% correct). The method of probits (Finney, 1971) was used to establish the threshold value. 500 trials were sufficient to produce acceptably small fiducial limits (95% confidence intervals).

The second procedure used was a one interval two alternative forced choice (1TAFC) paradigm with the method of constant stimuli. Stimulus timing, response and feedback was the same as with 2TAFC with the exception that the one second interinterval delay and the second interval were omitted. The Observer's task was to decide in which of two sets the displayed stimulus belonged. All stimuli were presented an equal number of times in a randomized order. Threshold (75% correct) was calculated with the method of probits for each stimulus set independently and then averaged. This method of computing threshold produces a criterion free measure since a bias for one stimulus set is counterbalanced by the concomitant bias against the other stimulus set. Any resulting threshold shifts are equal and opposite, leaving the average unchanged.

The Observers were two of the nicest people you'd ever want to meet: neat, well-educated and cosmopolitan; totally incapable of producing spurious data. Measured on the Armed Forces Vision Tester (Bausch and Lomb), Observer BCM had 20/20 acuity (binocular, corrected); Observer DLG had 20/17 acuity (binocular, uncorrected).

data

Estimates of the sinewave sensitivity for both Observers (DLG and BCM) were obtained for viewing conditions standard for the experiments in this thesis (figure 2.1). The CSF's at 200 msec duration for both Observers are considerably more lowpass than is usually found with unrestricted viewing. The high sensitivity at low spatial frequencies can be attributed to the presence of high temporal frequency components in the spectrum of the 200 msec test interval. The sensitivity of both Observers begins to decline above 2 cpd and reaches high frequency cutoff at 51 cpd (BCM) and 49 cpd (DLG). The high frequency cutoff is defined by the straight line extrapolation on logarithmic coordinates of the CSFs to a sensitivity of one. Insofar as the initial stages of the visual system are linear, these measurements of sinewave sensitivity can provide a basis for the prediction of the sensitivity for any stimulus. It remains to relate these sinewave sensitivities to a model of spatial vision in order to predict the Observers' responses to broadband stimuli.

model

The theoretical relations presented in this thesis are based on a model of spatial vision that is composed of a collection of coarse (relative to seconds of arc offsets) spatial filters, each localized, oriented and bandpass. The partitioning of spatial visual processing into independent frequency bands has massive support drawn from a variety of paradigms (e.g., detection, discrimination, masking,

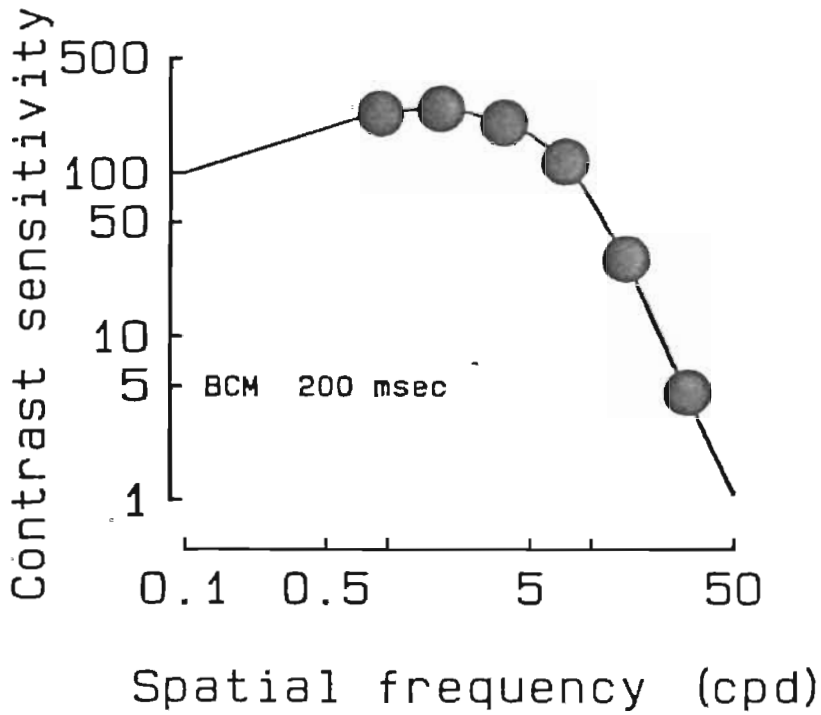

Figure 2.1 Spatial sinewave contrast sensitivity.

Contrast sensitivity measurements were obtained at 200 msec duration using a 2TAFC procedure with feedback. Each threshold was based on 500 trials. The trials were run in blocks of 100. A staircase procedure was used to concentrate the stimulus contrasts near threshold. The Observers have similar sensitivities: lowpass; peak sensitivity, c. 220; high frequency cutoff, c. 50 cpd. Data plotted is for Observer BCM (data for Observer DLG is within ±0.08 log units).

The gratings were vertically oriented and subtended 4.4 by 2.2°. Both the stimulus aperture and a uniform surround (17.6 by 8.8°) were 1.3m down the line of sight. Both the mean luminance (6 cd/m^2) and the chromaticity (pale green; p31 phosphor) of the surround matched that of the display.

Estimates of nonsampled frequencies were calculated by fitting cubic splines to the obtained sensitivities (solid curve). Probit analysis of the psychometric functions for sinewave detection yields fiducial limits (95% confidence interval) that are smaller than the symbols.

adaptation, matching and magnitude estimation). The empirical data presented herein are not used to defend a specific multiple filter theory. Rather, the predictions of the filter model (CELT) are used to demonstrate the adequacy of conventional mechanisms occasionally to produce apparently exceptional performance. To this end, CELT is expanded only to the extent required to make a plausible account of the spatial resolution data in terms of sinewave contrast sensitivity and is not proposed as a comprehensive model of spatial vision. With the exception of the filter gains, parameter estimates for detection were taken from the literature and were not optimized to fit the current data (see table 2.1).

The initial transformation of CELT is an approximation to the optical transfer function (OTF) of the eye. The OTF embodies the effects of both diffraction and the geometrical aberrations. The approximation used in CELT was derived from Campbell and Gubisch's 5.8mm pupil line spread function (LSF) (figures 2.2, a and 3.3). The 5.8mm pupil diameter matches that of the Observers under the conditions of the experiment. A sum of exponentials function is used to approximate the Observers' LSFs:

$$LSF(x) = 0.23\ e^{-2.3x^2} + 0.77\ e^{-0.54\ |x|} \qquad [2.1]$$

x is visual angle in minutes of arc.

The Fourier transform of the LSF (figure 2.2, b) acts as a spatial frequency weighting function when applied to the objective stimulus spectrum. The transform of [2.1] is used to approximate the OTF of the human eye with a 5.8

Table 2.1 CELT: Summary of model parameters.

OTF	sum of exponentials function based on 5.8 mm LSF (4 parameters).
linear summation	64 filter center frequencies; gaussian weighting profile as measured with linear weights against log spatial frequency; center frequencies range from 0.5 to 32.0 cpd in 0.5 cpd increments; bandwidth is constant at 1 octave.
phase	filter phase spectra are constant across spatial frequency; each filter location contains filters with six fixed phases (0, 30, 60, 90, 120 and 150°).
spatial density	filters are positioned across space with a density that is proportional to center frequency.
gain	64 filter gains, each adjusted to produce an aggregate response that models NTF; individual filter gain falls off exponentially from fixation with a space constant that is proportional to center frequency and at twice the rate in the vertical, as compared to the horizontal, direction.
compression	the cutoff for response compression is 0.4 (where 1.0 is the aggregate response detection criterion); responses above the cutoff are attenuated in proportion to the degree they exceed the the cutoff (the Weber fraction equals 1.0).
nonlinear exponent	the vector magnitude exponent used to model probability summation is 3.5.

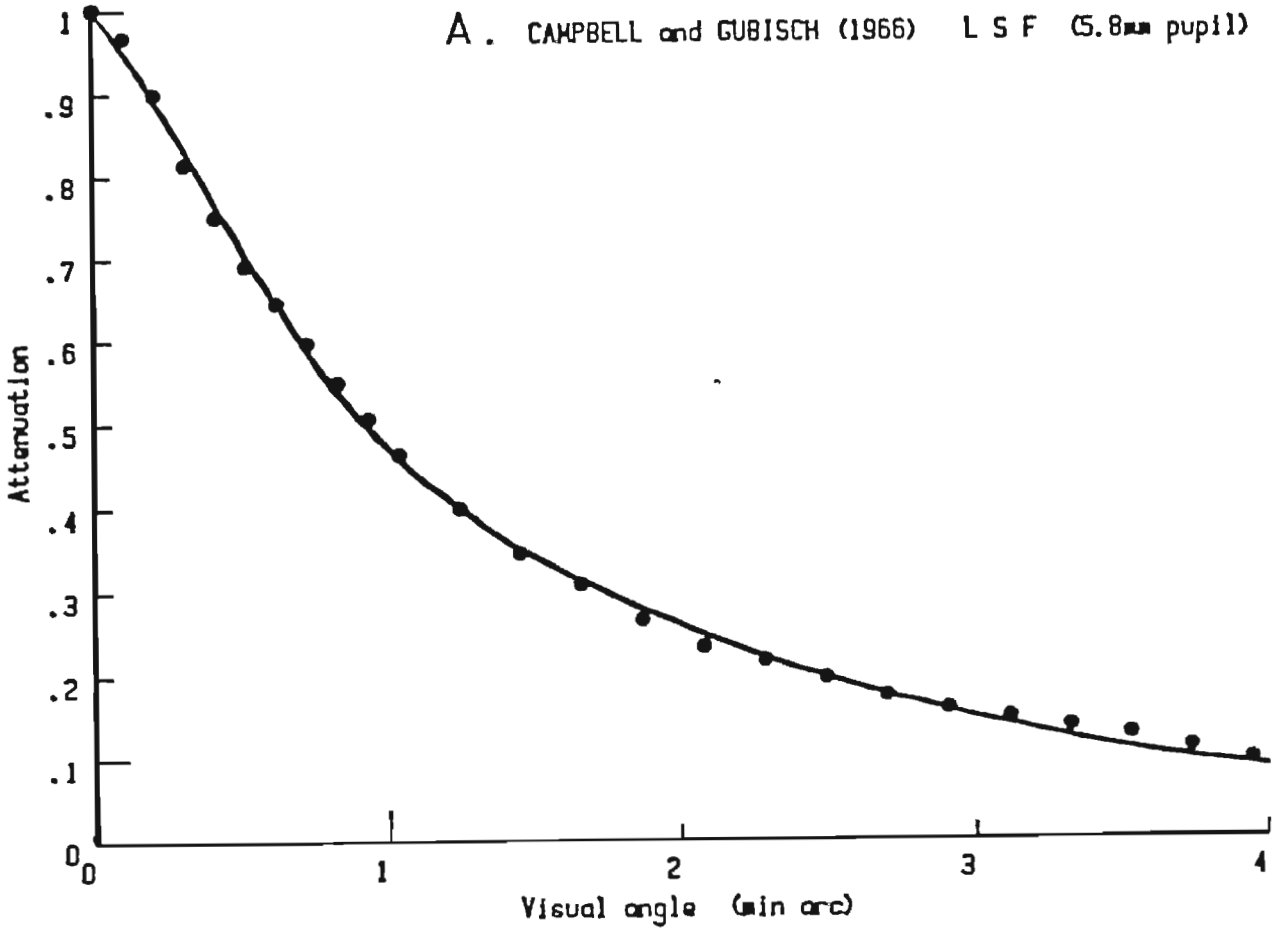

Figure 2.2 Attenuation by the optics of the eye.

Optical aberrations and diffraction combine to degrade the retinal image. The broadening of the image of a narrow line (a) reflects these imperfections. The line spread function shown here (solid dots) is the estimated line image for a 5.8mm pupil (Campbell and Gubisch, 1966). The solid line is an optimized fit of a sum of exponentials function.

In lieu of convolving the line spread function with the stimulus, their Fourier transforms may be multiplied. The Fourier transform of the line spread function, the optical transfer function (b), describes the degree of attenuation each spatial frequency by the optics of the eye. The transform of the data for the 5.8 mm pupil is well fit by the transform of the optimized function.

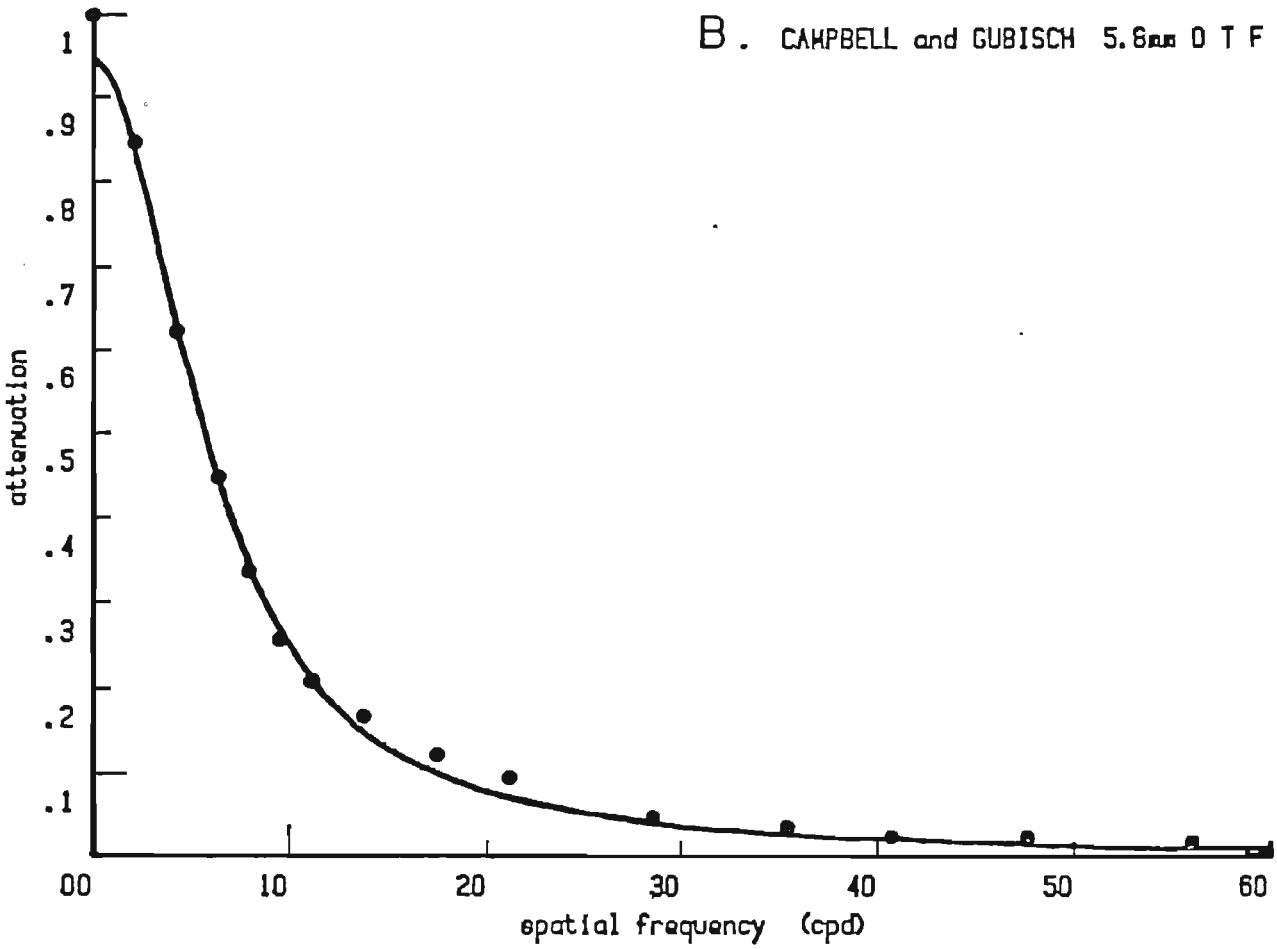
B. CAMPBELL and GUBISCH 5.6mm D T F
attenuation
1
.9
.8
.7
.6
.5
.4
.3
.2
.1
00
10
20
30
40
50
60
spatial frequency (cpd)

mm pupil:

$$F(\omega) = 0.076\, e^{-\left\{\frac{\omega}{0.12}\right\}^2} + \frac{1346}{1430 + \omega^2} \qquad [2.2]$$

ω is spatial frequency in radians.

The frequency by frequency product of the OTF and the stimulus spectrum, then, is the spectrum of the retinal flux distribution, the actual filter input.

The basic partitioning mechanism of CELT is a spatial filter. Each filter is composed of spatially-localized, antagonistic regions that vary in their sensitivity to flux. Apart from probability summation among filter responses, the filter activity is independent. There is no preferred combination of filter response by spatial frequency, phase or orientation. The absence of any special combination of subsets of filter output across space greatly lessens the difference between the frequency and feature characterizations. Without channeling as defined by Graham (1977), the filters become localized, relatively coarse image processors. The selectivity may be viewed as result of a need to improve signal to noise ratios through spatial pooling within a filter while maintaining a generalized basis of representation through the diversity of distinct bands of spatial frequency and orientation among filters (q.v., Geisler, 1984). This description is in contrast to theories that hold that the filters are highly selective for perceptually salient features. In models such as CELT, an odd-symmetric bandpass spatial filter is no more an edge detector than a long wavelength sensitive cone is a red detector.

Specialized bar and edge detectors discard too much information to comprise an efficient first stage of spatial vision.

The initial stage of a spatial filter is characterized by a linear summation of the weighted point by point response to the retinal flux distribution. Although it is possible to use the point-intensive representation of a filter (figure 2.3, a and b), the spatial interactions are more simply described by the filter's spatial frequency sensitivity (figure 2.3,c). When plotted on a linear abscissa and a logarithmic ordinate, each filter has a gaussian sensitivity profile. The gaussian profile was selected because it provides an analytic expression similar in shape to the unimodal straight-flanked sensitivities (logarithmic axes) obtained in both adaptation and masking studies (e.g., Blakemore and Campbell, 1969; Stromeyer and Julesz, 1972). The use of a filter spatial frequency weighting function that is gaussian on logarithmic spatial frequency coordinates produces a relatively greater high frequency response and a more sharply localized spatial profile than is obtained with a profile that is gaussian on a linear frequency axis. It should be noted, however, that the filter weights are applied to retinal contrast. When the attenuation of the OTF is included, the filter profiles become less skewed.

The ratio of the upper to lower spatial frequencies that mark the 50% attenuation weights is two. The one octave filter bandwidth is a compromise between somewhat larger estimates obtained in adaptation studies and smaller estimates derived from masking experiments. The response of each filter for a given stimulus is computed by taking the linear sum of the frequency by

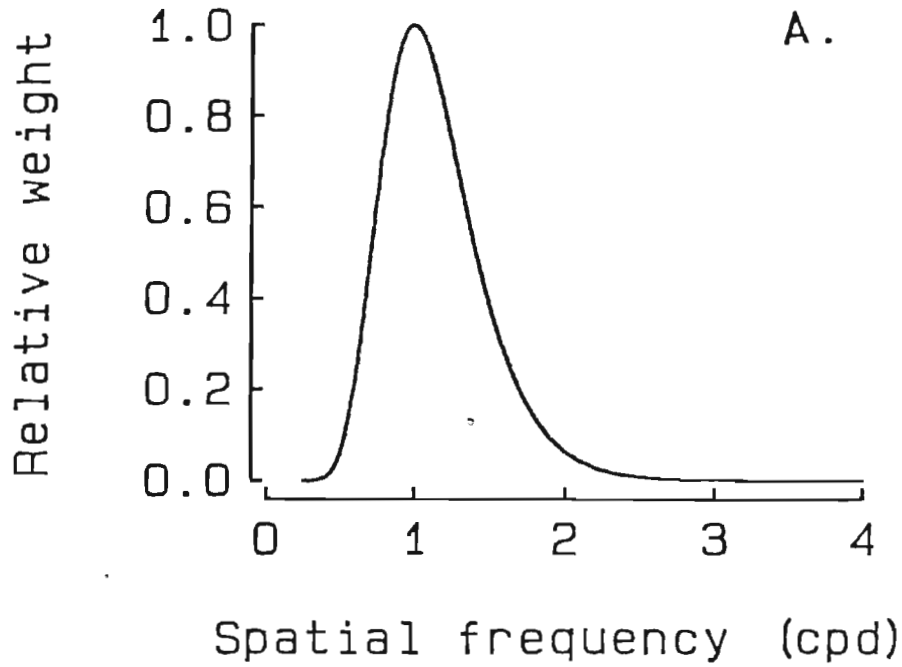

Figure 2.3 One octave gaussian filter.

Spatial filters early in the visual system are characterized by localized linear summation regions whose response contributions are antagonistic. Antagonism between the regions of opposite weighting limit the filters' sensitivity to low spatial frequencies while summation within each region limits the response to high spatial frequencies. The limited spatial extent of the filters is inversely related to the range of its spatial frequency sensitivity. For the unimodal filter profiles used in this model the peak response is referred to as the center frequency (CF) and the range of spatial frequencies separating the upper and lower weights that are half the peak response is the filter bandwidth. All filters in CELT have a one octave bandwidth about their CF. The filter weighting profiles are simply scaled in direct proportion to CF in spatial frequency, and in inverse proportion to CF in space. The summation of the weighted spectrum takes into account phase when computing the net response. The response of the linear summation stage is bipolar. There is no thresholding mechanism to truncate the summation output.

In CELT, all filters at a given center frequency (1 cpd shown) have the same modulus (a) but vary in phase (b). Six flat (constant) phase spectra are used (0, 30, 60, 90, 120, and 150 degrees). Since the filter response is bipolar the filter phase spectra need span only 180 degrees.

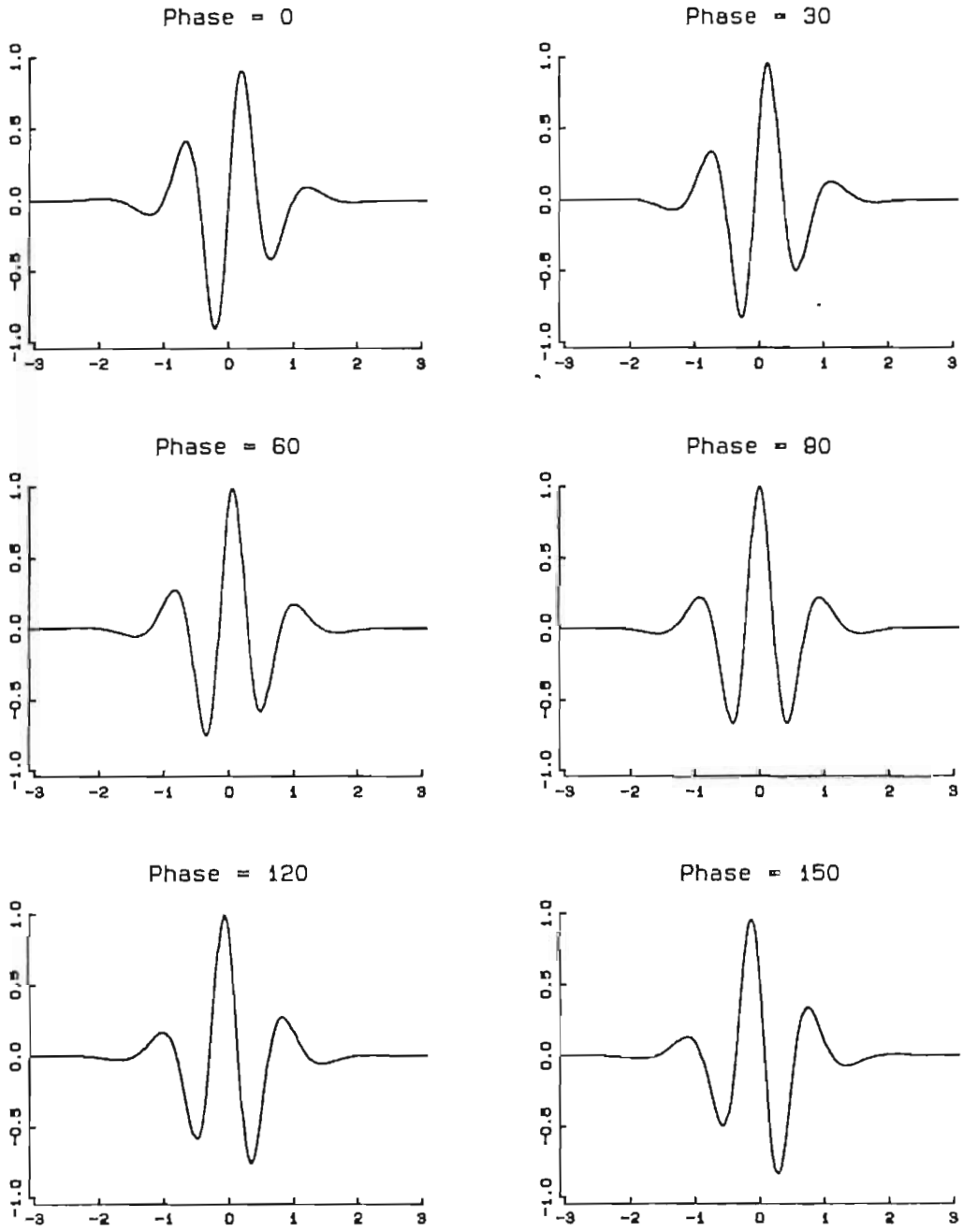
Phase = 0
Phase = 30
Phase = 60
Phase = 90
Phase = 120
Phase = 150
1.0
0.5
0.0
-0.5
-1.0
-3
-2
-1
0
1
2
3

B.

frequency product of the stimulus spectrum (attenuated by the estimated OTF) and the Fourier transform of the filter's spatial sensitivity. The frequency domain product is equivalent to convolution of the stimulus and the filter weighting profile in space and is used to estimate the variation in filter response to the stimulus across the visual field.

Responses to impulsive spectra (e.g., sinewaves) are related to continuous amplitude density spectra (e.g., lines) by the raster rate of the display. It is the raster rate of the display which determines both the width of a line and the spatial sampling rate of the continuous functions and thus provides a common basis for spectrum amplitude calculations.

Filter center frequencies ranged over six octaves, from 0.5 to 32.0 cpd (figure 2.4). The lower bound coincides with the lowest spatial frequency for which an adaptation stimulus was coupled to the maximum loss in sensitivity (Blakemore and Campbell, 1969). The upper bound was derived from filters composed of elements having minimum receptor diameters (Marr et al., 1980). Filter calculations were performed over this frequency range at 0.5 cpd increments. The 0.5 cpd center frequency sampling rate was used to approximate the presumed underlying continuum of potential center frequencies. It is assumed here that a given visual system is similarly composed of a finite number of samples taken from this continuous distribution. When compared to absolute bandwidth, the sampling is relatively coarse in the low frequency region; however, any variation in the sampling density would correspond to a departure from simple linear

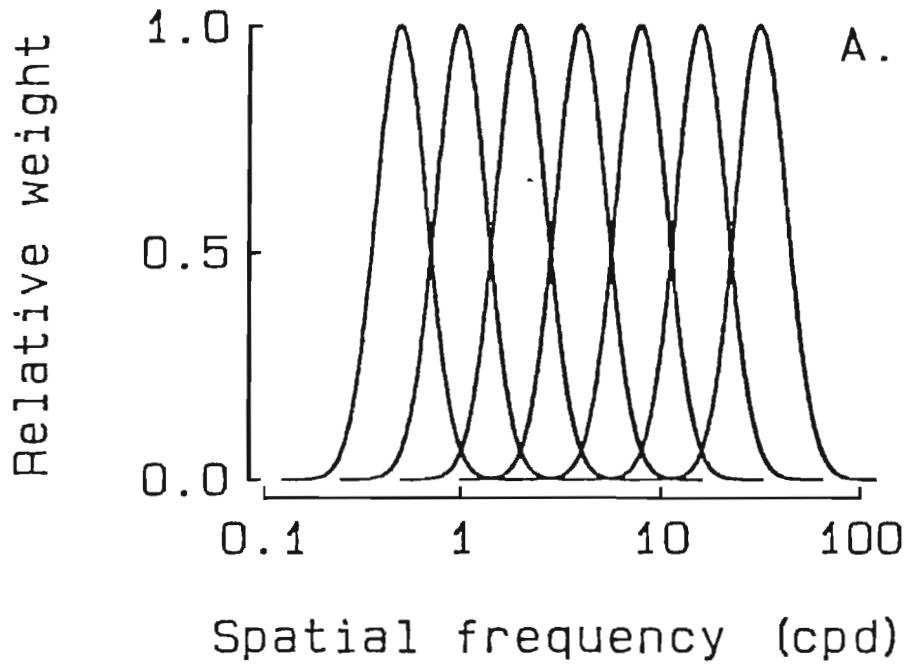

Figure 2.4 Range of filters.

The model is composed of a six octave span of one octave bandpass filters. The underlying continuum is approximated by sampling at 0.5 cpd differences in center frequency between 0.5 and 32.0 cpd. The gaussian nature of the filter weights may be seen when the profiles are plotted on semilogarithmic coordinates (a). The constant octave bandwidth produce a template that is merely shifted along the spatial frequency axis. The constant filter profile is also preserved in the more commonly used logarithmic representation (b). However, if the spectrum is assumed to be uniformly sampled in the linear summation stage, then a linear representation is more appropriate (c). The advantage that high spatial frequency filters have in detecting broadband stimuli relative to sinewaves can be seen from the increase in absolute bandwidth in proportion the center frequency.

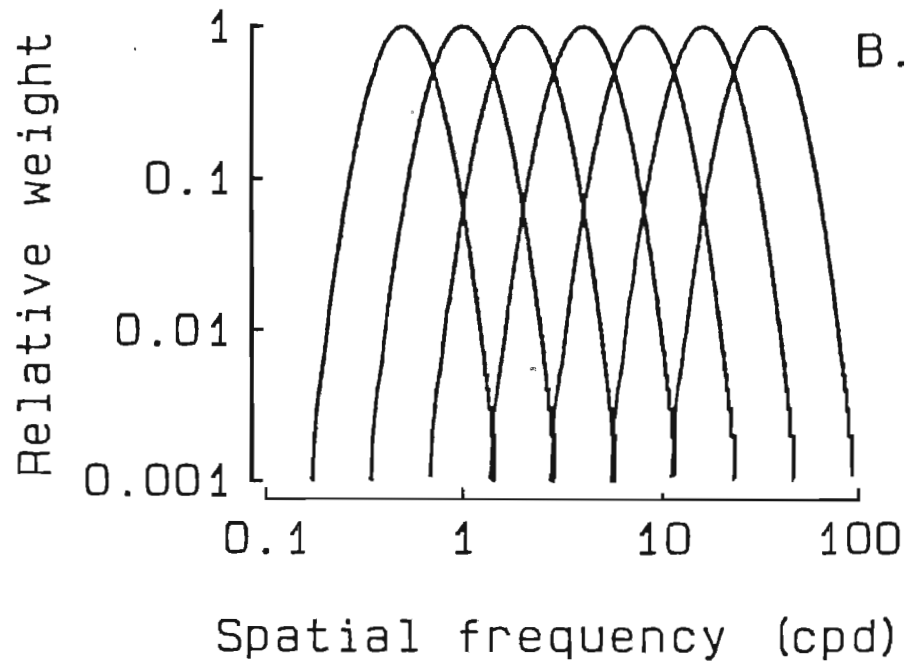
B.
Relative weight
1
0.1
0.01
0.001
0.1
1
10
100
Spatial frequency (cpd)

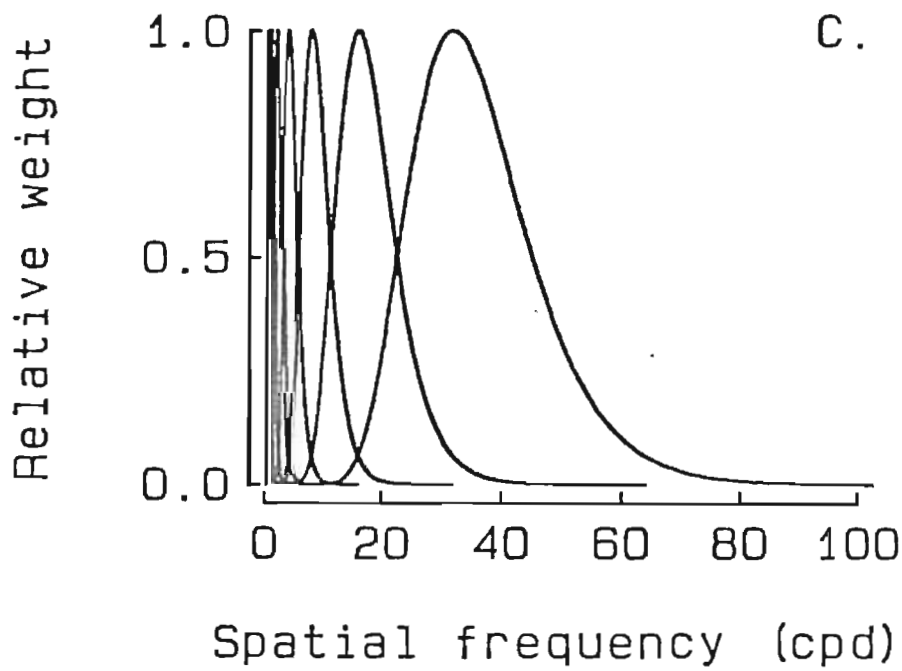
C.
Relative weight
1.0
0.5
0.0
0
20
40
60
80
100
Spatial frequency (cpd)

summation. Any changes in the density of the underlying continuum might be more appropriately incorporated in some other parameter in the model (e.g., gain). A filter in this model may be viewed as representing the net activity of a continuum of actual filters whose center frequencies fall within a region that is equal to the filter sampling rate (0.5 cpd).

Bandpass filters are also limited in spatial extent. The spatial extent is inversely proportional to filter bandwidth. After Robson and Graham (1981), it is assumed that the sampling array of filters is simply scaled in proportion to their extent and that there is one filter per period of the filter's center frequency (figure 2.5).

With a rectangular sampling grid of filters, beating may be produced in the pattern of filter responses to periodic stimuli. A sinewave of any amplitude that is 90° out of phase with respect to a filter's phase will elicit no response. To combat this potential artifact, six filter phases are applied at each filter location. The filter phase spectra are flat and differ by 30° (0, 30, 60, 90, 120, and 150°). The flat phase spectra yield an orderly and gradual transition between pure odd and pure even symmetry. When applied to sinewaves, the aggregate response of the six filters (with the vector metric equal to 3.5) is 28% larger than the response to a single filter with the optimal phase; however, the larger response varies only 0.02% with sinewave phase.

This distribution of filter center frequency, phase and spatial density requires 1,342,074 filters to span the 4.4 by 2.2° stimulus aperture. The vast majority of

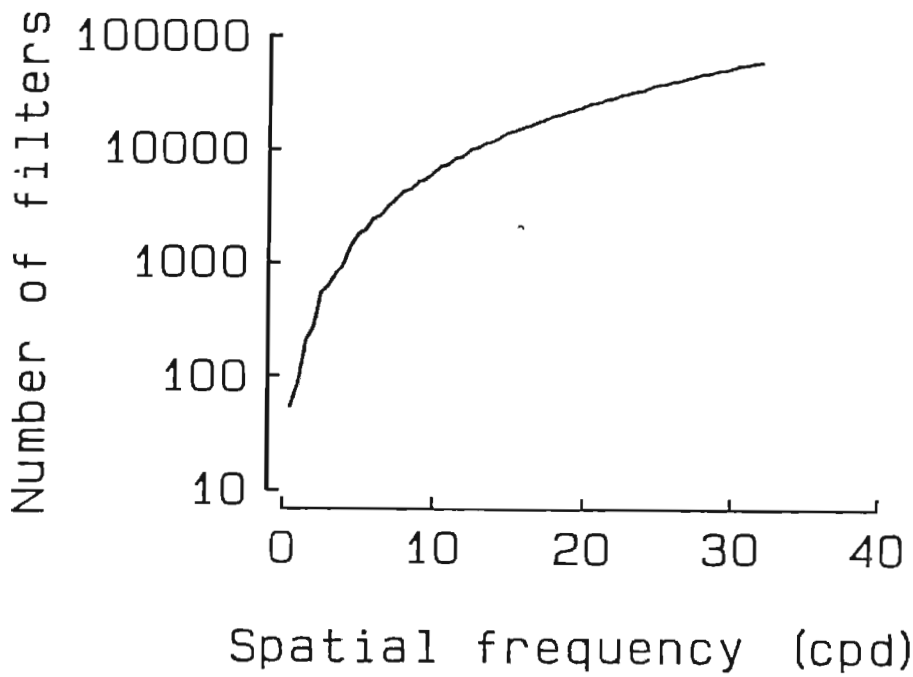

Figure 2.5. Number of filters.

The spatial extent of the model is limited to the 4.4 by 2.2° display aperture. Filters of the same type are positioned in a rectangular lattice with nodes that are separated by one period of their center frequency. Six filters with the same modulus but different phase spectra are located at each node. This arrangement yields as few as 54 (at 0.5 cpd) and as many as 60,066 (at 32.0 cpd) filters.

the filters are incorporated because of the one filter per period assumption applied to high center frequencies. Only 8.8% of the filters are required to serve 50% (0.5 to 16.0 cpd) of the center frequencies.

In addition, filters with a given center frequency lose sensitivity exponentially with eccentricity (figure 2.6; Robson and Graham, 1981). The space constant of the decline in sensitivity is inversely proportional to center frequency. This decline in sensitivity is not uniform across orientations: in the vertical direction, the rate of decline is twice as fast as on the horizontal. The end result of differences in density and eccentricity is a weighting of the filter response as a function of center frequency (figure 2.7). The effective contribution of the ensemble of filters at 32 cpd is more than 4.5 times that at 0.5 cpd when normalized to the individual filter response.

Apart from any change in the aggregate response of an array of filters due to number or eccentricity, there is the inherent sensitivity of the filter itself. Within each filter, the integral of the weighted stimulus spectrum is multiplied by the filter's gain. In CELT, individual filter gain varies as a function of center frequency. Estimates of the individual filter gains may be derived from sinewave contrast sensitivity if detection is mediated by a constant criterion decision rule applied to an aggregate measure of the filter response (see appendix C). Gain estimates are constrained by the obtained contrast sensitivity with the OTF factored out. The resulting neural transfer function (NTF) is based on sensitivity to retinal contrast (figure 2.8). A wide range of filter parameters and combination

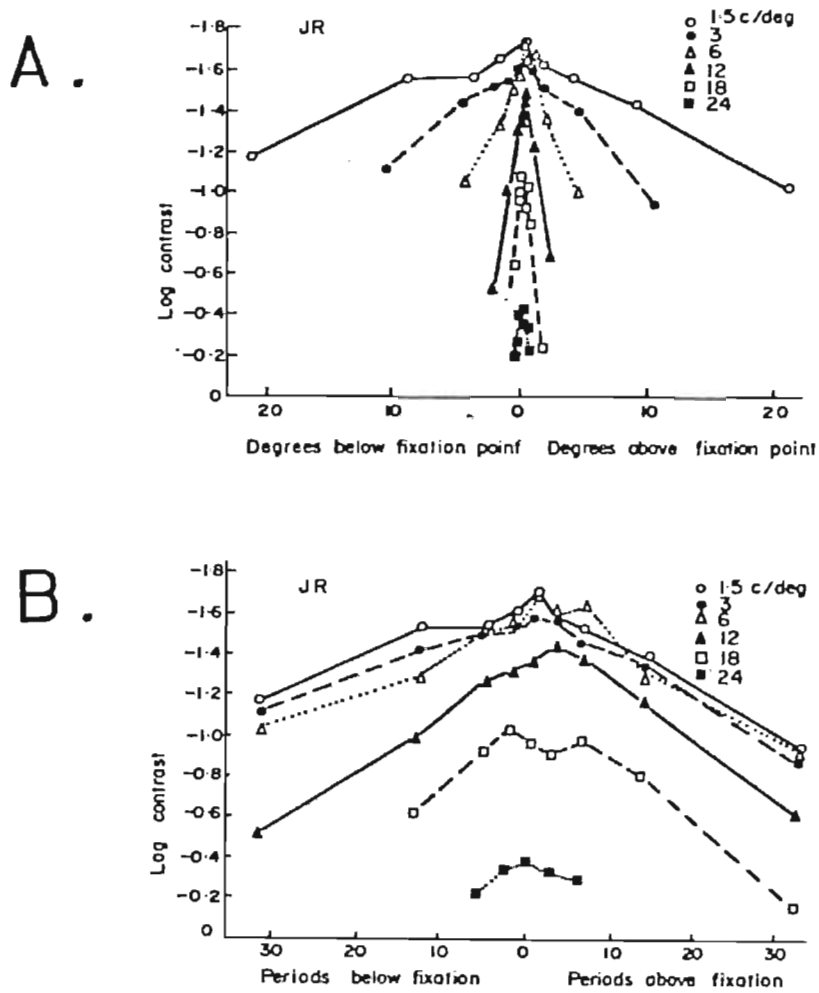

Figure 2.6 Decline in sensitivity with eccentricity.

Robson and Graham (1981) determined the log threshold contrast for 4-cycle patches of horizontal gratings as a function of distance above and below the fixation point. Sensitivity declined more rapidly with eccentricity at higher spatial frequencies (a). When normalized by the spatial frequency of the grating, however, the rate of decline was quite uniform across spatial frequency (b). In CELT, the decline in sensitivity was fit by:

$$S_{eccentric} = S_{fixation}\ 10^{-0.0094\,(\#\ periods)}$$

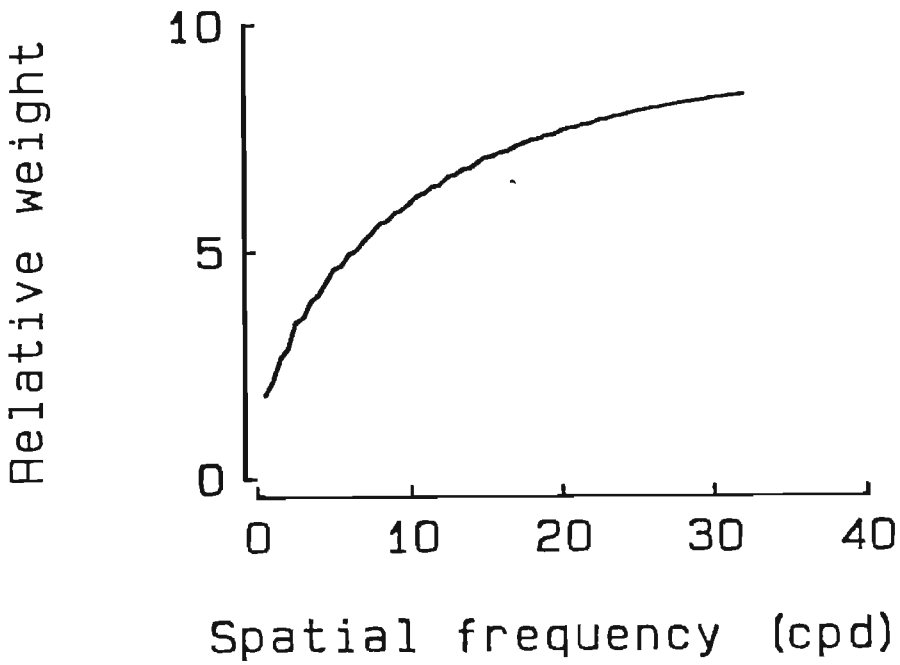

Figure 2.7. The effect of filter distribution on the aggregate response.

As center frequency increases, there is an increase in the ratio of the aggregate to individual response for a collection of spatially distributed filters of the same center frequency. Although sensitivity drops off faster at high spatial frequencies, the increase in the number of filters with center frequency more than compensates for the decline.

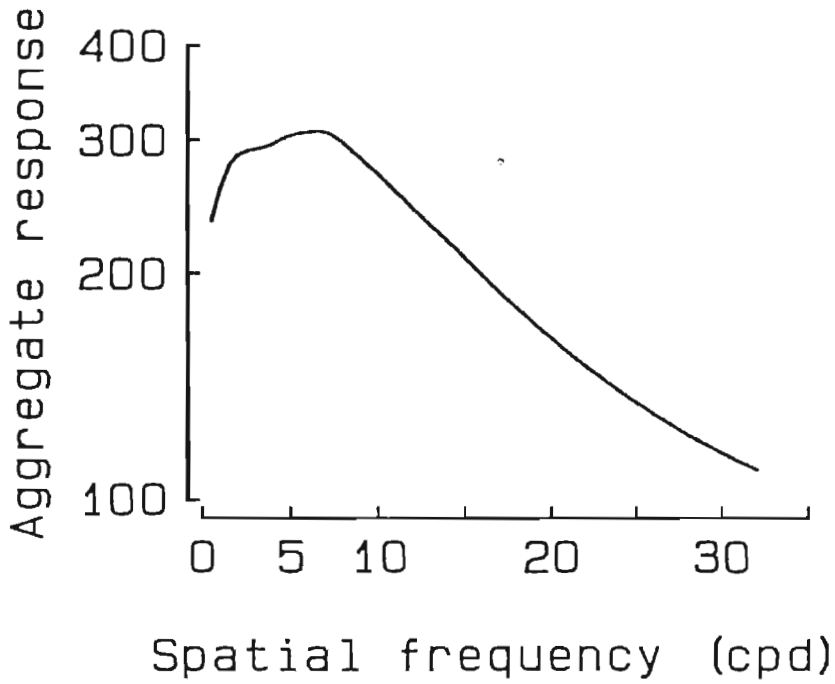

Figure 2.8 Neural transfer function.

When the Observer's sinewave contrast sensitivity is adjusted to compensate for the attenuation by the optics of the eye the resulting function reflects changes in neural sensitivity to sinewaves (solid curve). The advantage of this representation is the possibility of demonstrating more clearly invariances in neural mechanisms.

rules were tested. None of the models could simulate a smooth, continuous contrast sensitivity function with positive gains. Although it is possible that the visual system is composed of filter gains that vary in sign across spatial frequency (e.g., off-center units dominate and overpower the response to on-center units at some spatial frequencies while the reverse occurs at others), there is no evidence in hand that could be used to constrain the parameters of such a model.

Analysis of the failed simulations suggests an alternative explanation. The mathematical solutions were disproportionately sensitive to filter shape at the extremes of the contrast sensitivity function. Most models that simulate a smooth contrast sensitivity function with a finite number of filters do so with overlapping filter sensitivities. The slope of the gaussian filter profiles are too shallow to simulate the rapid fall-off in sensitivity at high spatial frequencies while maintaining sufficient sensitivity at lower ones. Although they preclude an exact solution with gaussian filters, the deviations do not produce distortions of large magnitude. Indeed, it is possible to fit the NTF for Observer BCM to within 1.5% of the obtained values over a 6 octave range (figure 2.9). The individual filter gains decrease monotonically with a slope of approximately 1/21 on semilogarithmic coordinates (figure 2.10). An exponential function was fit by eye to the 64 individually adjusted gains to determine how well the model would perform with fewer degrees of freedom. The deviations of aggregate filter response from obtained contrast sensitivity remained less than 30 percent over the same 6 octave interval. The largest errors were at the extremes of the range.

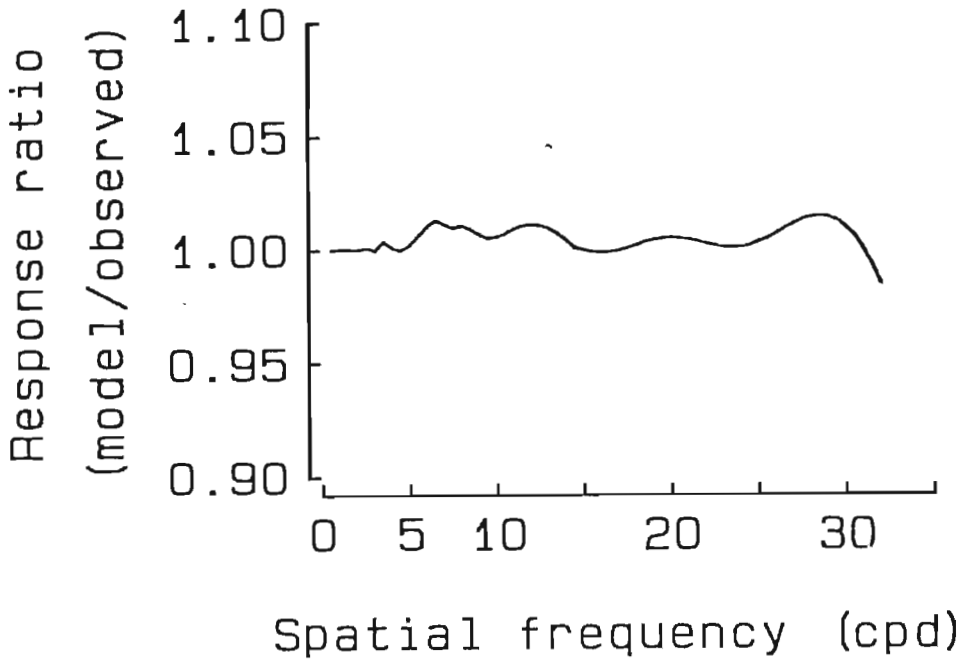

Figure 2.9 Comparison of model responses to the NTF.

The model responses remain with 1.5 percent of the NTF (Observer BCM) across the entire range of center frequencies. The individual filter gains were adjusted to reduce the difference between the NTF and CELT's response. The gain is the only model parameter that is specifically fit to the current detection data. The other parameters were obtained from the literature.

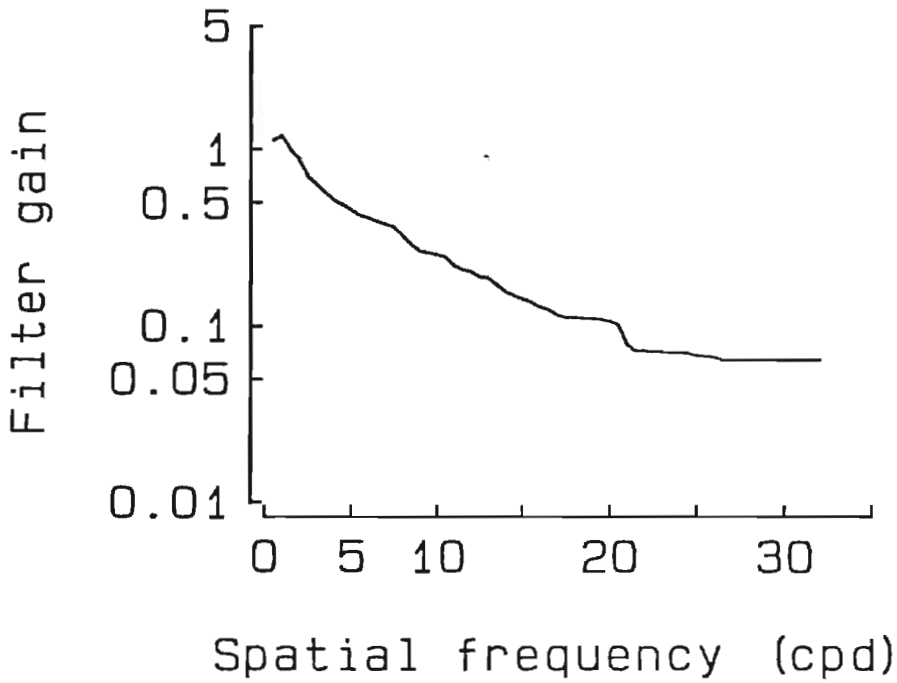

Figure 2.10 Individual filter gains.

The relative amplitudes of the 64 individual filter gains in the model were were adjusted to minimize deviations of the aggregate filter response from the obtained contrast sensitivity (Observer: BCM). Overall, the pattern of filter gains is well fit by a straight line on semilogarithmic coordinates:

$$g(f) = 10^{-(0.0475\,f) - 0.04}$$

Keeping in mind that CELT is a generic model, that is , it is defined by consensus parameters and is not optimized, the fit to the data by a single two parameter function is exceptional. However, since the goal is to establish the plausibility that contrast sensitivity supplements acuity measures and not to defend a particular filter model, it is important to determine the source of any errors in prediction. To this end, the individually adjusted gains will be used. Any errors in the prediction of responses to other stimuli, therefore, will contain minimal departures due to deviations in the contrast sensitivity predictions.

Although it is not of consequence in the modeling of most detection experiments, there is a degree of freedom in the trade between gain and filter density in the determination of individual sensitivity: gain may be increased at the expense of filter density. To the extent that the early filter stages are linear, sensitivity should be a function of the total flux summation area (i.e., with filter sensitivities that are inversely proportional to bandwidth). For each filter, gain acts as a scalar that relates flux to response. Other filter parameters, such as bandwidth and intrinsic noise, also may vary with eccentricity and may be traded off against the gain estimate. These trades may become of consequence in modeling discrimination experiments.

The effects of probability summation among the array of filters produces a markedly nonlinear relation between the stimulus spectrum and the Observer's response (see appendix C). The mechanism selected here to model this nonlinear behavior is the vector magnitude sum (Quick, 1974). After the output of the

linear summation stage is scaled by the gain and spatial weighting factors in the individual filters, each filter's response was raised to the B^{th} power. The value of B determines the metric of the vector space. The exponentiated responses are calculated for each spatial frequency and phase and summed. The response of the entire array of filters is then taken to be the Bth root of that sum. In CELT, B is set to 3.5. This value has been used in the literature to fit a range of grating summation data (e.g., Graham et al., 1978). Robson and Graham (1981) measured the change in sensitivity obtained when the spatial extent of narrowband stimuli at a constant eccentricity was increased. The changes in sensitivity were consistent with a vector magnitude metric that had an exponent of 3.5.

The consequence of a vector metric with an exponent greater than one is to increase disproportionately the weight of large filter responses in the aggregate response. This nonlinearity might be a consequence of oversimplifications in CELT. Either noise sources or thresholds could cause the diminished effective contribution of the smaller signals to the aggregate. On the other hand, there is nothing sacred about an exponent of one (linear summation of response across filters). It is quite possible that the visual system distorts the responses in forming internal representations.

The end product of these computations is a pattern of filter response profiles that vary markedly across spatial frequency (figure 2.11). Response profiles for sinewaves change from virtual impulses at 0.5 cpd to a broad region of activity at 32cpd. The aggregate responses in figure 2.11 are subdivided by spatial frequency

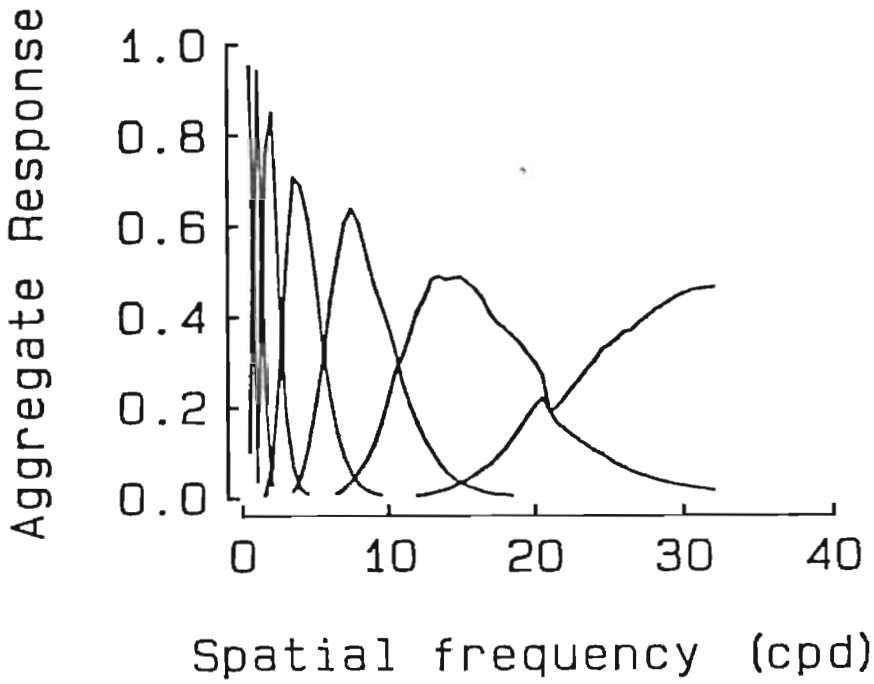

Figure 2.11 Filter responses to single sinewaves.

Filter response profiles for sinewaves differ greatly with stimulus frequency. The responses for sinewaves from 0.5 to 32.0 cpd are plotted at one octave intervals. The response amplitude for a given center frequency represents the aggregate response of all filters at that center frequency at all phases and positions.

and combined across space and phase. This display format is used because it accentuates changes in the spatial frequency domain. It is in this dimension that the major changes among the stimuli are most readily discerned. The use of this simplification does not imply that that the changes in response of individual filters that occur across phase and eccentricity do not contribute to detection and discrimination. It is simply an informative condensation of a complex multi-dimensional response surface.

Not included in this model are the consequences of variability in gain, threshold and intrinsic noise among detectors at a given filter center frequency. The range of filter phase spectra also alters the expected contribution of probability summation to detection, especially with broadband stimuli. Insofar as the linear summation assumption and the bandwidth estimates are correct, the ratio of the broadband to sinewave filter responses will be valid; however, the absolute height and shape will change as a function of filter density and parameter variability. Some models in the literature (e.g., Graham, 1977) have incorporated simplified filter characteristics and have presumed perfect probability summation. Gross simplifications that circumvent some of these difficulties cannot be applied here because of an ultimate interest in the response to stimuli whose amplitude spectra change significantly within the bandwidth of an individual filter. Although there is evidence for summation across a few filters (e. g., Graham and Nachmias, 1971) there has been none to suggest how broadband that summation can be nor how equivalent the summation process is for stimuli with different spatial extent.

summary

In summary, it is proposed that sinewave detection is mediated by a collection of linear one octave bandpass filters whose center frequencies are distributed along a continuum between 0.5 and 32.0 cpd. The filter phase spectra are flat and have a range of values at each location in space. The actual distribution of a finite number of filters is presumed to be closely spaced with sufficient density to preclude localized insensitivities either in spatial frequency or in space. The combination of filter response is modeled by a nonlinear vector magnitude metric with an exponent of 3.5. A constant criterion, aggregate response decision mechanism is used to assess to ensemble filter response. Measurements of sinewave sensitivity, therefore, reflect the the vector sum of a collection of filter responses centered about the region of the spatial frequency being tested.

The next step is to determine if any amendments are required for a model based on the sensitivity to narrowband stimuli to predict the response to broadband stimuli.

Detection of a single line

background

From a feature perspective all one-dimensional stimuli may be viewed simply as a combination of lines of varying intensity located at different positions in space. In combination with other elemental patterns (e.g., edges, corners), lines comprise a patchwork of juxtaposed features that are processed independently to

form the composite two-dimensional percept. The first stage of this class of model is characterized by the preferred processing afforded the elemental patterns by a corresponding set of feature filters.

Based on their subthreshold summation results, Kulikowski and King-Smith (1973) proposed that there existed a range of filter bandwidths at each center frequency; from 0.3 octave grating detectors to 2.1 octave line detectors. The cosine phase of the line detectors' MTF at the most sensitive center frequency (5 cpd) was consistent with a summation region a few minutes of arc wide and two shallower inhibitory flanks. King-Smith and Kulikowski (1975) went on to show that probability summation across narrowband grating detectors underestimates obtained line sensitivity by an average of 0.2 log units (58%). They suggested that line detection is indeed a composite of probability summation among subunits but that the bandwidth of the subunits is still very wide (c. 2 octaves). Further work (King-Smith and Kulikowski, 1981) showed that their model for the detection of a line could be improved by a combination of localized (line) detectors and narrower bandwidth "bidetectors". Bidetector bandwidth was determined by the minimum spatial offset that produced no line interaction; however, the criterion as to what is negligible is strongly dependent on the slope of the filters' psychometric function and the number of filters that combine to form the aggregate response.

In comparison to features, the spatial frequency description of a line is quite complex, being composed of all spatial frequencies at equal amplitude and in cosine phase. Graham (1977) proposed that the "conglomerate action" of a collection of narrowband filters could account for the detection of broadband stimuli such as lines. The conglomerate action was not a direct pooling of filter responses, but rather, a reduction in the probability of detection required of each filter because of the activation of a range of significantly driven filters across spatial frequency. The more extensive the population of active filters, the more probability summation allows the threshold contrast to shift down an individual filter's psychometric function. The obtained psychometric function for a given stimulus, then, would be the product of individual filter functions. Much of the nonlinear nature of the detection process is derived from the shifting of the operating point along the psychometric function, for it is the slope that determines the marginal gain associated with the incremental filter contributions, and that slope is not constant.

Graham modeled sine plus line data with narrowband (0.4 octave) filters by assuming that noise was correlated across space within channels. Narrow filter bandwidths based on sine plus sine experiments (e.g., Sachs et al., 1971) were acknowledged as minimum estimates. The incorporation into the model of uncorrelated noise in filters of the same center frequency but at different spatial positions increases the estimated bandwidth of individual filters; however, the degree of the bandwidth increase depends strongly on the density and distribution

of filters.

Wilson (1978) argued that line plus line experiments could not be accommodated by models with narrowband filters. He concluded that narrowband estimates are the result of models with insufficient probability summation. If probability summation across spatial frequency and across space characterizes early visual processing, as Graham and Rogowitz (1976) and Wilson (1978) argue, then the responses of mediumband (c. one octave) gaussian filters possess the appropriate relative sensitivity to broad and narrowband stimuli. With the incorporation of probability summation across space it is not necessary, therefore, to include a multiplicity of bandwidths at each center frequency.

data

The Observers' contrast threshold for a line was determined in this thesis by presenting individual narrow lines at one of four positions spaced 640" arc apart. On a given trial, line position was selected at random in a 2TAFC procedure. Randomization of position was used to prevent the focus of attention from converging on a single location. This modification was introduced to increase the similarity in task demands between the single and four line detection experiments. Threshold contrast was 26.8% (±1.5%) for BCM and 28.1% (±2.4%) for DLG. Threshold contrast as used here is stimulus contrast (dL/L) times 100.

model

Broadband stimuli at threshold contrast produce activity in a range of filters. There is a non-zero but subthreshold probability that any one of them would exceed the detection criterion on a given trial. The form of the modeled filter response for broadband stimuli reflects a trade among the greater summation of the frequency spectrum associated with the larger filter bandwidths present at higher spatial frequencies and the greater neural gains and smaller attenuation by the optics at lower spatial frequencies. Stimulus contrast linearly scales the aggregate response determined by the relative magnitude of the filter responses across space and spatial frequency. Figure 2.12 (dotted line) shows the filter response to a single narrow line of threshold contrast ($dL/L = 0.268$). According to CELT, the aggregate response to this stimulus is 0.84. The 16% deficit (1.0 is required for detection) is small considering the fact that no parameters other than gain were adjusted to fit the Observers responses. A different collection of model parameters than used in CELT produced an aggregate response for a threshold line that was 1.5. It is not unreasonable, therefore, to expect that this class of model may be tuned to produce aggregate responses for threshold lines that are arbitrarily close to one. (A likely candidate to increase the model's relative response to broadband stimuli is a slight reduction in filter bandwidth.) The effect of such tuning on the qualitative aspects of the model is negligible.

The peak response by filters of any center frequency is only 42% of that required for detection (or 50% when normalized to the aggregate response of 0.84).

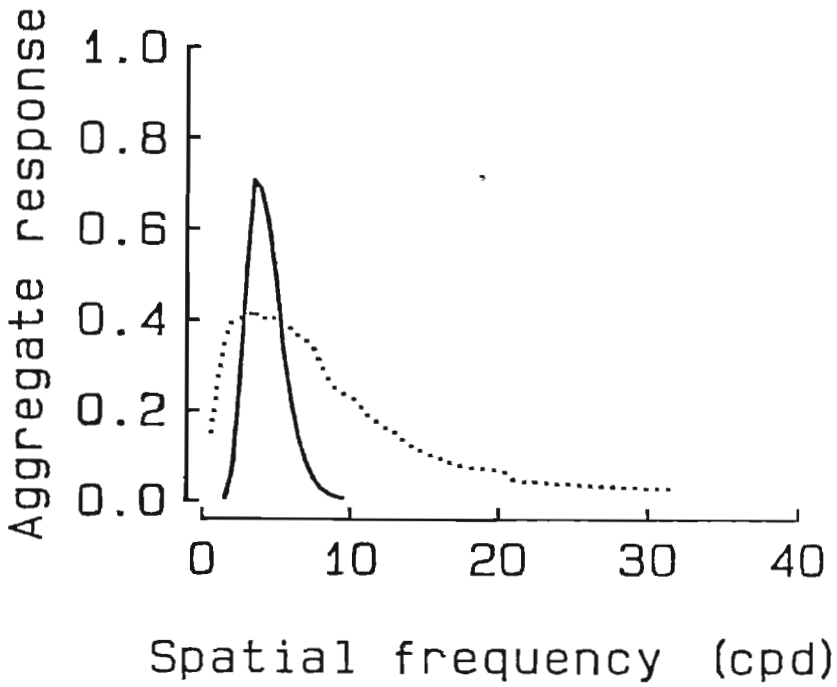

Figure 2.12 Filter response to narrow- and broadband stimuli.

The dotted curve describes the theoretical pattern of filter response produced by CELT for a single bright line. The aggregate response is subdivided according to center frequency but is combined across space. An aggregate response of one is required for detection. The distribution of activity induced by a 4 cpd sinewave grating is plotted for comparison (solid curve).

At higher mean luminances than used in these experiments, the peak of the line filter response profile would be shifted toward higher spatial frequencies. The shift is a consequence of smaller pupil diameters and a concomitant reduction in optical attenuation.

The distribution of activity, however, is quite widespread. While the peak response is near 4 cpd, the half amplitude frequencies are less than 1 and almost 11 cpd. The response declines much more slowly on the high frequency side of the peak response.

By comparison, the response to a 4 cpd grating is very peaked (figure 2.12, solid line). The maximum response at any one frequency is 71% of the detection criterion. The fact that the two curves elicit very nearly the same aggregate response from CELT illustrates the disproportionate weighting a vector metric greater than one gives to large responses. In a linear model, equal areas under the curves would suffice for matched response. In the present case, a much larger region of moderate response is required to balance a small region of greater activity. For higher mean luminances than used here, the attenuation of high spatial frequencies would be reduced and consequently the region of moderate activity would spread to higher frequencies.

Figure 2.12 also demonstrates the difficulty of extending the distinction of broad- and narrowband stimuli into the response domain. The extent of activity induced by each of the two spectral extrema is not that disparate. Indeed, the absolute bandwidth of the response to a threshold 16 cpd sinewave grating is greater than that of a threshold line (c.f., figures 2.11 and 2.12). Bandwidth differences between the responses to narrow- and broadband stimuli are further reduced at higher levels of contrast.

Equally important to stimulus bandwidth in the establishment of relative threshold is the spatial extent of the stimulus. In the spatial domain, the pattern of the distribution of activity is reversed (figure 2.13). In the localized region about fixation, filter activity induced by a threshold line is greater than that of a threshold sinewave even at frequencies where the total aggregate response to the sine dominates (e.g., 4 cpd). Comparison of the line weighting function of the filters and the line spread function illustrates the source of the trades in the spatial domain (figure 2.14).

summary

The detection of a single line is well modeled by the probabilistic combination of individual one octave gaussian filter responses. Sinewave and line thresholds are reconciled in CELT by appropriate weighting of the spatial advantage possessed by gratings and the spatial frequency advantage possessed by lines.

The detectability of the stimuli in one of the most frequently used tasks in this thesis, the four line interval judgment, is examined next.

Detection of four lines

background

For separations beyond 14' arc, the detection of two lines is well modeled by the independent detection of the individual lines (King-Smith and Kulikowski,

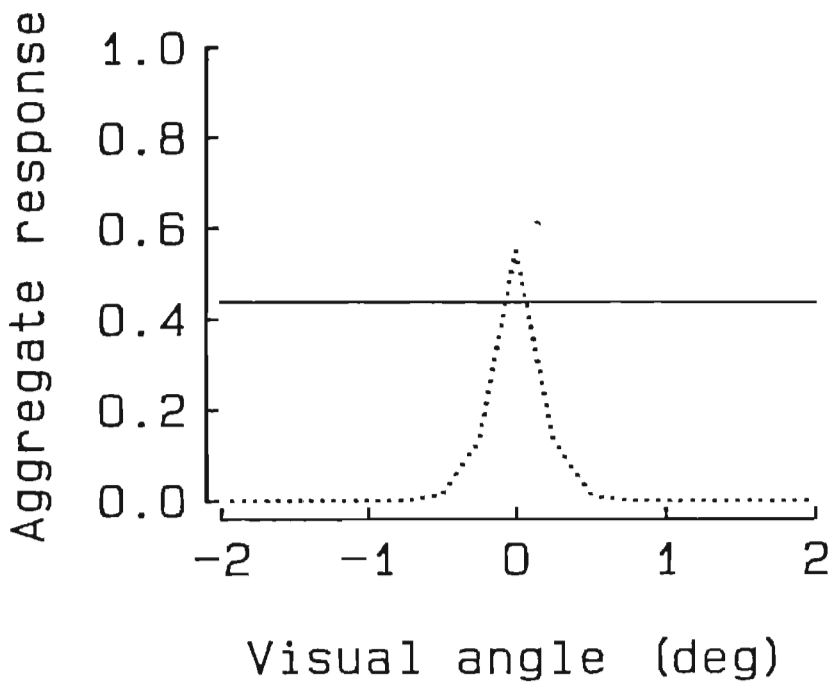

Figure 2.13. Filter response to localized and spatially extensive stimuli.

With the exception of the region close to fixation, the aggregate response of 4 cpd filters at each position in space for a threshold sinewave grating (solid line) exceeds that for a single line at threshold (dotted line). The aggregate response represents filters at all vertical positions and all phases at a given horizontal position.

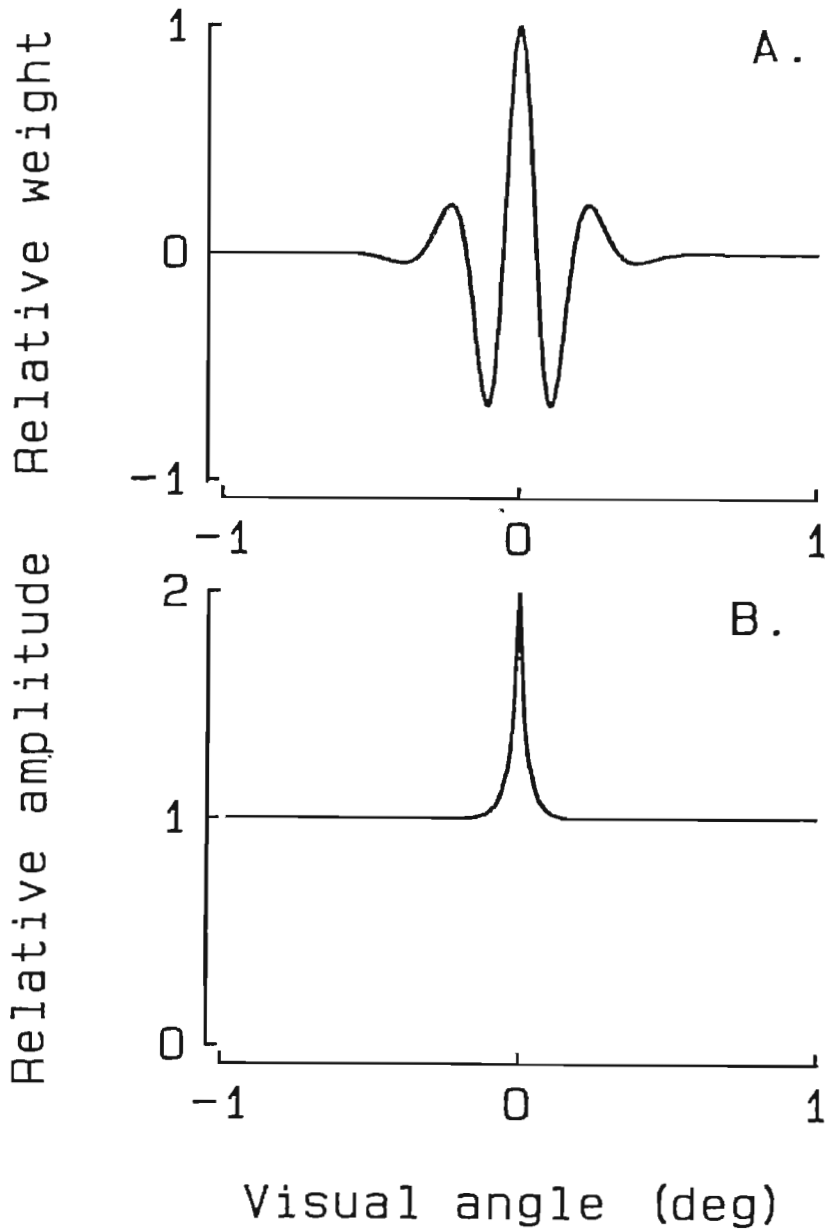

Figure 2.14 A one octave filter at 4 cpd.

The spatial extent of a 4 cpd one octave filter (a) is less than a half degree, the region of greatest sensitivity is even smaller (c. 4' arc). The number of such filters required to prevent spatial notches in sensitivity in the display aperture would be large (c. 171); however, the nonlinear nature of vector magnitude summation severely diminishes the incremental effect of legions of filters. Detection based on a small portion of these spatially distributed filters (10%) would be less sensitive by a factor of only two than that based on probability summation among the entire population.

For comparison, the line spread function (b) estimated to be appropriate for the experimental conditions is also shown (Campbell and Gubisch: 5.8 mm pupil).

1981); however, optimal separation for the detection of positional offset is less than half this value (Westheimer and McKee, 1977c). In this section the spatial interactions that are manifest in the detection of broadband stimuli at small separations will help to define the filters that are active (and inactive) under these conditions and are therefore potential contributors to the detection of positional offsets.

Kulikowski and King-Smith (1973) measured the effect of two flanking lines on the detection of a single line. Although evidence was found for a range of filter types (line, edge, and grating), they assumed that the linearity of spatial summation within a filter operating near threshold allows their subthreshold summation technique to isolate the character of the most sensitive filter for a given stimulus; in this case, a line. King-Smith and Kulikowski (1975) went on to show that the detection of line pairs, sets of lines, and even gratings could be broken down into the visibility of the constituent lines if probability summation and disinhibition were included in the model. They asserted that these two mechanisms account for the differential in obtained and predicted (based on amplitude spectra) sinewave and line sensitivity. King-Smith and Kulikowski (1981) further modified their model to include bidetectors, filters that are optimally sensitive to two lines at small separations and have bandwidths slightly smaller than their line detectors

In contrast to the King-Smith and Kulikowski model, Glezer, Kostelyanets and Cooperman (1977) found a marked increase in two line sensitivity at

separations less than 25' arc over that predicted by independent detection and suggested that observed sensitivity was well matched by the mediation of medium bandwidth mechanisms. In an extension of the theoretical approach of Quick and of Graham, Wilson (1978) demonstrated that probability summation of medium bandwidth filters across spatial frequency and across space eliminates the need for more than one filter bandwidth at each center frequency.

data

In order to measure these multiple line interactions with stimuli relevant to localization tasks, the Observers' contrast threshold for 4 equally spaced lines was obtained for a range of line separations (figure 2.15). A 2TAFC procedure with feedback was used to obtain thresholds for line separations between 40 and 640" arc. This range of separations was used in an attempt to span the transition between complete summation of the 4 lines and independent detection of the individual lines. At 40" arc separation, the threshold contrast of the 4 lines was approximately 1/4 that of a single line, indicating near complete summation. At the largest separation (640" arc), threshold contrast approximated that expected from probability summation among 4 independently detected lines. This value was calculated using the slope of the psychometric function for the detection of a single line. The probability summation threshold was taken to be the contrast that corresponded to a probability of nondetection equal to the fourth root of 1/2. It appears then, that within a factor of 10 change in line separation, processing of the

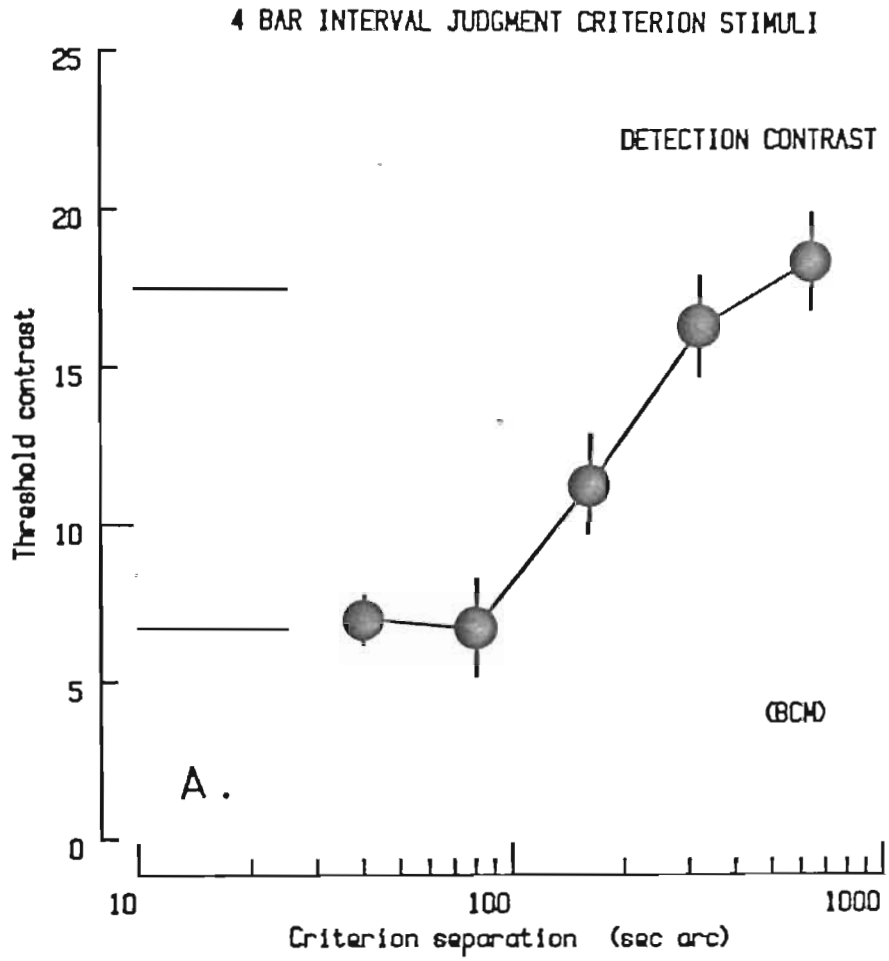

Figure 2.15 Four line detection threshold.

Measures of contrast threshold for 4 equally spaced lines were obtained from both Observers (a and b). At narrow separations, contrast threshold is consistent with that for a single line (lower horizontal line). At the larger separation (640" arc), the threshold was close to that expected for probability summation among four independently detected lines (upper horizontal line). For both Observers, the amount of contrast required to detect the criterion of the 4 line interval judgment task increased with increasing line separation. The error bars correspond to 95% confidence intervals.

In (c), the filled triangles represent the threshold contrast required by CELT (normalized to the response for a single line).

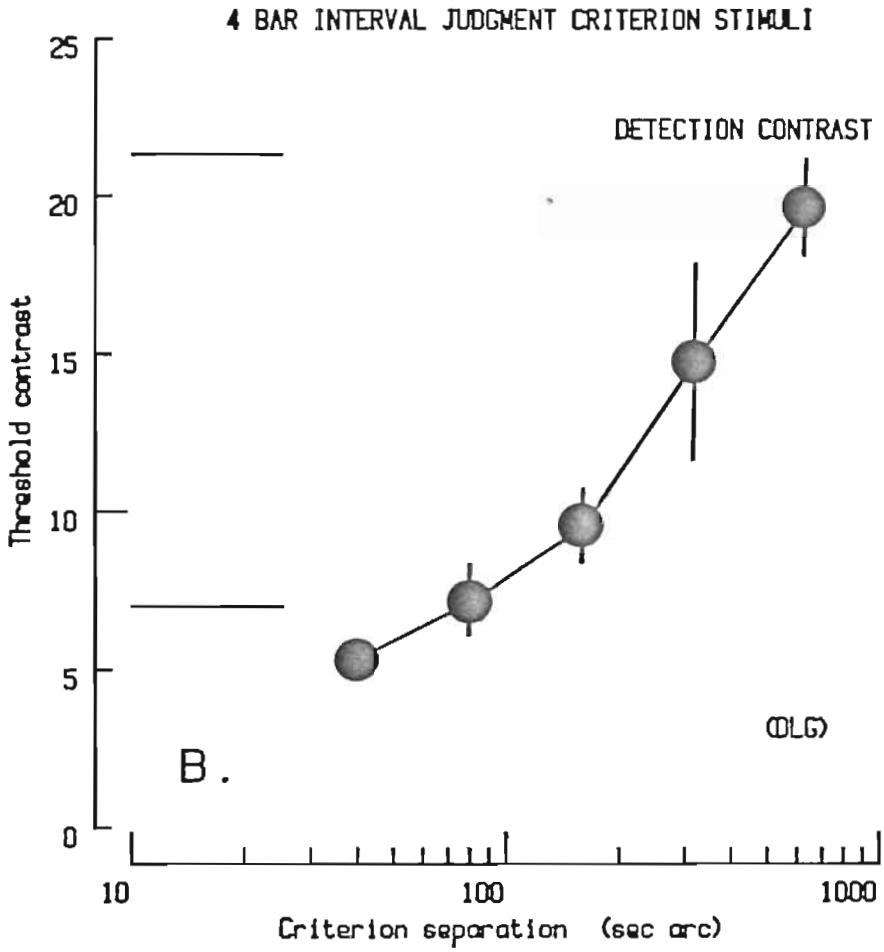
4 BAR INTERVAL JUDGMENT CRITERION STIMULI
DETECTION CONTRAST
Threshold contrast
25
20
15
10
5
0
B.
(DLG)
10
100
1000
Criterion separation (sec arc)

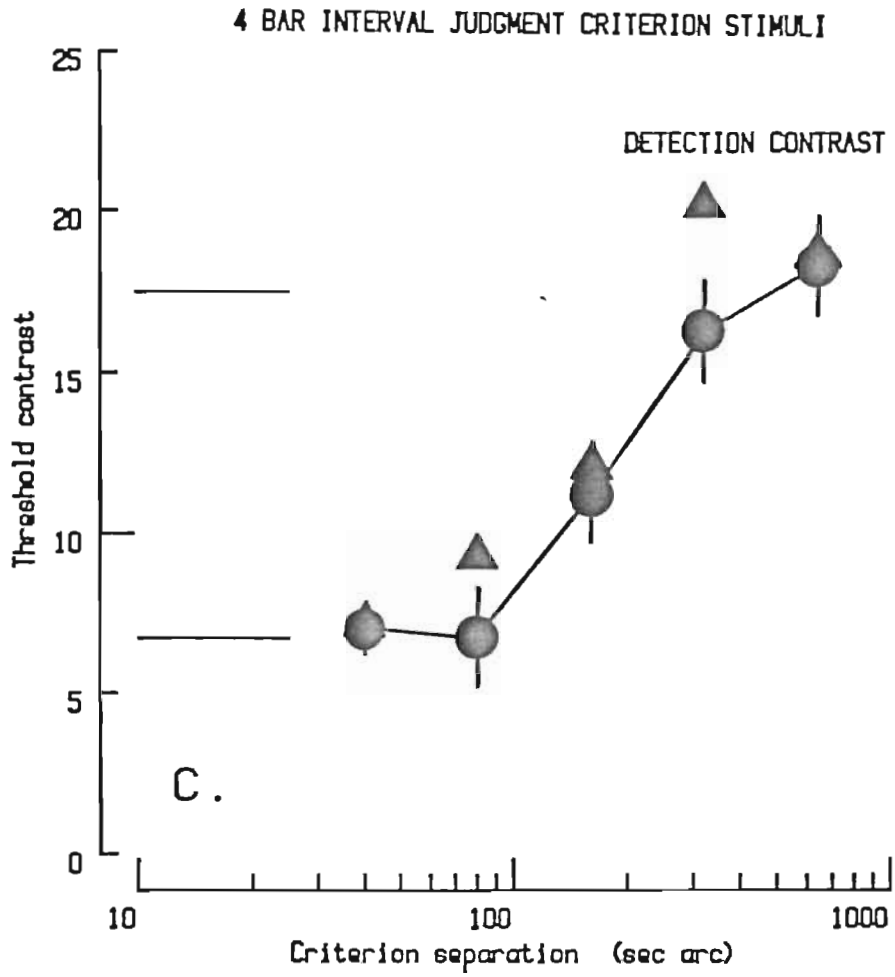
4 BAR INTERVAL JUDGMENT CRITERION STIMULI
DETECTION CONTRAST
Threshold contrast
25
20
15
10
5
0
C.
10
100
1000
Criterion separation (sec arc)

4 line stimuli goes from unification to independence and that the transition coincides with the optimal separations for the detection of positional offset (c. 3' arc, see appendix A).

model

As with the detection of a single line, CELT overestimates the contrast required at threshold for four lines. An examination of the 4 line spectra and the response they induce in filters that vary in position and center frequency should help define the basis of the sensitivity differences during the transition.

The amplitude spectrum of a 4 line stimulus is the product of two cosines; one "frequency" (measured in cycles per cycle per degree) is proportional to the line separation, the other is twice the first (figure 2.16). For small separations (c. 40" arc), the spectrum amplitude decreases slowly with increasing spatial frequency and differs little from the spectrum of a single line, especially in the region of greatest contrast sensitivity. As separation increases, the undulations become increasingly compressed until, at 640" arc separation, there are peaks of opposite sign within an octave of spatial frequency.

As with a single line, the 4 line stimuli produced activity in a range of filters (figure 2.17, a to e; c.f., figure 2.12).; however, at more than the minimum separation, the amplitude envelope differs significantly in shape. At 40" arc separation the response profile is very similar to that for a single line. The greatest

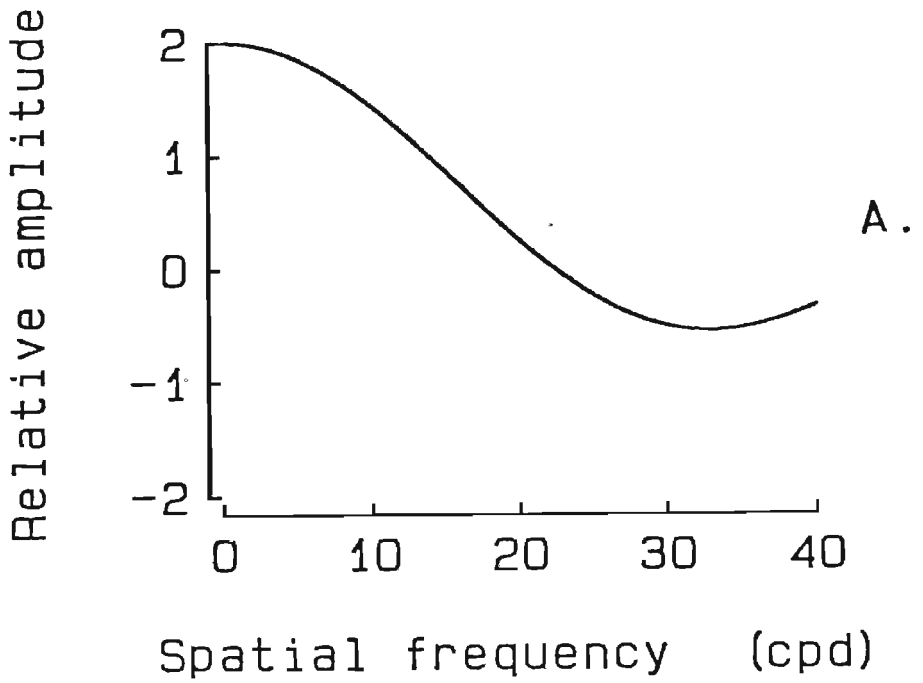

Figure 2.16 Four line amplitude spectra.

The periodic amplitude spectrum of 4 equally spaced lines is:

$$F(\omega) = 2\ cos(\omega\ s)\ cos(\omega\ \frac{s}{2})$$

where s is the line separation in degrees
and ω is the spatial frequency in radians.

The rate of oscillation, therefore, increases with increasing separation (a, 40; b, 80; c, 160; d, 320; e, 640; and f, 1280" arc). For a phase reference centered on the stimulus, the phase spectrum is constant (cosine). Changes in polarity reflect a 180° phase shift.

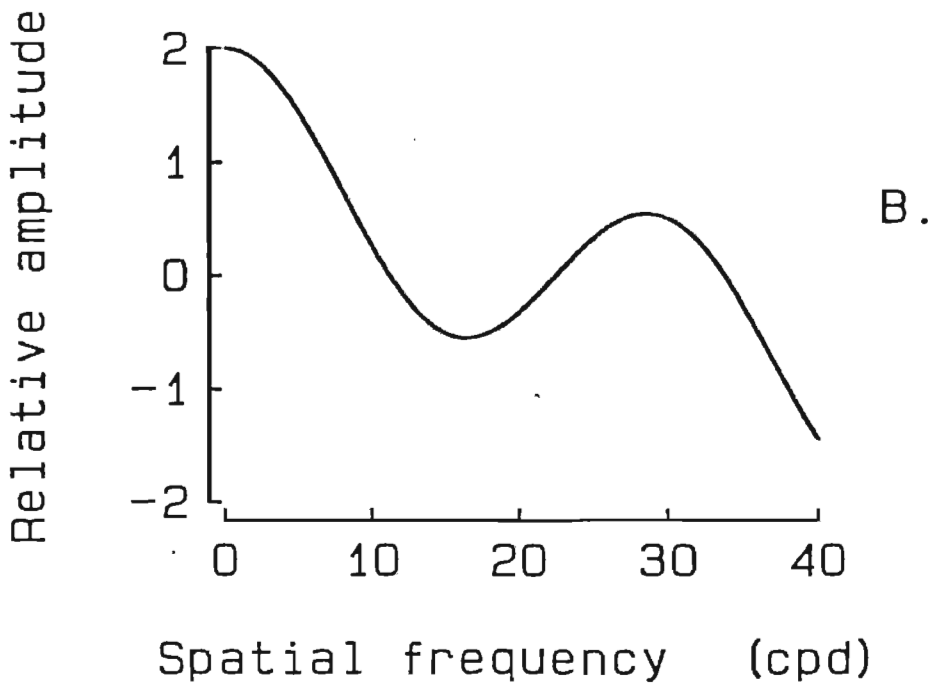
Relative amplitude
2
1
0
−1
−2
0
10
20
30
40
Spatial frequency (cpd)

B.

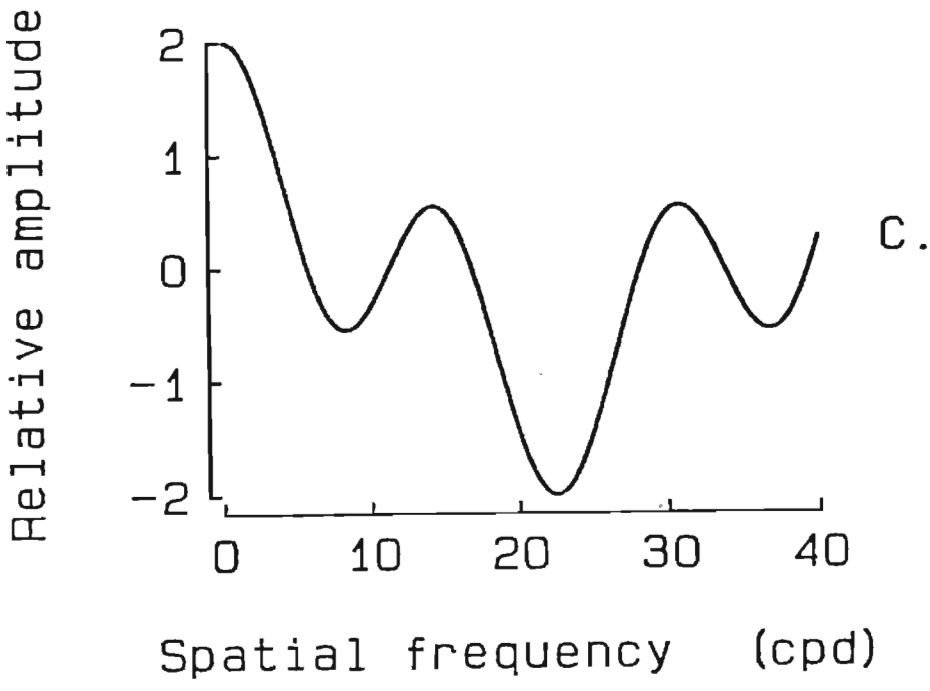
Relative amplitude
2
1
0
−1
−2
0
10
20
30
40
Spatial frequency (cpd)

C.

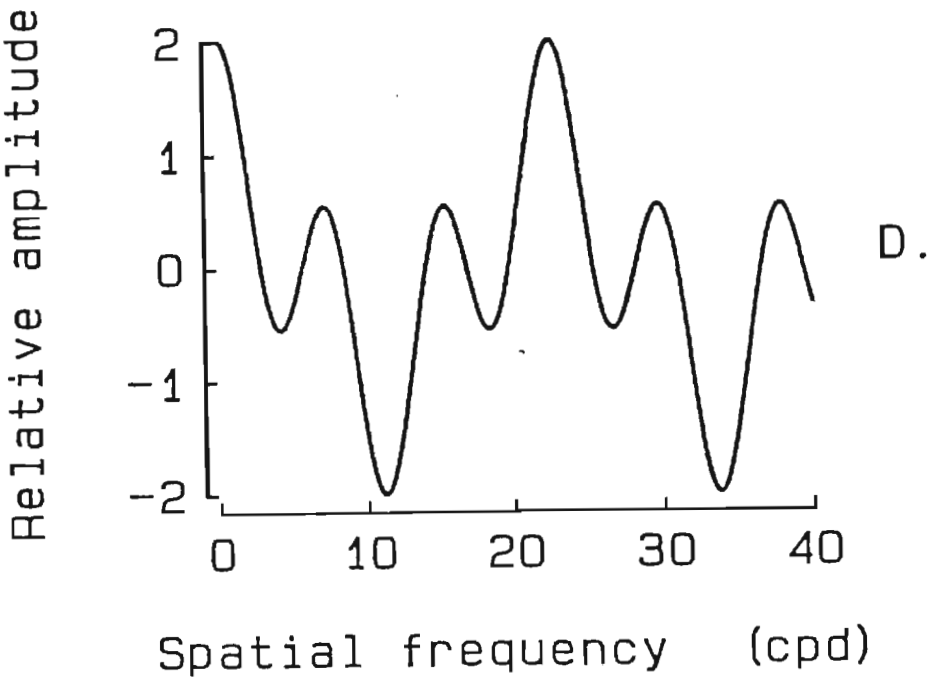
Relative amplitude
2
1
0
−1
−2
0
10
20
30
40
Spatial frequency (cpd)

D.

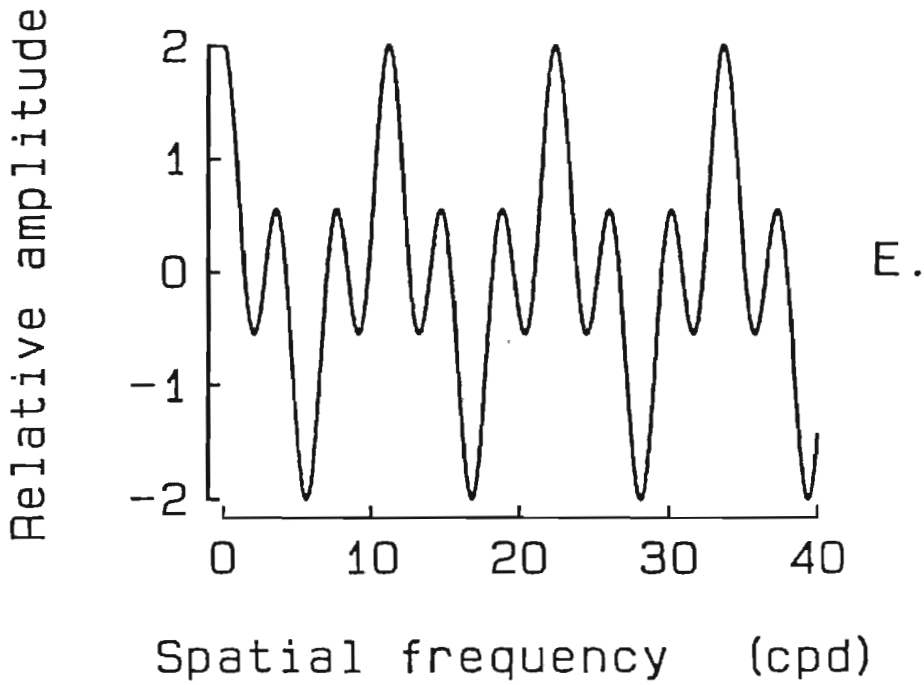
Relative amplitude
2
1
0
−1
−2
0
10
20
30
40
Spatial frequency (cpd)

E.

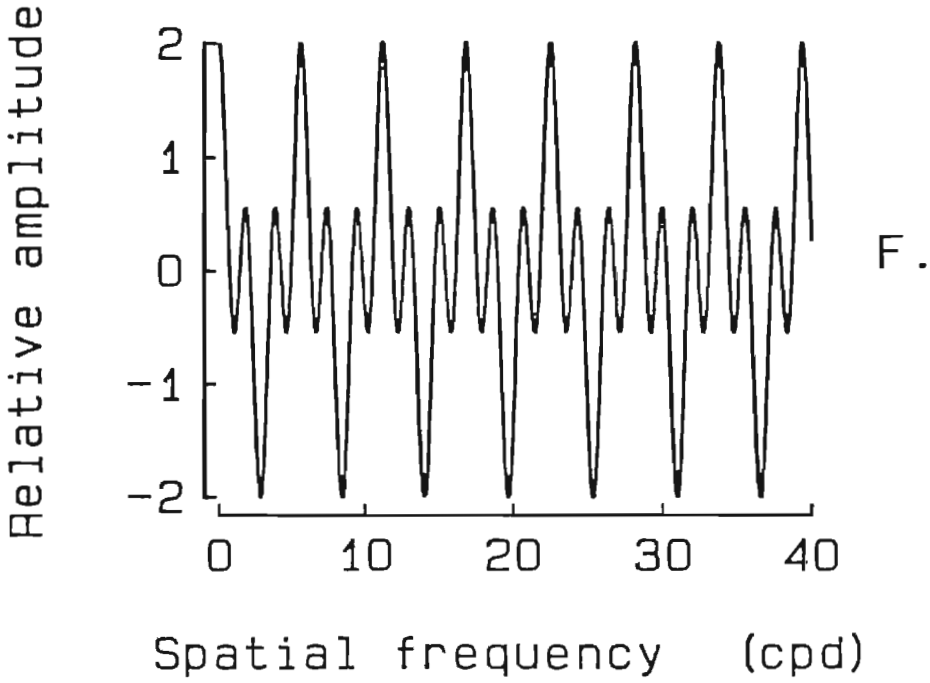
Relative amplitude
2
1
0
-1
-2
0
10
20
30
40
Spatial frequency (cpd)

F.

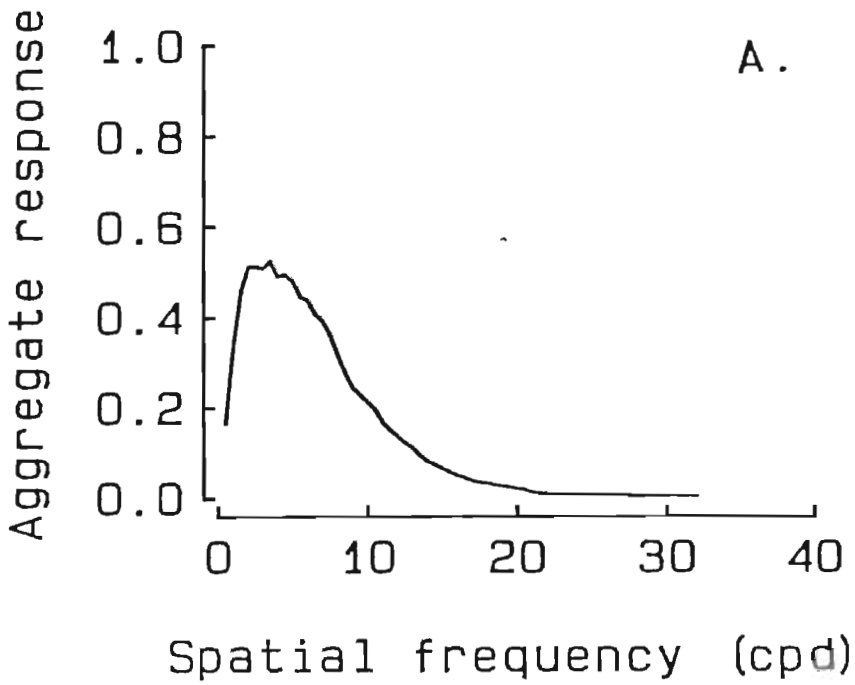

Figure 2.17 Filter responses to 4 lines.

The graph represents the theoretical filter response obtained from CELT for 4 lines over a range of separations (40 to 640" arc). The filter responses are subdivided by center frequency but collected across space and phase. A filter output of 1 corresponds to the aggregate response magnitude required for detection.

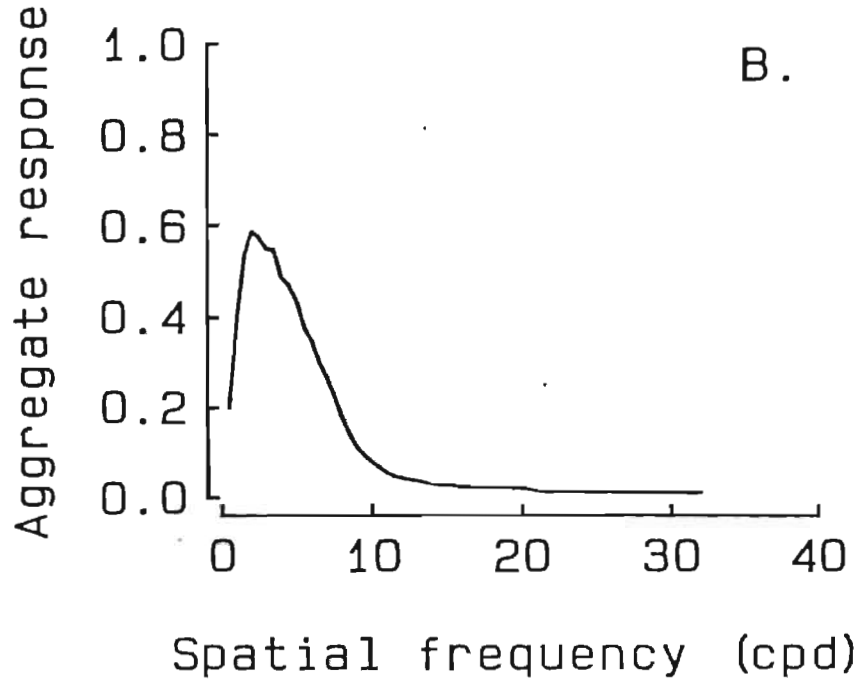
B.
Aggregate response
1.0
0.8
0.6
0.4
0.2
0.0
0
10
20
30
40
Spatial frequency (cpd)

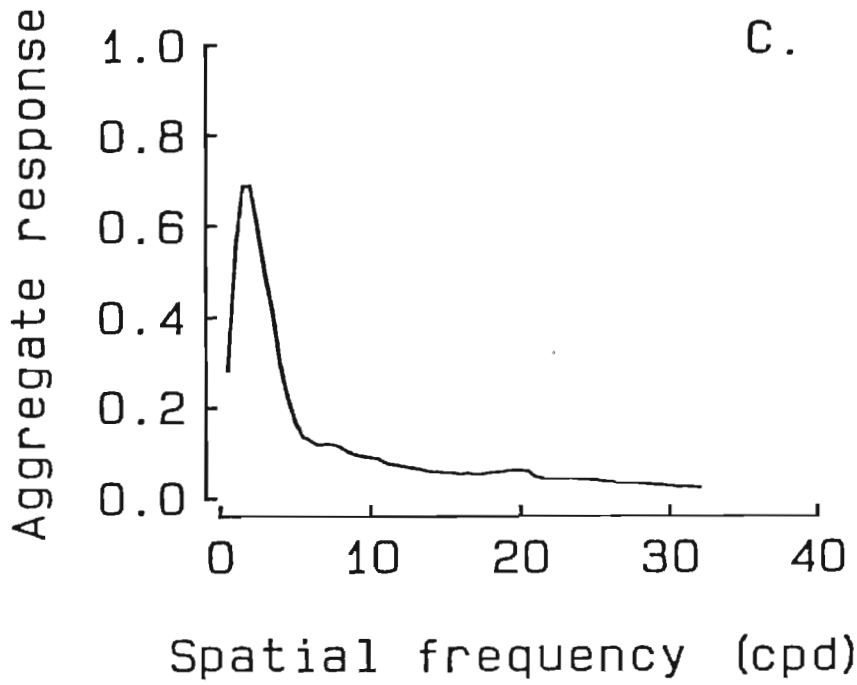
C.
Aggregate response
1.0
0.8
0.6
0.4
0.2
0.0
0
10
20
30
40
Spatial frequency (cpd)

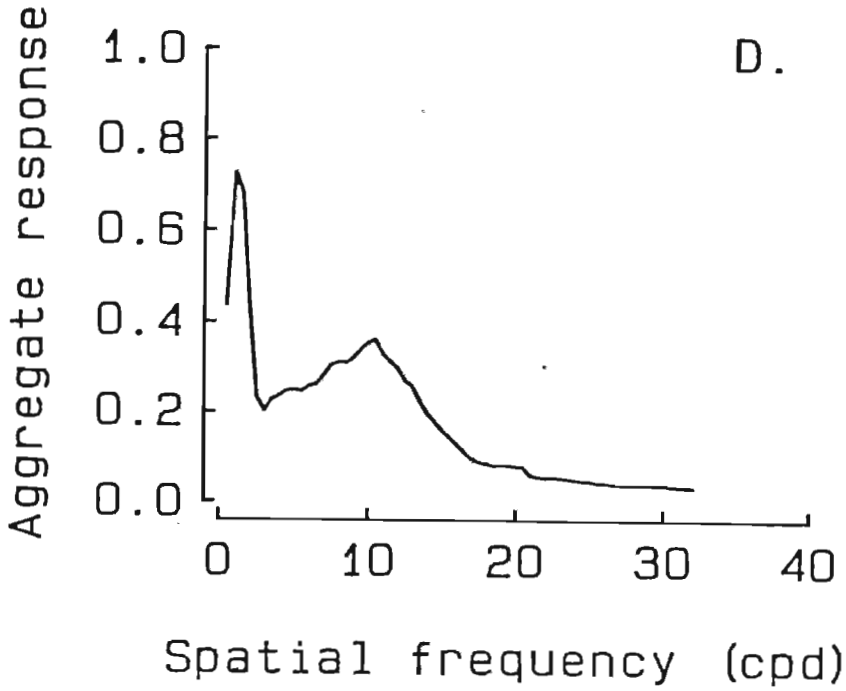
D.
Aggregate response
1.0
0.8
0.6
0.4
0.2
0.0
0
10
20
30
40
Spatial frequency (cpd)

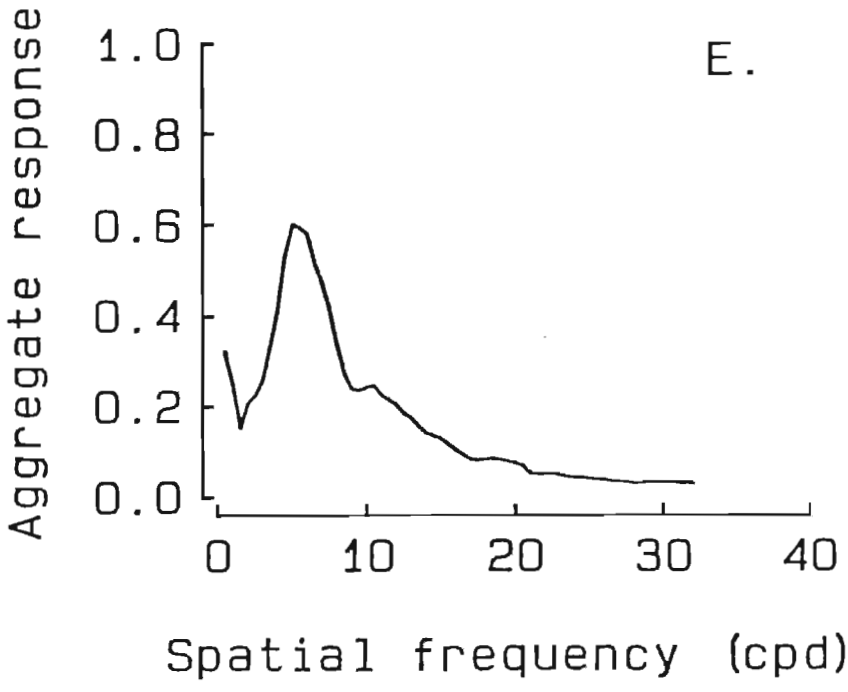
E.
Aggregate response
1.0
0.8
0.6
0.4
0.2
0.0
0
10
20
30
40
Spatial frequency (cpd)

differences occur above 10 cpd where there is a significant decline in stimulus amplitude. As the period of spectrum oscillation decreases with larger line separations, the peak of response activity narrows and is compressed toward the low frequency range of the filter center frequencies. At 320" arc separation the original peak is compressed even further while a second, broader peak appears around 10 cpd. While the original peak reflected the collection of four lines as a single unit, the second reflects the periodicity implicit in their separation. At 640" arc separation the initial peak is severely diminished in amplitude and the second peak dominates the response. The reduction of the initial peak occurs because there are few filters large enough to integrate the widely separated lines. The second peak now occurs at 5 cpd, reflecting the lower periodicity of the lines. At greater separations (neglecting the effects of large eccentricities), the pattern would come full circle and the response profile would again approximate that of a single line.

Although it is the regions of high activity that are important for detection, the distribution of regions of low activity should also be noted. In particular, as the first peak is compressed and the second peak grows, there is a notch of low activity that shifts toward lower spatial frequencies, frequencies that correspond to filters with greater gains. It is the filters in these regions of low activity that are most sensitive to changes in response. Contrast discrimination is optimal here because large spectrum differences coincide with filters at threshold sensitivity.

In feature theories, the interactions of lines at various separations have been described as summation, inhibition and disinhibition (e.g., Wilson, 1978). No clear distinction is made between the mechanisms that underlie the selectivity of a line detector and mechanisms that describe interactions between filters. Can a need be demonstrated for mechanisms beyond the tuning inherent in one octave filters? A one octave filter (q.v., figure 2.3, a) has a line weighting function that can be parsed into several regions. Interactions within the center region, between the center region and a side-lobe of the opposite sign, and between the center region and a side-lobe of the same sign can account for most of the effects attributed to summation, inhibition and disinhibition, respectively. From a spatial frequency perspective, then, multiple-line interactions are characteristic of tuning in a linear system and do not require the addition of separate mechanisms.

summary

The analysis of Observer sensitivity to four lines extends the application of the model to complex broadband stimuli. The shift between independent detection and complete summation defines a region where the four line stimulus is processed as a unitary pattern that is more complex than an individual line and possessing interactions not present in four widely-spaced lines. Examination of activity in the model suggests that while some of the medium bandwidth filters are highly active, others respond nearly not at all. The stage is nearly set, therefore, for an analysis of the filter responses to small changes in position. Prior to that

analysis, however, there remains the fundamental question as to the definition of position. This question is examined next.

Density of labeled positions

background

Position is a spatial attribute that can be used to classify visual objects solely by their distribution across the visual field. Of special interest here is the density with which objects may be labeled by position. Most commonly, positional resolution is determined by a forced-choice psychophysical procedure wherein threshold is defined to be the minimum spatial offset required to produce a proportion of correct responses that is midway between chance and certainty. For at least as far back as Stratton (1900), researchers have considered labeled responses such as lateralization (left/right) as a sufficient safeguard against the potential recruitment of auxiliary stimulus attributes. As an example of an auxiliary dimension, consider the case when stimulus wavelength is made to covary with spatial offset. The obtained threshold would not be considered a measure of spatial resolution alone. The enhanced performance would be attributed to additional information supplied by a dimension independent of position.

Unfortunately, the analogy to the relation between position and form is not as clear. Since both position and form are spatial attributes, it has been commonplace to merge the two into the single dimension of position; however, this convenience may not be an appropriate way to model performance. Although

position is a qualitative dimension, form has both qualitative and intensive properties. In the context of the current model, the spatial filters are labeled according to their position in the visual field as well as by their center frequency. Intensive changes (contrast) produce changes in the magnitude of filter response. Resolution of position to the degree obtained in localization tasks would require a transformation that would map the responses of the filter array onto the position dimension. As yet, no transformation has been discovered that will model observed performance (see appendix B).

The alternative proposed here is that the Observer makes use of the intensive properties of the contrast-sensitive filters to enhance performance beyond the resolution supported by positional labeling. The enhancement in performance is not necessarily accompanied by a change in the perceived position of the stimulus or of its constituent features with the magnitude or even in the direction that is commensurate with the physical offset. What occurs is a discriminable change in the appearance (form) of the stimulus. For example, a region may appear darker when there is a positional offset. The sensitivity for small offsets is different for different stimuli because the capacity to detect contrast differences varies with the criterion stimulus spectrum. The transformation between a physical offset and the corresponding change in the response of the contrast sensitive filters, therefore, is not constant across stimuli. If the perception of perceptual differences were based on such a transformation, the distance an object appeared to move for a given offset would change from object to object and with the contrast of the same object.

In the view proposed here, the operational definition of position in most forced-choice localization tasks includes information derived from contrast detection and discrimination.

The classification of sensory input according to labeled and intensive dimensions has a long history, going back at least to Boring's (1935) distinction of place and frequency coding (see Burgess et al., 1984). A qualitative (labeled) view of position is supported by studies that have shown position to be independent of stimulus luminance (Leibowitz et al., 1955 a, b). They found that near-threshold stimuli can be located to the same accuracy as much brighter targets. In an analysis of positioning accuracy relative to ideal performance, Andrews and Miller (1978) concluded that positional resolution was quite coarse, more than 30 times that of other measures of visual acuity. They attributed the low-grade positional performance to the contribution of many inputs to the representation of a local portion of the visual field. The convergence of the responses of many filters does not maintain the fine registration afforded by the retinal mosaic, and the representation of position suffers. Using similar arguments about the restrictions imposed by a complete representation of all attributes at each position in space, Erickson (1968) proposed a dichotomy of sensory processing based on whether or not the neural representation was spatially organized. In this system, topographic filters span only a small portion of their entire stimulus dimension (space). Changes in value along topographic dimensions involve different sets of filters. Non-topographic filters are broadly-tuned (i.e., are sensitive to a large portion of

their stimulus dimension and represent changes in value by the ratio of responses in a fixed set of filters at each location in space. In the present context, the non-topographic synthesis is provided by sets of bandpass spatial frequency filters at each labeled position in the visual field.

data and *model*

It is of interest, therefore, to obtain an estimate of positional resolution that contains no contribution from contrast (form). To this end, the Observers were asked to label the position of an isolated line when presented in the standard format used in the experiments in this thesis: fixation point off, 500 msec delay, 200 msec line, 500 msec delay, fixation point on (see chapter 2, methods). The line was presented in one of 8 positions centered on the fixation point. Within a session the separation of line positions was kept equal and constant. Across sessions line separation ranged from 80 to 1280" arc. The results from pilot experiments with from 2 to 8 lines indicate that 8 is not an excessive load on the Observers' capacity to maintain distinct labels. There was a small effect on resolution across different numbers of lines at the largest separation (1280" arc), but the decrease in resolution was commensurate with the cortical magnification factor at 1.25° eccentricity (Cowey and Rolls, 1974). Since the effect occurred at an eccentricity that was more than twice that present in the localization stimuli used here in the other experiments, it was not considered to be a factor in the two and four line acuity estimates.

The variation in line separation across sessions may be viewed as changes in the criterion of a two-tailed test of the normal distribution of position labels associated with a given objective position (figure 2.18). After the proportion correct at each separation is adjusted for guessing (1 in 8), a bell-shaped error distribution can be constructed from the responses at different separations. A probit analysis of the cumulative error distribution produces an estimate of the standard deviation of the error of labeled position (BCM: 5.5, DLG: 6.8' arc). When an adjustment is made to the proportion correct to include the single-tailed nature of the judgments at the most eccentric positions, the estimates of standard deviation increased slightly (BCM: 6.1, DLG: 8.6' arc).

These measures of standard deviation of positional error are undoubtably overestimates. Although the Observers made an effort to maintain fixation, eye movements were unavoidable in the 1.2 second interval the fixation point was off. An estimate of the eye movement distribution was obtained by analyzing the Observers' ability to correctly locate which side of the fixation point the line appeared. The proportion of incorrect responses for a given eccentricity of the line was interpreted as the proportion of times an eye movement that large or larger occurred. This measure (BCM: 3.4, DLG: 3.3' arc) is certainly an overestimate of the actual eye movement distribution for it does not incorporate the positional error in the perceived location of the midline (fixation point), but it does not greatly exceed the 1' arc estimates obtained under optimal conditions for 200 msec intervals (Riggs et al., 1954). When the eye movement variance is

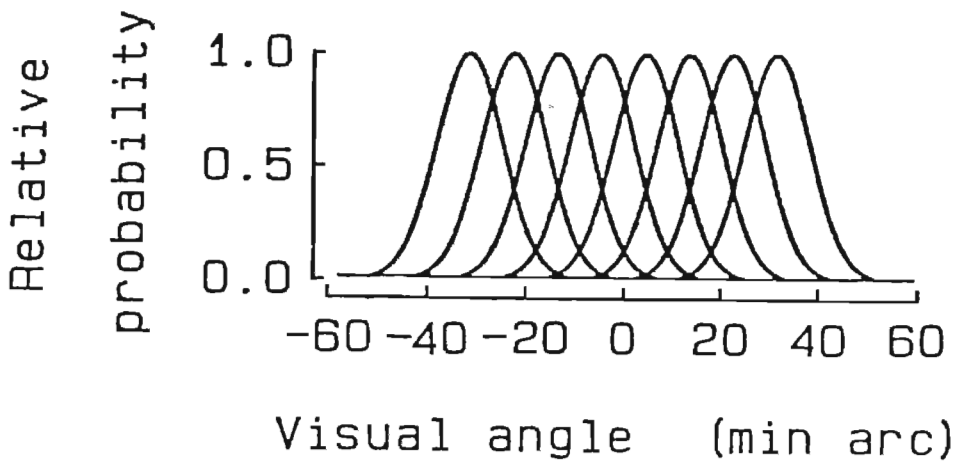

Figure 2.18 Distribution of labeled position.

The error in labeled position has a probability distribution that is approximately normal and a standard deviation that is several minutes of arc (BCM: 5.1; DLG: 8.0' arc). A region is defined by the label with the highest probability. The response distributions are separated so that each region contains 50% correct responses. The mean 50% criterion separation for the two Observers (9' arc) is plotted above. This separation yields a label resolution of 4.5' arc (270" arc).

factored out of the 8 line positional error distribution, the result is a conservative lower bound on positional error, conservative in the sense that positional error is not being overestimated. This correction results in a decrease in the estimate of the standard deviation of positional error (BCM: 5.1, DLG: 8.0' arc).

Threshold positional resolution is defined to be the visual angle within which 50% of the responses associated with a particular label fall. For a normal distribution this condition is met when the criterion is set to ± 0.675 standard deviation of the response distribution. For Observer BCM this limit is 3.4' arc; for DLG, 5.4' arc.

These estimates of positional resolution are outstanding in that they are quite coarse, an order of magnitude more than two line resolution and two orders of magnitude larger than the optimal localization estimates. It is proposed here that the minutes of arc resolution estimate is a measure of the perceptual correlate of location and that the traditional measures are enhanced by the intensive properties of the contrast dimension. This formulation maintains that changes in the form of an object are not inexorably linked on a continuum to its perceived position.

summary

The perceptual correlate of location was found to be coarse, minutes of arc in resolution. Each labeled region contains a range of filters, themselves coarsely tuned for different spatial frequencies, that share the label. The crudeness of these mechanisms is compensated for by the intensive nature of the contrast response.

Chapter 3

OFFSETS AND CONTRAST

In chapter 2, the relative detectability of narrowband and simple and complex broadband stimuli was established. The aggregate activity elicited in a range of moderately coarse (one octave) spatial filters with overlapping sensitivities varied inversely with threshold contrast. The positional labeling of the filter mosaic was found to be coarse, several minutes of arc in resolution. In chapter 3, this analysis is extended to the discrimination of stimuli that have the same contrast but differ in the relative position of their spatial detail. (Note that it is the contrast of the individual lines in the stimuli as they are presented on the display that is held constant; the amplitude of the retinal flux distribution will vary with the relative position of the lines.) Offset thresholds are presented for resolution (two line) and localization (four line interval judgment) tasks. Variation in offset threshold with changes in the contrast of these stimuli are then related to responses of the bandpass filters commensurate with the detection and near-detection discrimination of sinewave gratings. Threshold offsets for two and three line interval judgments are shown to vary in accordance with the optimal conditions for contrast discrimination. The contrast discrimination capacity of the bandpass filters allows the detection of small spatial offsets to be subserved by a relatively small range of center frequencies at a given location in space. In this way the

quantitative dimension afforded by the response to contrast is used to extend performance measures of positional acuity by one (resolution) and two (localization) orders of magnitude beyond the actual positional labeling without requiring an excessively high density of filters across space.

Two line resolution

background

Optical measures of resolution, such as the Rayleigh and Sparrow criteria, are based on objective features of the image (figure 3.1). Under the Rayleigh criterion and with monochromatic light, the images of two points are considered resolved if the centroid of one diffraction pattern is positioned over the dark ring of the other (Airy, 1834). The coincidence of peaks and dark rings is accompanied by a region of reduced intensity between the two peaks. The Sparrow criterion is somewhat less stringent; two monochromatic points are considered resolved at the widest separation their combined peak is monotonic (Sparrow, 1916). With 550 nm light and the entrance pupil consistent with the conditions in the experiments in this thesis (5.8 mm apparent pupil diameter multiplied by 1.15 to obtain entrance pupil diameter; Laurance, 1926), the Rayleigh criterion resolution separation would be 24.1" arc; the Sparrow, 19.7" arc. Although these measures are useful as theoretical limits, their extension to white light or line stimuli, much less human performance, is not as clear.

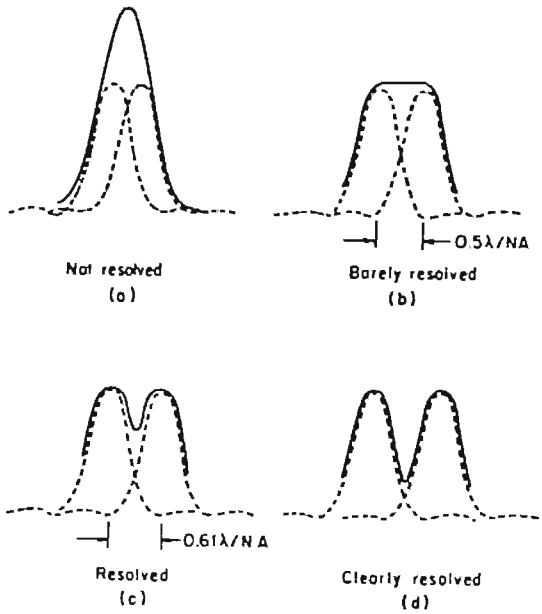

Figure 3.1 Resolution criteria.

Characteristics of the distribution of illumination of the diffraction pattern (circular aperture) of monochromatic point images (Rayleigh) or of the envelope of two point images (Sparrow) have commonly been used to assess the quality of optical systems objectively. As two point images are separated the peaked envelope first flattens (b, Sparrow criterion) and then becomes bimodal (c, Rayleigh criterion).

(from Driscoll and Vaughan, 1978)

The Airy disk of the diffraction pattern of white light is much less peaked (44%) than for monochromatic light and has a sloping shoulder instead of a set of discrete rings (figure 3.2). The combination of multiple point spread functions into a line adds a further distortion to the theoretical limit (figure 3.3). This integration steepens the slope of the central region and also washes out the discrete ring pattern. Any structural analogy to the Rayleigh point resolution criterion for white or line stimuli is lost; however, the Sparrow criterion may still serve as a useful benchmark.

At large pupil diameters, the effect of geometrical aberrations become dominant in the transfer function of the human eye. When the Campbell and Gubisch (1966) estimate of the human line spread function for a 5.8 mm pupil is used, monotonicity in the image of two lines (Sparrow criterion) is maintained for separations out to 48" arc. Given the severe departures from the theoretical limiting flux distribution, human performance measures derived under such conditions may rely on quite different properties of the image than are used to establish the objective measures.

Early measures of two point resolution (e.g., Volkmann, 1863; Aubert, 1865) were based on subjective criteria for the separateness of two points. Modern studies that used forced-choice procedures obtained smaller thresholds (1.3' arc; Martin et al., 1950) than those determined by subjective methods. Even with the improved techniques, however, the results did not approach the theoretical limit proposed by Airy. Measures of human resolution using thin bright lines on a dark

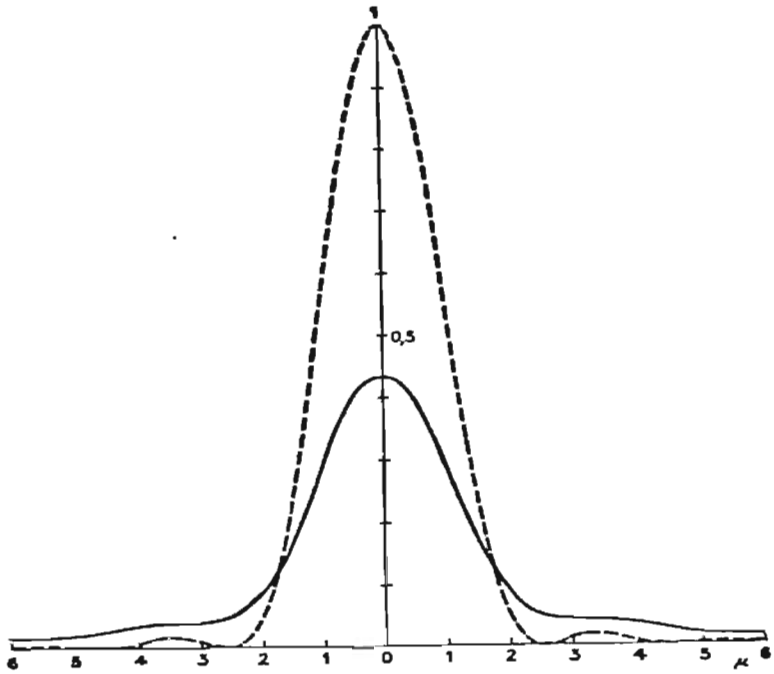

Figure 3.2 Diffraction pattern of a point source.

The continuous line represents the illumination of a diffraction pattern (circular aperture) of a point source of white light (illuminant C), assuming the eye to be free of spherical aberration and in focus for 560 nm. The dashed line represents the Airy disk, assuming that the same luminous flux is concentrated at 560 nm. (A micron on the retina subtends approximately 12.5" arc.)

(from Le Grand, 1967)

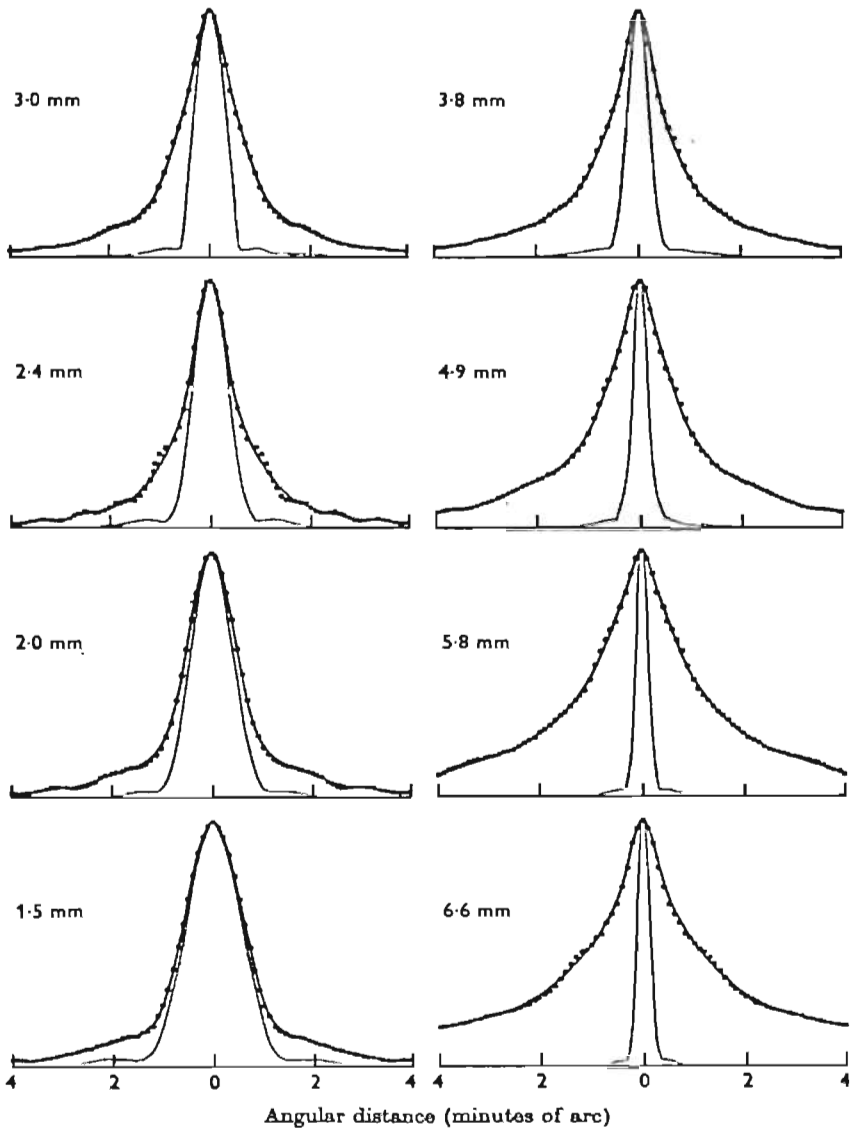

Figure 3.3 Diffraction pattern for a white line and the human line spread function.

The narrower curve at each pupil diameter represents the diffraction image of a thin line of white light (circular aperture). The integration of the point spread function and the superposition of many wavelengths preclude the complete cancellation of flux at any position.

The wider curves demonstrate the increasing departure of the human line spread function from the diffraction limit with increasing pupil diameter. This departure is based on an increase in the Seidel and chromatic aberrations. The curves for the 5.8 mm pupil most closely correspond to the experimental conditions in this thesis.

(from Campbell and Gubisch, 1966)

background were between 40" and 1' arc (Roelofs, 1918; Wilcox and Purdy, 1933; Fry and Cobb, 1935). Minimum resolution with dark backgrounds was obtained with intermediate line luminance. Under these conditions, incomplete adaptation alters the apparent contrast of the image and reduces the discriminability of flux differences at the higher luminances (Le Grand, 1967). When adaptation was controlled, however, acuity continuously improved up to high luminances (Eguchi, 1931 (ref. in Le Grand, 1967)). A theoretical analysis that included uniform background luminance (Coleman and Coleman, 1947) concluded that obtained minimum separable resolution was similar to the theoretical limit when small pupil diameters were used. A number of other optotypes (Landolt, Snellen and Foucault) demonstrated the concordance as well, producing a modern consensus of resolution measures of approximately 30" arc.

Early theories of the limitations of human resolution were anatomically oriented. Helmholtz maintained that resolution and receptor diameter were matched (1' arc). When later research halved the prevailing estimate of receptor diameter, he adjusted his criterion (after Weber, 1846) to require a nonstimulated cone to reside between two stimulated ones in order for image details to be resolved. Pure receptor-resolution theories have difficulty explaining the resolution by Observers of unimodal images as well as the continued improvement in acuity with increases in luminance well into the photopic range.

Subsequent theories downplayed the influence discontinuities in the receptor mosaic had on resolution. In the extreme, these theories considered the retina to

be a smooth continuum characterized only by intensity discrimination. Observer performance is consistent with the limitations imposed by diffraction and brightness discrimination for the detection of points and lines and the resolution of detail with small pupil diameters. On the other hand, the brightness discrimination theories have difficulty modeling resolution performance with wider pupil diameters and with more complex images. Shlear (1937), for example, found that the relative resolvability of Landolt C's and Foucault gratings reversed with changes in luminance. Especially difficult to explain is the obtained variation in threshold contrast with the spatial frequency of interference fringes on the retina. The lack of unification led Riggs (1965) to conclude that the commonly used measures of acuity reflect a number of fundamentally different tasks.

data

A measure of two line resolution threshold was obtained here for both Observers. The separation of two 2.2°-long single-raster bright lines was varied in a 2TAFC paradigm under standard viewing conditions (see chapter 2, methods). The experiment was repeated at each of five contrast levels (figure 3.4). Line contrast (dL/L on the display) was varied from 0.45 to 4.5. This range of line contrast goes from just above (1.6 times) single line detection threshold to moderately bright (16 times threshold contrast). Resolution threshold decreases sharply with increasing contrast at low contrasts, but ultimately approaches an asymptote near 30" arc at moderate contrasts. For a ten-fold increase in contrast,

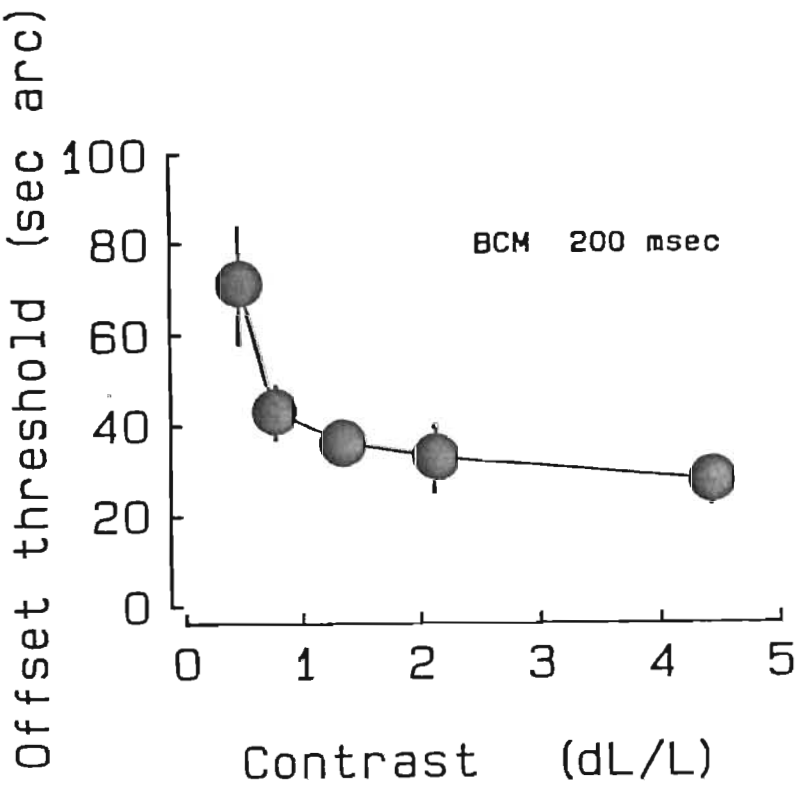

Figure 3.4 Variation in two line resolution with contrast.

The resolution threshold increases rapidly with contrast at low contrast levels. At moderate contrast levels, resolution threshold asymptotes near a half minute of arc separation. The data were obtained with a 2TAFC procedure with feedback. The error bars correspond to 95% confidence intervals.

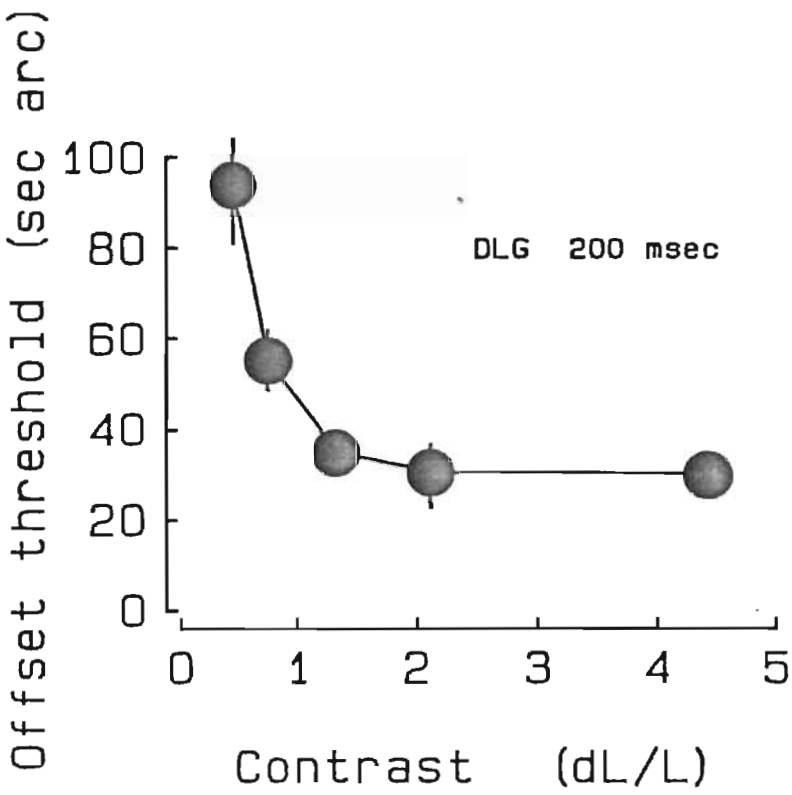
Offset threshold (sec arc)
100
80
60
40
20
0
DLG 200 msec
0
1
2
3
4
5
Contrast (dL/L)

B.

resolution threshold decreases by a factor of three. The half second of arc resolution limit agrees well with modern estimates of spatial resolution obtained under laboratory conditions.

Since the resolution stimuli were presented against a constant background, total flux did not vary greatly over the course of a trial. Consequently, pupil diameter is well approximated by a constant value (5.8 mm) across all contrast conditions. An estimate of the retinal flux distribution for threshold separations was derived from Campbell and Gubisch's (1966) measure of the line spread function that corresponds to this pupil diameter (figure 3.5). Only at the lowest contrast is there a clear bimodal distribution of flux on the retina analogous to the Rayleigh criterion and consistent with the theory of Helmholtz. The constant background luminance makes it unlikely that there is a neural reorganization that requires a depression, but only at low line contrasts. The maximum flux difference between two superimposed lines and two lines at resolution threshold does not appear to be a better alternative criterion. With a constant background luminance, the required flux difference for resolution threshold increases with increasing line luminance. At the higher contrasts, the ratio of the flux difference at separation threshold to the peak criterion luminance (background plus twice the line luminance) is a stable measure of threshold at about 11% for both Observers (figure 3.6). The ratio, however, increases at low line contrast. A decrease in incremental sensitivity near the adaptation luminance is difficult to explain with the mechanisms usually proposed for brightness discrimination. The lack of a

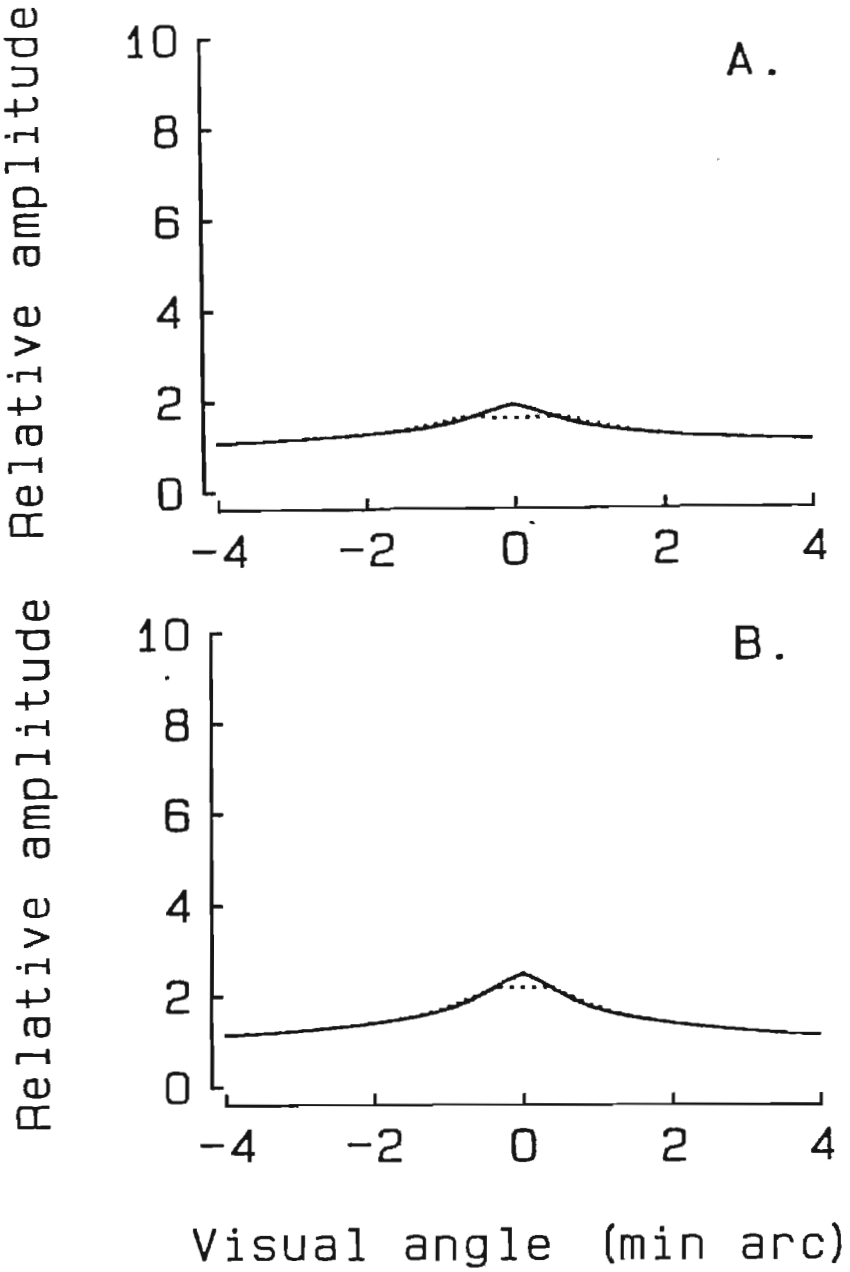

Figure 3.5 Retinal flux distribution at threshold separations.

An estimate of the human line spread function with white light for a 5.8 mm pupil diameter (Campbell and Gubisch, 1966) was used to calculate the retinal flux distribution for the threshold separations obtained at different contrast levels (a to e; Observer BCM). At the higher contrast levels the two line envelope is unimodal.

When normalized to line luminance, the distribution of flux at threshold differs markedly between contrasts of 0.45 (f, dotted) and 4.5 (f, solid). For a constant contrast increment criterion, the peaks would be equal in height.

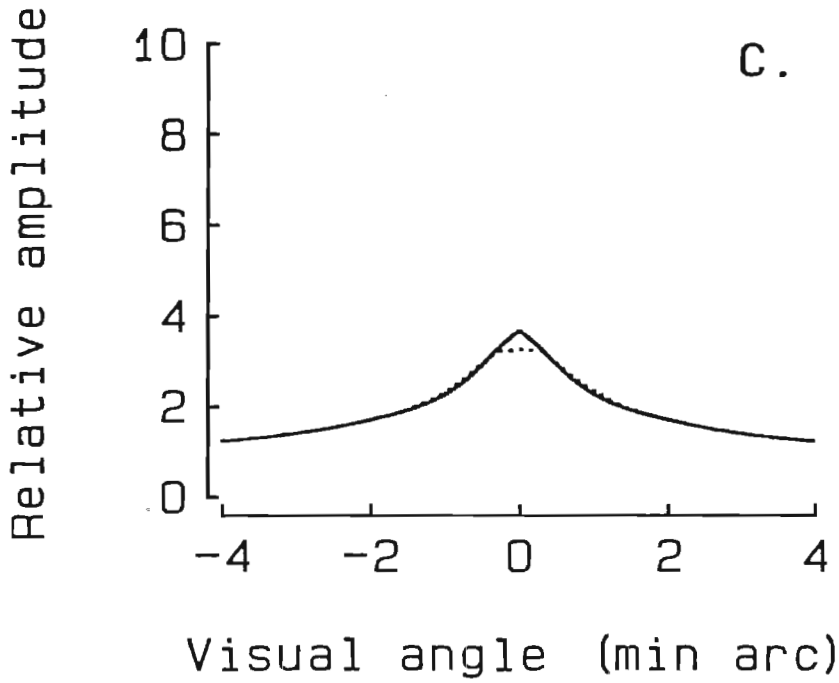
C.
Relative amplitude
10
8
6
4
2
0
-4
-2
0
2
4
Visual angle (min arc)

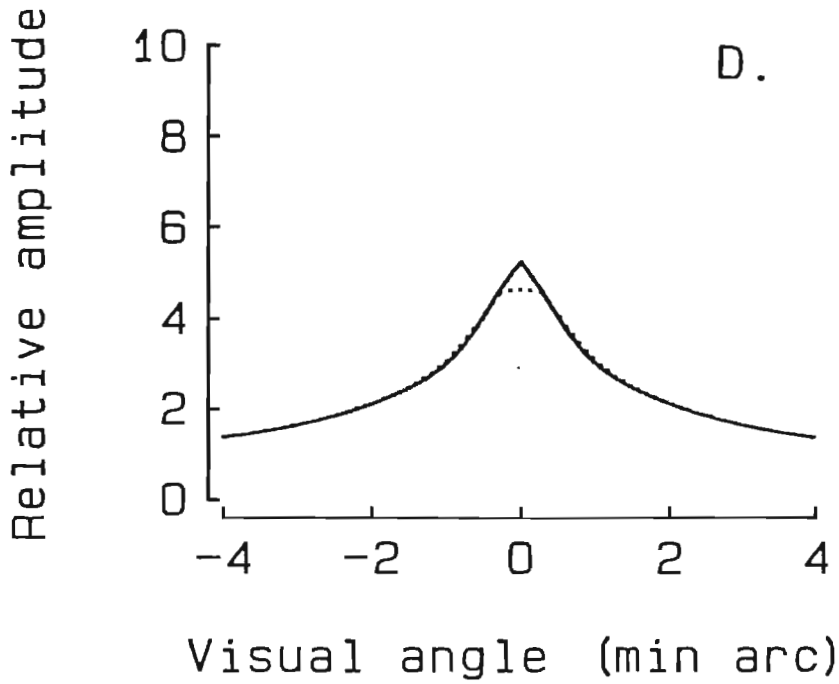
D.
Relative amplitude
10
8
6
4
2
0
-4
-2
0
2
4
Visual angle (min arc)

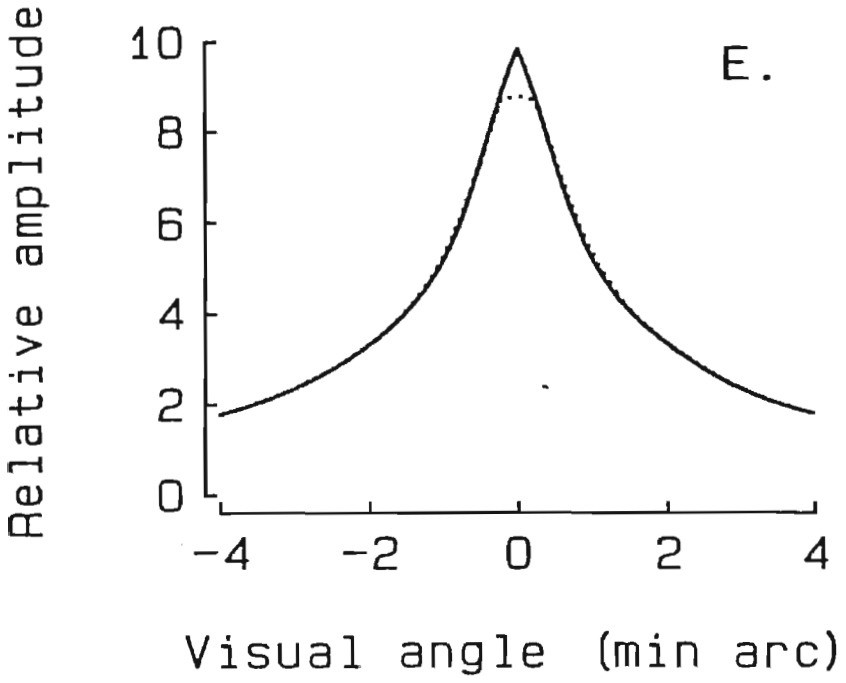
E.
Relative amplitude
10
8
6
4
2
0
-4
-2
0
2
4
Visual angle (min arc)

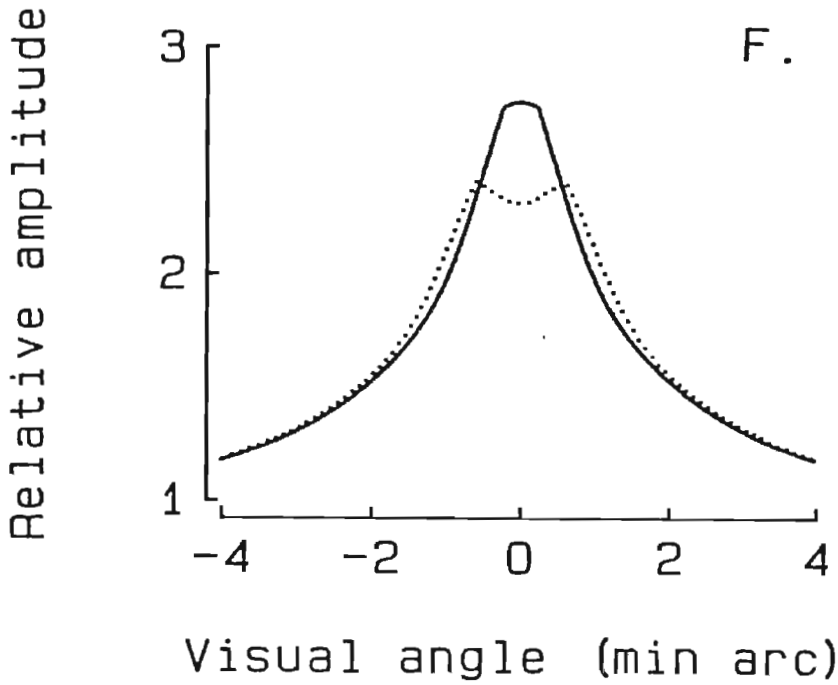
F.
Relative amplitude
3
2
1
-4
-2
0
2
4
Visual angle (min arc)

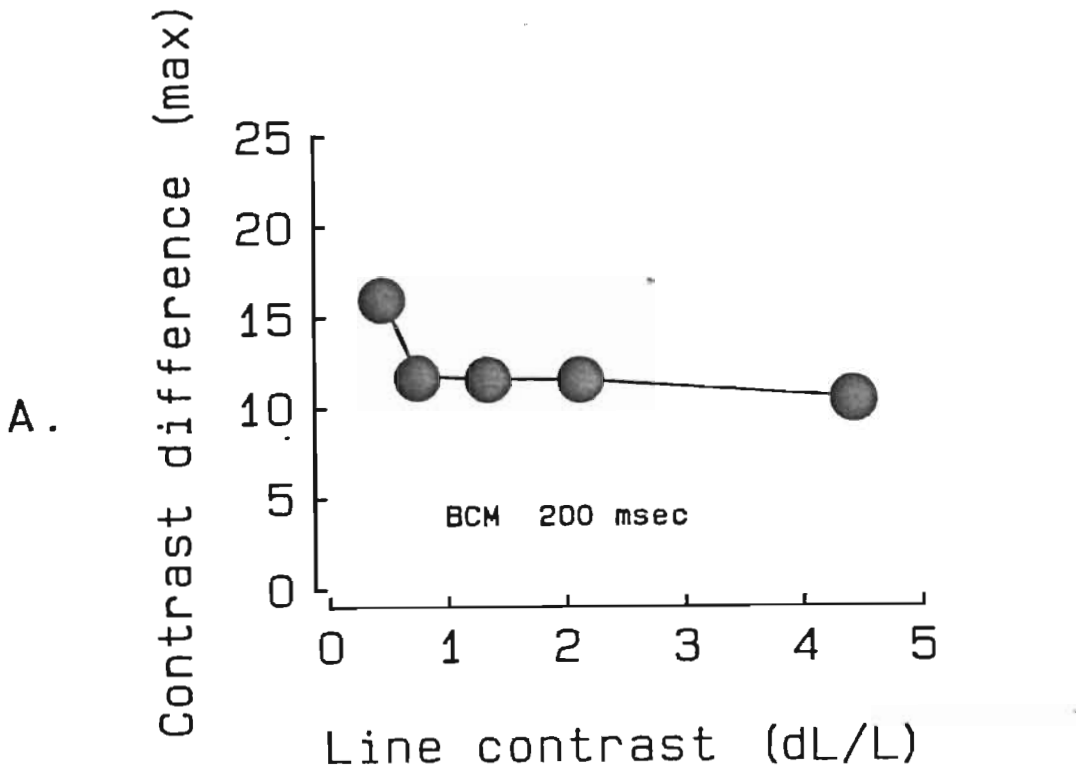

Figure 3.6 Maximum flux change at resolution.

The retinal flux distribution was calculated for two superimposed lines and two line that were just resolvable at each of the five line contrasts. The ratio of the peak flux difference to the peak luminance is nearly constant at 11% for moderate line contrasts; however, at low line contrasts this ratio increases.

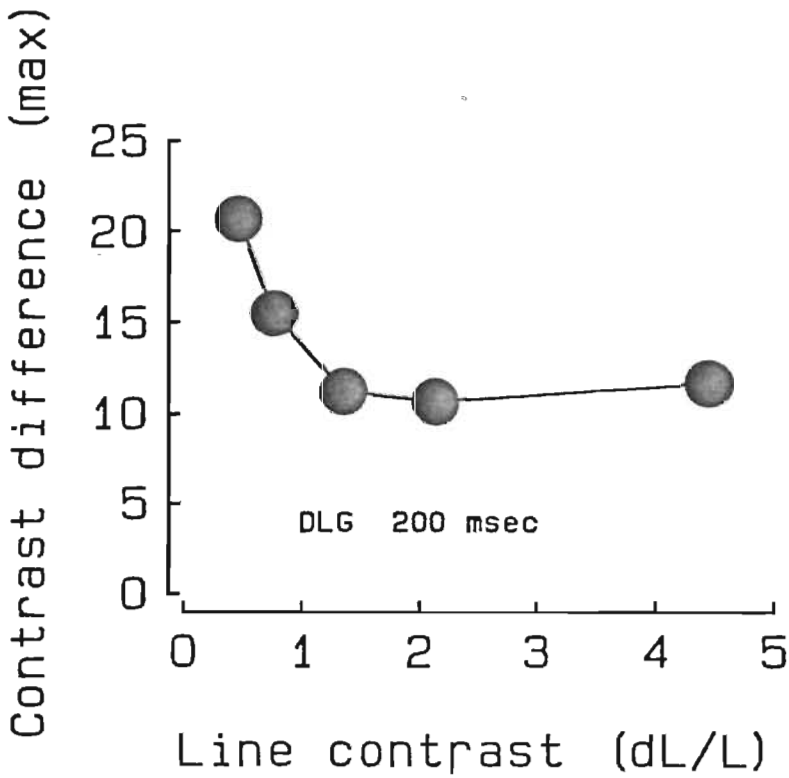
Contrast difference (max)
25
20
15
10
5
0
DLG 200 msec
0
1
2
3
4
5
Line contrast (dL/L)

B.

constant criterion across contrasts and changes in relative resolvability with other resolution targets cast doubt on the brightness discrimination theories of Hartridge and of Hecht and their derivatives.

model

As an alternative to resolution theories that depend on flux differences at a single point or at most between two points, it is proposed here that the same spatially extensive, weighted flux summation that was used to model detection of gratings and lines may be used to establish criteria for minimally separable stimuli. As with detection, the responses of the bandpass spatial filters to resolution stimuli are more easily determined by examining their Fourier spectra. The spectrum modulus of a thin narrow bright line, or for two lines superimposed, has a constant amplitude. The phase spectrum is also constant (90^o). The phase coherence is the only difference between a line and white noise. As two narrow lines are separated the phase coherence relative to a reference midway between them is maintained while the modulus begins to undulate in a cosinusoidal fashion (figure 3.7). The periodicity of modulus oscillation in cycles/cycles/degree is proportional to line separation. The cue to the Observer for separation must be entirely contained in the difference between the flat and sinusoidal moduli. As separation increases from zero, the greatest difference occurs in the filters with the highest center frequency. Unlike detection where filter responses are compared to

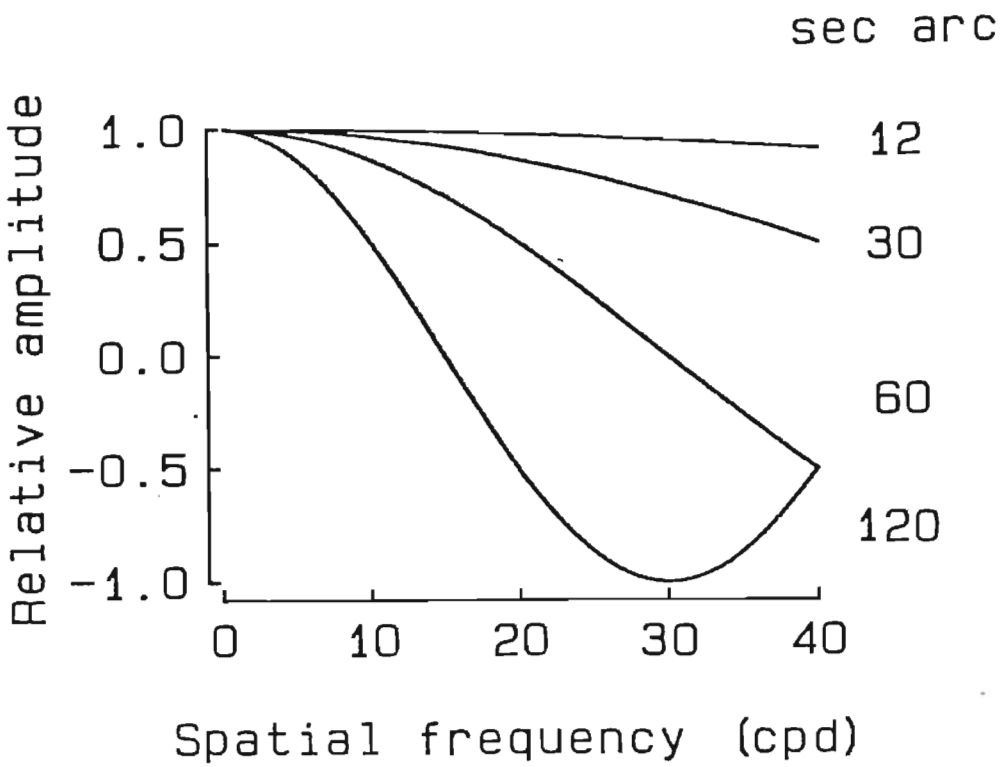

Figure 3.7 Two resolution line spectra.

The spectrum of two bright narrow lines has a sinusoidal amplitude envelope with a period (in cycles per degree) that is inversely proportional to line separation and a phase spectrum that is constant (90°) with respect to the midpoint between the lines.

zero response or to internal noise, resolution tasks generally require the comparison of nonzero driven responses. Before examining the way positional shifts alter the responses of these contrast sensitive mechanisms, it is necessary first to propose a model of the ability of the Observers to discriminate among levels of filter response.

background (contrast discrimination)

In detection paradigms using near threshold contrasts it is commonly assumed that in the initial stage of the spatial filters stimulus contrast is processed linearly. The responses to subthreshold sinewaves are presumed to sum arithmetically with one another and with the internal noise of the filter. The relation between the linear sum and the final filter response, the transducer function, may be nonlinear. Certainly, in the limit, the instantaneous response of the filter cannot follow any arbitrarily large input and, therefore, must be compressive. In the small signal range, however, a different characterization may be appropriate. Nachmias and Sansbury (1974) and Stromeyer and Klein (1975) found that an accelerating transducer function with an exponent slightly greater than two best fit their data. No rationale is given for the source of the small signal nonlinearity. In contrast, Sachs et al. (1971) found that a linear transducer function gave an optimal fit. Nachmias and Sansbury attributed the linear finding to the higher contrasts involved. They proposed that linearity was observed because the operating point was in the transducer region between acceleration and compression. An

alternative explanation which preserved linearity in the small signal regime was proposed by Hamerly (1975). If the output of the linear spatial filter had to pass a threshold, the total response of a collection of filters whose thresholds varied would experience a form of recruitment as stimulus contrast increased. The disproportionate growth in total response with contrast for a population of filters having a distribution of thresholds would be equivalent to a uniformly accelerating transducer function. Because of computational complexity, the effects of parameter variability are seldom included in models. In simplified models, changes in the transfer function are used to accommodate the functional consequences of variability. Of interest here is the manner in which such transducer functions alter the Observers' ability to respond to changes in stimulus contrast. (Further consequences of these simplifications are discussed in chapter 5.)

Contrast discrimination thresholds are determined by the contrast increment that is detectable against a background contrast with a criterion probability. The definition is easily extended to include sinewave detection: detection threshold is the contrast that can be discriminated against the internal noise of the detector. As the background contrast is increased from zero to approximately detection threshold, discrimination thresholds are reduced to less than half that of detection threshold (Campbell and Kulikowski, 1966; Nachmias and Sansbury, 1974; Stromeyer and Klein, 1974; Legge and Foley, 1980). The decrease in detector threshold at low background contrast has been named the pedestal effect (after

Nachmias and Kocher, 1970), wherein the background was thought to add constructively with the increment at low background levels (figure 3.8). Beyond the discrimination minimum, threshold increases monotonically with increases in background contrast. When plotted on log-log coordinates the later portion of this relation may be well fit by a straight line. Estimates of the slope of this line depend on how much of the pedestal region is included in the estimate. However, even taking this source of variability into account, slope estimates obtained from different experiments are discrepant. Several studies have found evidence for a compressive response function (Nachmias and Sansbury, 1974; Tolhurst and Barfield, 1978; Pelli, 1979; Legge, 1979, 1981; Legge and Foley, 1980; Foley and Legge, 1981). In these studies, the discriminable contrast increment did not grow in proportion to background contrast. The exponents were between 0.4 and 0.7, appreciably different from the 1.0 required for Weber's law to hold for contrast discrimination.

On the other hand, several studies have found contrast discrimination to be consistent with Weber's law - an exponent of one (Kulikowski, 1976; Kulikowski and Gorea, 1978; Campbell and Kulikowski, 1966; Bodis-Wollner et al., 1972; Bodis-Wollner et al., 1973; Carlson and Pica, 1979; Burton, 1981). However, even in these studies, there often appeared to be a decrease in the exponents obtained at lower spatial frequencies.

Burton (1981) was able to model much of the sinewave contrast discrimination data, including the pedestal effect and the steepening of the

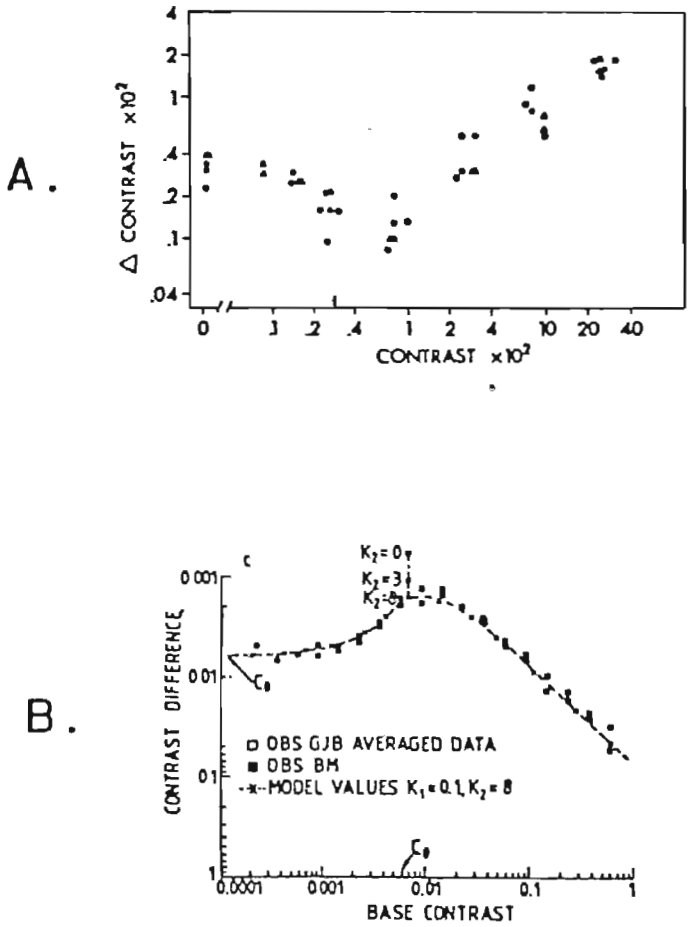

Figure 3.8 Contrast discrimination functions.

The ability to discriminate changes in contrast is as good or better than the ability to detect a sinewave for a considerable range of background contrasts. This exceptional near-threshold contrast discriminability occurs under experimental conditions that produce Weber (a; Nachmias and Sansbury, 1974) or power (b; Burton, 1981) discrimination functions for moderate and high background contrasts.

psychometric function at zero background contrast, by assuming the presence of two uncorrelated noise sources. One of the noise distributions was proposed to be constant for a given detector, varying across detectors in proportion to threshold contrast. The other noise source was proposed to vary in proportion to signal contrast. Within each detector, the noise and signal were linearly summed and the output transformed by a subtractive threshold. An alternate model that would produce the same result would be to pass the signal and constant noise sum through a gain control mechanism and then add in the second (now constant) noise source. The advantage of the second model comes from factoring the system into constant noise distributions and isolating the adaptation mechanism.

There is considerable discrepancy about the conditions necessary to obtain responses consistent with Weber's law (Legge, 1980). Kulikowski and Gorea (1978) maintained that it is necessary and sufficient to adapt completely to the background contrast before proportional discrimination thresholds are obtained. In disagreement with this position are the studies that use 2AFC paradigms with the background present only during the test intervals. This difference is equivalent to the distinction between a Weber's law for instantaneous (compressive) nonlinearities and dynamic (adaptive) nonlinearities. Further complications arise from the possibility of detectors with different spatiotemporal tuning characteristics subserving the different (adaptive vs. temporally coextensive) discrimination thresholds. Similar difficulties have been observed for purely intensive changes (Mansfield, 1976).

model (contrast discrimination)

Sinewave contrast discrimination is modeled here in a qualitative manner. Contrast differences equal to or less than threshold contrast may be discriminated from backgrounds of up to ten times threshold contrast (q.v., figure 3.8). Beyond this region discriminable contrast increases either in proportion to background contrast (Burton, 1981) or obeys a power relation of less than one (Nachmias and Sansbury, 1974). The exact form of the discrimination function is still an open question (Legge, 1980); however, the form of the increase in discriminable contrast has little effect on the qualitative predictions of the model to resolution stimuli and even less to vernier offsets. Optimal offset sensitivity, in large part, depends on the near threshold discrimination properties of the filters.

In CELT, the discrimination process is modeled by a probability summation mechanism that is similar to the one proposed to subserve detection. As in the detection task, the stimulus spectrum is passed through an array of bandpass spatial filters. In each filter, the stimulus spectrum is weighted by the filter and then linearly summed. This sum, the response of the filter, is then raised to the 3.5 power. The filter by filter difference between the exponentiated responses to the criterion stimulus and those to the criterion plus offset is summed across space and phase.

The contribution of filter response differences to the aggregate metric is reduced when the differences are associated with large criterion responses. The proportional reduction of the response differences (Weber region) that are

discriminated against high background levels is applied center frequency by center frequency to vector magnitude sums collected across space and across phase. A single background response level was used to define the knee of the discrimination response curve for all center frequencies. The knee of the discrimination response function is the aggregate response at which the Observer's just discriminable response difference exceeds the response value required at threshold (with no background contrast). Exponentiated response differences below this value are simply added to the vector magnitude sum. The piecewise linear approximation of the Observer's discrimination performance does not contain enhancement at near-threshold backgrounds (the pedestal effect). Above the knee, the differences at each center frequency are attenuated by a factor equal to the ratio of the response to the criterion stimulus and the response level at the knee, all raised to the 3.5 power. The simple ratio corresponds to the Weber fraction with an exponent of one. A knee value of 0.4 produced a good fit to both the resolution and localization data.

The weighted difference of the exponentiated responses is an estimate of the distance between the internal representations of the two stimuli. As reflected in the vector magnitude exponent of 3.5 and the discrimination response function, the internal representation space is nonlinear. The exponentiation was made to precede the differencing operation so that the calculated distance reflects the effective or "perceived" changes in the response profile. Reversal of the sequence would require storage of a response pattern that does not reflect the apparent

magnitude of the response. The differencing operation, although acting on exponentiated and therefore positive response values, preserves sign. The bipolar nature of the linear filter stage allows both positive and negative excursions. Positive and negative excursions are presumed to be differentially labeled. Accordingly, the exponentiated values of responses of opposite signs are summed in the computation of the aggregate measure of interstimulus representational distance.

The attenuated, exponentiated response sum is then reduced by root 3.5 to obtain the aggregate response measure. An aggregate value of one is necessary and sufficient for the response to the stimulus with the offset to be discriminated from the response to the criterion. This is the same constant criterion that was used in CELT for the detection of sinewaves and lines.

Two features of this discrimination model should be noted. First, the combination of responses at all positions across the 4.4 by 2.2° aperture and at all phases is a very conservative simplification. The simplification is necessary because the proper balance among individual filter gain, the number of filter phases and the filter density is uncertain. The simplification is conservative because contrast discrimination undoubtedly can be localized to regions smaller than the entire stimulus aperture. Moreover, filter parameters are conservatively held constant that, in all liklihood vary considerably across space and across spatial frequency. Since the ratio of response difference to criterion response varies considerably with position, it is possible that a large response difference in a

region of small criterion response is attenuated because there are regions of large criterion response elsewhere in the stimulus aperture. Unfortunately, the evidence does not exist that will specify the degree that local discrimination pools vary with spatial frequency or eccentricity. The spatial uniformity of the narrowband stimuli and the restricted extent of the broadband stimuli examined here should reduce the amount of distortion introduced by the simplification. The issue of local discrimination pools will be expanded in later sections.

Second, the difference of exponentiated responses measure of stimulus difference has an implicit assumption about the processing and representation of stimuli. A vector magnitude sum with an exponent greater than one disproportionately emphasizes larger responses in the aggregate measure. It is possible that the emphasis of large responses reflects a response truncation (rectification in a distal filter component) and/or signal to noise limitations. The discrimination of small signals against small backgrounds are more likely to be affected by such distal limitations and the vector magnitude sum may serve as an aggregate surrogate for the limitations in the probability summation model. As with pooling extent, the evidence for local noise levels or rectification thresholds is sparse or nonexistent.

Augmented by these contrast discrimination features, the same probability summation model (CELT) used to simulate the detection results was applied to the two line resolution task. The results not only matched the form of the contrast-

offset interaction, they produced the correct levels of absolute response required for a constant criterion detection/discrimination mechanism (figure 3.9; cf. figure 3.4, a). As before, the filter gain estimates were determined by the contrast sensitivity of Observer BCM.

In order to study the interactions between probability summation and contrast discrimination, filter responses at each center frequency were calculated for the two line stimuli. Both the superimposed lines (criterion) and line pairs at threshold offset were applied to the model at each of the five contrast levels. The spectrum of the superimposed lines produces a peak response near a center frequency of 4 cpd (see figure 2.12). The response profiles may be simply scaled in proportion to stimulus contrast (n.b., these profiles do not contain Weber compression). As the line separation increases the rate of oscillation of the stimulus modulus also increases. Although the stimulus spectrum is flat over the range of human sensitivity, the maximum filter response occurs near 4 cpd. In large part the location of the peak response reflects the profile of the MTF. The individual filter responses to the two line resolution stimuli (figure 3.10) reflect the increasing spectrum oscillation that accompanies larger offsets; however, the changes in the stimulus spectra are small in the region of high contrast sensitivity. For the range of offset thresholds obtained in this task, the largest spectrum differences occur above the highest filter center frequency (32 cpd). At the highest contrast examined, the largest contributions to the aggregate difference measure come from the highest spatial frequencies (figure 3.11, a). Not only are

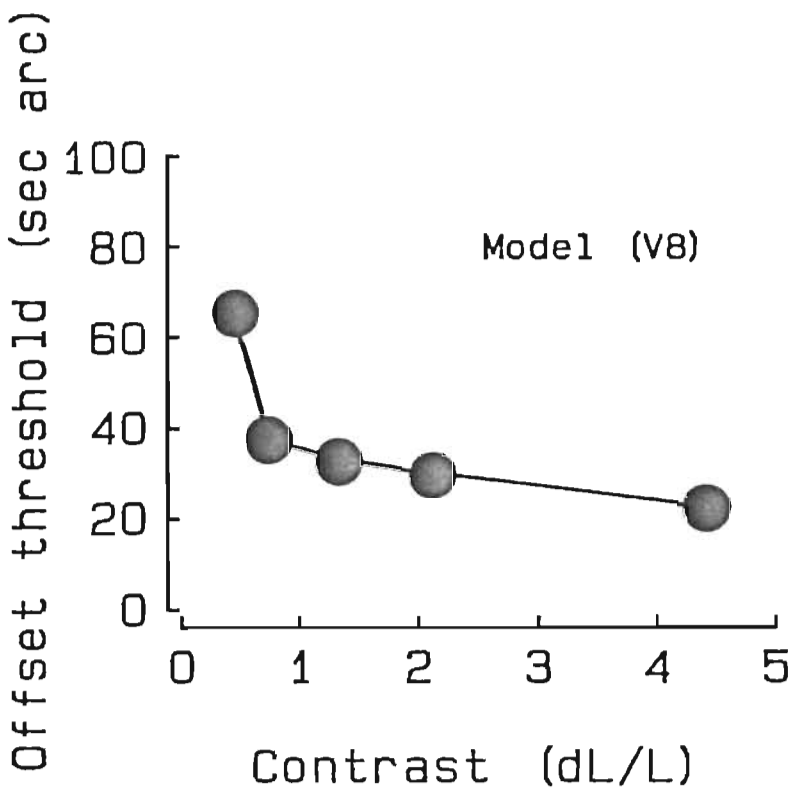

Figure 3.9 Aggregate discrimination responses for two line resolution.

The aggregate responses for a probability summation model of contrast discrimination (CELT) are presented for the threshold offsets required for a range of line contrasts (Observer BCM). The exponent of the Weber fraction is one and the response at the knee of the response discrimination function is 0.4. Any response differences that at compared to a criterion response that is greater than 40% of the aggregate response required for detection or discrimination is reduced by the ratio that the criterion response exceeds the value at the knee.

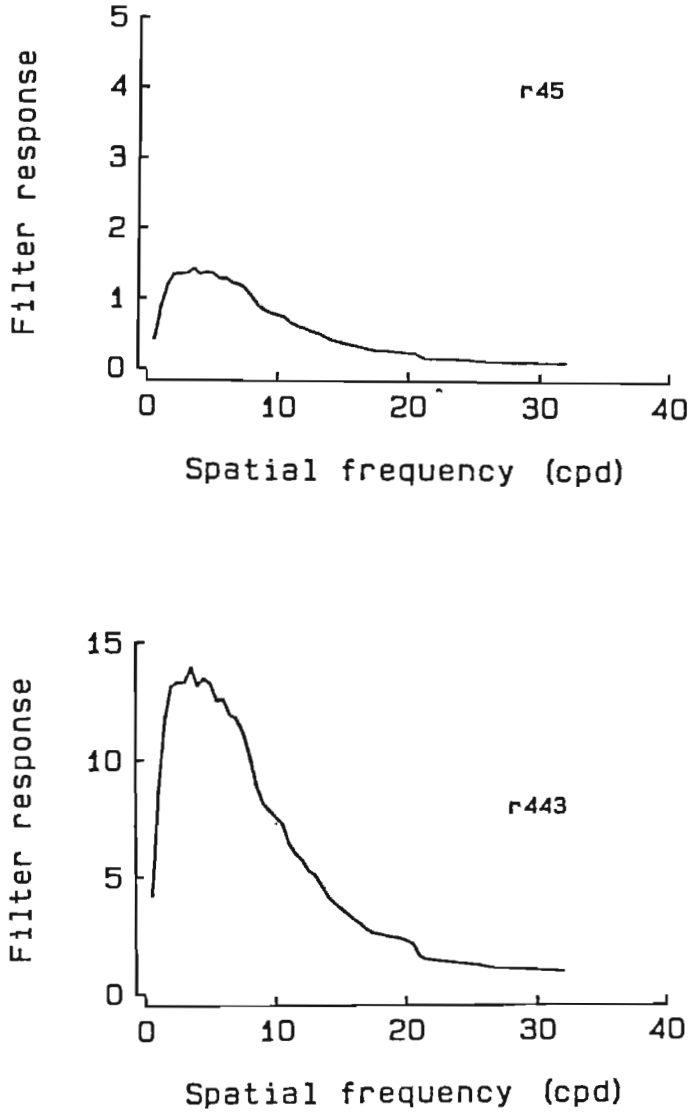

Figure 3.10 Filter responses to two line resolution stimuli at threshold offset.

The aggregate response produced by CELT is subdivided by filter center frequency. The frequency by frequency profile of the resolution stimuli at threshold offset does not differ greatly with contrast (a, 0.45; b, 4.43). The form of the profile changes only slightly with the approximately 3 to 1 change in threshold offset. The major difference is the amplitude of the envelope. The amplitude increases in proportion to stimulus contrast.

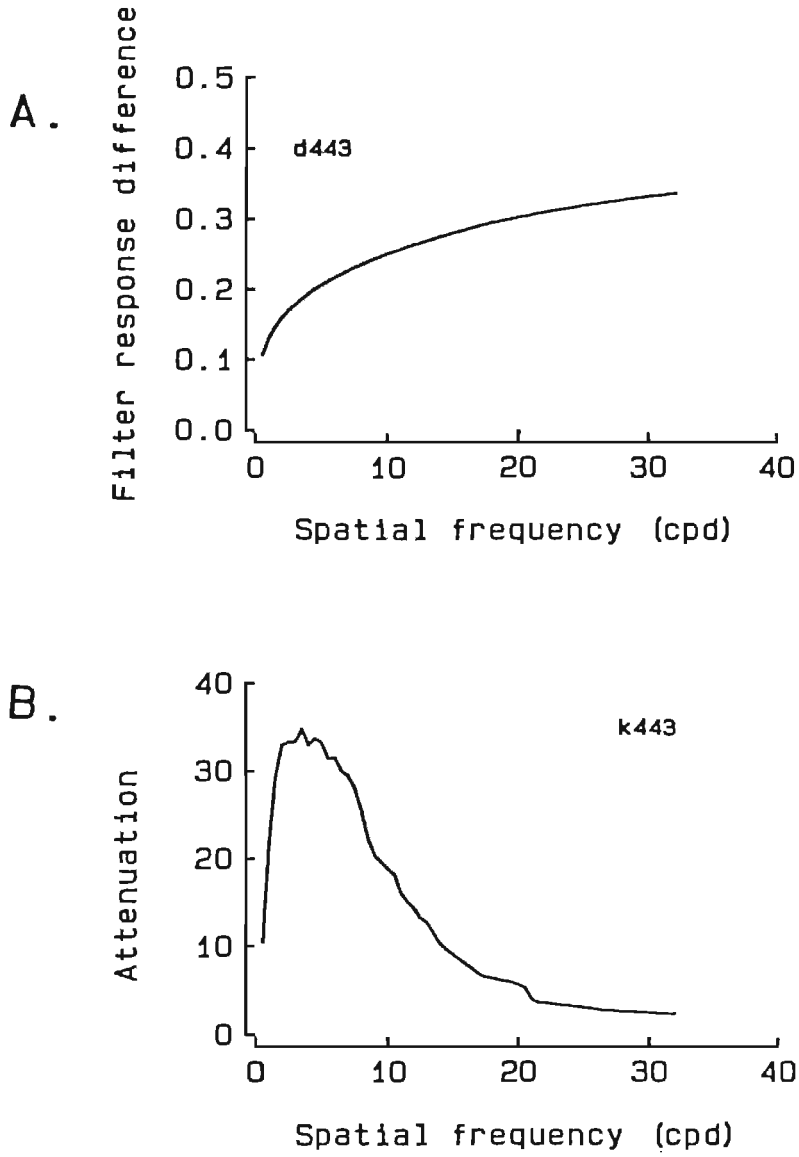

Figure 3.11 Response differences for two line resolution threshold offsets.

The contribution to the aggregate response difference is subdivided by center frequency. At moderate contrast (a, $dL/L=4.43$), the entire range of response differences are compared to criterion responses in the Weber region. The attenuation (b), although much higher in the low frequencies, is above one for all filters. At lower contrast (c, $dL/L=0.45$), only the filters below 14 cpd are in the Weber region; however, the response difference is also less. The trade produces a response difference peak at 14 cpd.

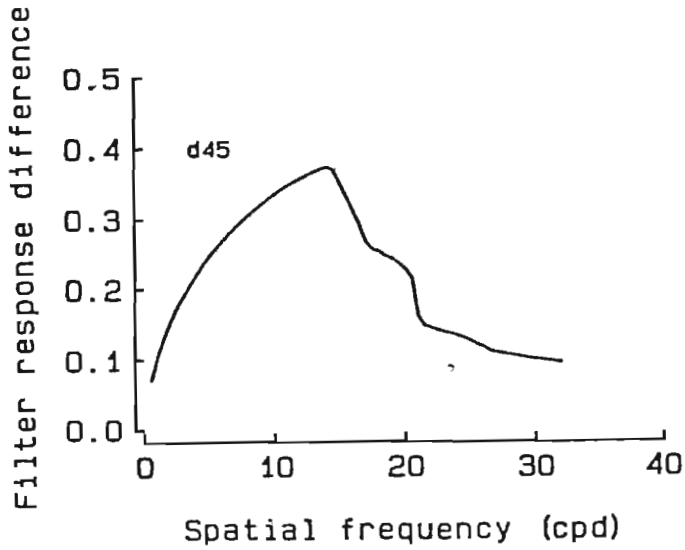
Filter response difference
0.5
0.4
0.3
0.2
0.1
0.0
d45
0
10
20
30
40
Spatial frequency (cpd)

C.

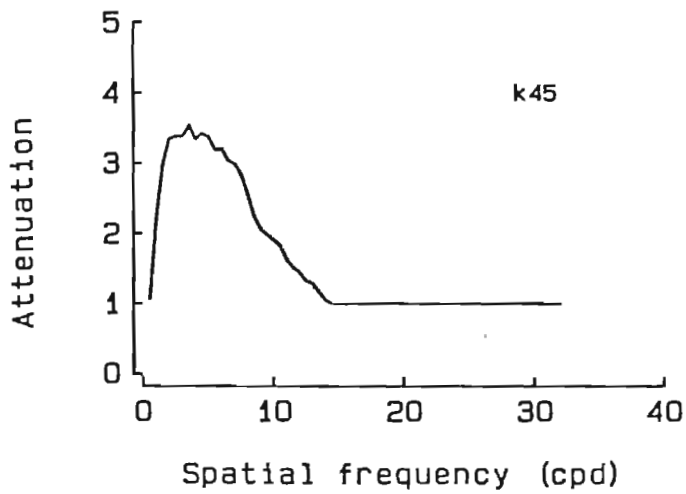
Attenuation
5
4
3
2
1
0
k45
0
10
20
30
40
Spatial frequency (cpd)

D.

the greatest spectrum differences in the high frequency end, but the greatest attenuation is at the low frequencies (figure 3.11, b). At this contrast (dL/L=4.43), all filter responses are in the Weber region. As stimulus contrast is reduced, however, more and more of the high frequency responses to the criterion slip below the knee of the contrast discrimination curve. A trade between the reduced amplitude of the difference response and the reduction in attenuation by the Weber region results in the maximum difference response coinciding with the lowest (most sensitive) center frequency at which threshold sensitivity is maintained (figure 3.11, c and d). At 0.45 contrast (1.6 times single line threshold), the knee is shifted to 14 cpd. This trade also underlies the change across contrasts in the form of the flux distribution at threshold offset (q.v., figure 3.5, f).

summary

Two line resolution at a constant background luminance may be viewed as a contrast discrimination task - a task that, at threshold, does not require the labeling of the position of features but, rather, requires the discrimination of contrast. Obtained thresholds are better fit over a range of line contrasts than either the individual receptor response differences (e.g., Helmholtz) or maximum flux difference models (e.g., Hecht) (cf. the ratio of responses in figure 3.6 and the two line resolution data in table 5.1). Discriminable changes in the separation of two line stimuli occur when the weighted vector magnitude sum of the change in

amplitude of the stimulus spectrum exceeds a criterion amount, a condition that may be met when neither of the local flux-based criteria are above threshold.

Two line interval judgment

theory

In the previous section, contrast detection/discrimination was shown to be a possible mechanism for the enhancement of performance in operationally defined positional resolution tasks. It remains to demonstrate why the enhancement varies so considerably even when the same constituent elements are involved.

Consider the two line interval judgment task. As in the two line resolution task, Observers are required to discriminate the relative position of two lines; however, in the interval judgment task the criterion separation of the two lines is nonzero. At criterion separations of a few minutes of arc, spatial offsets of a few seconds of arc may be resolved (see appendix A). Why are small criterion separations so conducive to the detection of small offsets?

The spectra associated with the two line resolution stimuli diverge increasingly from the flat criterion spectrum at high frequencies (see figure 3.7). At a given contrast level, displacement increases until there is a decrement in activity in the filters in the high frequency range that is sufficiently large to be discriminated. As line contrast increases, the associated increase in the difference amplitude is negated by a decrease in the sensitivity to change (the Weber

fraction).

Now consider the spectrum of two lines at larger separations. As the line separation increases, the period of spectrum oscillation (in cycles per cycle per degree) decreases (figure 3.12). One effect of the increase in oscillation is the occurrence of a spectrum null in the range of filter center frequencies. A spectrum null is characterized by a frequency of zero amplitude in-between adjoining regions of opposite phase. In a linear sum, spectrum amplitudes of opposite sign add algebraically, and cancel. The regions of opposite sign reduce activity induced in filters with center frequencies that are close to the spectrum null. The cancellation is especially great for a subpopulation of filters with both a center frequency near the spectrum null and a position near the midline of the two lines. This subpopulation of filters is able to maintain near threshold sensitivity even when presented with high contrast lines. The optimal position for the nulled response in filters at one center frequency coincides with the position of maximum response in filters at other center frequencies, especially in those filters with sensitivities that span regions of the spectrum with like phase.

A two line stimulus at the selected criterion separation, then, will be represented by a wide range of activity across space and spatial frequency. Some filters will be highly activated, while others will not be stimulated at all. Deviations from the criterion separation will produce changes in the periodicity of the spectrum oscillation. The spectrum of the offset itself may be represented by the difference of two cosines, or equivalently, by the product of two sines:

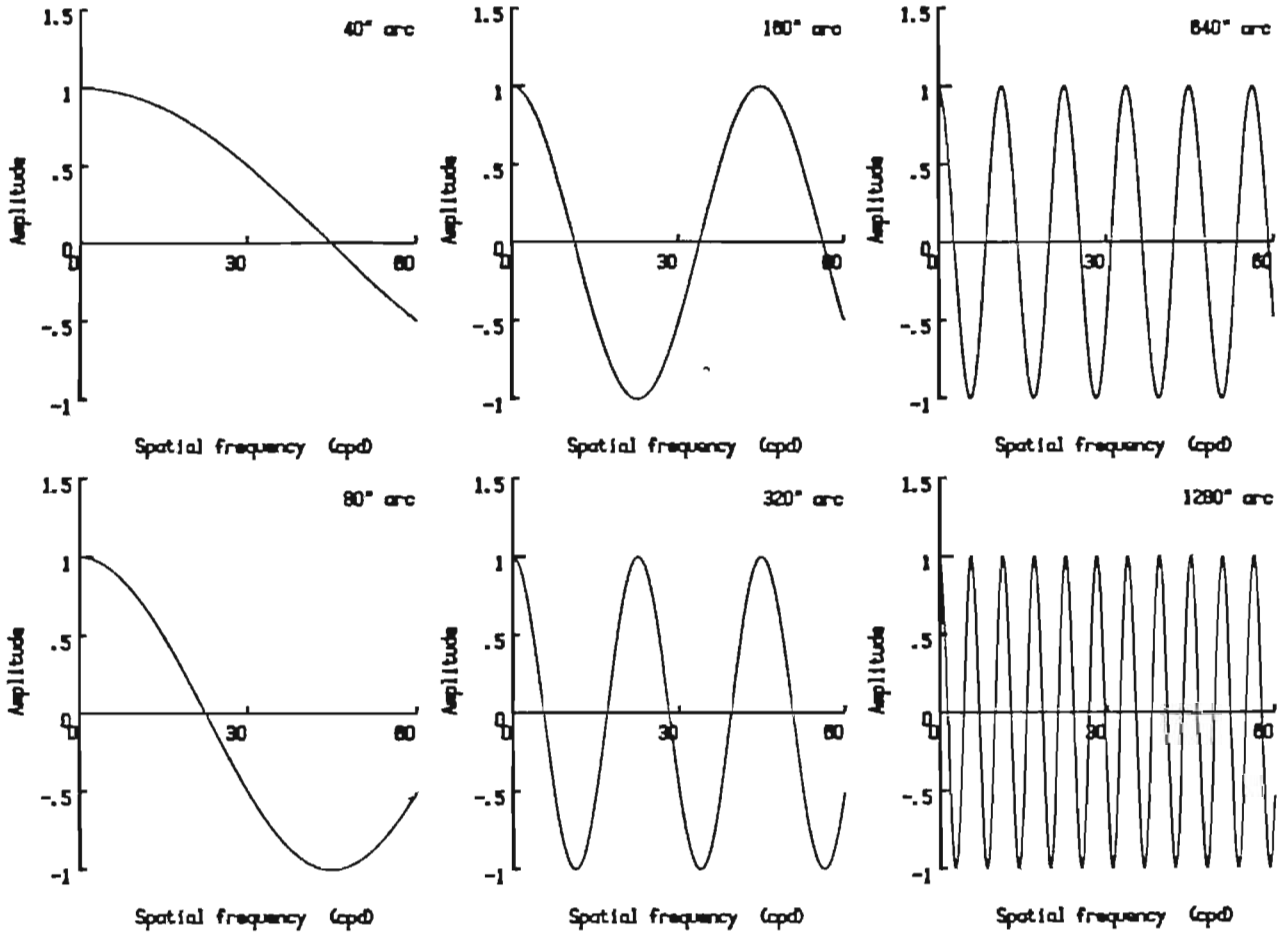

Figure 3.12 Two line localization spectra.

The spectrum oscillation of the two line localization stimuli increases in proportion to the separation. At 40" arc separation, the first spectrum null occurs barely within the range of visual sensitivity. By 320" arc separation, the first spectrum null is close to the peak of visual sensitivity and there are several nulls within the range. With larger separations the rate of oscillation increases rapidly. At these separations, spectrum nulls of opposite slope fall within a single bandwidth.

$$\cos O - \cos C = - \sin \frac{O + C}{2} \sin \frac{O - C}{2}$$

where O is the separation of stimulus with offset
and C is the criterion separation (in radians).

When the offset is small relative to the criterion separation, the period of the offset spectrum, now in sine phase with respect to zero cpd, is close to that of the criterion but amplitude modulated by a sine of much longer period (figure 3.13). There are two important corollaries of this relation. First, since the period of the beat envelope decreases in proportion to the offset while the peak amplitude of the envelope remains constant, the amplitude of the initial portion of the difference spectrum increases in proportion to the magnitude of the offset: and second, the peak of the difference spectrum always occurs near a spectrum null. The net result is that the change in the stimulus spectrum due to a small spatial offset coincides in spatial frequency and phase with that subpopulation of filters least desensitized by the criterion stimulus and induces activity that is proportional to the magnitude of the offset. It is the presence of the spectrum nulls that allows threshold sensitivity to coexist with large amounts of induced activity that is proximal both in space and spatial frequency.

data

Thresholds were obtained for the two line localization task at a separation of 160" arc and a moderate contrast (dL/L=4.43). A 2TAFC procedure with feedback was used under standard conditions (see chapter 2, methods). Observer

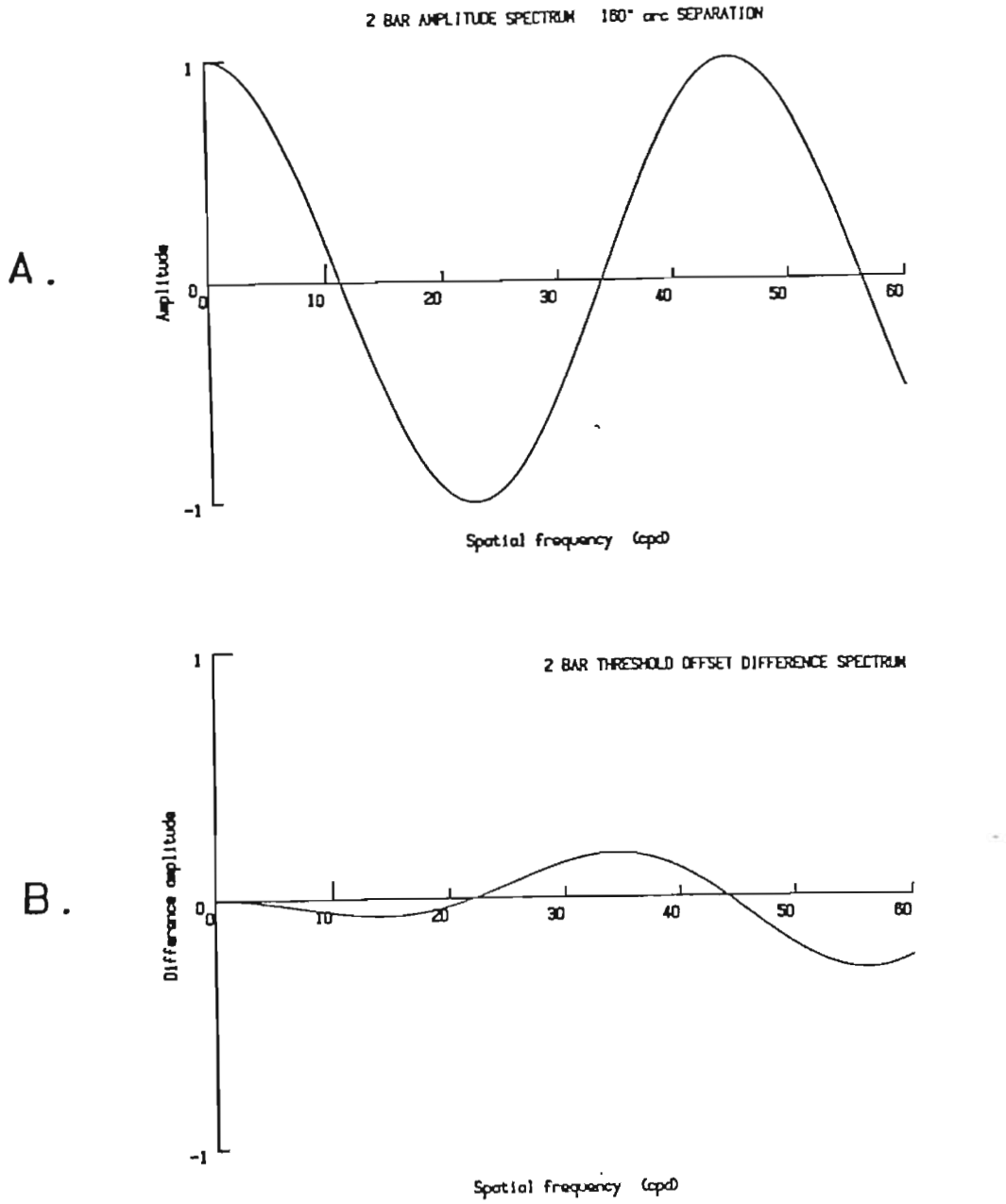

Figure 3.13 Correspondence between two line criterion and difference spectra.

The change in the amplitude spectrum due to small displacements of the lines is itself periodic at a rate close to that of the criterion. The oscillation of the difference spectrum, however, is advanced in phase relative to the criterion oscillation by 90°. As a consequence, the maximum difference amplitudes occur at frequencies close to the spectrum nulls. The sign of the spectrum difference alternates with successive nulls.

BCM had a threshold of 13.4" arc (±3.9" arc). When the 160" arc criterion stimulus was applied to CELT with the same discrimination parameters used to model the two line resolution task, an offset of 12.7" arc elicited a just discriminable response. The profile of the modeled filter responses peaks in the low frequencies near 2 cpd and declines rapidly with increasing spatial frequency (figure 3.14, a). Although the entire range of filters is in the Weber region, the peak of the difference response is near 13 cpd (figure 3.14, c). This measure of the peak of the modeled difference response is close to the lowest spectrum null for 160" arc separation, 11.25 cpd. The peak difference is apparent even though a conservative measure of response compression is used, one that includes filter responses from all six phases and the entire aperture in the computation of background response. A more local discrimination response measure could take advantage of the coincidence of larger differences and smaller backgrounds in an optimal subpopulation. Together with a smaller response value for the knee, the local measure would eliminate much of the high frequency contribution to the difference response.

Any attempt to cluster optimal subsets of filter response without independent evidence of their existence would degenerate rapidly into a form of filter phrenology, an exercise in the use of excessive degrees of freedom. Although the conservative approach of applying compression according to the total response at each filter center frequency will be used throughout this dissertation, it is illustrative to probe the pattern of responses to see what benefit might be gained

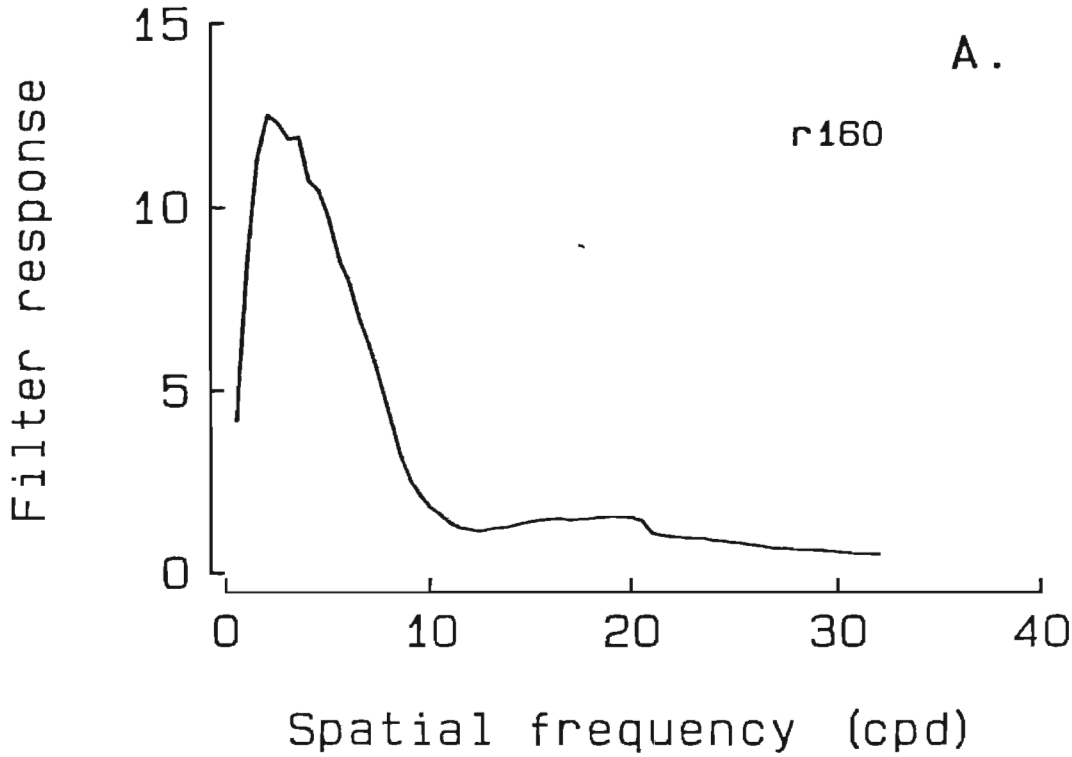

Figure 3.14 Model responses for two line localization.

For two lines of moderate contrast (dL/L = 4.43) at 160" arc separation the filter response profile, subdivided according to center frequency, peaks in the low frequencies and declines rapidly. At this contrast, however, all filters are in the Weber region. Attenuation is proportional to the criterion response for all center frequencies. The peak of the difference response occurs near 13 cpd, just above the first spectrum null.

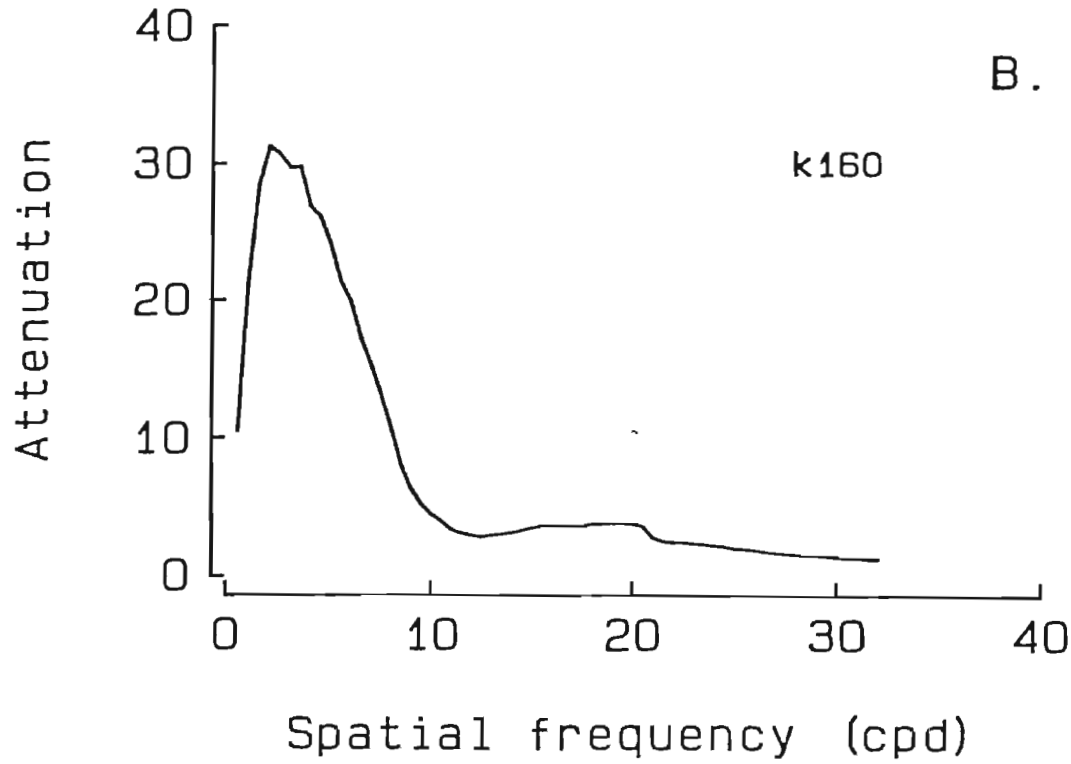
B.
k160
Attenuation
40
30
20
10
0
0
10
20
30
40
Spatial frequency (cpd)

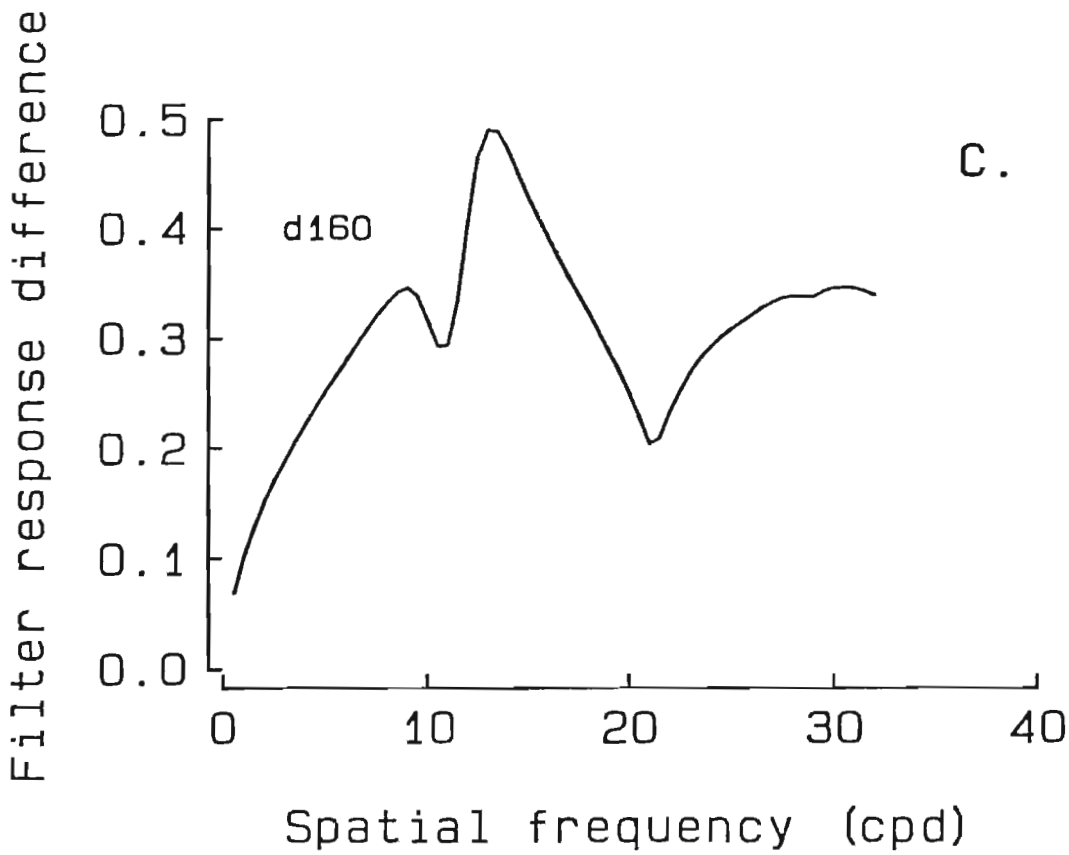
C.
d160
Filter response difference
0.5
0.4
0.3
0.2
0.1
0.0
0
10
20
30
40
Spatial frequency (cpd)

should data on filter clustering (e.g., attentional focusing) become available. For the two line localization task (160" arc separation) described above, the aggregate response of the subset of filters with center frequencies ±1 cpd of the optimal, with a cosine phase spectrum and located on the vertical axis of symmetry of the stimulus is 52% as large as the aggregate response of the entire population. Even this calculation is conservative since the Weber compression used was based on the response of the entire population of filters, not just the subset located on the midline. If the subset is expanded to include all cosine phase filters located on the midline, the relative aggregate response increases to 72%. Inclusion of all filters located on the midline (all phase spectra) ups the relative aggregate response even further (92%). It is apparent from this exercise that the response changes in the filters responsible for the brightness of the center interval alone are sufficient to support discrimination.

The preceding analysis establishes the ability of contrast detection/discrimination mechanisms to enhance performance estimates in both resolution and localization tasks while maintaining a constant decision criterion. The problem of explaining localization, however, is twofold. Practically any interpolation scheme could do as well as the contrast mechanisms in resolving small offsets with a fixed criterion. It is much more difficult to find a mechanism that matches the variation in the Observer's threshold with changes in stimulus parameters. One spatial interaction observed in the interval judgment tasks is a

strong relation between offset threshold and criterion separation (Westheimer and McKee, 1977c). Optimal offset thresholds are reported in the literature for criterion separations of 2 to 6' arc. To establish critical criterion interval commensurate with the conditions used here, thresholds were obtained for two octaves above and below the 160" arc separation already described. The pattern of interaction between offset threshold and criterion separation does indeed replicate the U-shape reported in the literature, with a minimum around 2' arc (figure 3.15). With the same parameters as used in the detection and two line resolution simulations, the stimuli were applied to the model. The fit was quite good, both in form and in absolute value of the criterion. In addition, the peak of the response difference occurred at spatial frequencies that occur near the first spectrum null.

The pattern of filter responses in the model suggests that the U-shaped function is a result of a trade between the effects of filter sensitivity and filter bandwidth as well as changes in the difference spectra with criterion separation. As criterion separation increases from zero (with the two line resolution task as the limiting case), the first spectrum null occurs at lower and lower spatial frequencies. As the spatial frequency of the spectrum null decreases, the attenuation by the OTF decreases and the sensitivity of the filters centered near the null increase. The enhanced detectability of offsets with increasing separation continues until two spectrum nulls occur within the bandwidth of the optimal filters. The changes in response associated with successive spectrum nulls are opposite in sign.

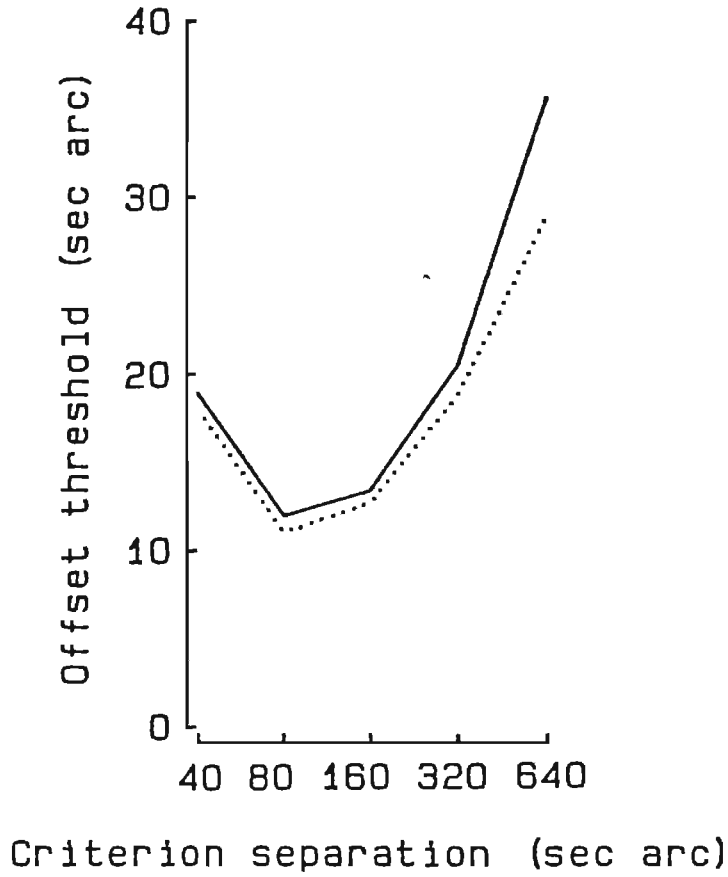

Figure 3.15 Two line critical interval: observed and modeled thresholds.

As reported by Westheimer and McKee (1977c) and replicated here (solid line), detection of offset for two lines is optimal at criterion separations of a few minutes arc. The responses of the model (dotted line) follow the same U-shaped pattern and have very nearly the same absolute values.

Therefore, the response difference is reduced by algebraic cancellation at the linear summation stage of the filters. (The analysis of critical intervals is continued in chapter 5 where it is extended to the two-dimensional case.)

Three line interval judgment

theory

Although it conveys as much information as the amplitude spectrum, the phase spectrum is often neglected in models and descriptions of spatial vision. Phase is of special importance here since translations in space may be produced solely be changes in the phase spectrum. In CELT, phase is incorporated by six filter spectra, all flat, at 30° increments, at each filter position. In the two line interval judgment task both the criterion and the offset spectra were in constant cosine phase with respect to a phase reference at the center of the stimulus. Although phase as well as position were combined in the calculation of responses at a given filter center frequency, it is still possible that the model is not robust enough to simulate Observer sensitivity when criterion and offset phase are disparate. To test this possibility measurements were obtained for the three line interval judgment (bisection) task. The Observer was required to decide whether or not the right-hand interval was smaller or larger than the left-hand (criterion) interval. As in the two line case, the criterion spectrum is cosinusoidal with a constant 90° phase term (figure 3.16, a); however, the oscillation of the spectrum

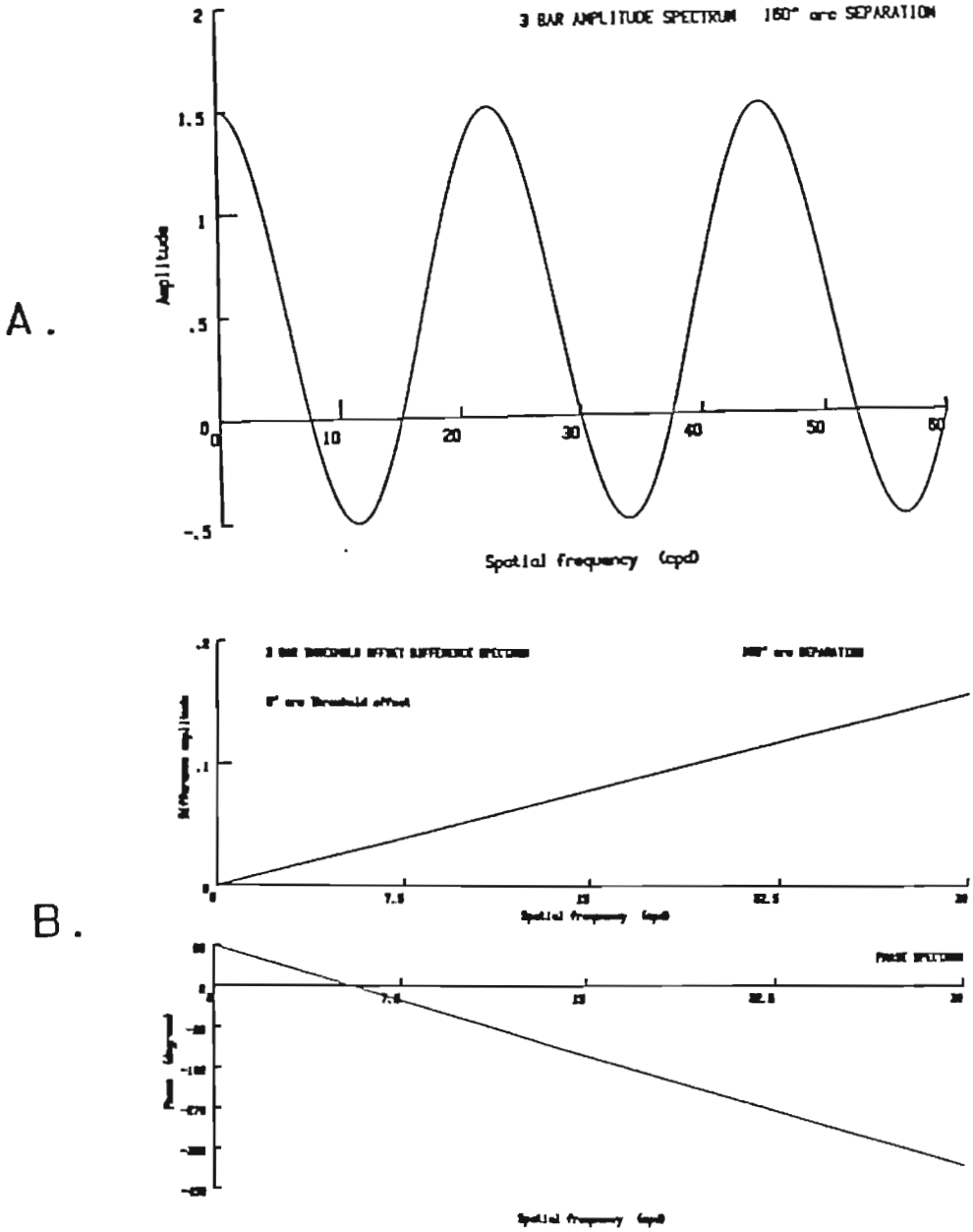

Figure 3.16 Correspondence of three line criterion and offset spectra.

The spatial frequency amplitude envelope of three equally spaced lines oscillates in proportion to the separation of the outer lines (a). The envelope is displaced above the spatial frequency axis by the addition of the flat spectrum of the center line. Relative to the center line, the phase spectrum of the criterion is at 90° at all frequencies. Displacement of the right-hand line causes a change in the amplitude spectrum that has a sinusoidal envelope and a period (in cycles per cycle per degree) that is equal to half the offset. The phase term of the offset is linear with a slope that is proportional to half the sum of the offset and criterion separation (b).

envelope is raised an amount equal to one half the oscillation amplitude. The amplitude spectrum may be factored into an oscillation determined by the separation of the outside lines and a vertical shift due to the center line. Although the rate of oscillation is determined by the separation of the outer lines, the criterion separation is defined by convention to be the width of the interline interval. Also as in the two line case, a displacement of the right-hand line changes the period of the spectrum oscillation. The amplitude of the offset spectrum is sinusoidal with a period equal to one half the offset (measured in cycles per cycle per degree). The important difference is that the offset induces a phase change (figure 3.16, b). The linear phase term has a slope that is proportional to one half the sum of the offset and the criterion separation of the outer lines. The shifting phase associated with the offset will serve as a probe to assess the ability of the model to adequately process phase changes.

data

Observer responses for criterion intervals between 40 and 640" arc produced threshold offsets that followed the characteristic U-shaped critical interval curve (figure 3.17). When the same stimulus parameters were used as input to the model, the responses that correspond to a constant decision criterion closely match the obtained data. With a caveat that the results are based on the compression of responses over six discrete filter phases as well as over space, phase change appears to be well handled by CELT. The is no reason to believe that this performance

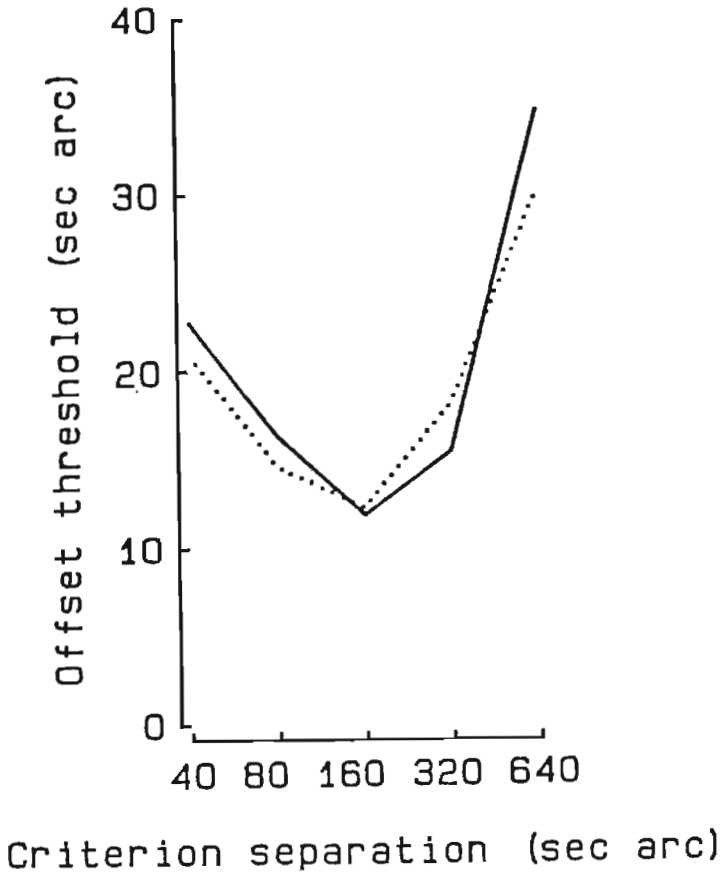

Figure 3.17 Three line critical interval: observer and model data.

As with the two line stimuli, the three line interval judgment task elicits the lowest thresholds for intermediate separations (solid line). The model was able to reproduce both the form and absolute sensitivity of the critical interval even though the offset spectrum changes markedly in phase (dotted line).

won't be maintained for local discrimination pools as well. There is no evidence to support a separate labeling of detectors as to phase and so none will be incorporated.

Four line interval judgment

theory

The equation of the separation of four lines is an example of a localization task that is self-evident. The criterion interval is present during every trial. In this task Observers are required to detect an increment or decrement in the width in the middle of three intervals. The adjoining intervals are maintained at a criterion separation. The four line stimulus was selected for analysis because the complex amplitude spectra (see figure 2.16) provide a more critical test of the model than the simple harmonic oscillations of the two and three line patterns. Additional insights may be gained into the way localization judgments are made from a functional factoring that is possible with the four line stimulus. The amplitude envelope of four equally spaced lines may be decomposed into the product of two cosines (figure 3.18). The cosine envelope with the longer period oscillates in proportion the the criterion separation. The other cosine oscillates in proportion to the separation of the midlines of the outer intervals. They may be functionally described as form and position spectra, respectively. Of special interest is the property that offset causes changes in amplitude only about spectrum nulls

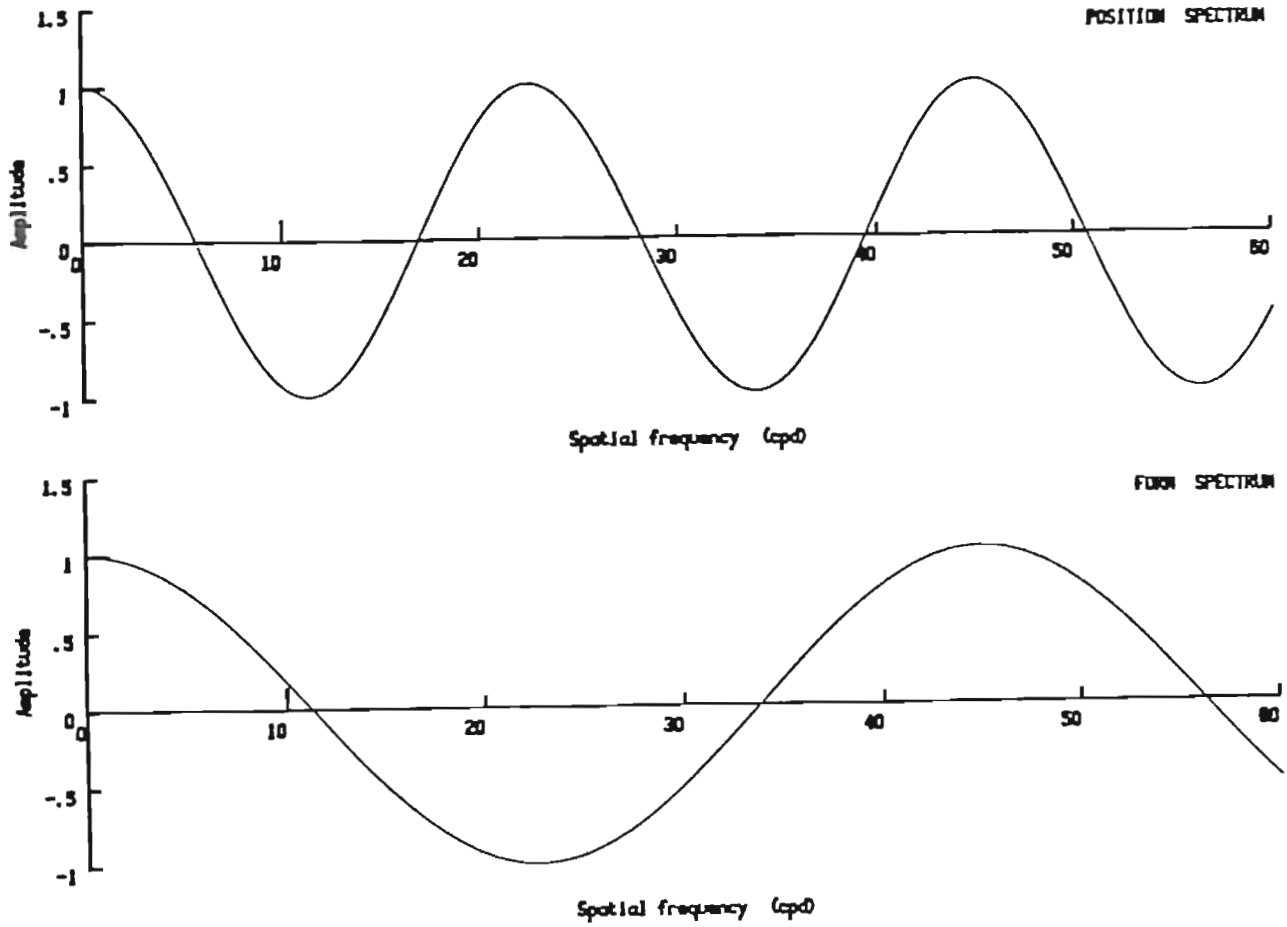

Figure 3.18 A decomposition of the four line spectrum.

The criterion four line amplitude spectrum may be represented by the product of two cosines, one twice the frequency of the other. When an offset is added to the center interval change occurs only the cosine with the greater periodicity, the one related to the relative position of the left and right line pairs. This example is for 160" arc criterion separation.

associated with the position spectrum (figure 3.19). Negligible amplitude change occurs near spectrum nulls associated with form.

data

The patterns of threshold offsets for the two Observers were very similar (figure 3.20, a and b). Optimal separations were obtained at the highest line contrast and at a medium separation. The thresholds increase rapidly as the criterion separation decreases, and more slowly as it increases. As line contrast decreases, the optimal criterion separation shifts toward smaller values. Of interest to the relation among absolute position, resolution and localization is the finding that even at 640" arc separation the offset thresholds for clearly visible lines are disparate across contrasts and have larger threshold offsets than for two line resolution at comparable contrasts. This divergence lends support to the presence of an additional mechanism that supplements labeled position. In addition, the tuned nature of the curves can be attributed to the interaction of the sinusoidal stimulus spectra and the sensitivity of the bandpass filters that integrate these amplitudes. As in the two line resolution task, the stimulus spectra oscillate more rapidly as the separation increases. The difference between the stimuli with offsets and the criteria get proportionately larger at lower spatial frequencies, a region of greater sensitivity. The increase in sensitivity in the region of greatest response difference decreases the required offset for detection until the oscillations in the response difference contain amplitude components of the opposite sign within a

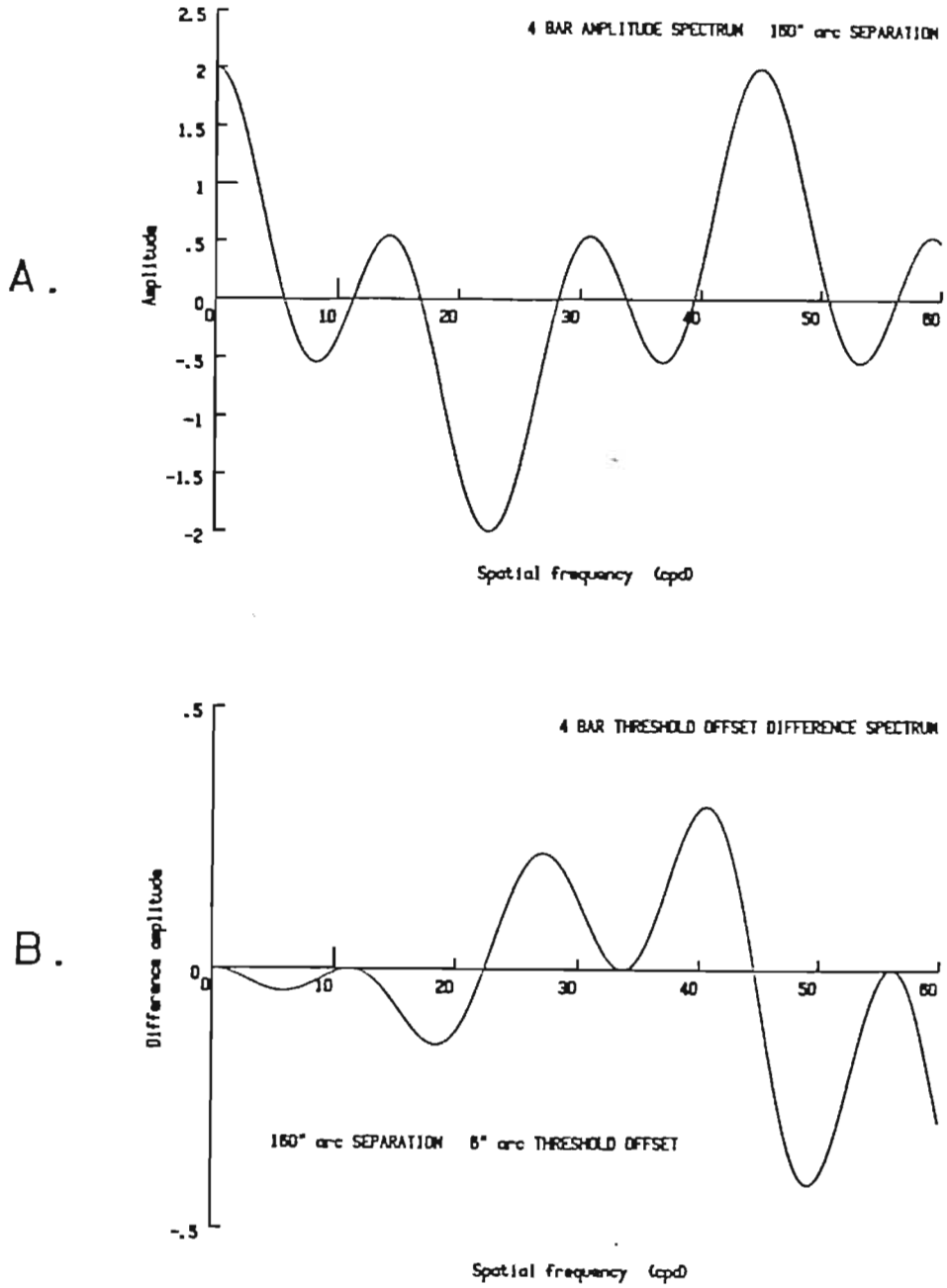

Figure 3.19 Correspondence of four line criterion and offset spectra.

The spectrum nulls of the four bar spectrum follow a complex pattern of alternation. The nulls associated with the form change correspond to zeros in the difference spectra. Nulls associated with position occur in pairs of like sign and correspond with peaks of like sign in the difference spectra.

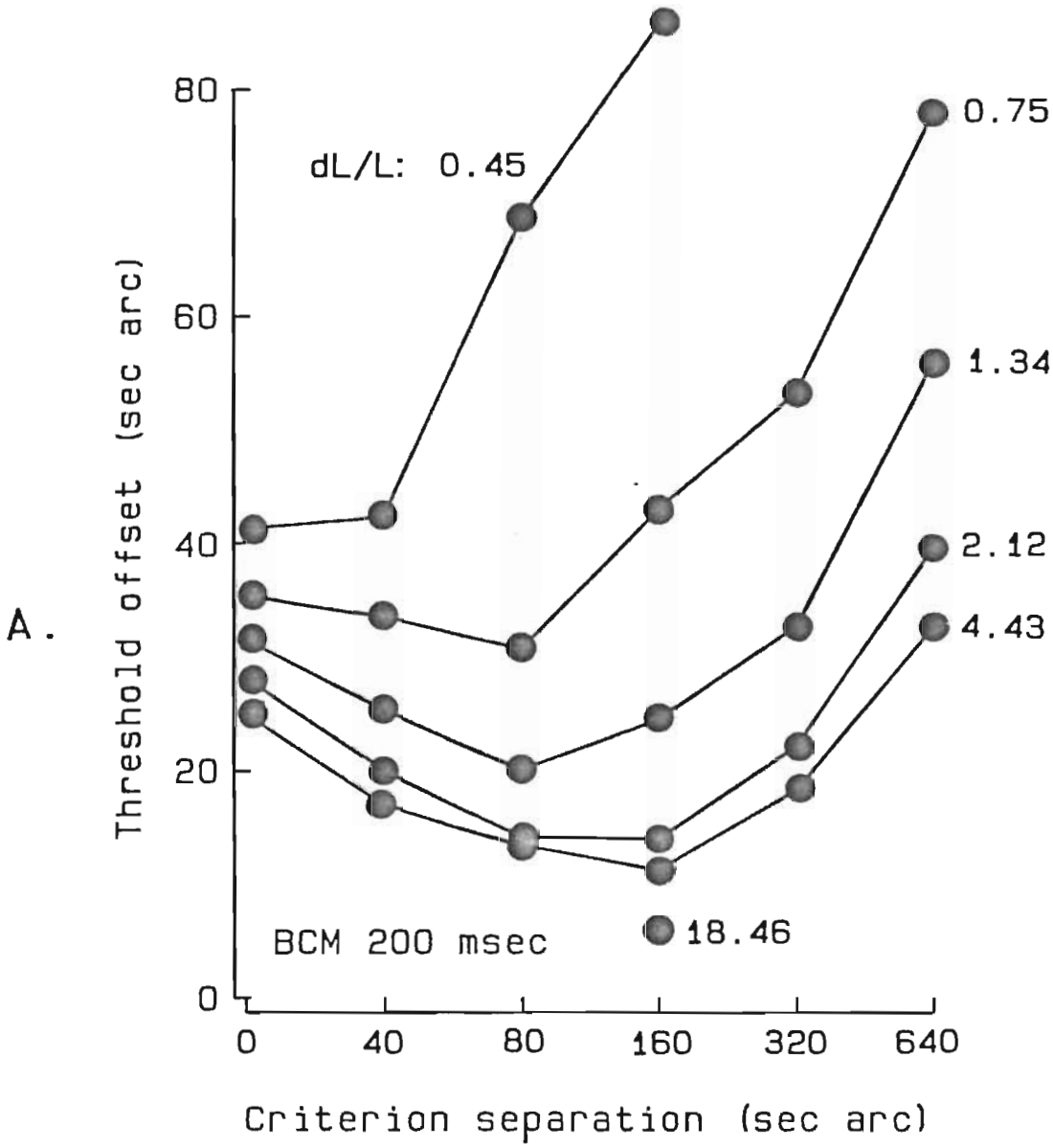

Figure 3.20 Variation of 4 line offset threshold with criterion separation and contrast.

The interaction of criterion separation and contrast on offset threshold was investigated using a 2TAFC procedure with feedback. For both Observers offset threshold increased with decreasing contrast at all separations. The rate of increase varied across separations, however, causing the optimal separation to shift toward smaller separations at lower contrasts.

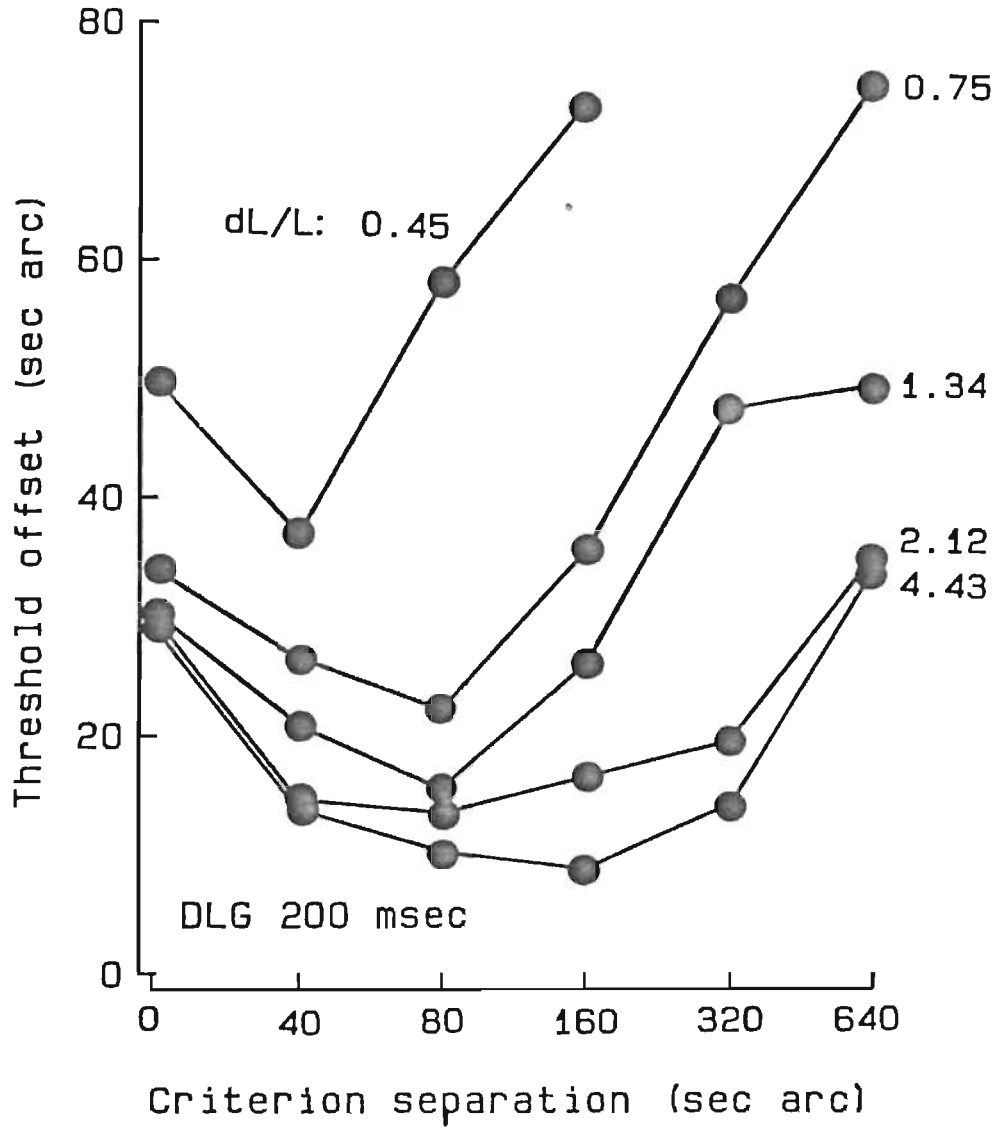
80
60
40
20
0
Threshold offset (sec arc)
dL/L: 0.45
0.75
1.34
2.12
4.43
DLG 200 msec
0
40
80
160
320
640
Criterion separation (sec arc)

B.

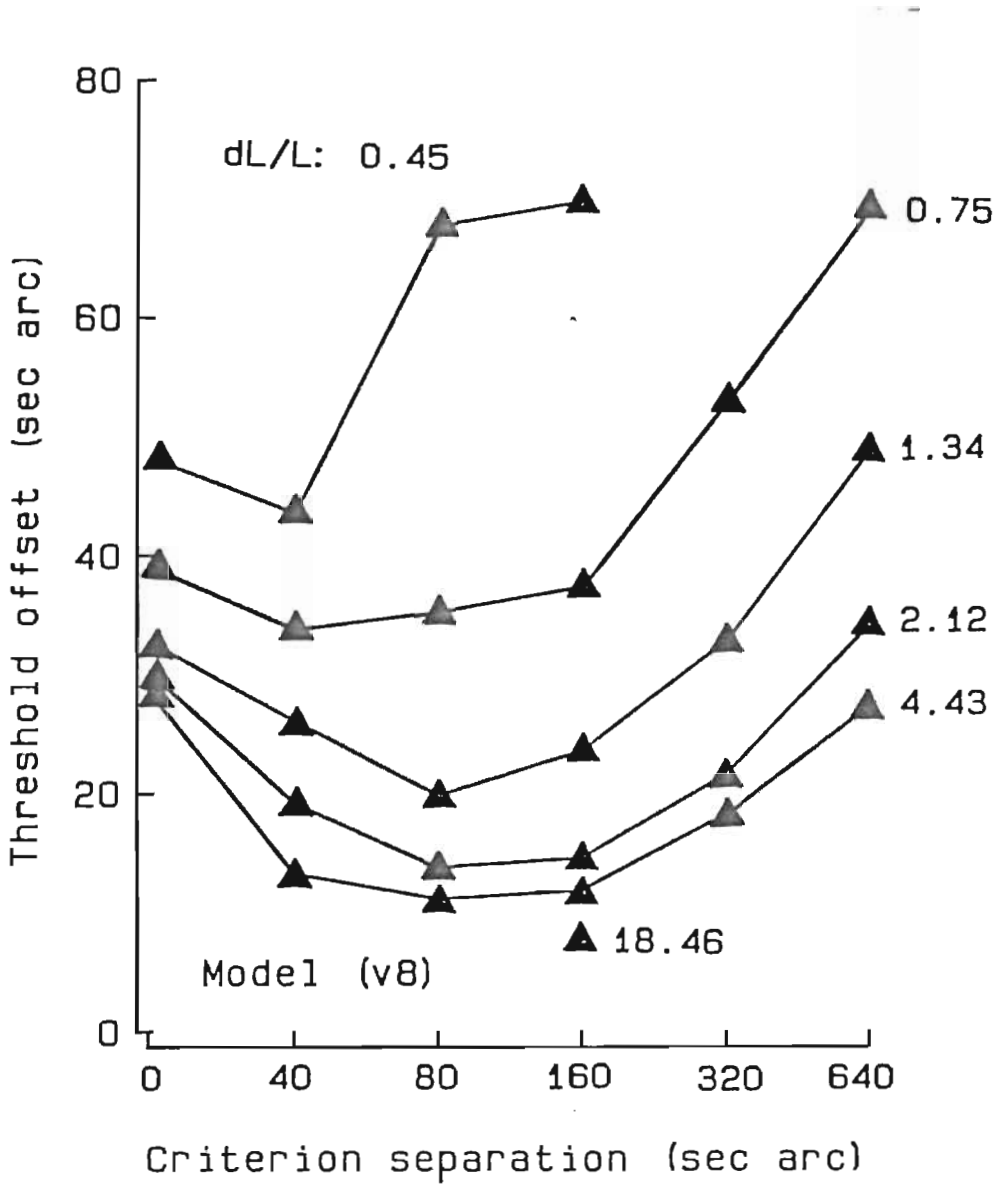
80
60
40
20
0
Threshold offset (sec arc)
dL/L: 0.45
0.75
1.34
2.12
4.43
18.46
Model (v8)
0
40
80
160
320
640
Criterion separation (sec arc)

C.

single bandwidth, a limitation caused by the lower bound on filter center frequencies. Algebraic cancellation occurs within a single filter reducing the net response to the offset. In addition, the integrated difference spectrum at the first spectrum null decreases with increasing criterion separation. The latter influence is reflected in the slower increase in threshold at larger criterion separations. (This analysis is expanded in chapter 5).

summary

Localization is found to be an extension of the same process that aids resolution: a supplementation of absolute position labeling by mechanisms sensitive to contrast. The order of magnitude improvement in resolution over absolute position is derived from the intensive nature of the contrast discrimination response. The order of magnitude improvement that localization has over resolution is derived from the location of spectrum nulls in the stimulus spectra; the difference spectra have peaks in amplitude in regions of greater filter sensitivity. Consequently, smaller offsets are necessary to reach contrast detection/discrimination threshold.

Chapter 4

AN OFFSET BY ANOTHER NAME

The preceding chapters contain a unified framework for spatial acuity. In this system, the position of objects in the visual field can be localized and labeled at best to within a few minutes of arc. Measures of spatial acuity finer than this mosaic of perceived position are based on discriminable changes in the response of bandpass spatial filters. Although these filters underlie the apprehension of spatial contrast and form, there is no reason to believe that the visual system creates a fine positional metric based on changes in the responses of these filters that is separable from a particular stimulus configuration. Fine resolution and localization are a consequence of an operational definition of position that, in itself, does not have a uniform perceptual correlate. The failure over the last one hundred years to find a metric that is consistent with both the fine resolution and the many spatial interactions, especially in localization, stems from the nonexistence of such a perceptual correlate.

Sinewave masks

If this framework is correct it should be possible, therefore, to interfere with the detection of small offsets by raising the background activity in those filters

most affected by the changes in the frequency spectrum due to offset. The masking effect of spatial offsets by sinewaves of the appropriate spatial frequency and phase in comparison to the masking effect by other sinewaves would provide a critical test of the theory. A series of pilot experiments were run on Observer BCM to test the effect of sinewave masks on the four line interval judgment task. The four line stimulus was selected because both the criterion spectrum and the spectra for the stimuli with offsets have the same phase. Consequently, fewer assumptions were required in the selection of optimal sinewave masks. In addition, the stimuli were self-evident. Stimulus parameters were selected to correspond to the optimal conditions found in the contrast and critical separation study. The lines were moderately bright ($dL/L=4.43$, on the display) and the criterion separation was 160" arc. A 2TAFC procedure with feedback was used under standard viewing conditions (see chapter 2, methods). Sinewave masks with modulations that ranged up to 18 times threshold contrast were superimposed on both the criterion and offset stimuli. One mask was used per session. Among the masks tested were some whose spatial frequency and phase corresponded to regions with both relatively high difference spectrum amplitudes and low criterion spectrum amplitudes (optimal condition). If the theory were correct, these masks would act to raise the level of the response to the difference spectrum required for contrast discrimination in the vicinity of the mask.

No loss of sensitivity for offsets was observed with either the non-optimal or the optimal masks. *Mene, mene, tekel, upharsin*! Either the theory is wrong or

the Observer had information available to counteract the effect of the masks. A reanalysis of the model responses to the four line stimuli, this time with the mask present, suggested a solution. When added to the oscillating spectra of the four line stimuli the sinewave mask did not eliminate a region of low filter response, it merely shifted it. Algebraic cancellation of the mask and a region of the four line spectra of the opposite phase created a new spectrum null. The shift of the spectrum null was small because of the relative amplitude of the bright lines and the sinewave mask. The Observer still had access to a region of high difference spectrum amplitudes and low criterion amplitudes. Feedback could then be used to train the Observer to attend to changes in response at the new spectrum null. Although it would be possible to apply sinewave masks to dim four line stimuli, the larger thresholds normally obtained with low line contrast might be interpreted as being outside the vernier-like range and not reflective of the localization process.

Sinewave cancellation of offset

As an alternative, a method was employed that allowed the sinewaves to masquerade as spatial offsets in localization stimuli that can be used to produce thresholds of less than 10" arc under optimal conditions. As in the four line interval judgment experiment where contrast and criterion separation were varied, stimuli with both positive and negative offsets were interleaved. In addition, each

stimulus was paired with two phases, 180° apart, of a sinewave overlay. A ITAFC procedure with no feedback and standard viewing conditions was used (see chapter 2, methods). The Observers, who were well practiced at the interval judgment task, were instructed to respond as to whether the center interval appeared to be larger or smaller than the adjacent intervals. In the ITAFC procedure the criterion stimulus (four equally spaced lines) is not presented for comparison. With no feedback to train the Observers to the location of a spectrum null consistent with the response to the criterion plus sinewave (actually with this stimulus set there would be two null locations to be learned, one for each phase of the sinewave), the effect of the sinewave is uncoupled from the response to the criterion stimulus. Under these conditions a positional theory based on a contrast discrimination mechanism would predict that the major perceptual consequence of the addition of a sinewave with the appropriate spatial frequency and phase would be the appearance of an offset. An appropriate sinewave would induce activity in the filters at the spectrum null, adding linearly to the activity caused by any actual offset present in any of the four line stimuli. Sinewaves with a spatial frequency away from the spectrum null should not alter the detectability of offsets at any phase.

Cosines at ±90° phase relative to the center of the four line pattern were superimposed on a set of stimuli that had a criterion separation of 160" arc and a moderate contrast (dL/L=4.43). Four spatial frequencies (2.8, 5.6, 11.2 and 22.5 cpd), corresponding to regions of both high and low filter response, were added to

stimuli with positive and negative offsets that ranged from 0 to 60" arc. For four lines separated by 160" arc, 2.8 and 22.5 cpd sinewaves correspond to regions of high spectrum amplitude (nonoptimal) while 5.6 and 11.2 cpd sinewaves correspond to regions of low amplitude (optimal) (See figure 2.16, c). The sinewave contrasts were either 1, 2.5 or 5 times their respective detection threshold.

For nonoptimal sinewaves, the psychometric functions relating offset magnitude to probability of detection are not distinguishable from the functions obtained without the sinewaves (figure 4.1). As in chapter 3, the psychometric functions are corrected for guessing. The curve for negative offsets is reflected about the origin and is combined in a single graph with the curve for positive offsets. The general tendency of the curves for positive and negative offsets to form a single ogive is consistent with a bipolar filter whose response is combined with gaussian noise prior to an all-or-nothing decision mechanism. The individual psychometric functions for either positive or negative offsets rise steeply from the zero probability of detection axis and approach an asymptote at 100% detection. As a notational convention, probability of detection for smaller (negative) offsets are labeled with a minus sign. A single ogive yields as good or better fit to the data than two ogives forced to asymptote to zero detection probability. The unity of the combined psychometric functions support a model with a single mechanism subserving the detection of both positive and negative offsets. The positive and negative offsets would appear, then, to lie on a sensory continuum and not be

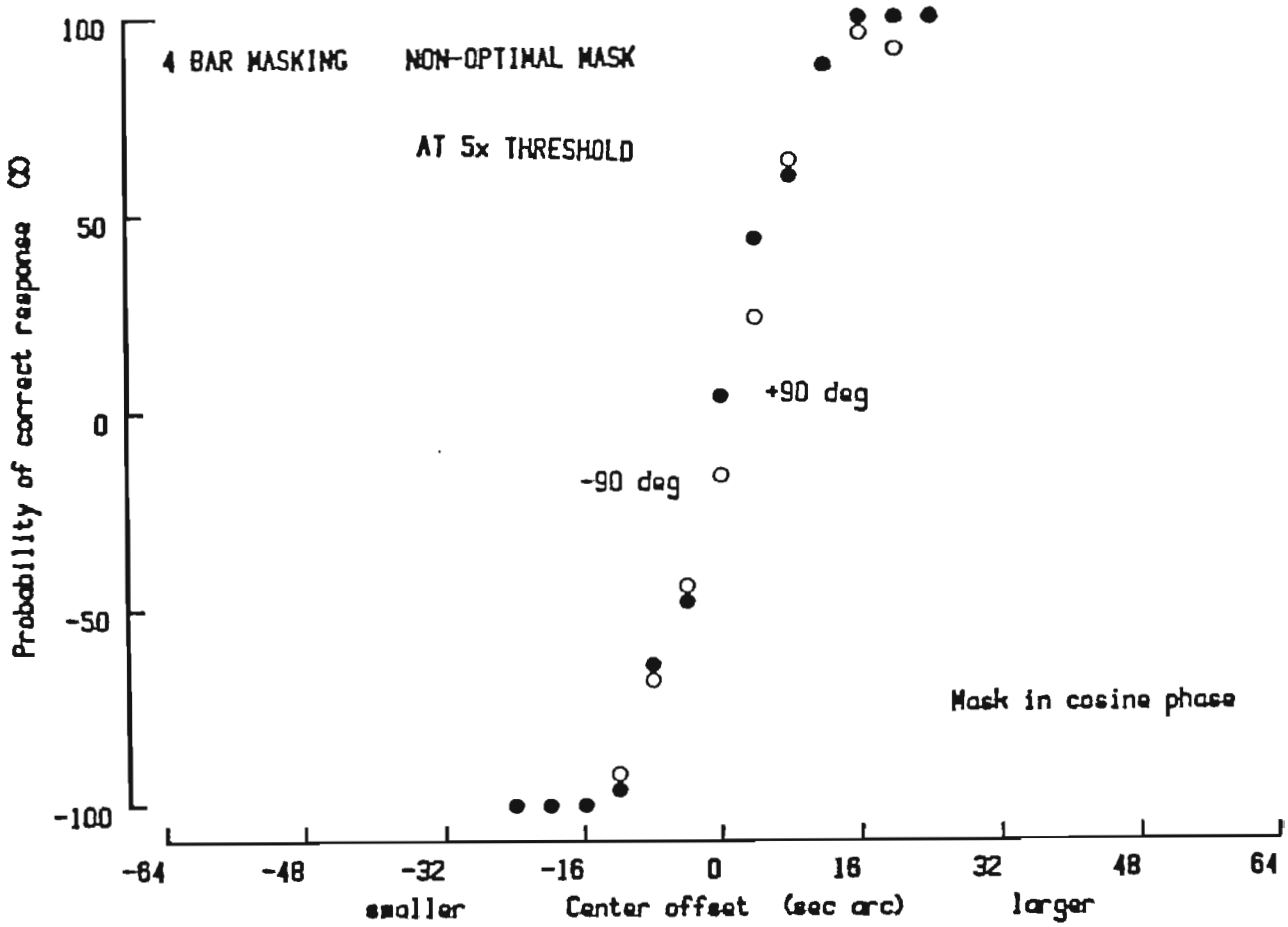

Figure 4.1 Psychometric functions for the detection of offsets in the presence of a nonoptimal sinewave.

The results of a four line interval judgment task are displayed in a single graph. The criterion separation was 160" arc and the line contrast (on the display) was 4.43. The offsets ranged from -24 to +24" arc. Each stimulus was paired with each of two sinewaves (2.8 cpd, 2.2% contrast, and -90 or +90° phase). According to the theory, these conditions are nonoptimal since the sinewaves correspond to a region of large criterion spectrum amplitude. The curves for both phases of the sinewaves are superimposed and the curves pass through zero probability of offset detection when there is zero physical offset. The error bounds are fiducial limits calculated for the combined positive and negative offset stimulus sets by the method of probits (see chapter 2, methods).

qualitatively different stimuli. As in chapter 3, offset threshold is, by convention of the literature after Stratton, computed to be half the difference between the positive and negative offsets that are detected 50% of the time. Computed with either single or double ogives, the offset threshold for the interval judgment task is not affected by the presence of a nonoptimal sinewave.

The effect of an optimal sinewave on the detection of an offset is markedly different (figure 4.2). The ogives formed by the combined psychometric functions for positive and negative offsets are translated along the offset axis. The direction of translation is dependent on the phase of the superimposed sinewave. The divergence of the two ogives, constructed from data points collected on interleaved trials, cannot be due to response bias. A preference for either response would translate both curves in the same direction. The alternative theory proposed here is that sinewaves act as offsets where the filter response to the difference spectrum is large and the response to the criterion is small. It is the limited extent of this coincidence that allows a narrowband stimulus such as a sinewave to constitute a good approximation to a broadband offset spectrum. When weighted by the criterion amplitude spectrum, as in the contrast discrimination function based on filter response, the most effective portion of the offset spectrum is quite narrow. Although the aggregate response to a stimulus may include contributions over a range of filter center frequencies, it is the nature of probability summation mechanisms to disproportionately weight responses that are even slightly larger than the rest. With the exponent of 3.5 used here, this advantage is no small

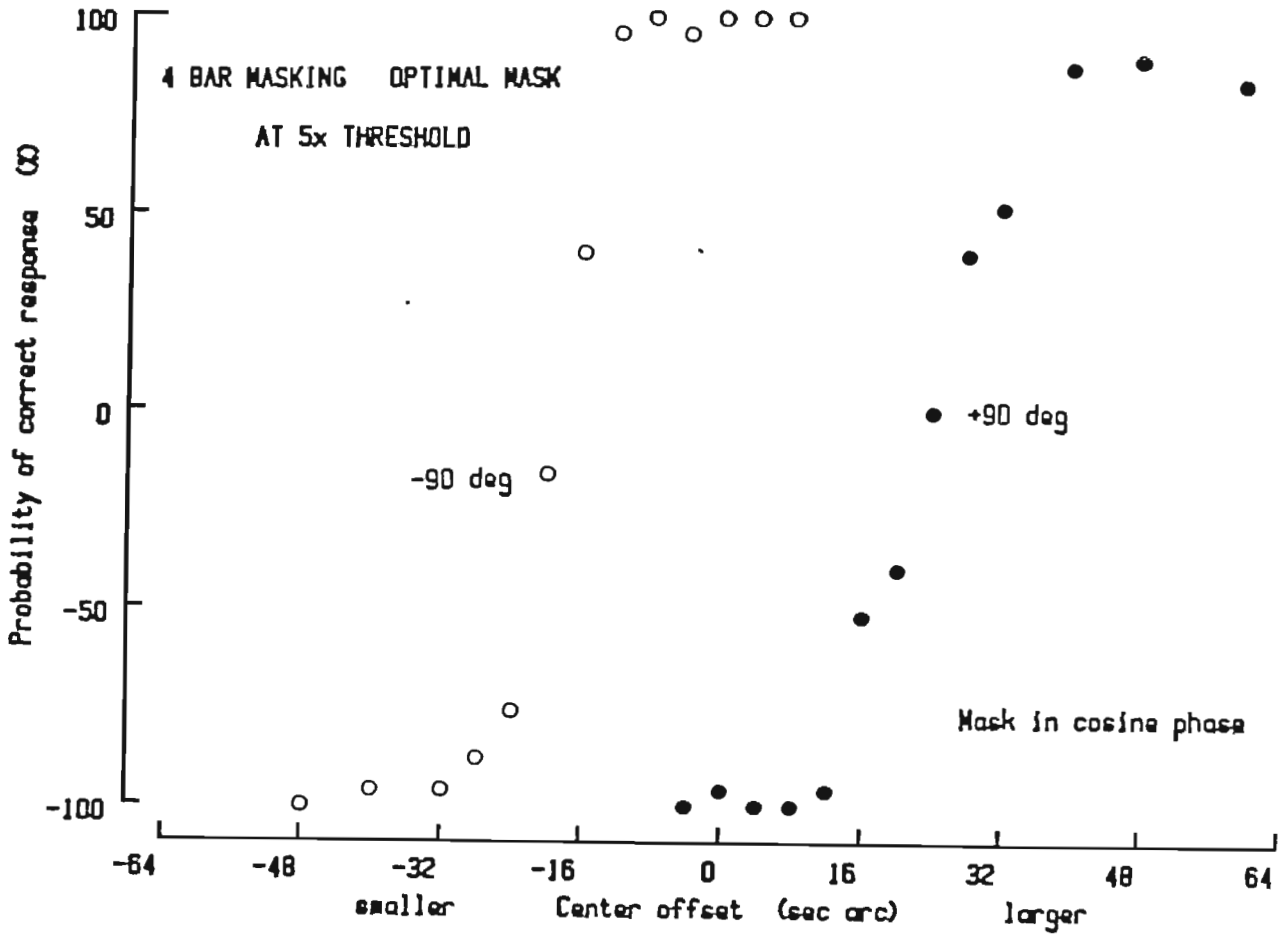

Figure 4.2 Psychometric functions for the detection of offset in the presence of an optimal sinewave.

The four line stimulus is as in figure 4.1; however, the sinewave frequency now corresponds to a spectrum null (11.25 cpd, 10% contrast and $\pm 90^{\circ}$ phase). The sinewaves translate the psychometric functions along the offset axis as if they were actual increments (decrements) in the physical offset.

effect. A 22% increase in a filter's response doubles its contribution the the aggregate measure. It is the presence of these peaks in the offset response and their coincidence with spectrum nulls that universally characterize stimuli that are able to elicit seconds of arc offset thresholds. Depending on the particular stimulus, there may be more than one peak, but there is always one. The size of the offset at threshold depends, in part, on the contrast sensitivity of the filters near the discrimination peaks. The theory proposed here is in contrast to those that contain broadband mechanisms that require many sinewave components to be simultaneously present to signal the presence of an offset.

The same linear summation stage in the filters that cause the spectrum nulls also cause the phase specific effects of the superimposed sinewaves. The sinewaves sum with the spectra of the stimuli containing the physical offsets, changing the magnitude and sometimes even the sign of the filter response in the regions of optimal contrast discrimination. In the case of the four line stimulus, the spectrum differences between the equally spaced stimulus and those containing offsets is entirely in cosine phase with respect to the center of the stimulus. The low frequency spectra of the positive offsets (at -90^{o} phase) is 180^{o} out of phase with those of the negative offsets (at $+90^{o}$). Since the amplitudes of the offset spectra are proportional to offset for small offsets, the shape of the psychometric functions should be preserved, and they are. The presence of an optimal sinewave, therefore, does not alter offset threshold. However, an optimal sinewave in -90^{o} phase (simulating a positive offset) does reduce the detectability of

negative physical offsets and enhance the detectability of positive ones. Data points in the second quadrant indicate some stimuli with negative physical offsets may nonetheless appear more often to contain a positive offset (probabilities corrected for guessing). In these cases, the sinewave overwhelms the relatively weak response of the physical offset. A sinewave in +90° phase has a similar effect (but opposite in sign) on the physical offsets.

One metric that can be used to measure the relation between sinewaves and physical offsets is the extent that perceived zero offset is shifted. Perceived zero offset occurs when the forced choice (larger, smaller) responses are equally probable. For the response proportions to be equal, the response to the narrowband sinewave must cancel the response to the broadband offset. With 160" arc criterion separation, the largest shift occurs for an 11.2 cpd sinewave (figure 4.3). At that spatial frequency, the sinewave in +90° (cosine) phase and at 5 times detection threshold is able to cancel a positive 35" arc physical offset (Observer BCM). At 5.6 cpd the magnitude of the shift is smaller and, at the other frequencies, the shift is nonexistent. This pattern of response provides strong support for the theory. The shifts occur for frequencies that correspond to filters with good contrast discrimination sensitivity when presented with the criterion stimulus. For frequencies that correspond to regions with large responses to the criterion and consequently have poor contrast discrimination sensitivity, no shifts in perceived offset occur.

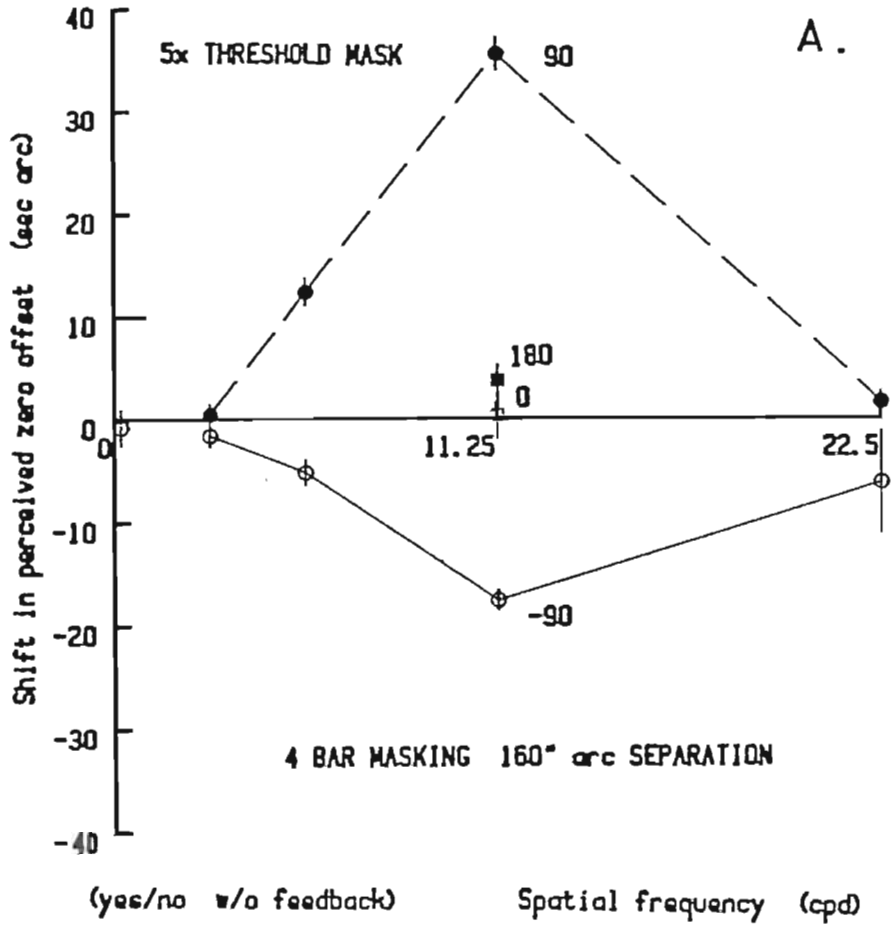

Figure 4.3 Perceived zero offset (160" arc criterion separation)

The ability of a superimposed sinewave at 5 times detection threshold to cancel a physical offset varies as a function of spatial frequency and phase. The cancellation is maximum in the region where the response to the difference spectrum is large and and that to the criterion spectrum is small (11.2 cpd). The magnitude of the shift is smaller where the difference spectrum response is smaller but the criterion spectrum is still small (5.6 cpd). In the regions where the criterion spectrum response is large (2.8 and 22.5 cpd), the magnitude of the shift is small or nonexistent. Sinewaves in cosine phase have a larger effect on perceived offset than the corresponding negative cosine.

When sinewaves at the optimal spatial frequency are in sine or negative sine phase, there is no shift in perceived offset. The Observers (BCM, a; DLG, b) are able to maintain perceived zero offset to within a few seconds of physical equality both for the positive and negative sine phase conditions and for the no sinewave condition (0 cpd).

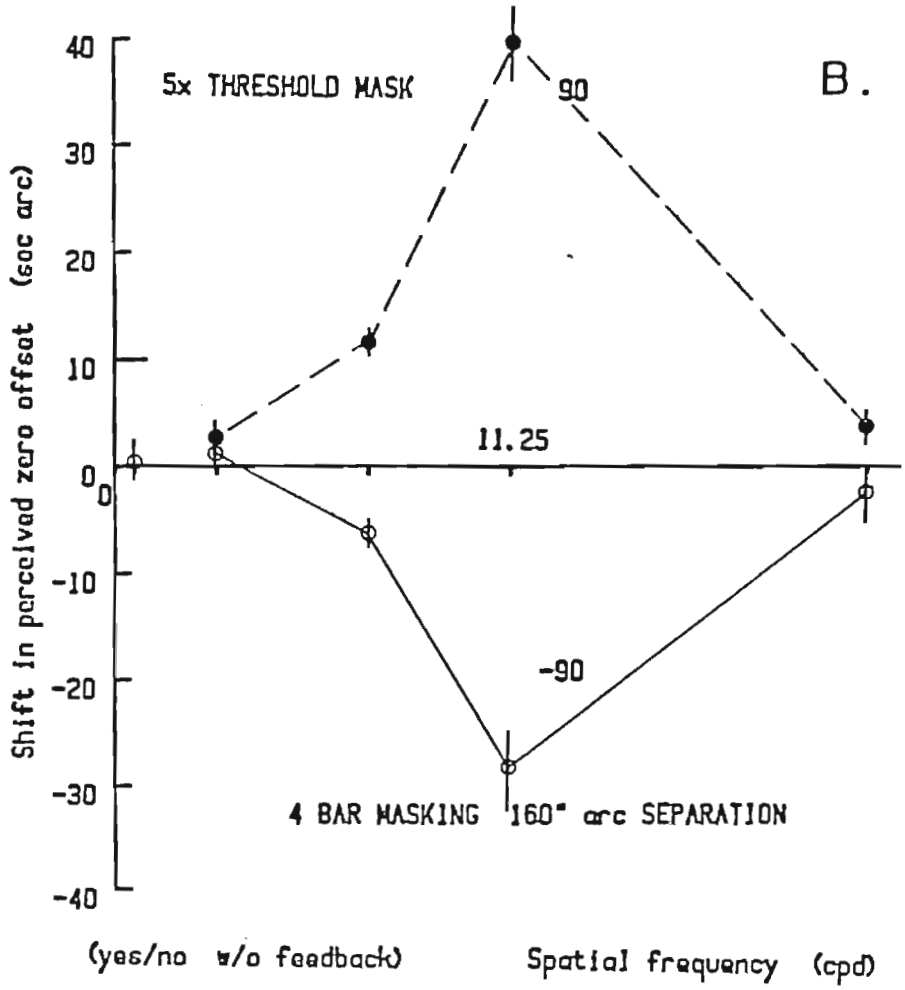
40
30
20
10
0
-10
-20
-30
-40
5x THRESHOLD MASK
90
B.
11.25
-90
4 BAR MASKING 160" arc SEPARATION
Shift in perceived zero offset (sec arc)
(yes/no w/o feedback)
Spatial frequency (cpd)

A similar pattern of cancellation occurs between sinewaves at -90^{o} phase and negative physical offsets; however, the shifts are smaller. It is likely that this difference in magnitude as a function of phase is real since not only were the trials interleaved but the test sessions were interleaved with sessions with no sinewave superimposed. In the latter condition (figure 4.3, 0 cpd), no change in Observer criterion for equality of separation was seen. The difference may be related to a family of effects that mitigate against the averaging of positive and negative offset data in computing threshold because of a difference in the relation between offset magnitude and filter response for positive and negative offsets. Alternatively, the masks may have a differential effect on the form spectra (q.v., figure 3.18).

Further strong evidence for the CELT is the phase specific nature of the shift effect. If the sinewaves act in a truly additive relation with the physical offsets there should be no disruption of the localization process by sinewaves that are orthogonal to the phase of the offsets. The filters that are most sensitive to the cosine phase of the offset spectra will have a spatial weighting that makes them insensitive to the sine phase. Indeed, sinewaves in sine or negative sine phase produce no shift of perceived offset even though the same spatial frequency produces large effects in cosine phase. It is also important to note that there is no elevation of the thresholds, either by optimal or by nonoptimal sinewaves. Seconds of arc thresholds are maintained throughout all conditions.

When the criterion separation is halved (80" arc), the period of the four line amplitude spectrum is doubled (see figure 2.16, b). According to a contrast

discrimination based theory, the pattern of optimal and nonoptimal spatial frequencies should also be doubled, and indeed it is (figure 4.4). The maximum shift of perceived zero offset now occurs at 22.5 cpd for 5 times detection threshold sinewaves in cosine phase. A smaller shift is seen at half the spatial frequency and none at all for the nonoptimal frequencies. Again, the shift is larger for $+90^{o}$ phase than for -90^{o} phase and there is very little effect for sinewaves in sine phase. The Observers were able to maintain a criterion at this separation as well. The estimated perceived zero offset in the absence of any sinewave was within a second of arc of physical equality. Consistent with the 80" arc criterion separation, the offset thresholds were slightly larger than those obtained at the optimal 160" arc separation. The offset thresholds at 80" arc separation were not degraded by the presence of the sinewaves.

When the criterion separation is doubled from the optimal 160" value, the period of oscillation in the amplitude spectrum is halved (see figure 2.16, d). The pattern of sinewave cancellation of physical offsets now peaks at 5.6 cpd (figure 4.5). As in the other separation conditions, the sinewaves do not perturb the sensitivity of offset detection. In the condition where a 22.5 cpd sinewave is superimposed, there is a reversal in the relation between sinewave phase and cancellation of offset. This reversal evinces the transition wherein the four line stimulus with more than 5' arc interval separation begins to be processed as individual lines as well as a collective pattern. The small spatial extent of the bandpass filters centered at high spatial frequencies allows only individual lines to

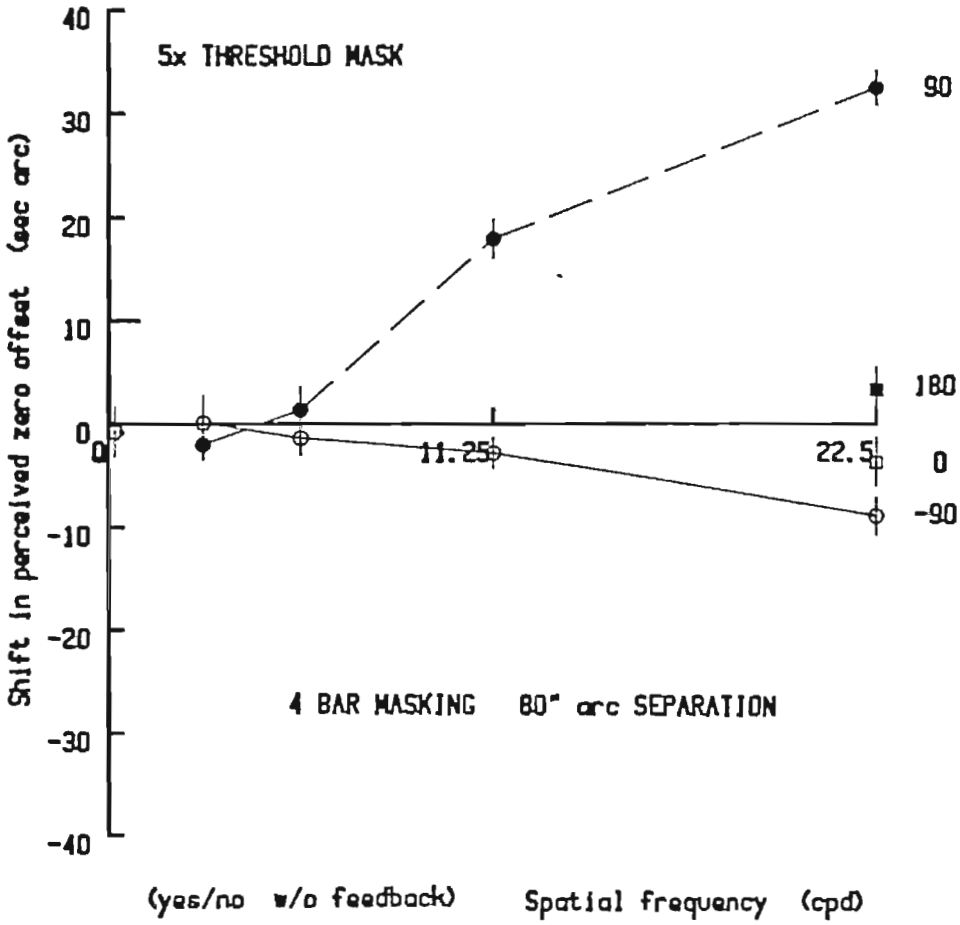

Figure 4.4 Perceived zero offset (80" arc criterion separation)

The criterion separation of the four line stimulus is 80" arc. All other conditions are the same as for the 160" arc condition (figure 4.3). The same pattern of sinewave cancellation of offset is observed here. The pattern is simply shifted to twice the spatial frequency. (Observer BCM)

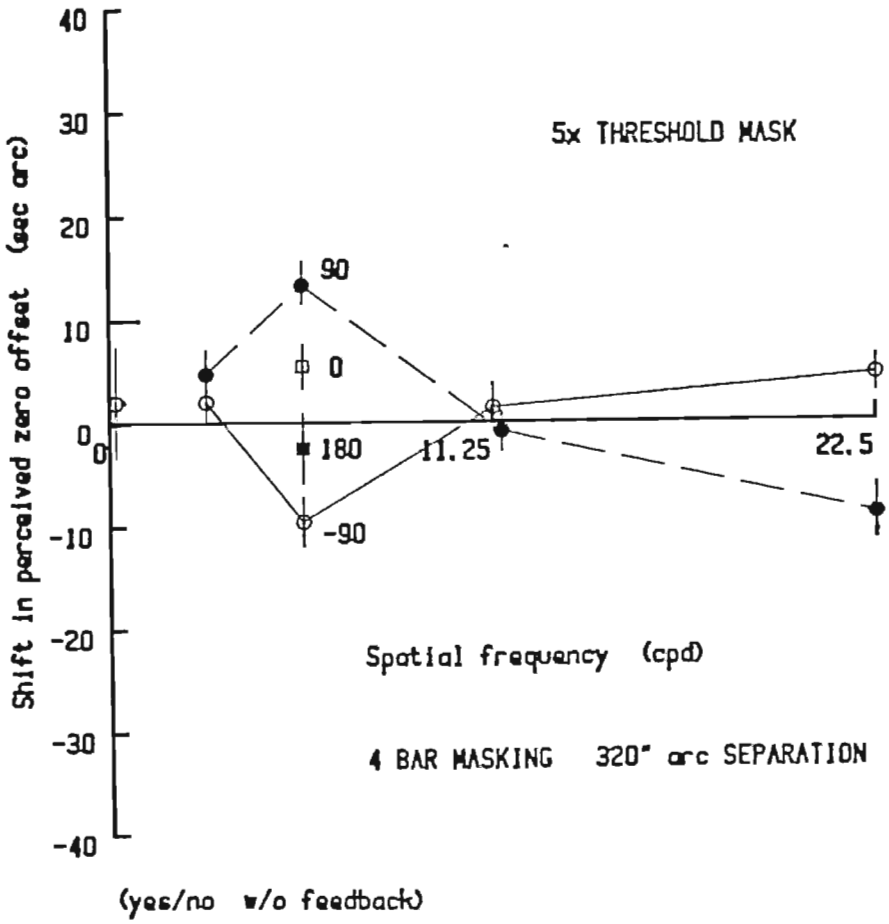

Figure 4.5 Perceived zero offset (320" arc criterion separation).

The criterion separation of the four line stimulus is 320" arc. All other parameters are the same as for the 160" arc condition (figure 4.3). The pattern of sinewave cancellation is now shifted down to half the spatial frequency.

stimulate a given filter.

The transition from unified to individual processing of the lines is even more apparent when the criterion separation is doubled again, to 640" arc (figure 4.6). The pattern of sinewave cancellation of offset is not present. In its place is the interaction of the superimposed sinewaves and the individual lines. The domination by individual interactions at large separations reflects the reduction in contrast sensitivity at low spatial frequencies as well as the lower limit on center frequencies of the filters themselves. When the change in offset causes the individual lines to beat with the local phase of the superimposed sinewaves, the perceived position of the individual lines is altered. This shift in the position of individual lines is reflected in a disruption of offset threshold. At 11.25 and 22.5 cpd. there are large disparities in threshold with opposite phase sinewaves. The beating of the individual lines with the phase of the sinewaves may be seen in the psychometric functions obtained under these conditions (figure 4.7).

Effect of contrast on cancellation of offset

The change in the amplitude spectrum of the four line stimulus due to offset is proportional to the magnitude of the offset for small offsets (figure 3.19). If the shift in perceived zero offset is due to algebraic cancellation of offsets by the superimposed sinewaves in the linear summation stage of a limited and critical range of spatial frequencies, the magnitude of the shift should be proportional to

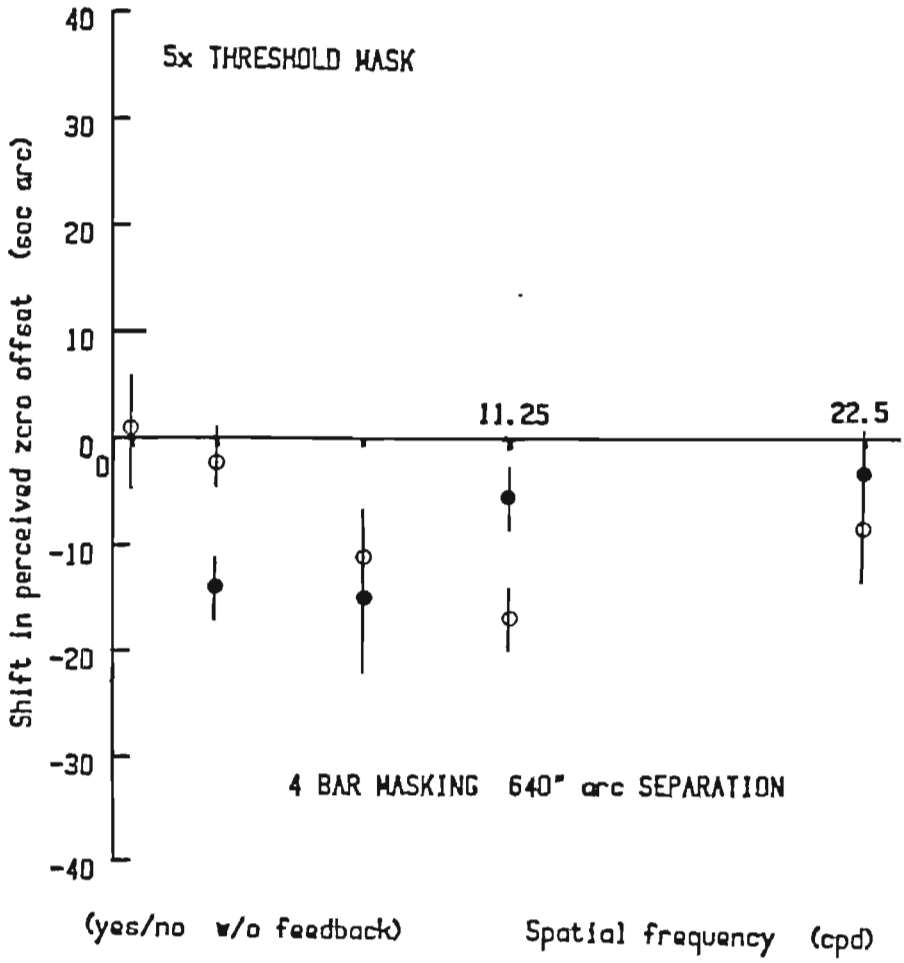

Figure 4.6 Perceived zero offset (640" arc criterion separation).

The criterion separation of the four line stimulus is 640" arc. All other conditions are the same as for the 160" arc condition (figure 4.3). At this large separation the pattern of cancellation of offset by a superimposed sinewave is no longer apparent. The the detection of offsets is dominated by the interaction of single lines with the sinewaves.

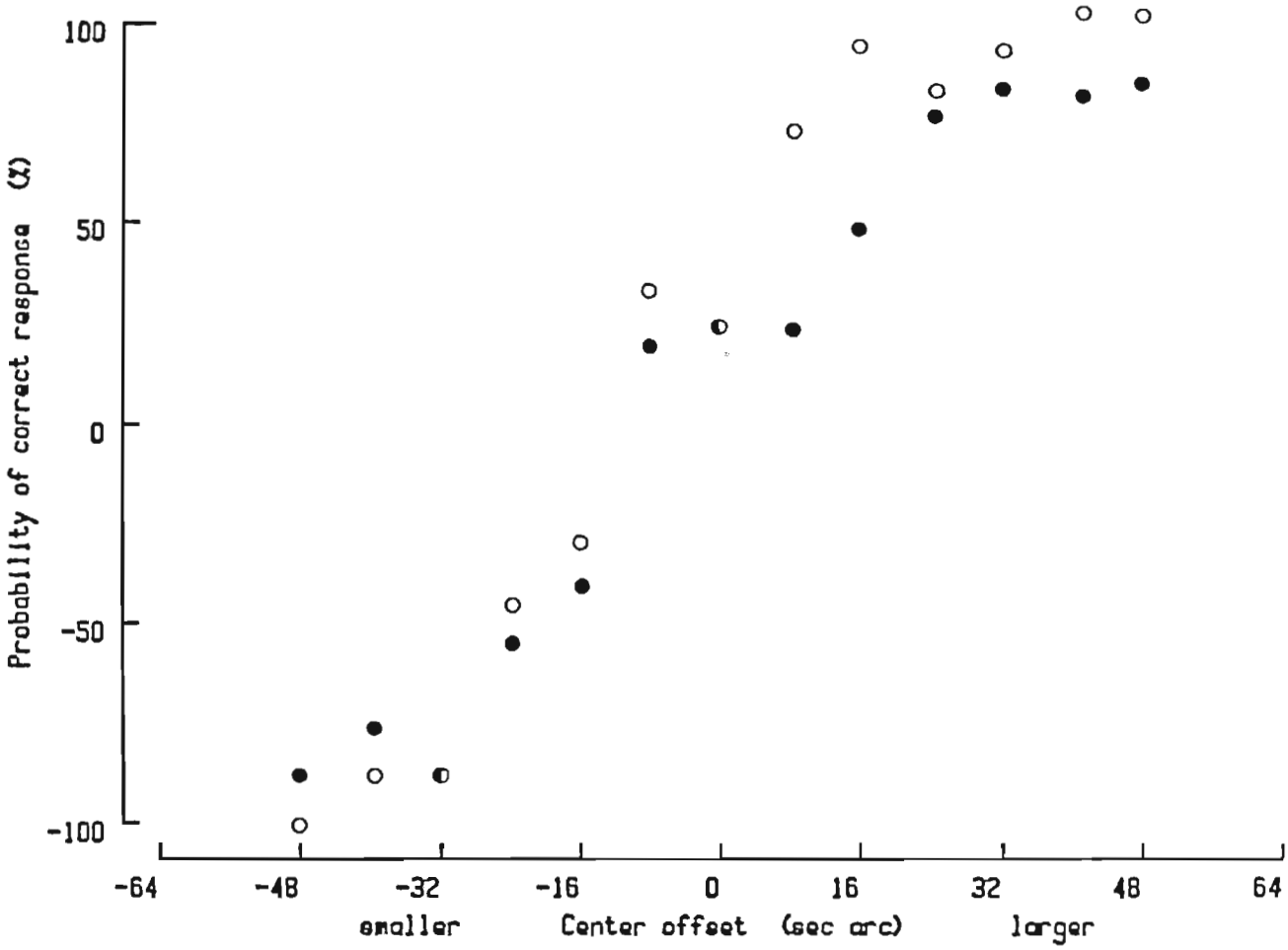

Figure 4.7 Psychometric function for the detection of offset obtained at a large criterion separation.

For a large criterion separation (640" arc), the individual lines beat with the high frequency (22.5 cpd) sinewave as the offset of the four line stimulus is changed. The net result is that the beating produces shifts between the psychometric functions of opposite phase at some separations while leaving them coincident at others.

the contrast of the sinewave. The effects of sinewave contrast were tested by superimposing sinewaves at 1.0 and 2.5 times detection threshold on four line interval judgment stimuli at the optimal critical separation (figure 4.8). In agreement with CELT, the lower contrast sinewaves have less of an effect on physical offsets. At the spatial frequency that elicits the greatest shift in perceived zero offset (11.25 cpd), the reduction in shift is proportional to contrast for both phases of the sinewave.

Giving particularly strong support to the theory, is the match between the shift in perceived offset induced by a threshold sinewave at the optimal spatial frequency and the just detectable physical offset. This condition demonstrates the ability of contrast sensitive mechanisms to subserve the detection of seconds of arc positional offsets without exceeding measured contrast sensitivity. As with the higher contrasts the shift in perceived zero offset occurs because the entire ogive for each phase is shifted (figure 4.9).

To underscore the exquisite sensitivity afforded by the arrangement of bandpass spatial filters in the visual system, consider the change in retinal flux distribution associated with a threshold offset in the four line interval task (figure 4.10, a). The misalignment of the four lines results in a flux change that has a peak contrast of 0.25 (dL/L). This undulating pattern must be discriminated against a criterion retinal flux distribution with a peak contrast of 7.2 (figure 4.10, b). The contrast of a sinewave at the optimal spatial frequency and phase to induce the apprehension of an offset needs only 0.0042 contrast (retinal dL/L).

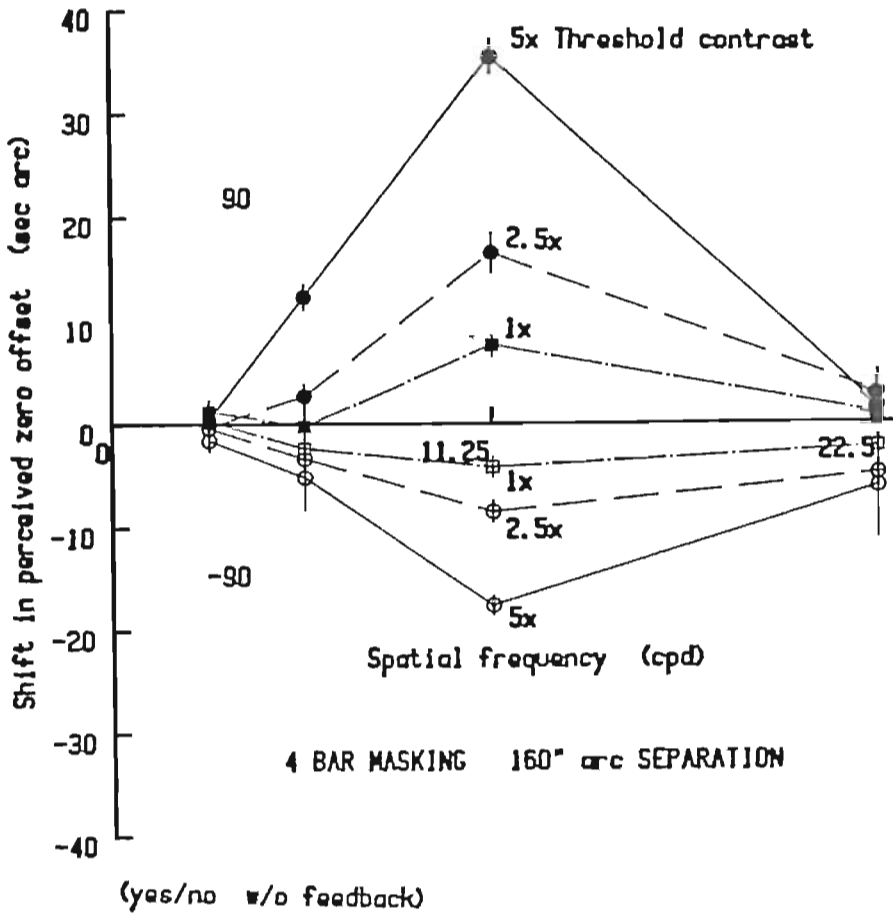

Figure 4.8 Effect of sinewave contrast on offset cancellation.

Sinewaves of 1, 2.5 and 5 times detection threshold are superimposed on four line interval judgment stimuli with a criterion separation of 160" arc and a line contrast contrast of 4.43 (dL/L). The cancellation strength of the sinewaves is reduced for lower contrasts.

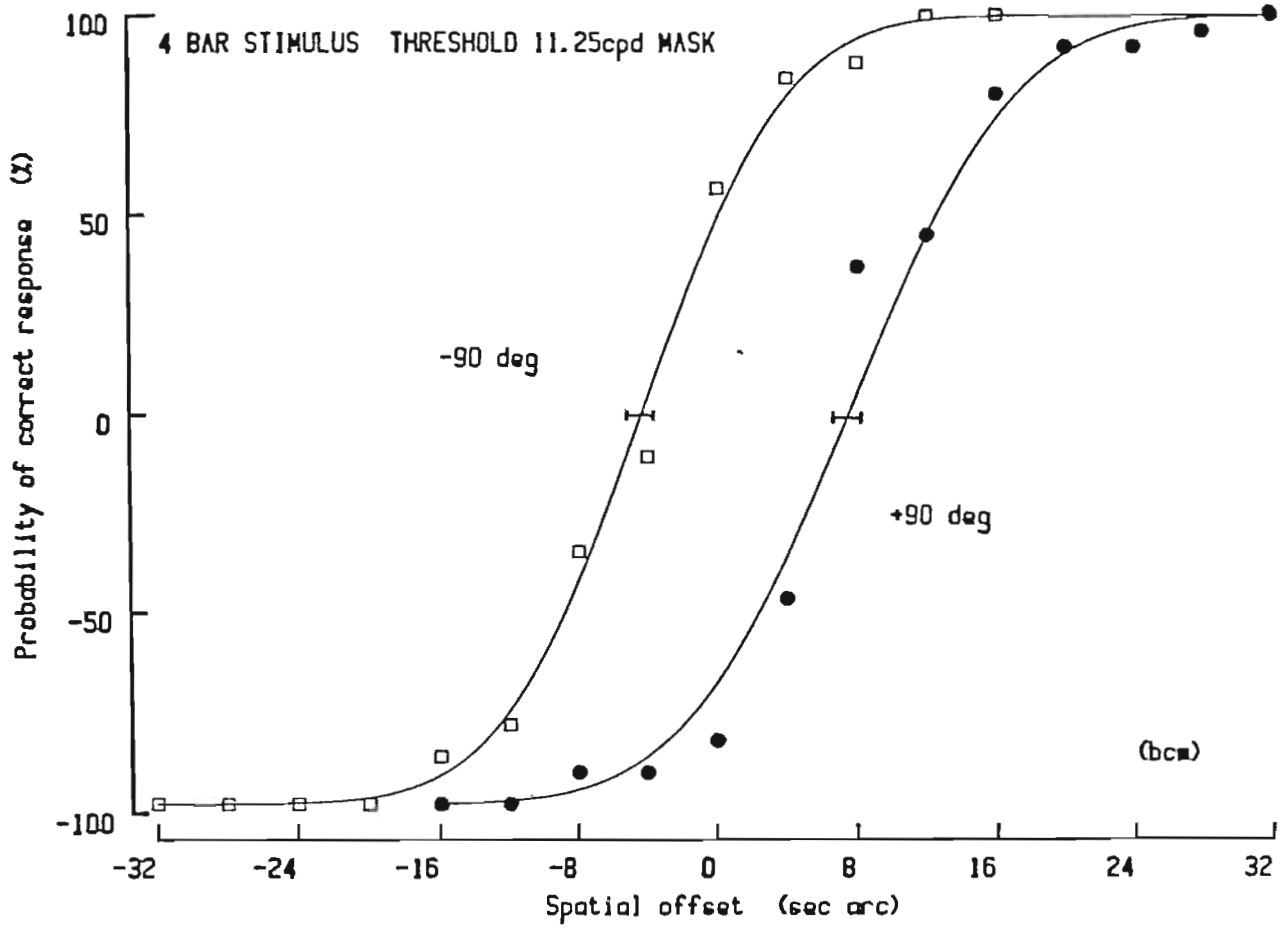

Figure 4.9 Psychometric functions for the detection of offset in the presence of a threshold sinewave.

A 2% 11.25 cpd sinewave in positive and negative cosine phase is superimposed on four line interval judgment stimuli with small physical offsets. The shift of the data points on each ogive en masse is consistent with the linear summation of the sinewaves and the offset spectra over a limited region.

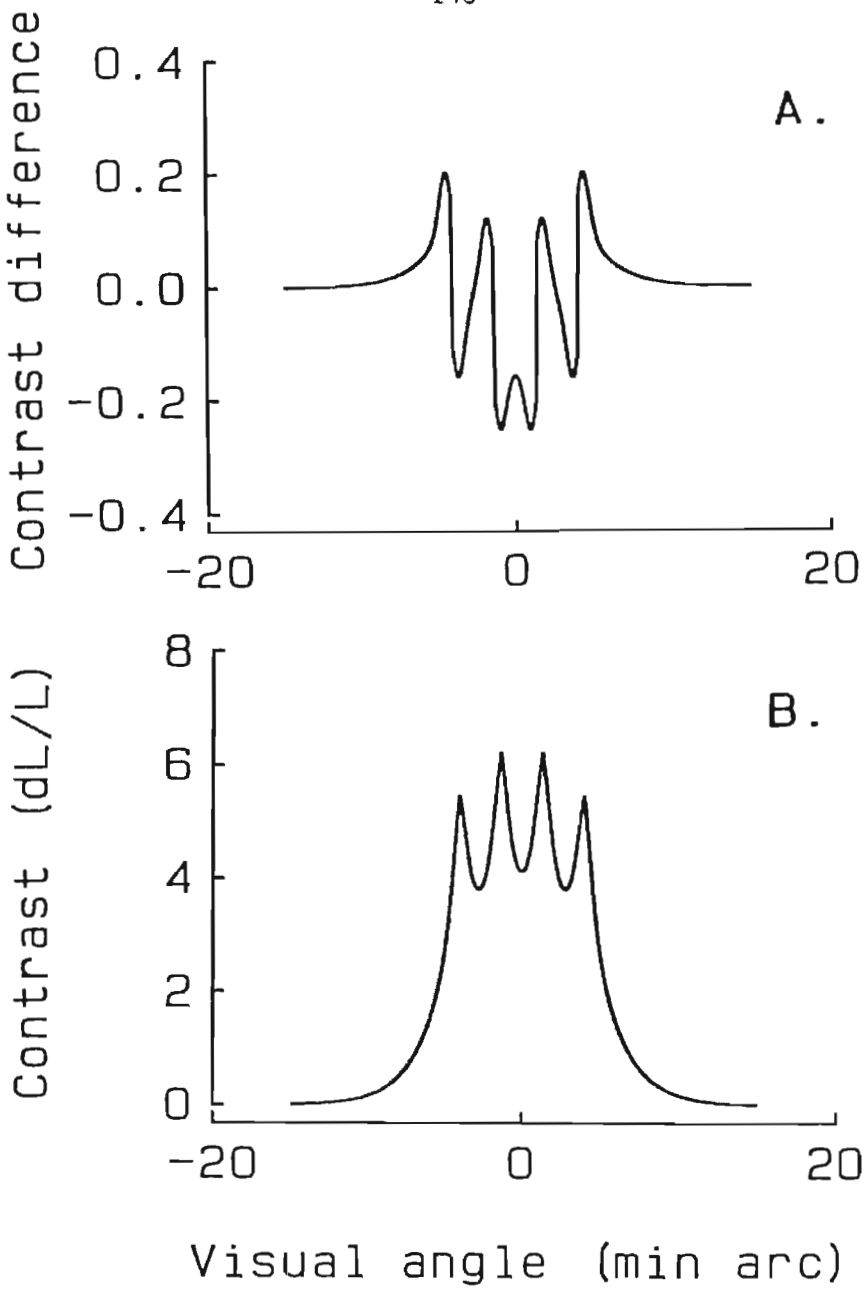

Figure 4.10 Relative retinal flux distribution of offset and criterion.

The retinal flux distribution that corresponds to the difference of the four line 160" arc criterion and the four line stimulus plus 8" arc offset at moderate contrast (dL/L = 4.43) is a pattern of four dipoles with a peak contrast of 0.25 (a). The undulating flux pattern is just discriminable against the retinal flux distribution of the criterion (b). The superposition of a sinewave mask of 11.25 cpd (5.3' arc period) in 180° (negative cosine) phase with the center of the stimulus of 0.0042 retinal contrast resulted in the same apparent displacement.

The ratio of peak criterion amplitude to sinewave amplitude (more than 1700:1 on the retina) is difficult to reconcile with a general flux discrimination or interpolation scheme.

Cancellation in asymmetric stimuli

When referenced to their centers, the stimuli used in the four line interval judgment task, as well as differences between them, all have cosine phase spectra. Consequently, at all spatial frequencies, the filters most sensitive to the criterion amplitude spectrum are also most sensitive to the offset spectrum. Calculations of filter responses for contrast discrimination are relatively straightforward. This coincidence of phase does not occur for the three line interval judgment (bisection) task. The addition of an offset to one of the two intervals introduces spatial frequencies at phases for which there is no common axis of symmetry (see figure 3.16). The change in the amplitude spectrum due to offset increases almost linearly over the range of human contrast sensitivity. At the same time the phase changes linearly with spatial frequency. The rate of phase change is approximately proportional to the criterion separation. As with the four line stimuli, the amplitude (slope) of the modulus is proportional to offset magnitude for small offsets.

In chapter 3, the detection of small positional offsets in the separation of three lines was shown to be consistent with the discrimination of the difference in contrast response generated by the criterion and offset stimuli. If the sinewaves are indeed acting as offsets, the the pattern of perceived offset should reflect not only the background response amplitude but also the phase of the offset as a function of spatial frequency.

With CELT, regions of high contrast discrimination sensitivity should occur near the change in sign of the phase of the criterion amplitude spectrum; that is, at a spectrum null. For a criterion separation of 160" arc these changes occur near 7.5 and 15 cpd. The sinewave cancellation technique used in the previous section with the four line stimuli was repeated here for the three line stimuli. The Observers were asked to respond as to whether the right interval was larger than the left. Stimuli with larger and smaller offsets were interleaved within a single session. Each stimulus was paired with sinewaves that had the phase of the offsets at the spatial frequency being tested. Along with the two lowest optimal spatial frequencies, four other nonoptimal spatial frequencies were used (3.75, 11.25, 18.75 and 22.5 cpd). Again the results are in agreement with the theory (figure 14.11). Shifts in perceived zero offset occur only in the regions of high contrast discrimination sensitivity (7.5 and 15 cpd). Importantly, the results also show the predicted change in the sign of the shift. While an increment in the response of the filter at the first spectrum null is indicative of a positive offset, the change in the slope of the spectrum envelope at the second spectrum null results in a

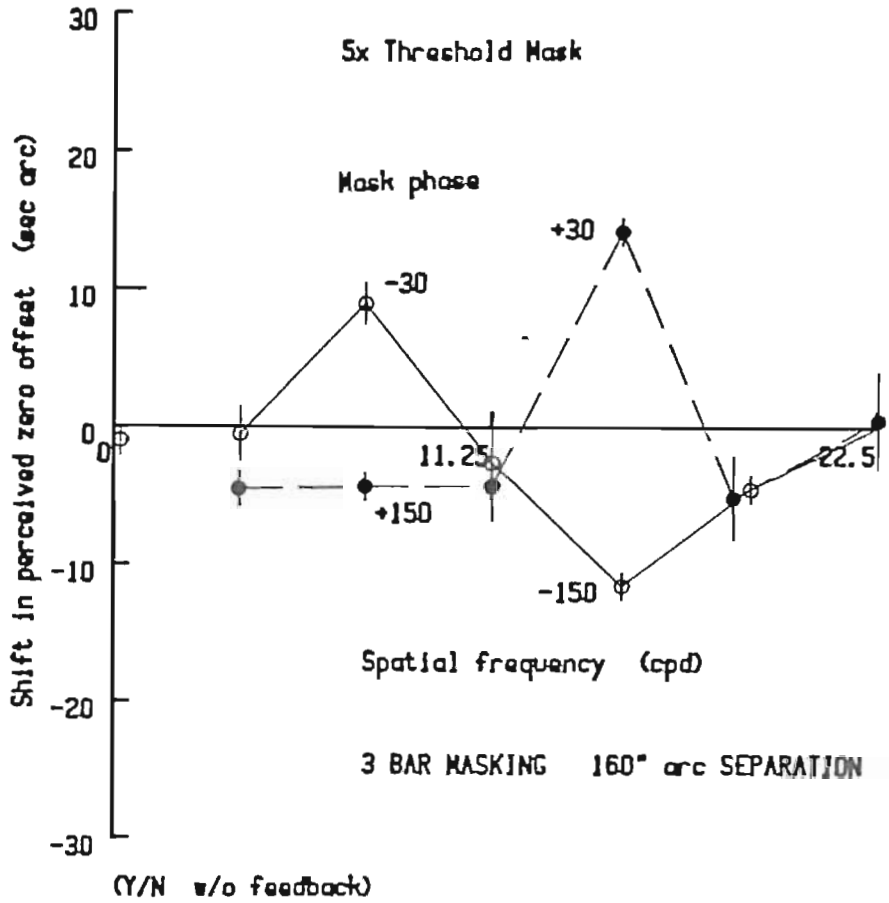

Figure 4.11 Perceived zero offset, three line stimuli (160" arc criterion separation).

Sinewaves superimposed on three line stimuli sum and cancel physical offsets when they have the appropriate phase and spatial frequency. Observers were required to judge whether the right interval was larger or smaller than the left. Changes in perceived offset from that physically present occurred only when the sinewaves had the phase of the offset spectrum at that spatial frequency and contrast discrimination sensitivity was high.

decrement in response for a positive offset. A -30^o phase 7.5 cpd sinewave will cancel a positive offset, yet a -150^o phase 15 cpd sinewave (the appropriate linear phase shift for a 7.5 cycle frequency increment) cancels a negative physical offset. The opposite relations are observed for sinewaves with the opposite phase. As was the case with the interval judgment task, the presence of the sinewaves did not disrupt localization in the bisection task.

summary

The ability of sinewaves to masquerade as broadband offsets when the sinewave spatial frequency coincides with spectrum nulls in the criterion spectra and the sinewave phase agrees with the offset spectra, strongly supports the theory of contrast enhanced localization. The peak of the distribution of sinewave induced offsets shifts in the expected manner with changes in both criterion separation and offset phase. The threshold positional offsets that threshold sinewaves induce in highly superthreshold stimuli clearly demonstrate the advantage that spectrum nulls give to localization stimuli.

Chapter 5

WHAT'S IN AN OFFSET?

"Walls has pointed out that vernier and stereoscopic acuities have little in common with visual acuity as measured by line or grating test objects."

Berry, Riggs & Duncan (1948)

"The spatial localization of a feature to an accuracy of one-fifth the width of a photoreceptor would seem to demand more complex neural processing than is needed for ordinary visual acuity."

McKee & Westheimer (1978)

"On the other hand, vernier acuity, which measures the ability to detect misalignment of edges or bars, is not constrained by the same factors as the other acuities."

Freeman & Bradley (1980)

Rationale

The central issue in the unification of measures of visual acuity is the definition of position. Position here is held to be an orderly labeling of regions in the visual field. Like color and depth, position is a perceptual attribute that is attached to variations of flux. It is the sensation that is tapped by the experiment described at the end of chapter two. The stimuli in that experiment are distinguished purely by position. Identical lines elicit different responses when

they fall on regions that are sufficiently disparate to have distinct labels. At issue in this thesis are the operational criteria for sufficiently disparate that are used to obtain the various measures of visual acuity.

Does Stratton's (1900) left/right judgment isolate the sensation of position? Is "intensity" eliminated as a source of information in his paradigm? At a time when the theoretical influence of a discrete retinal mosaic was great, Stratton's argument was compelling. From this perspective, foveal cones could be individually labeled. The orderly mosaic allowed higher visual processing to "know" in some sense (i.e., make use of) the position of individual photoreceptors relative to the visual field. The averaging of local sign (interpolation between labels) over space and time was used to explain the gap between the density of the mosaic and measures of performance. Although the retinal interpolation schemes [As should be clear by now: A scheme is a theory I don't espouse.] have been discredited by subsequent research, measures of performance have retained the assumption that displacements of stimulus elements elicit changes only in positional sensations.

In the last twenty years, a different view of the organization of spatial representation has emerged. In place of a "connect the dots" approach, the intensity responses of many photoreceptors are thought to be weighted and combined in different ways over the same region. The responses of filters with different spatial weighting distributions, but labeled for the same position in the visual field, form the basis for the detection, discrimination and recognition of different flux variations at any single position. In this context, the validity of

traditional measures of positional acuity depends on establishing the continuity between the two mechanisms. Are sensations that are elicited by gross displacements in the visual field on a continuum with those elicited by seconds of arc changes in the relative distance of two closely spaced features?

The distinction between the two mechanisms subserving spatial acuity is made less apparent perceptually by an overlap in the range of separations for which there is distinct positional labeling and the spatial extent of contrast sensitive filters. Some positional changes of the individual elements may still be discerned well into the range where those elements both fall within the extent of a single contrast sensitive filter. Ultimately, however, it is purely changes in the contrast mechanisms that underlie the discrimination of the smallest offsets.

There is a considerable divergence of opinion on how best to describe the function of these contrast sensitive filters. On one hand is the class of theories that propose that the visual system decomposes the visual field globally into sinewave spectra (e.g., Pollen et al., 1971; Pollen and Ronner, 1982). Implicit in this type of analysis is that there is a demonstrable relation between the spectrum amplitudes and the percept. The pitfalls of such a global analysis have been pointed out early on (e.g., Cornsweet, 1970). The failure of global spectrum analysis to extend much beyond simple detection results may be seen in the perception of a checkerboard (Marr, 1980). The percept of a checkerboard is manifestly vertical and horizontal while the spectrum is diagonally dominant. There is no evidence, here or in the literature, that suggests that a preferred

combination of the responses of subpopulations of filters could be combined into global spatial frequency analyzers that form an acceptable metric for position.

On the other hand, the confusion is not relieved by assuming that bar and edge feature labels are assigned to the individual contrast sensitive filters. Feature theories depend on a collection of spatially local descriptors to characterize stimuli. The feature descriptors are selected because of their manifest and distinct appearance in the percept. The discreteness of the descriptors is maintained in the depiction of composite stimuli; a bar is a bar, whether viewed alone or in the presence of other bars. Any changes in the detectability of a feature when in combination are attributed to higher level interactions among the recognized features. Unfortunately, feature descriptions have not evolved into a comprehensive theory. Either the analytic functions that describe contour interactions are highly selective and therefore a large number of detector types are required (e.g., "grandmother cells"), or they are more cognitive in nature, containing abstractions that only work in restricted environments (e.g., Guzman, 1968). Both types of feature theories depend heavily on the labeling of individual detector output and formation of the percept from the peak activation of those labeled lines.

The traditional feature theory approach fails to capture the full extent of the relation between spatial contours and the sensitivity of detectors in the visual system. To characterize the line weighting function consistent with a one octave spatial filter, for example, as a "size" detector for the bar that produces a large

response from that detector by being equal in diameter to the central summation region is to gloss over much of the detector's diverse nature. It is no more appropriate to assign a perceived size to the activation of a detector having a given bandwidth and center frequency than it is to attribute perceived color to a given wavelength. The superficiality becomes even more apparent when a line weighting function with the same amplitude spectrum, now in odd-symmetric phase, is characterized as one of an undifferentiated set of "edge" detectors; the feature characterization makes no use of the information available in the different spatial frequency sensitivity profiles.

Consider, as an alternative approach, a representation that depends on the pattern of activation among a range of filters to determine the percept. A representation where the utility of a filter is not coopted by premature assignment to an abstraction (as in the feature theories) nor submerged in a global amalgam (as in the frequency theories). In this approach, the natural balance between spectrum bandwidth and spatial extent is the only constraint. The broadband spectra associated with two features, bars and edges will serve as good examples. An infinitely narrow bar (a one-dimensional spatial impulse) has a flat amplitude spectrum with a cosine phase term (figure 5.1). The broad spectrum induces activity at all center frequencies in even-symmetric filters centered on the bar. Each filter weights the spectrum according to its sensitivity and computes a linear sum. As the phase of the filter differs from 90°, the responses decrease until at 0°

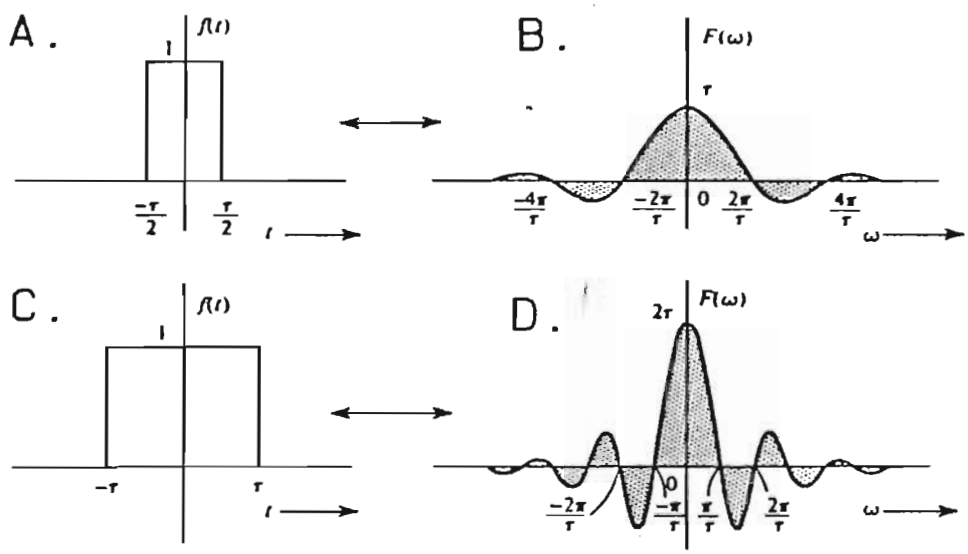

Figure 5.1 Spatial frequency spectra at different line widths.

The amplitude spectrum of luminous line has a $\frac{\sin x}{x}$ profile with a magnitude that is proportional to the product of the luminance and the width. The rate of oscillation of this amplitude spectrum envelope is inversely proportional to line width (compare a and b to c and d). For an infinitely wide line, the frequency spectrum becomes an impulse at zero cpd; in comparison, reflecting the symmetry of the Fourier transform and its inverse, the amplitude spectrum of an infinitely narrow line is flat.

(from Lathi, 1968)

there is no activity. The pattern of responses in filters offset from the bar, however, is markedly different. The phase shift associated with moderate offsets is sufficient to induce significant activity even in odd-symmetric filters. The peak response of an optimally positioned odd-symmetric filter to a narrow bar approaches that of a centered even-symmetric filter. Ultimately, at large offsets, the phase shift is large enough to produce cancellation of contributions to the linear sum within individual filters. The offset tolerated before cancellation occurs depends in large part on the spatial extent of the filter and, by extension, to its bandwidth. The net result is an island of activity distributed in space and spatial frequency associated with each discrete stimulus. This entire response ensemble comprises the representation of the bar - at detection, in discrimination and for recognition.

As the width of the bar, τ, increases, its frequency spectrum, $F(\omega)$, changes:

$$F(\omega) = \tau \left\{ \frac{\sin\left\{ \frac{\omega \tau}{2} \right\}}{\frac{\omega \tau}{2}} \right\} \qquad [5.1]$$

The relation between bar width and amplitude spectrum may be viewed as a consequence of the way a fixed spatial offset produces larger and larger phase shifts as the spatial frequency increases. A finite width bar is the sum of many impulses, each with a different offset and consequently, a different interaction of phase. Carried to the semi-infinite limit, the extended superposition results in an edge (figure 5.2). The amplitude density distribution of the edge is different from

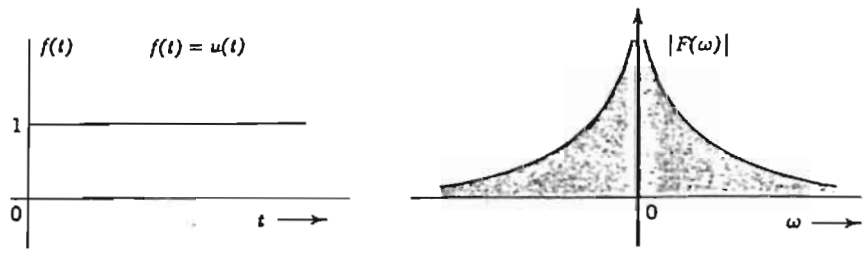

Figure 5.2 Fourier spectrum of an edge.

The amplitude spectrum of an edge has a spectrum density that is inversely proportional to spatial frequency. The odd symmetry of the exponential representation reflects the sine phase of the spatial frequencies that comprise the edge. The impulse at zero cpd is a consequence of the step function going from 0 to 1 rather than maintaining a symmetry about the origin.

that obtained with an impulse because of the way the offset impulses are summed within each filter, but nonetheless remains broadband. Both features stimulate many detectors, although to varying degrees. It is important to note that all stimuli induce activity that is extensive in both space and spatial frequency. The extensive detector activation is especially true for acuity targets where the contrast of discrete contours is generally high and, consequently, even relatively low amplitude spatial frequency components are above threshold.

It is possible, then, that measures of spatial acuity are enhanced by pattern discrimination wherein the small positional offsets produce changes in the frequency spectrum large enough to alter significantly the response of a group of contrast sensitive filters. To establish the credibility of this argument, the preceding chapters examined the relation between contrast and measurements of acuity. In addition, a probability summation model was expanded to account for discrimination of superthreshold stimuli. What emerged was a consistent flow of results and reasoning in support of contrast enhanced localization as a unifying approach to spatial acuity.

First, a baseline of pure positional performance was established. The mosaic of labeled regions appears to be no finer than 5' arc. Within and among these regions, detection of both narrow- and broadband stimuli may be modeled by probability summation among the responses of one octave spatial filters. With the addition of an additional mechanism to adjust gain at high response levels, the probability summation mechanism will simulate the discrimination of resolution

and localization stimuli as well. The simulation of localization performance was accomplished entirely with contrast sensitive filters. No recourse was made to any positional interpolation scheme.

The answer to the continuity question posed above, then, is no. There is no need to posit a facility that extends the performance of the position sense to "hyperfine" resolution. An analogy may be made to the discrimination of temporal duration by the visual system. A linear system with a finite integration time can be used to form a simple model for the discrimination of temporal duration. Durations that are grossly disparate are associated with clear and isolated changes in the pattern of the model's temporal responses. Changes in the model's response associated with the beginning and end of the interval shift with changes in duration. At very short durations, however, the discrimination of durations occurs uncoupled from changes in the shape of model responses. Only the amplitude of a fixed shape (the impulse response) changes. Although stimuli of different short durations may be discriminated based on intensity differences, no claim would be made that the perceived duration of two brief stimuli is distinguished. The major difference between the temporal and spatial domains is that the temporal filters are lowpass while the spatial filters are bandpass.

Now that a theory of contrast discrimination as a mechanism for resolution and localization has been given substantial analytical support, it remains to demonstrate its utility by accounting for the interactions that abound in the

literature.

Analysis of interactions

critical interval

One of the most consistent findings in localization is that detection of positional offset is optimal when stimulus features are separated by 2 to 6' arc (e.g., Westheimer and McKee, 1977c; see figures A.7, 3.15, 3.17 and 3.20). This property of localization may be understood by examining the effect of criterion separation of features on the stimulus spectrum and the relation of the different patterns of spectrum amplitude to the response of the contrast sensitive filters. Commonly, although not universally, the elemental features of a localization stimulus are small and uniform in type. As described in chapter 3, the stimuli in these cases may be viewed as the convolution of the feature and a set of impulses, one for each feature site in the composite stimulus. The spectrum of such a stimulus, then, is the product of the feature spectrum and the spectrum of the impulse array. Due to their small size the features have Fourier spectra that are relatively constant in the low and moderate spatial frequencies, the range where human contrast sensitivity is greatest. As a consequence, in the convolution the positional spectra are relatively unmodulated by the form spectra and the effect of a positional change is largely independent of the form of the elements being moved. The undulating spectrum envelopes that are characteristic of the impulse arrays is apparent in the cosinusoidal spectra of a simple one dimensional

stimulus, a line pair (see figure 3.12). Changes in position about a criterion separation are reflected in the period of oscillation of the spectrum envelope.

The existence of a critical interval reflects a trade among stimulus and filter properties. At small criterion separations the slow oscillation of the spectrum envelope positions the first spectrum null in the high spatial frequencies. As the criterion separation is increased the period of oscillation of the amplitude envelope decreases proportionately. The decrease in period of oscillation moves the initial spectrum null to lower spatial frequencies. The combination of higher filter gains and lower optical attenuation increases the detectability of changes in the amplitude spectrum due to offsets. The subsequent spectrum nulls make less of a contribution to the increase in sensitivity because the spatial frequencies of succeeding spectrum nulls are proportionately closer. Filters in the region of the second zero-crossing are broad enough to be sensitive in the region of the third as well (zero-crossings of bright line pairs fall at odd multiples of the frequency of the first). The relation between the stimulus spectrum and the span of filter sensitivity is maintained at different criterion separations because of the constant octave bandwidth assumption contained in the model. Filters that span more than one zero-crossing are less sensitive to offset because the offset spectrum at adjacent zero-crossings are of opposite sign and cancel when integrated within a single filter (see figure 3.13). This process continues until a lower bound is reached both in the increase in filter gain and in the population of filter center frequencies. As the initial zero-crossing of the amplitude envelope moves below 0.5 cpd, not only are

there no filters that have an optimal weighting function needed to form a null, the best available filters are now sensitive to multiple zero-crossings. Ultimately, the separations are large enough that the rapid oscillations place many zero-crossings within the integration region of a single filter. The multiple cancellations eliminate any contribution to the detection of offset; however, the separations are now easily large enough to activate distinct regions of position. Any continued increase in offset threshold (e.g., Andrews and Miller, 1978) is due to the cortical magnification present at larger eccentricities.

The isolation of the integration at the initial spectrum null is dependent on the constant bandwidth assumption. Larger bandwidths (in octave terms) would reduce the detectability of offsets. Data relevant to filter bandwidth over the entire range of spatial frequencies, however, are painfully scarce. There are suggestions, especially from electrophysiological data (e.g., DeValois et al., 1982), that bandwidth (in octaves) decreases with increasing spatial frequency, although it increases in absolute terms. If the relation between bandwidth and spatial frequency were more appropriate than the constant bandwidth assumption, there would be less isolation of the initial spectrum null and therefore a diminished contribution to sensitivity at the low frequencies and relatively less integration of the spectrum differences at high spatial frequencies.

Another factor that reduces sensitivity to offset at larger separations is the decrease in the magnitude of the difference spectrum for a given offset as measured by the area under the first lobe of the difference spectrum. Therefore,

not only does the absolute filter bandwidth decrease with decreasing spatial frequency, there is less there to be summed. In spatial terms, the decrease in response to a fixed offset in filters sensitive to lower spatial frequencies is due to the shallower slopes of their weighting profiles (all else being equal).

In summary, the range of optimal criterion feature separations known as the critical interval is the result of a trade between the improvement in sensitivity obtained as small separations are increased and a decrease in the signal available to be integrated. Ultimately, at large separations, sensitivity to offset is limited by a lower bound on the range of filter center frequencies.

length versus separation

That the threshold for offset decreases with increased line length was known at least as for back as French (1920; see appendix A). An additional complication for localization theories was introduced by Ludvigh (1953). He found that even dots could be aligned as well as lines if they were separated by a few minutes of arc. Most attempts to explain the interaction have centered on featural interactions among the proximal ends of the line segments. If, instead, the coincidence stimulus is viewed as the convolution of a line segment (form) and impulses located at each feature site (position) the problem decomposes into a two dimensional case of the the critical interval. In this analysis, it is the separation of the impulses that is the important factor, not the distance between the proximal ends. The traditional vernier coincidence task contains two impulses (form sites)

and is the two dimensional analog to the line pair.

The Fourier transform of the coincidence stimulus may be represented by an equation that is factorable into vertical and horizontal frequency components related to form and a third component related to the separation of the impulses. Coincidence targets have a two-dimensional point of symmetry, a property that produces spectra that are entirely in cosine phase (i.e., $\pm 90^{o}$). The rectilinear profile of the form components corresponds to a two-dimensional sampling function amplitude profile; the positional separation between the midpoints of the bars (not the separation between the proximal ends) produces a cosinusoidal modulation of the sampling function profile in the orientation containing the midpoints of the bars. The entire expression is:

$$F\{\omega_h,\omega_v\} = \left\{W \frac{\sin\left\{\frac{W\,\omega_h}{2}\right\}}{\frac{W\,\omega_h}{2}}\right\} \left\{L \frac{\sin\left\{\frac{L\,\omega_v}{2}\right\}}{\frac{L\,\omega_v}{2}}\right\} *$$

$$\cos\left[\left\{\omega_h^2 + \omega_v^2\right\}^{1/2} \cos\left\{\tan^{-1}\left(\frac{L+S}{dx}\right) - \tan^{-1}\left(\frac{\omega_v}{\omega_h}\right)\right\} \left\{\left(\frac{dx}{2}\right)^2 + \left(\frac{L+S}{2}\right)^2\right\}^{1/2}\right]$$

The separable sinc functions that comprise the spectrum of the rectangular line create an island of spectrum amplitude that is centered on zero cpd and has principal dimensions that are inversely proportional to the length (L) and width (W) of the line. The island is surrounded by elliptical rings of alternating positive and negative amplitudes that decrease in amplitude with increasing spatial frequency. This concentric pattern of oscillation is itself modulated by a

horizontal sinusoid in cosine phase with the origin that has a period inversely proportional to the sum of the line length and the separation of the proximal ends (S). A major consequence of this modulation is the creation of a series of lines with constant vertical (but varying horizontal) spatial frequency that form the boundaries between regions of opposite amplitude. These boundaries are the two-dimensional equivalent of a zero-crossing.

Figure 5.3, a illustrates the pattern of spectrum amplitudes corresponding to a criterion coincidence stimulus with line segments that are rectangular (8 by 0.2' arc) and are separated by 3' arc. The large ratio of length to width is reflected in the narrow horizontal slice of activity that forms the central island. Superimposed on this is the rapidly oscillating cosine that is a consequence of the magnitude of the length and separation. When line length is reduced to 0.5' arc (figure 5.3, b) the rate of horizontal oscillations from both the sinc and the cosine are markedly reduced. The central island is much more oval reflecting the smaller length to width ratio. The shorter lines also cause peak amplitude to be proportionately smaller. Nonetheless, the 3' arc proximal separation is sufficient to cause horizontal striations of zero-crossings at fairly low spatial frequencies.

Reduction of the proximal to 0.5' arc produces little change in the spectrum of the 8' arc long coincidence target (figure 5.4, a). Periodicity of both the island/ring structure and the cosine modulation is slightly lower. As a consequence the zero-crossing striations are more widely separated and occur at slightly higher spatial frequencies. For the short lines the island/ring structure

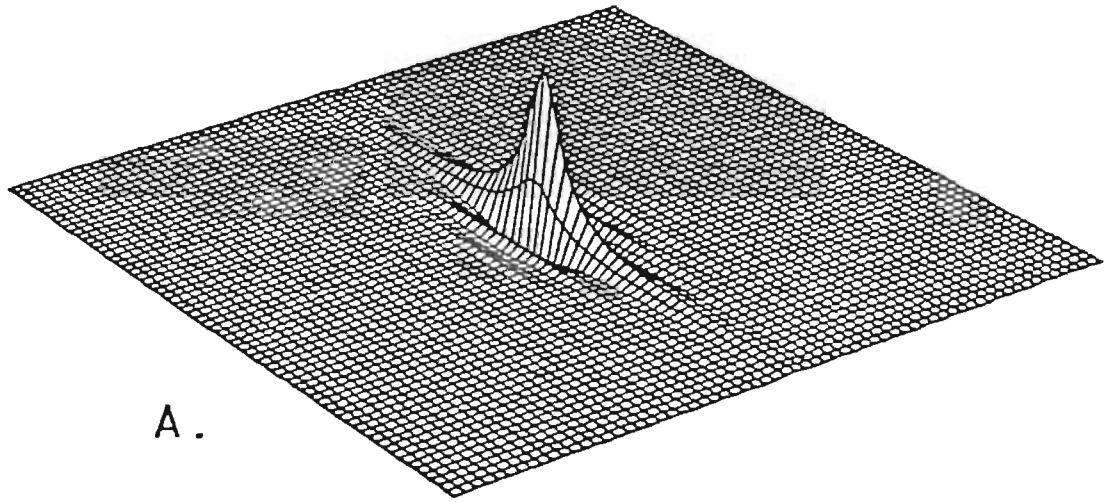

Figure 5.3 Fourier spectra for coincidence stimuli (separation = 3' arc).

The two-dimensional Fourier spectra for two line segments can be plotted in a Cartesian grid. The origin is located in the center of a plane where spatial frequency increases radially and orientation varies with the angle of the vector connecting any point with the origin. The axis of vertical modulation (gratings with horizontal bars) runs SW to NE through the origin. The axis of horizontal modulation runs NW to SE. Spectrum amplitude is positive up and negative down in this perspective view (which usually asymptotes to zero by the edge). Grid resolution is 2 cpd with an upper limit of 64 cpd. In a, the parameters are: length, 8' arc; width, 12" arc; and separation 3' arc. In b, they are 30", 12" and 3" arc, respectively. All spectra reflect the attenuation by the OTF (retinal contrast for a 5.8mm pupil). In b, the amplitudes are increased by a factor of 10.

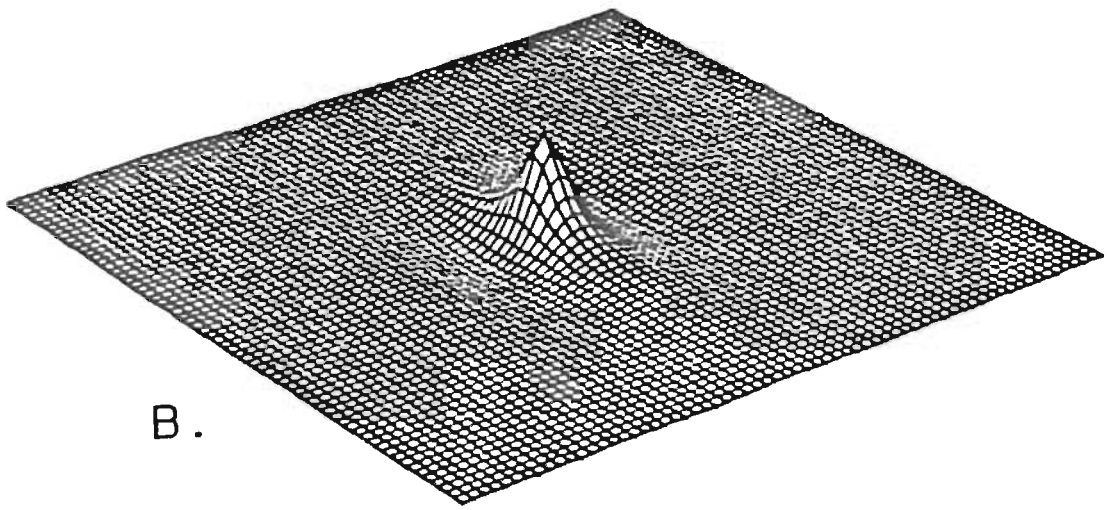

B.

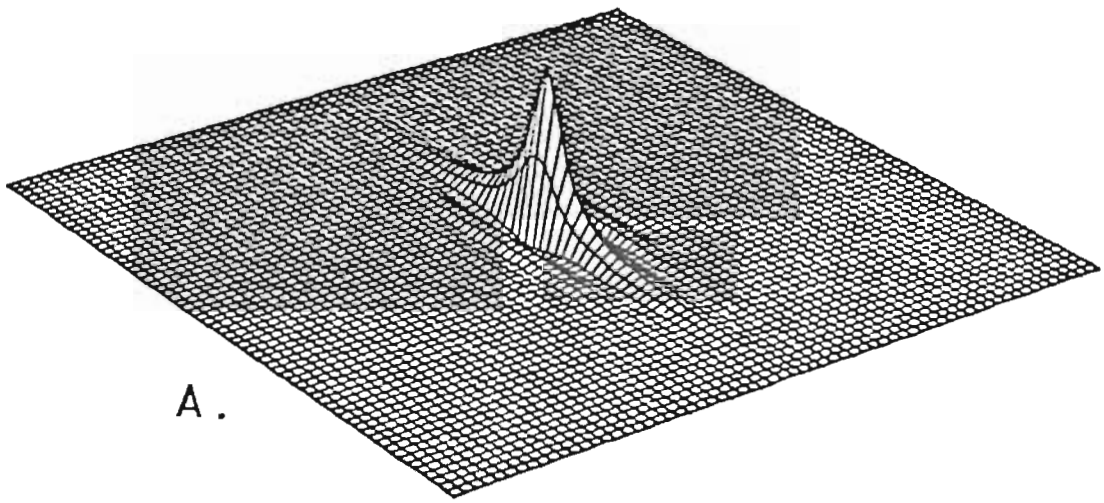

Figure 5.4 Fourier spectra for coincidence stimuli (separation = 30" arc).

All conditions are the same as in figure 5.3 with the exception of the decrease in proximal separation.

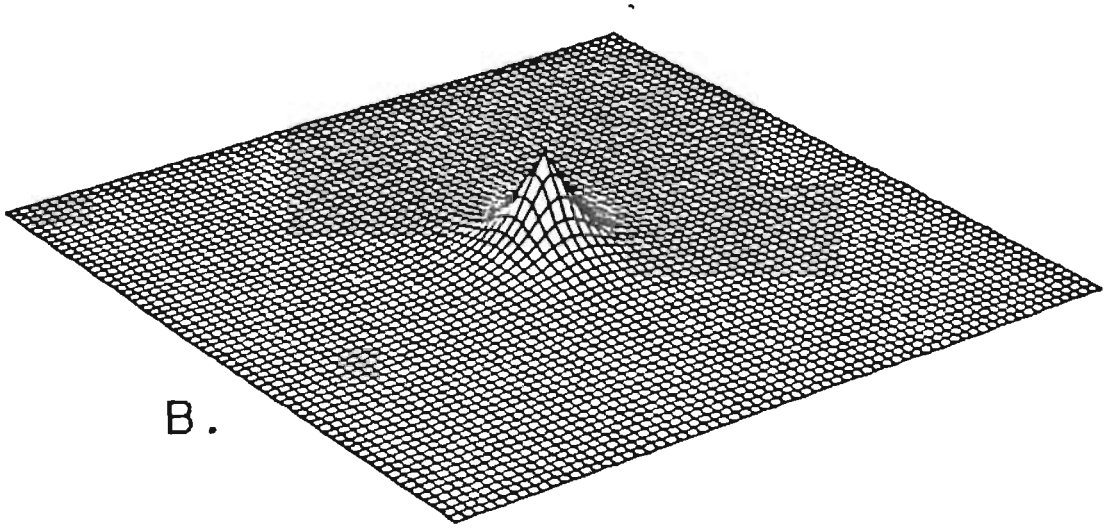

B.

remains the same as with the larger separation; however, the period of cosine modulation is greatly altered (figure 5.4, b). The short line length and small separation combine to yield a modulation with an initial zero-crossing at high spatial frequencies. It is the absence of zero-crossings in the range of high contrast sensitivity that sets this last condition apart. Only when the lines are both short and proximal is there a marked increase in offset threshold (see figure A.5). Any combination of of length and separation that totals a few minutes of arc moves the impulses into the optimal range of spacing (the "critical interval").

An examination of the two-dimensional difference spectra for the coincidence stimuli further supports the critical interval analogy. As in the one-dimensional conditions (cf. figure 3.13) the peaks of the difference spectra coincide with their respective zero-crossing loci. The reason for the correspondence is the same in both conditions, changes in position alter the periodicity of the cosine modulation of the stimulus spectrum. The difference of two cosines is sinusoidal and the phase relation between sine and cosine yokes the sine peak with the cosine zero. It is important to note that it is the amplitude envelope that is in sine phase, not the actual frequency components (they are in cosine phase). An additional complexity in the two-dimensional condition is a shift in orientation of the modulation that is a function of the offset magnitude. The net result is that the difference spectra are antisymmetric about both axes. The modulation of the amplitude envelope along the horizontal frequency dimension, however, remains in sine phase. Again, exceptional sensitivity to offset is derived from the match

between maxima in the band-limited integration of the spectrum differences and minima in the band-limited integration of the criterion spectra.

Figure 5.5 illustrates the difference spectra associated with a fixed 4" arc offset in the criterion stimuli with a 3' arc separation (figure 5.3). The difference spectra are antisymmetric about both axes and the modulation of the amplitude envelope is at a lower frequency for the shorter lines. The ridges and crevasses flow along the zero-crossing loci of the criterion spectra. The amplitude of the difference spectrum for the shorter lines is smaller reflecting the reduced amplitude of the sinc function associated with length. The difference spectra for long lines at smaller separations is very similar to that obtained for larger separations (figure 5.6, a). The difference spectra for closely spaced short lines shows a much greater change (figure 5.6, b). Although the spectrum changes are quantitative (all graphs can be derived from the same function), they follow the same pattern as obtained offset thresholds. Increasing the proximal separation of long lines to several minutes of arc improves the peak difference response by only 15% while the same change in separation with short lines increases the peak response by a factor of 2.4.

Although the model was not expanded to include probability summation among filters of different orientations it is likely that the same principles would apply. In particular, it is likely that in such a model discrimination would still exhibit a Weber region, a region where high background responses would attenuate sensitivity to change in offset. This gain mechanism would account for

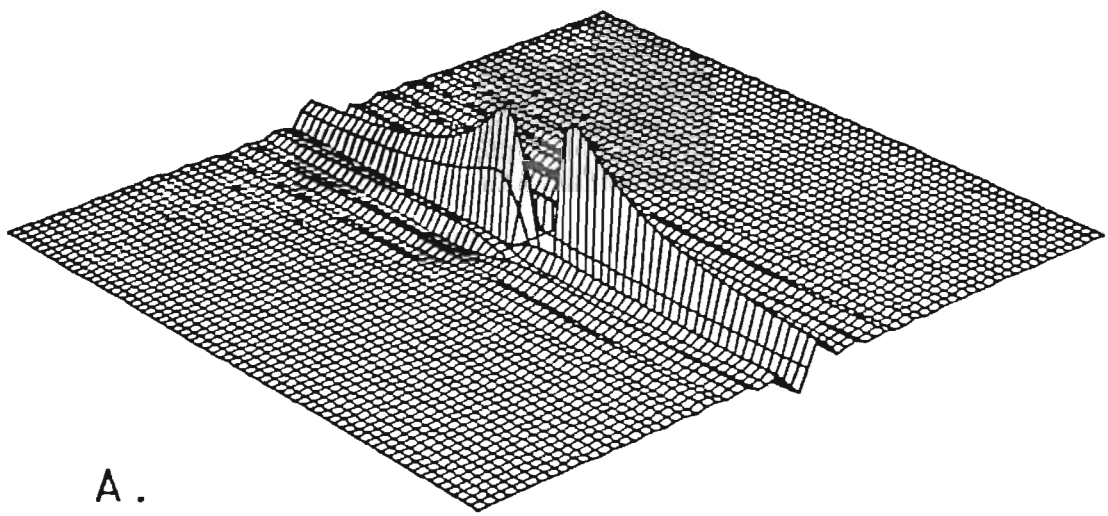

Figure 5.5 Fourier difference spectra for coincidence stimuli (separation = 3' arc).

All conditions for the criterion stimuli are the same as in figure 5.3. The offset is 4" arc

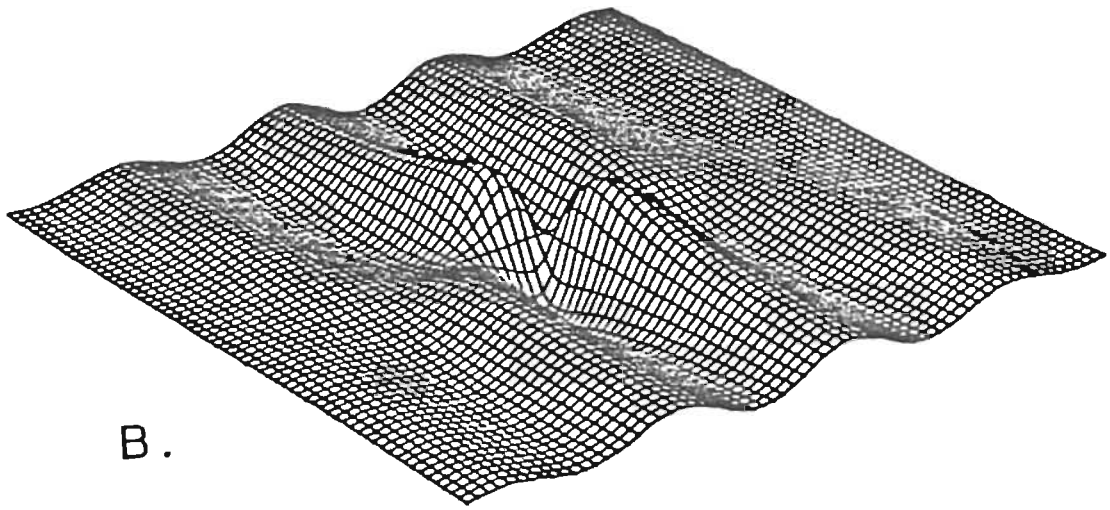

B.

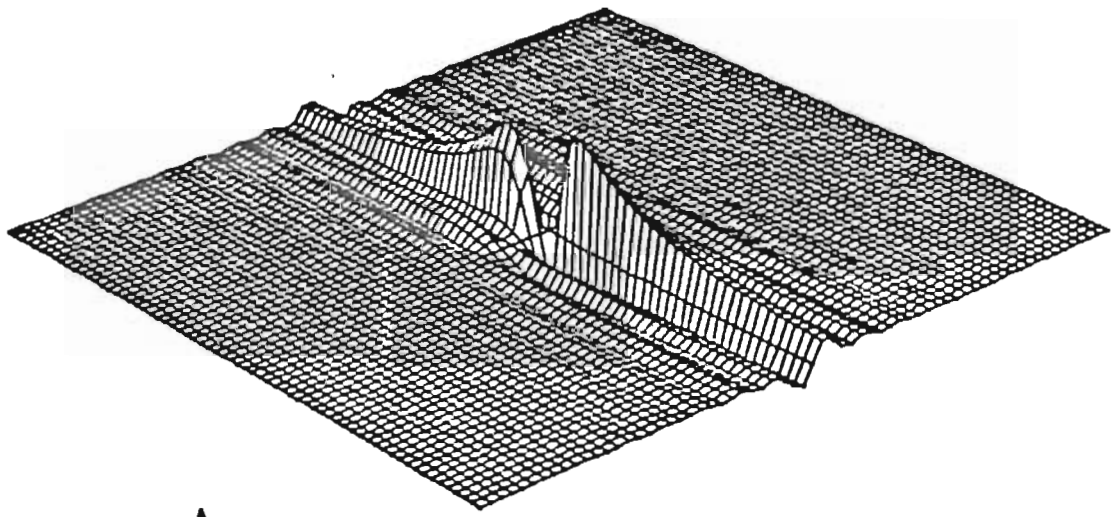

A .

Figure 5.6 Fourier difference spectra for coincidence stimuli (separation = 30" arc).

All conditions for the criterion stimuli are the same as in figure 5.3. The offset is 4" arc

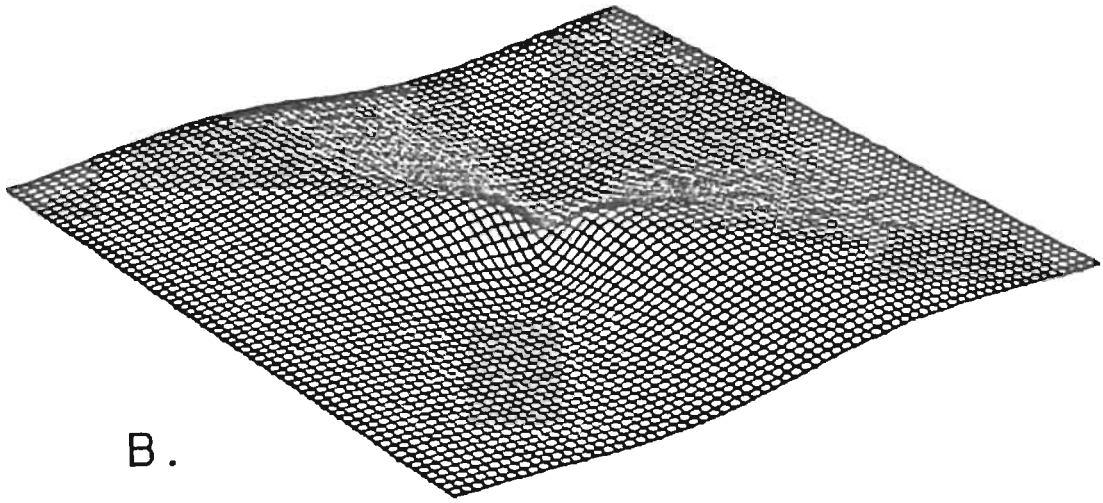

B.

the similarity in sensitivity for offset with long and short lines at moderate separation even though the absolute spectrum amplitudes are more than an order of magnitude apart. Ultimately, the effective length of a line is limited by the center frequency of the largest filter. Even though the centroids of line segments move apart with increasing length, the centroids of the line segments weighted by filter sensitivity profiles asymptotically approach a limit set by the largest receptive field.

The importance of the peaks of the difference spectra in the detection of offset is supported by Findlay's (1973) masking results (see figure A.14). In that study, sinewave masks interfered maximally with the detection of offset when the mask orientation was $\pm 20^{o}$ from the vertical. An examination of the threshold difference spectrum for a coincidence target 8' arc in length reveals that there is a correspondence between stimulus spectrum zero-crossings and peaks of the difference spectrum both above and below the horizontal frequency axis. A $\pm 20^{o}$ angle measured from the origin would intersect the zero-crossings of the amplitude spectrum in a region of high contrast sensitivity. The exact locus of optimal sensitivity would depend on the specific parameters of the stimulus.

flanking lines

The addition of parallel lines to localization stimuli also produced results that were difficult to explain. Andrews (1967a, b) used a single long horizontal line as a reference in orientation discrimination tasks with no untoward consequences for

threshold. Rather than serving as a reference, however, flanking line pairs interfere with performance on both coincidence and orientation tasks (Westheimer and Hauske, 1975; Westheimer et al., 1976). This interference effect manifests a tuning of threshold that is reminiscent of critical interval interactions. Thresholds for offset or change in orientation is increased over those obtained with no flanks only for stimulus-flank separations of a few minutes of arc; for narrower or wider separations, the effect diminishes rapidly.

The cause of the lowered performance may be seen by comparing the spectrum amplitude distribution of the flanking bars and the offset difference spectrum (figure 5.7; c.f. figure 5.5). If the spectrum amplitudes are high in the region where the difference spectrum of the coincidence lines is also large (near a spectrum null), the sensitivity to the difference spectrum will be reduced. Changing the separation of the flanks will vary their effectiveness as a mask in a manner similar to the variation of offset threshold for the two-bar stimulus, and for the same reasons: the sensitivity for the spatial frequencies in the region of the initial side-lobe increases with line separation, the integrated amplitude of each side-lobe decreases with increasing line separation and, ultimately, cancellation of the responses of opposite phase occurs within even the largest detectors when the line separation nears the spatial boundaries of the filters. In this interpretation, the broadband amplitude spectrum of the flanking lines accounts well for the insensitivity of the masking effect to the orientation of small elements in the flanking array found by Westheimer and Hauske (1975). It is the dependency of

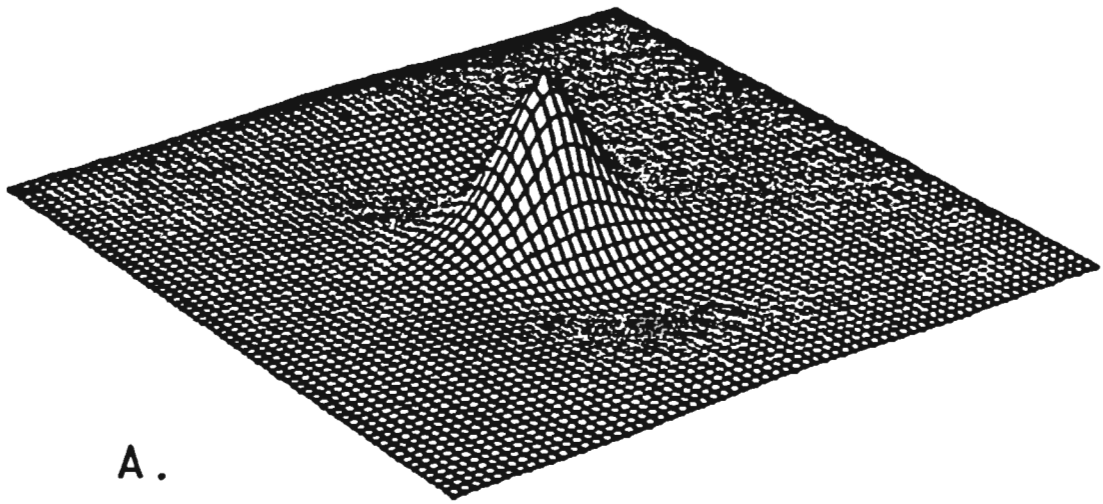

Figure 5.7 Fourier spectra of flanking lines.

The two-dimensional Fourier spectrum of two thin vertical lines is characterized by a cosinusoidal oscillation of the horizontal frequency components that varies inversely with line separation and a vertical modulation (sinc) that oscillates at a rate that is inversely proportional to line length. The spectra for 4' arc lines is shown for three separations: a, 8; b, 16; and c, 32' arc. All conditions are the same as in figure 5.3.

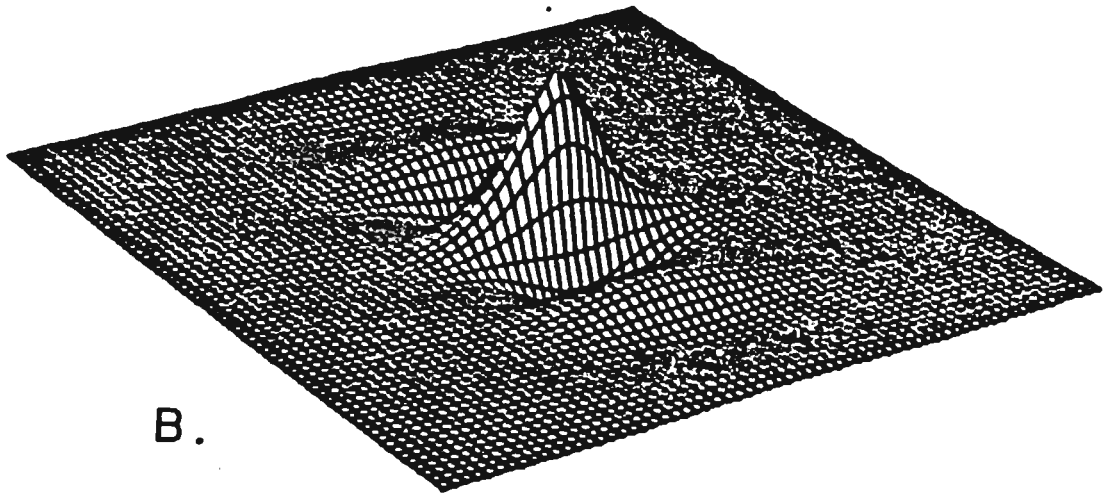

B.

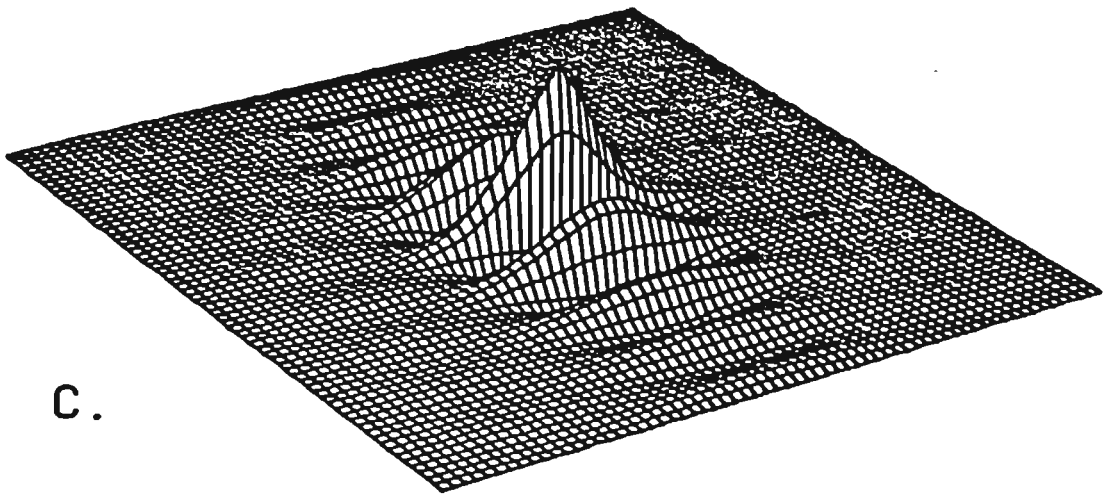

C.

the oscillation of the spectrum envelope on line separation (especially at the low spatial frequencies) that determines the masking effectiveness of the flanks. The distance between the centroids of the flanking arrays determines most strongly the spectrum shape, not the high frequencies of the individual elements in the array.

Further, the effect of the flanking stimuli is not constrained to be normal to the orientation of the bars; the two-dimensional Fourier transform of the flanks contains large amplitude spatial frequency components over a wide range of orientations. The difference limen in filters of many orientations is increased by the presence of flanking lines, thus decreasing the detectability of activity in the detectors that are the primary contributors to the detection of spatial offset in the absence of flanking lines. Masking effectiveness at oblique orientations contains a trade between the scalar increase in spectrum amplitude and the increase in the periodicity of the sinc function along the vertical frequency axis, both of which are proportional to line length. Contributions to an optimal trade come from many filter and stimulus parameters. Such a trade may have contributed to the selection by Westheimer of flanks that were only half the length of the lines in the coincidence stimulus being masked. The shorter lines would have a broader primary spectrum lobe in the vertical direction, producing a relative increase in the amplitude of the oblique components.

width

As long as the width of each element is narrow (< 1/2' arc) then those aspects of the spectrum attributable to the form of the stimulus have little effect on the positional interactions over the range of greatest contrast sensitivity. For those localization configurations where the elements are all of the same form, the spectrum is simply the frequency by frequency product of the form and position spectra. Figure 5.1 and equation [5.1] describe the inverse relation between bar width and the width of the primary spectrum lobe. The form spectrum usually acts like a scalar over a limited region of the position spectrum; however, with wider bars the shape of the form spectrum may become significant. A form spectrum with a zero-crossing at the peak of a positional difference band would greatly reduce its contribution to the discrimination task. The widths typically used in the majority of localization experiments do not produce such a destructive coincidence and should not therefore significantly alter threshold.

There is an another factor that may have a significant effect on the detection of offset with wide bars: the width acts as a scalar multiplier of the entire amplitude spectrum. There are always some filters with sensitivities close enough to the spectrum null to have criterion responses below the knee of the discrimination function. The larger spectrum difference that accompany shifts of the wider bars would be expected to produce larger discrimination responses in these most sensitive filters. On the other hand, the Weber region gain adjustment proportionately reduces much of the response of the nonoptimal filters to the

difference spectrum while at the same time, the steeper slope of the scaled criterion response reduces the range of filters with responses that are below the knee (optimal), mitigating the aggregate contribution of the filter ensemble to the detection of offset with wider bars. The fact that offset threshold does not decrease inversely with bar width does put a lower limit on the range of filters that can be isolated by attention or labeling either across space or spatial frequency, or both. This balance of trades also occurs for changes in line length of coincidence stimuli.

The data on variation of threshold as a function of width are sparse, offering little to constrain the parameters that would determine these trades (see appendix A). One illustration of the consequences of these trades may be seen by comparing the results from the two and four line interval judgment tasks. The four line condition can be viewed as a form of the two bar task where the separation of the outer intervals corresponds to bar width. Even though the peak amplitude of the four bar spectrum is twice that of the two, the four line threshold is not halved. The spectrum of the two lines that constitute the bar width reduces the amplitude of the positional spectrum around the spectrum null (see figure 3.18).

While the more rapid undulations of the form spectrum of wide bars in coincidence stimuli may reduce the positional difference spectrum at some spatial frequencies, the larger scalar multiplier may increase it at others. The two-dimensional amplitude spectrum of an 8 by 15' arc bar is a factor of 75 greater

than those of narrow line stimuli used in some studies (e.g., Westheimer and Hauske, 1975). For some intermediate widths, the secondary lobes of the sampling function amplitude profile [5.1] are larger than the primary lobes of the narrow bar spectra. This trade, between the shape and the scale of the bar amplitude spectra, combined with limited sampling of stimulus parameters, may account for the mixed results found with variation of the width of the coincidence targets.

orientation

The relative orientation of spatial detail within two-dimensional localization stimuli has often been cited as the cue for detection of offset (e.g., Ludvigh and McKinnon, 1967; Andrews, 1967). In fact, orientation discrimination of a line itself may be interpreted as a localization task when the displacement of the end of the line is used as a metric. The use of proximal lines ends as a cue, however, fails to account for the effect line length has on offset sensitivity and does not at all address one-dimensional localization capabilities.

In models such as CELT, orientation tuning of the linear spatial summation stage is applied in the same way as spatial frequency tuning. The detection of offset in two-dimensional stimuli depends on the correspondence between the two-dimensional offset spectrum and the two-dimensional criterion spectrum. While it is true that offset spectra do vary in orientation with the magnitude of the offset, the orientation of the largest contributions to offset detection do not

correspond to the orientation of manifest features in the stimulus. The lack of correspondence stems both from the broadband nature of most localization stimuli and the reduction of filter response contributions to discrimination when compared to large criterion responses (the Weber region).

The 20' arc orientation discrimination thresholds, as well as the threshold decreases that are associated with increased length, are presumed here to be mediated by the responses of two-dimensional orientation tuned ($\pm 12^{o}$) bandpass (1 octave) filters. Within the linear summation stage of a detector, the change in response produced by a discriminable rotation of a line are not very different from that produced by changes of contrast or of spatial frequency.

Orientation is a special characteristic in that it is both a contour (feature) parameter and a spatial frequency parameter. However, it should be emphasized that the orientation of local contours does not necessarily signify the orientation of the principal spectrum amplitudes in a stimulus. Consider the checkerboard pattern. The compelling perception is one of rows and columns of squares. In fact, there are no horizontal or vertical spatial frequency components in its two-dimensional spectrum. The major activity is in the oblique orientations. Similarly, the major components of the two-dimensional difference spectrum (corresponding to the difference between aligned and offset coincidence lines) appear at oblique orientations. A 12 cpd sinewave grating oriented $\pm 20^{o}$ from vertical was found to interfere maximally with the a coincidence task. The major determinant of the beating pattern that is the difference spectrum is the orientation of the centroids of

the two bars. The orientation of corresponding points on the proximal ends of the bars varies widely with end separation, but has little effect on offset threshold when the centroids are sufficiently separated by line length.

A feeling for the types of spectrum differences that occur with vernier stimuli having more than two components can be acquired from viewing optical Fourier transforms (see Harburn et al., 1975). When the two-dimensional spectra for aligned and offset 3-dot stimuli are compared, it can be seen that asymmetries in the stimulus resulting from the offset produce gaps in the amplitude spectrum. These gaps correspond to maxima in the two-dimensional difference spectrum. Positional offsets in the two-dimensional stimuli can produce difference energy at many orientations. As with the effects of width, orientation effects may interact with form if the shape becomes either large or complex. For example, consider the complex pattern of zero-crossings that occurs when line length is not an integral multiple of centroid separation. The zeroes due to line length (a sinc function) form a beat pattern with the zeroes due to centroid separation (a cosine function).

luminance

The improvement of vernier acuity with increased levels of luminance is similar to that found for contrast sensitivity. Acuity improves, rapidly at first, then more slowly as the luminance increases from mesopic levels. The improvement in sensitivity is found to some extent for all spatial frequencies.

wavelength

Localization improves very little when the illumination is changed from white to monochromatic light. The lack of improvement in performance as a function of chromatic bandwidth is consistent with results obtained in the literature for normal acuity targets. The relative diffraction-limited attenuation at both high and low spatial frequencies is small compared to the attenuation at intermediate spatial frequencies. If the discrimination involved in localization is mediated by spatial filters with sensitivities near the low end of the spectrum, the monochromatic illumination would offer very little advantage.

contrast

Along the same line of reasoning used in the analysis of wavelength effects, it is not surprising that blurred and sharp stimuli can be aligned with similar precision. Moderate defocusing acts somewhat as a low-pass filter and would leave the difference spectrum in the low spatial frequency range relatively unattenuated. The correlation between localization thresholds and contrast sensitivity further supports the hypothesis that contrast discrimination underlies the detection of small offsets. Localization improves with increases in target contrast (especially at low contrasts). In this view, the contrast of a discriminable stimulus may be reduced until the peak activity generated by the difference spectrum reaches threshold for the most sensitive detector(s).

temporal

The relation between exposure duration and localization is like that found for resolution acuity tasks. The metacontrast effects obtained with localization stimuli are also very similar to those found with more conventional spatial stimuli. The improved resolution of the temporal asynchronies at spatial separations of 2 to 6' arc are consistent with the interaction between the spatiotemporal bandwidths of the detectors and the positional and temporal spectra of the offset.

The low spatial frequency nature of some difference spectra should result in a decrease in localization threshold when the bars are counterphase modulated if free viewing is used in place of flashed presentation. The decrease in threshold should be proportional to the increase in sensitivity obtained when low frequency gratings are temporally modulated.

motion

Even moderate rates of motion smear the retinal images of very small offsets across distances much larger than a receptor diameter. Since the difference spectra produced by threshold offsets contain significant amounts of low and moderate spatial frequencies, the spectrum differences at these frequencies may be used to detect small offsets. Further, the visibility of low spatial frequencies has been found not to degrade with moderate image motion. Hence the fact that vernier offsets are robust with respect to moderate amounts of motion should not be surprising given the proposed discrimination mechanism.

monocular:binocular viewing

The dichoptic experiments indicate that there is significant cortical processing involved in localization. Sensitivity to an offset presented to one eye is degraded by flanking lines presented to the other eye. A cortical locus is consistent with the nature of the detectors, especially their orientation selectivity. Sharp orientation tuning is a property of the cortex and is essentially absent in the concentric receptive fields of the lgn and retina.

summary

In chapter 3, a mechanism was proposed that passed the first requirement of localization: the production of seconds of arc thresholds. Bandpass spatial filters sensitive to contrast enhance performance in positional tasks. It is clear now that these filters also fulfill the second requirement: the simulation of obtained spatial interactions. The properties of the contrast-sensitive filters provide a unified source for the divers interactions.

Next, the performance of the particular model used here to demonstrate the feasibility of the enhancement theory is examined and alterations are proposed.

Comments on the model

One of the major assertions in this thesis is that all of the spatial acuity measures are consistent with the responses of an array of medium bandwidth spatial filters. In support of the assertion, an instance of this class of models was

used to simulate Observer performance in the experiments presented here. In this section, the simulations are reviewed first to reassert the overall validity of the model; then, the contributions of each component of the model are analyzed. Based on the review and analysis, improvements in the parameter values and of the formulations themselves are suggested.

model performance

The majority of the degrees of freedom in CELT are taken up by the adjustment of filter gain as a function of filter center frequency. (The only other parameter that is optimized specifically for the current data is the threshold response for gain compression, the lower region of the Weber region.) All other parameters are taken directly from the literature. The values used are mostly consensus estimates that represent a large body of data. The parameters from the literature were selected prior to the simulations and were not altered subsequently.

The model contains filters at 64 center frequencies that are spaced at 0.5 cpd intervals between 0.5 and 32.0 cpd. The gain at each center frequency was determined in an iterative adjustment process that was repeated until the aggregate response was close to 1.0 for a range of threshold sinewaves. Threshold contrast was estimated by fitting the observed data with cubic splines and interpolating the contrasts at the 64 center frequencies. Although an exact solution with positive gains could not be found (see appendix C), the iterative procedure produced a solution that was within $\pm 1.5\%$ of the desired response aggregate at all spatial

frequencies (table 5.1). The ratio of modeled to observed responses is quite flat over the entire range of spatial frequencies, dropping slightly at the high end. In linear terms, then, the absolute contrast error increases with spatial frequency. Thus determined, the 64 gain estimates form the only portion of the model tailored to the Observer's sensitivity under the conditions of the detection experiments.

When applied to the detection of a single line the model overestimates the contrast required at threshold by 16%. The same underestimation of aggregate filter response is seen in the simulation of the four line detection performance. Although the pattern of increase in contrast threshold with criterion separation is maintained by the simulation, the modeled estimates of contrast threshold are markedly higher than those observed. The simulations of the detection of intermediate criterion separations were the poorest fits produced with the current parameters.

By comparison, the simulations of the resolution and localization tasks somewhat underestimated the contrast required for discrimination. The only parameter that was optimized for the current discrimination data was the lower response cutoff of the Weber region. A value of 0.4 was found to be optimal (where 1.0 is the aggregate response required for discrimination threshold). With this value as the knee of the contrast discrimination function, not only did the absolute values of the simulation thresholds match the observed thresholds, the form of the interactions matched as well. Specifically, the decrease in resolution

Table 5.1 CELT: Summary of model performance.
(last model/version 8)

Sinewave Detection

spatial frequency (cpd)	modeled threshold (% contrast)	observed threshold (% contrast)	95% confidence interval (±% contrast)
0.5	0.55	0.52	0.06
1.0	0.44	0.42	0.06
2.0	0.41	0.41	0.04
4.0	0.52	0.52	0.05
8.0	0.98	0.99	0.07
16.0	4.35	4.37	0.51
32.0	30.58	30.93	4.85

Single Line Detection

modeled threshold (% contrast)	observed threshold (% contrast)	95% confidence interval (±% contrast)
31.9	26.8	1.5

Four Line Detection

criterion separation (sec arc)	modeled threshold (% contrast)	observed threshold (% contrast)	95% confidence interval (±% contrast)
40	8.8	7.0	0.8
80	10.6	6.7	1.7
160	15.3	11.2	1.7
320	24.9	16.2	1.7
640	22.2	18.3	1.6

Two Line Resolution

line contrast (dL/L)	modeled threshold (sec arc)	observed threshold (sec arc)	95% confidence interval (±sec arc)
0.45	64.9	71.3	12.8
0.75	37.5	43.1	6.0
1.34	33.2	36.1	4.6
2.12	32.2	32.8	7.5
4.43	22.7	27.7	4.0

Two Line Localization

criterion separation (sec arc)	modeled threshold (sec arc)	observed threshold (sec arc)	95% confidence interval (±sec arc)
40	17.9	18.9	4.8
80	10.9	12.0	3.7
160	12.7	13.4	3.9
320	18.7	20.5	2.9
640	28.8	35.6	7.4

Three Line Localization

criterion separation (sec arc)	modeled threshold (sec arc)	observed threshold (sec arc)	95% confidence interval (±sec arc)
40	21.0	22.8	5.6
80	14.6	16.3	2.5
160	12.3	11.9	2.2
320	18.2	15.5	7.2
640	30.2	34.8	26.9

Four Line Localization

line contrast (dL/L)	criterion separation (sec arc)	modeled threshold (sec arc)	observed threshold (sec arc)	95% confidence interval (±sec arc)
18.46	160	8.1	6.1	1.2
4.43	40	13.3	17.0	2.6
4.43	80	11.2	13.4	2.2
4.43	160	12.0	11.3	1.3
4.43	320	18.3	18.3	1.9
4.43	640	27.5	32.6	2.8
2.12	40	19.2	20.0	3.2
2.12	80	13.9	14.2	2.1
2.12	160	14.7	14.0	1.8
2.12	320	21.7	22.2	3.0
2.12	640	34.3	39.6	3.5
1.34	40	26.1	25.4	3.5
1.34	80	19.9	20.1	4.3
1.34	160	23.7	24.5	11.2
1.34	320	33.1	32.7	3.6
1.34	640	49.0	55.8	5.7
0.75	40	33.8	33.5	
0.75	80	35.4	30.7	5.4
0.75	160	37.5	42.8	11.9
0.75	320	53.3	53.1	6.6
0.75	640	69.3	77.7	9.0
0.45	40	43.6	42.4	11.3
0.45	80	67.7	68.4	22.2
0.45	160	69.8	85.4	8.2

threshold with increasing line contrast, the U-shaped "critical interval" relation between criterion separation and offset threshold in the two, three and four line localization tasks, and the shift of the four line critical interval to smaller criterion separations at lower line contrasts are all present in the simulations.

analysis of filter components

The initial stage of the model, the optical transfer function, is the most secure. Even when quantitative variations across subjects and within subjects over time are considered, optical attenuation for a given pupil diameter is well bounded and well defined. Very little attenuation occurs below 0.5 cpd and very little contrast passes above 60 cpd. In between, there is a nearly exponential decline in weighting. The effect of smaller pupil diameters (higher mean luminances) would be to increase the relative contribution of the high spatial frequencies, but only to a limited degree. Unfortunately, the rest of the components are not as defined.

In fact, given twenty years of spatial frequency research, the paucity of data available on filter parameters is surprising. Most of the literature establishes a parameter interaction only over a limited range of spatial frequencies. The data base necessary to construct a model such as CELT to the degree that the small 3 dB effects used to discriminate among many psychophysical theories simply does not exist at present. As a consequence, the approach adopted here has been conservative. Many parameters are held constant that in all likelihood vary over spatial frequency or even at a given spatial frequency.

What is reliably known about the nature of the spatial filters in the human visual system is that the initial stage is spatially linear for low to moderate flux densities. It is likely that the initial transduction introduces an early point-intensive distortion at high flux densities. This potential source of distortion is not incorporated in the model. Within the linear stage the amplitudes (not amplitude squared or any other energy analog) of each stimulus spectrum are weighted and summed with phase taken into account. It is also likely that the lower and upper bounds on the peak frequency sensitivities do not depart significantly from 0.5 and 32 cpd, respectively. Knowledge of the distribution of the filters in-between, however, is less secure. There is psychophysical evidence that a range of filter center frequencies exists at each position in the visual field (Graham et al., 1978); however, a trade between spatial and spatial frequency resolution of the probe make it difficult to determine clearly the range or density of the filters. The electrophysiological results are difficult to interpret because of problems with electrode selectivity and the determination of functional taxonomy. Not only may the obtained distributions be skewed due to electrode bias, only a subportion of the recorded distribution may contribute to contrast detection.

Similar problems exist in the estimation of the individual filter weighting profile. The psychophysical evidence indicates that absolute filter bandwidth increases with center frequency and that filter shape is roughly gaussian when plotted on logarithmic spatial frequency coordinates. The conservative approach taken for the current model was to linearly space filter center frequencies between

0.5 and 32 cpd, each with a one octave gaussian envelope about the center frequency. The filters in the model are considered to be samples taken randomly from a theoretically continuous distribution of parameters. Any nonuniform sampling of center frequencies would represent a weighting of the filter responses that would be better incorporated in the distribution of filter shape, bandwidth, spatial density or gain. The gaussian weighting envelope of each filter is a approximation to the straight flanks (on logarithmic coordinates) of the interactions found in contrast masking (e.g., Stromeyer and Julesz, 1972) and adaptation (e.g., Blakemore and Campbell, 1969) studies. The constant octave bandwidth assumption is equivalent to maintaining that high frequency filters are simply spatially scaled-down versions of those found at low frequencies.

A design philosophy that minimizes the degrees of freedom in the model avoids charges of curve fitting but may do so at the expense of accuracy. Now that a conservative model has been shown to be adequate in the aggregate, there are several places in the model where it might be appropriate to tune or increase the degrees of freedom in some of the filter parameters. For example, a slightly smaller bandwidth estimate would increase the relative sensitivity of the model to broadband stimuli. This nonintuitive interaction is a consequence of the increase in effective attenuation that the nonlinear exponent has on the response to impulsive spectra (see figure C.6). The reduction in "recruitment" increases the gain estimates derived from the simulation of sinewave sensitivity. The summation within each of a range of filters responding to the broadband stimuli does not

suffer proportionately because the summation occurs before exponentiation.

There is physiological evidence from Tolhurst and Thompson (1981; cat) and DeValois et al. (1982; macaque) which suggests that although absolute bandwidth increases with center frequency, it does so at less than a proportional rate (i.e., the bandwidth in octaves decreases). If incorporated in the model, a variable bandwidth would alter many of the spatial interactions. The reduced bandwidths at high frequencies would increase the gain estimates in that region. In addition, the change in bandwidth would also shift the critical interval. For small criterion separations, filters near the high frequency spectrum nulls would integrate less of the spectrum difference and have a smaller response. As criterion separation is increased, a nonconstant octave bandwidth would alter the interaction between the first two spectrum nulls. The f/3f separation of the nulls would incur increasing filter overlap at the lower spatial frequencies (larger separations) and increase cancellation of the spectrum differences of opposite sign.

The gaussian filter template itself may be inappropriate. Although it is possible that the underlying physiological substrate exhibits a gaussian connectivity distribution, it is also possible that other mechanisms (e.g., competition among filters) alters the template. The inability to find an exact linear solution for the filter gains (appendix C) may be due to many causes, but the large degree to which an iterative solution reduces the error suggests that one of the current parameters such as the shape of the filter flanks imposes an inappropriate constraint. The rate of decline in response above 32 cpd (the highest filter center

frequency) also suggests that the current filter profile should be changed.

The spatial frequency characterization of filter sensitivity is only partially specified by the modulus. The phase spectrum must be defined as well. Models of phase spectra are most often derived from receptive field properties of cells found in striate cortex. Single units there are composed of several elongated regions that are antagonistic in their response to flux. The sensitivities of the regions are such that they can be closely approximated by gaussian moduli with constant phase terms. The current model employs six phases (30° apart) at each filter position. The distribution of phase spectra need span only 180° since the filter response is bipolar. The inclusion of six phases is very conservative in that the aggregate response of each sextet varies only 0.02% with changes in sinewave phase. With only a single filter phase, the regularity of filter position (a computational convenience for convolutions) would likely induce beating artifacts. A model with two or even a single phase spectrum might suffice for the simulation of detection and discrimination if the filter positions were randomly distributed. Evidence that large responses may be realized even though the filter phase spectra do not match the stimulus phase spectrum (where a match is the condition that yields peak response) comes from comparisons of convolutions with odd- and even-symmetric filters and the four line localization stimuli. Even the maximum mismatch of an odd-symmetric filter and the even-symmetric stimulus produces a peak response that is 92% of that obtained with an even-symmetric filter. This relation holds over seven octaves of criterion separation.

The filters in the model are distributed in 64 superimposed mosaics, each of which spans the 4.4 by 2.2° display aperture and contain a single center frequency. Within each mosaic the filters are spaced one per period of the center frequency, both vertically and horizontally. The collection of six filters (one for each phase spectrum) may be considered to represent the aggregate response of all the filters in that one period region of the Observer's visual field within ±0.25 cpd of the appropriate center frequency. The decrease in filter sensitivity at larger eccentricities was modeled after the results of Robson and Graham (1981). In that study sensitivity was found to decline exponentially from fixation with an exponent that is proportional to center frequency. They also found that sensitivity in the vertical direction declined twice as fast as that in the horizontal. It is likely that the decline in sensitivity reflects a decrease in filter density rather than a qualitative change in the composition of the filters in the periphery.

The one filter per period rule is included to eliminate sensitivity gaps in the model of the visual field as well as to simplify the convolutions; however, it is a simplification that leads to some unrealistic approximations. In particular, the model contains an inordinately large number of high frequency filters. If a random position feature was added to the model, there would be no reason not to replace the eccentricity weighting function with an actual decrease in filter density. Another improvement would be to replace the monotonically increasing relation between center frequency and filter density (a relation that occurs at fixation and forms the basis for the eccentricity calculations) with a tapered reduction of total

filter number at the high frequencies.

As used in the current model, gain is a factor that is used to scale the entire weighting profile of a filter relative to the other filter profiles. Gain is allowed to vary across filter center frequency and is the parameter used to tune the model to the Observer's contrast sensitivity. If the estimates of the filter profiles and density of filters across spatial frequency and across space are correct then gain should be related to some physical property of the filter such as width or total integrated weighting. The relation between gain and center frequency may be complex if the filters are not simply scaled versions of one another. For example, orthogonal length may not vary in proportion to center frequency. Such nonuniformities are likely since the human spatiotemporal MTF is not separable.

Attempts were made to determine an exact solution for the gain estimates (see appendix C). Solutions derived from contrast sensitivity data oscillate wildly between positive and negative values. It appears that in the limit the exact linear solutions are sensitive to simplifications contained in the analytic representations of the filter profiles, particularly in the rate of fall-off of sensitivity in the skirts. The hypersensitivity of an exact solution may be avoided by using an iterative method. A set of filter gains was found that produce aggregate responses that are within 1.5% of the detection criterion (see figure 2.10). Filter gain is highest for low spatial frequency filters and declines monotonically with increasing center frequency. Over the six octave range of center frequencies, the gains decline by a factor of about twenty. This ratio is less than the 64:1 figure expected if gain was

a function of a linear measure of filter profile and is much less than the 4096:1 ratio expected if gain had an areal dependency. As noted, however, these gain measures must absorb any errors in the estimates of filter density (c.f., figures 2.5 and 2.6) and the relevant empirical data are sparse. The required relative increase in gain at low center frequencies runs counter to a flux dependent adaptation (q.v., Enroth-Cugell and Shapley, 1973). If the adaptation pools were the size of concentric retinal ganglion cell receptive fields, the relation between gain (response per unit of flux) and filter center frequency should be positive, not negative; the larger receptive fields (lower center frequencies) should be at a higher state of adaptation. The extent of adaptational pooling in photopic primate (cone-based) vision is not resolved and may prove to different than the pooling found in cat.

Up to this point the weighted summation within each filter and the relative scaling of the responses among filters are linear. However, measures of suprathreshold performance such as perceived brightness and contrast indicate that at some point internal responses increasingly diverge from a linear rate of increase. Contrast discrimination data provide a good measure of the response compression. At high contrast levels, just discriminable responses increase in proportion to contrast. At low contrast levels, threshold contrast differences may be discriminated over a considerable range. The lowest contrast at which compression occurs is the only parameter tuned to fit the current discrimination data. A conservative approach was taken in the degree that responses were combined prior to compression. It is unlikely that the response of an individual

filter can be isolated; however, what the minimum number of filters that can be isolated actually is has not been determined. In the current model, the net response at each frequency after probability summation across space is compressed in proportion to the extent it exceeds 40% of the aggregate response required for detection (1.0). It is certain that regions smaller than the display aperture can be isolated; however, since the required data are unavailable, the more conservative constraints are used in demonstrations of the model's adequacy.

Adjustment of the compression boundary causes concomitant changes in the absolute sensitivity of the model. It is possible, therefore, to correct for the slight underestimation present in the model's simulation of the discrimination tasks. Unfortunately, the change in sensitivity is quite variable and the form of the spatial interactions become quite distorted. It is possible that the underestimation may be better corrected by adjusting the filter gains. For a fixed compression boundary, underestimation of discrimination response may stem from an overestimation of the detection responses. The greater the range of center frequencies for which the responses are in the Weber region, the smaller is the discrimination advantage offered by the remaining uncompressed regions.

If the Weber region represents an actual compression and not just a reduction in the ability to discriminate responses, it might be appropriate to compress some of the responses in the simulation of sinewave detection (see figure 2.11). Many of the aggregate responses at individual center frequencies exceed the 0.4 compression boundary. The large amplitude responses are especially evident at

low spatial frequencies where the response is concentrated in only a few filters.

Another possible improvement to the model might be the addition of a more complex compression function. Some discrimination data are consistent with a model wherein the compression changes as a function of center frequency. The compression may not even be the result of a single mechanism at each center frequency. Albrecht and Hamilton (1972) found that only the lower portion of the filter transducer function appears to adapt, suggesting the presence of more than one mechanism. It may be useful to modify the lower end of the discrimination function as well. The pedestal effect (Nachmias and Sansbury, 1974) could be incorporated to simulate the enhanced discriminability of responses at low background contrasts. Just as some nonlinearities induce nonmonotonicities in the discrimination function, other nonlinearities distort the symmetry of the transduction process. Simultaneous contrast effects and the narrow troughs perceived in high contrast sinewaves indicate that suprathreshold responses undergo a compression that is not symmetric about the mean luminance. This distortion represents a highly nonlinear transformation that is possibly an interaction between spatially adjacent filters rather than within an individual filter. The failure to incorporate this nonlinearity is perhaps the most significant omission in the current model.

The parameters used here to define the simulation of early visual processing have been expected values. It is unlikely that the human visual system is composed of an array of such exact replicas. With many linear systems,

approximation of distributions by the mean is an acceptable method of reducing computational requirements. In nonlinear systems, however, such simplifications may not produce an accurate model. For example, variations in bandwidth at a given center frequency would result in a corresponding variation of filter response. In a nonlinear system that disproportionately weighted larger responses, the sensitivity would be increased. Variability also may induce qualitative changes in functional relations. Hamerly (1975) demonstrated how variations in threshold could transform individual linear transducer functions into an accelerating function in the aggregate.

analysis of aggregate response

Complementary to the problem of simulating the initial sensory transformations is the specification of the rules of response combination. In general, the specifications are at a higher level of abstraction (i.e., more removed from direct physiological and anatomical analogies) than is characteristic of the filter simulations. These rules are a characterization of aggregate activity that are specific to the task being described. In particular, probabilistic models of detection and discrimination exhibit an emphasis on nonlinear behavior that is not likely a significant factor in "normal" visual perception. It is a mistake to extend characterizations beyond the tasks for which they were designed. An example of an aggregate characterization that is different than that used here is the simulation by Hamerly (1975) of perceived contrast. In this model, the responses of distinct

channels were linearly summed to obtain a measure that was proportional to perceived contrast.

The probabilistic nature of the detection/discrimination process perforce introduces nonlinear interactions. Even among completely linear filters, probability summation introduces gross nonlinearities (see appendix C). Most simulations that contain the probabilistic combination of filter response use some form of a vector magnitude metric introduced to vision models by Quick (1974). In this metric, the aggregate response is computed by raising each filter response to a power (B), summing the results and then extracting the B^{th} root. For values of B greater than one, the net effect of the metric is to disproportionately emphasize the contribution of large responses to the total response. Differences in the literature among the stimuli used and among the filter models that comprise the stages prior to the vector magnitude calculations has led to a wide range of exponent estimates. The estimate obtained by Robson and Graham (1981) using gratings of variable extent was included in the current model ($B = 3.5$).

In the vector magnitude calculations for discrimination, probability summation across space at each center frequency was computed prior to response compression. The adjusted response at each center frequency was then used in the probability summation determination of the aggregate response. The compression was applied subsequent to probability summation across space because there was no evidence that would help determine how compression should be factored across different size filter populations or across the decline in sensitivity with eccentricity.

The summation-compression-summation sequence was successfully applied here because of the nature of the stimulus sets. The stimuli were either narrowband and distributed over the entire display aperture or were highly localized. In both cases, any changes in response correspond spatially with appropriate levels of background activity. The analysis of two widely separated localized stimuli where only one of them contains an offset would violate this correspondence and it would therefore not be appropriate to take advantage of the simplification of calculating probability summation across space before response compression.

It is also important to note that the difference response is determined by a subtraction between exponentiated magnitudes and that the magnitudes retain the label of the sign of their response. The difference of the exponentiated responses, in effect, is a comparison of stored responses, not a direct comparison of inputs. The temporal separation of the test intervals forces the use of stored information. The retention of sign allows stimuli to be discriminated that are of the same magnitude (in the sense of detectability) but of different composition spectrally.

The addition of an ability to restrict the range of responses across space or spatial frequency (i.e., attention) would make qualitative differences in the performance of the model. It is possible that attention may be restricted to as small a region as the resolution of the labeled position mosaic. The sensitivity of contrast discriminations against the lower criterion activity would increase, allowing the knee of the Weber region to be lowered. The sensitivity advantage gained by restricting attention should not be offset by the reduced pool size. The

nonlinear nature of probability summation allows the number of contributing filters to be considerably reduced with little change in corresponding aggregate sensitivity. In addition, as demonstrated in the exercise in the decomposition of aggregate filter response (chapter 3), there is considerable spatial concentration of filter response in localization tasks.

There may be other problems with the vector magnitude formulation that cannot be repaired. The vector metric itself may be an adequate but inappropriate model, a mathematical convenience not at all isomorphic to the underlying activity. The disproportionate emphasis that an exponent greater than one places on large responses could be replaced by a threshold. A subtractive threshold would disproportionately reduce the contribution of small responses to the aggregate. A signal detection formulation might prove to be a better framework for the determination of global activity. The more complex nonlinearities proposed above would not be restricted to conform to some combination of Weibull functions.

What is the observer doing?

The thesis put forth in this dissertation is that the various measures of spatial acuity are consistent with one another and with the responses of an array of bandpass spatial filters thought to comprise the first stage of spatial vision. In order to achieve this goal, it has been necessary to dispel a misconception present in the literature for over a century; to wit, the presumption that the procedures

used to obtain these measures of acuity stimulate the position sense alone. The arguments, data and simulations presented here all support the contention that changes in objective measures of position stimulate a wide range of spatially related responses, not all of which may be directly attributed to the perception of position. The goal, then, has been met: the contrast sensitive filters not only possess sufficient sensitivity to changes in position, they also generate the many spatial interactions found to occur with measures of acuity. Care should be taken, however, that one misconception is not simply replaced with another. Just as top-down or manifest-feature based theories are bound to fail to account for the spatial interactions, the sensation based filter theories are bound to fail if they are extended to perceptual activities beyond their ken, such as across conditions where different task demands force the Observer to change strategies. The remainder of this section is an examination of sensation-perception interface. In particular, in what form does the initial sensory interface pass information on to the perceptual processes?

Differences in activity across the sensation-perception boundary may be represented by the questions: What is the stimulus doing to the Observer? and: What is the Observer doing to the stimulus? (or, at least: What is the Observer doing to acquire knowledge of the stimulus?). The initial sensory substrate is principally an adaptive mechanism used to constrain the large range of ambient conditions to responses that remain within the limited dynamic range of subsequent neural units. The early role of adaptation is not in dispute. It is the

bandpass nature of the early filters that raises the question as to how specialized their responses may actually be. Many theories of perception presume that because some feature is manifest in the percept, the information is available in a form that is isomorphic to the percept (e.g., lines are available as individual tokens). Projection of that presumption into the initial sensory stage simply begs the problem of visual processing. Historically, physiological findings have had a strong influence on the conceptualization of the organization of the visual system. Fifty years ago, equipment limitations forced the physiologist to obtain large responses in order to see any effect at all through the noise. The linkage between maximum response and function was retained long past any constraint by the technology, however. The tendency to attribute specific function to neurons was a consequence of the available experimental preparations - usually cold, wet creatures whose main advantage was the possession of visual cells with large somata but that unfortunately were not extensively cerebrate. The specificity found in the distal neurons of these creatures reflects a qualitatively different organization than that found in primates. Nonetheless, converging featural hierarchies such as Hubel and Wiesel's (1962, 1965) bar and edge detectors dominate the current models proposed for low level visual processing. Many computer models even take line and edges as the starting point for simulations of human vision.

Barlow (1972) summarizes the physiological underpinnings for this point of view. He asserts that the organization of the cortex is directed at successively

reducing the number of neurons active in the representation of an image (dogma 2). Neurons with sensitivities for simple elements converge at higher levels to form more complex percepts. In addition to the convergence principle, the magnitude of each filter response is interpreted as a measure of the certainty that a given feature is present in the image (dogma 5).

The characterization of the cortex as a muted filter comes largely from the use of "flash in the dark" stimulus presentations. During recording, single units are left unstimulated and then are presented with a high contrast contour of sudden onset. The famine and feast sequence is designed to elicit maximum firing rates. The dependence on maximum responses for functional categorization is tantamount to the presumption that signal to noise conditions are the limiting and driving influences under all viewing circumstances. From an engineering or systems perspective, this method of classification is flawed. Large signals are more likely to incur distortion than those lower down on a filter's operating characteristic. In addition to the statistical advantages of averaging many noise sources, distributed representation would lower the dynamic range required for each filter. The use of stimuli with statistics more characteristic of a moving and textured world gives a very different perspective of cortical activity (Madden and Mancini, 1980), one with widespread activity that would lessen the demand on any given sequence of neurons.

The early assignment of features to filters is a mistake. The flexibility of the later perceptual activity is lost through such preemption. The early processing of

meaningful features (sensation) is characterized by the output of meaning-free transformations. There is no reason to believe that it is either necessary or even advantageous for that organizing process to distill and purify the widespread activity that a feature initially induces and, indeed, such tendencies may lead to errors in the types of confusions that would be predicted to occur at higher levels. Theories that begin with crisp, labeled perceptual elements are devoid of the seeds of confusion and will not fail in the manner that a human fails.

This is not to argue that the initial distributed sensation representation is maintained throughout perception, just that it is the starting point. There is much subsequent abstraction; but abstraction doesn't require convergence. The tendency toward convergence (e.g., grandmother cells) speaks not of the poverty of distributed representations but only of the poverty of our ability to adequately describe and comprehend such activity.

As an illustration of such distributed representation, consider the responses of the probability summation model used in this dissertation when applied to threshold sinewave gratings (see figure 2.11). The induced activity in response to gratings over the range of filter center frequencies is not consistently narrow. The range of activity increases with increasing spatial frequency, a reflection of the increase in bandwidth at higher spatial frequencies. Maximum filter responses for high frequency gratings at threshold are a factor of two less than those at low frequencies. The decrease in response required at threshold is a consequence of the spread of activity, although the decrease is far from proportional to the area

under the envelope (linear). To such a visual system, a sinewave has no special standing. A grating, although a simple stimulus, elicits a composite response not qualitative different from, say, a toothbrush.

All perceptual features are the consequence of the responses of many bandpass filters, not just the result of the one with the peak response. Differential sensitivity in the filters that make up a feature allow changes in the more sensitive filters to disproportionately alter the appearance of the feature. Consider, for example, what happens when the contrast of a sinewave grating is increased from threshold. At low spatial frequencies the profile of filter activity is quite stable. The narrow response distributions, with much of their activity already in the Weber region, do not widen appreciably. At high spatial frequencies, the effect is quite different. Most, if not all, of the filter responses at threshold are below the cutoff for response compression. As contrast is increased, however, the large responses grow more slowly than the rest. An increase in suprathreshold contrast causes a disproportionate increase in responses at center frequencies away from the maximum response. The perceptual correlates of increased contrast are quite similar. The appearance of low frequency gratings is not distorted by increased contrast. The gratings appear to smoothly oscillate between peak and trough at all contrasts. The appearance of high frequency gratings is sinusoidal at near-threshold contrasts but becomes much sharper at higher contrasts. It is possible that the squarewave appearance is a consequence of the relative broadening of the filter activity at high contrasts. This consequence of distributed response would

reduce the amount of distal point-intensive compression required to account for the suprathreshold changes in appearance (c.f. Davidson, 1968).

Another interaction that is well accounted for by a distributed representation is the effect of adaptation on spatial frequency discrimination. If the just discriminable change in sinewave period is taken to be the measure of performance, sinewave discrimination may be classified as a localization task (Hirsch and Hylton, 1982; Regan et al., 1982). Observers are able to discriminate changes in sinewave period of only a few percent over more than a decade of spatial frequencies. The surprising finding is that although sinewave detection threshold is maximally elevated by adaptation at the same spatial frequency, discrimination thresholds are affected hardly at all; however, adaptation at half the spatial frequency greatly elevates discrimination threshold (Regan and Beverley, 1983). The reason behind the disparity between the discrimination and peak elevating frequencies may be seen by examining the envelope of activity induced by a high contrast sinewave in the one octave bandpass filters. Most of the responses are well into the Weber region. The response differences induced by small changes in frequency are rendered less discriminable by the high criterion activity at all center frequencies except at the edge of the envelope. Simulations with CELT (unpublished) confirm that the greatest discriminable response occurs a factor of two down from the test frequency. Such interactions away from the test spatial frequency are exceedingly difficult to explain with peak response models. The interactions are between suprathreshold gratings and cannot be

explained away as distortions present only at absolute threshold.

Added to the support given distributed representation by these examples are the many successful simulations presented in chapters two and three of detection and discrimination tasks, all unified by a single model. Together they provide the answer to the first question and fulfill the primary goal of this dissertation, the determination of a single sensory mechanism consistent with the sensitivity and interactions exhibited by the measures of spatial acuity. The answer to the second question requires more. That answer must define the degree to which the information in the responses of the initial sensory stage is unambiguously retained. Although little is known of the structure of the subsequent levels of filters, it is possible to infer some of the properties from both the physiology of visual cortex and Observer performance.

To a dualist, responses are at some point "read" by a homunculus, the mind's eye. In this view, there is little pressure to specify any complex mechanism in the corporeal domain. To a monist, labeling implies a pattern of connectivity from one level of processing, or representation, to the next. A label, as used here in a monist framework, has a much more mechanistic interpretation than the attachment of an abstraction to a given response. Labeling refers to the extent that the weighting profile of a filter at one level determines how it selectively combined with other filters at the subsequent level. The degree to which the responses of the initial level are labeled determines in large part the organization of subsequent levels. Labeled lines preserve information and, as such, they

diminish the amount of abstraction that occurs. Generalization occurs when information is combined across (i.e., without respect to) one or more labeled dimensions. Labeling may be implemented either by restricting which types of distal filters are combined or through selective weighting of the responses of the filters that do converge. Demonstration of labeling from physiological data is a matter of showing that distal neurons are combined in a restricted number of the potential combinations or that different distal pairs are combined to form one of a restricted distribution of proximal filters.

The potential degree of labeling is on a continuum. At one extreme, is a completely labeled system wherein the initial image is reconstructed within the limitations imposed by sampling. The only alternations would be adaptive and compressive transformations, but no selections. The other extreme would have the unrestricted combination of responses to contrast at each position in space. Specific knowledge of prior processing is nonexistent. A neural image would be created wherein the "flux" is a function of local retinal contrast. Where the human visual system resides on this continuum depends on a neural version of the Heisenberg uncertainty principle, a trade between specificity and generalization. It is likely that there is a high cost in maintaining a strictly labeled system. Generality in such a system is achieved only through a combinatorically large network. On the other hand, a sufficiently veridical spatial reconstruction of the environment must be available to the Observer as well.

What evidence is there for labeled dimensions? Does the initial stage act as an invisible and inaccessible transformation with only the magnitude of the responses available for subsequent processing, or, is it better characterized as a well-labeled array of filters that may be selectively and knowledgeably perused and combined? Certainly, the strongest case may be made for labeling of local regions of visual space. Retinotopic organization exists throughout a considerable portion of the visual pathways. The positional labels can be maintained by the simple mechanism of parallel projection from one level to the next. The limit of positional resolution is bound by variability in the registration of the projection. The resolution limit is further increased by physical constraints imposed by providing a nontopological synthesis at each position across space. The cost of labeling more than space increases dramatically because of the topological limitations that allow adjacency to work only for one parameter (e.g., space); although locally the adjacency mechanism appears to applied to orientation. Each patch of the visual field seems to be represented by an orderly sequence of cell orientations across the representation of local regions in visual cortex.

Apart from position and orientation (and ocular dominance), what evidence is there for labeling of other dimensions? In particular, to what extent are phase and spatial frequency labeled? In striate cortex, receptive field profiles come with a range of phase spectra, from even-symmetric (a dominant center region with two lesser antagonistic flanks) to odd-symmetric (two equal antagonistic regions). Undifferentiated combination of filter responses across such a range of phase

would wash out any internal structure in the aggregate response. Without labeled phase, a sinewave grating would be represented as a uniform rectangle of activity for all phases of the grating. The ability to discriminate two vertically adjacent gratings by their phase is easily demonstrated (in fact, under some conditions it is a localization task). Labeled phase also would explain the finding by Tolhurst and Dealy (1975) that a bright line may be discriminated from a dark one at contrasts just above threshold (although an auxiliary absolute luminance mechanism that operated in parallel to the bandpass spatial filters would suffice as well). On the other hand, the insensitivity of detection tasks to the phase of f/3f grating pairs suggests that at least in detection tasks phase is not labeled and that there is an undifferentiated combination of response in the pathways that lead to the detection decision. In the current probability summation model (CELT), the principal use of multiple phase spectra is to avoid beating artifacts caused by the regularity of sampling. In CELT, probability summation is combined across phase.

The extent to which filter center frequency is labeled is equally uncertain. Evidence obtained at threshold suggests that spatial frequencies can be perfectly discriminated if they are no closer than one octave (Watson and Robson, 1981). As a lower bound there must be as many labeled lines as there are spatial frequencies that are perfectly discriminated (i.e., seven). Although the concept of perfect discrimination has the advantage of an absolute criterion (the assumed equality of response at detection), it is unrealistically demanding. The

requirement that there be no confusion (overlap) between active filters results in performance that is limited more by filter bandwidth more than by label density. The reduction by more than half in the number of labeled spatial frequency lines at high temporal frequency may well reflect a broadening of the filter activity at high temporal frequencies rather than a decrease in the density of labeled lines. Such changes in activity are likely since the human spatiotemporal MTF is not separable across space and time. At suprathreshold contrasts, spatial frequency discrimination thresholds based on less stringent criteria (75% correct) are only a few percent of criterion frequency (Hirsch and Hylton, 1982; Regan et al., 1982); however, it is not clear that these thresholds are obtained through labeled lines alone.

Just as the absence of an absolute reference precludes the use of other than perfect discrimination to determine unambiguously the density of labeled lines, there is likewise no anchor to establish the relation between filter bandwidth and filter density when masking results are interpreted. A decrease in sensitivity brought on by the proximity of a mask usually is attributed to an increase in summation within the linear stage of filters used to detect the test stimulus. In this model, the increase in activity moves the operating region of the filter into the Weber region and the consequent response compression reduces sensitivity for the test. In a labeled system, the extent of the mask and test spectra that may be isolated is a function of label density. The degree to which regions of spatial frequencies are combined in the initial sensory stage (filter bandwidth) may be

determined by different considerations (e.g., s/n ratio) than is the density to which output is kept in registration in combinations at a later stage. Reduction in sensitivity caused by masking would depend not only on label density but also on the way the more numerous filters were combined to achieve the lower label density.

The seamless quality of the perceived image, both locally and over distances that are large as compared to receptive field diameters, can be interpreted as subjective evidence for the activity of a wide range of filters. Only at the highest spatial frequencies (as evidenced by the irregular appearance of high frequency squarewave gratings) does the continuity apparently break down. Even at threshold, a wide range of filter activity seems to be required. If the activity of only a single labeled filter led to detection, the percept associated with a threshold dot should be a patch of grating or perhaps a bull's-eye. A continuous range of activity would average out any Bessel-like ripples and summate over only the center region. As contrast is increased, the associated increase in subjective sharpness may well be a manifestation of the widening of the response envelope with increased contrast.

The continuously changing sequence of preferred filter orientations across local regions of visual cortex is capable of supporting the kind of summed activity of many filters across orientation that appears to be at work across spatial frequency. The distributed pattern of orientations also suggests that positional labeling is not being maintained to a degree finer than it takes to subserve one full

cycle of orientations. This nonretinotopic organization is likely to be the first stage of form perception. It is a mistake to characterize this continuity as an interpolation mechanism, a continuous extension of positional labeling. The search for an interpolation metric stretches Fechner's assumption of equal percepts at threshold beyond its original venue. Application of the assumption is valid if it is applied to different conditions of the same task requiring changes in the same filters. The assumption does not apply across different labels, different dimensions. A threshold red is not a threshold tilt; and, more to the point, a threshold change in contrast does not always lead to a threshold change in perceived offset.

While it is true that the patterns constructed at each position can have structure finer than the labeled mosaic, the individual peaks and troughs of apparent brightness cannot be broken out as individually processed elements, each with their own labels. The entire pattern is constructed as a whole out of the ensemble of responses of the contrast sensitive filters, each of which is only coarsely labeled as to spatial position. It is proposed that the elemental patterns constructed locally in this manner are fit together at higher levels of representation without recourse to an interpolation mechanism that extends the labeling of space. Although the widespread filter activity that forms the substrate of form perception is retained, it is further proposed that only the combined effect of the responses is available to further levels of processing. The Observer sees only a spatial distribution of perceived brightness and in no way directly senses the structure and

distribution of the underlying contrast filters. There is no analog to Ohm's acoustical law in vision.

Of particular interest here are the perceptual cues available to the Observer in localization tasks if the filter responses are available only as a composite. The exact form of the perception of offset will depend on the manner in which the frequencies in the difference spectra are labeled; however, an approximation to the percept can be obtained by examining the activity present at the sensory interface. In the coincidence task, a threshold offset appears as a "fuzzy knot" superimposed on an otherwise straight line (Andrews, 1968). The fuzzy knot is the perceptual correlate of the difference spectrum, the difference obtained by subtracting the aligned stimulus spectrum from that of the stimulus with offset. The location of the peaks and troughs of the difference spectra in terms of retinal contrast reflect a trade between the increase with spatial frequency of both the amplitude of the difference spectra and the attenuation by the OTF (see figure 5.5). After passing through a linear summation, a nonlinear compression and a nonlinear combination, the maximum responses are accentuated even more in the final response profile. The two peaks correspond to difference amplitudes that are in cosine phase (90^o) approximately one orientation bandwidth away from the vertical. The two troughs correspond to difference amplitudes in minus cosine phase (-90^o) approximately one orientation bandwidth away from vertical on the opposite side. When the two orientations are superimposed they form an oblique gingham pattern in space centered on the axis of symmetry for the aligned

stimulus. On one side of the vertical lines a bright patch is above a dark one; on the other side the reverse is true. When the offset is to the opposite side, the pattern of light and dark patches is reversed. The variation in the pattern of the knot allows the Observer to make the judgment as to the "position" of the line.

In the case of the four line localization stimuli both the phase and the orientation of the difference spectra match that of the criterion. The coincidence of peaks in the difference response and spectrum nulls occurs at frequencies and phases that contribute to the apparent brightness of the intervals between the lines (see figure 3.19). It should be emphasized that the apparent brightness is not a simple point by point transformation of retinal flux but is the consequence of a linear spatial summation, a nonlinear compression (Weber region) and a nonlinear combination (vector magnitude summation). Since the percept does not correspond directly to any intensive measure, a term such as spatial brightness might be more appropriate. The frequency and phase of the peak of the difference spectrum (larger offset) that coincides with the first spectrum null results in a trough centered on the middle interval with its limits close to the centers of the side intervals. The difference spectrum goes to zero at the second spectrum null due to a zero of the form spectrum (see figure 3.18). The third spectrum null corresponds to the second peak of the difference spectrum. The frequency and phase here causes a trough to coincide with the center interval and has a light/dark transition in the outer intervals that coincides with the edge of the first trough bit is of opposite slope. The net effect of the activity at these

spectrum nulls is a decrease in the apparent brightness of the center interval and almost no net change in the brightness of the side intervals. For smaller offsets the polarity of all of the brightness changes is reversed. The Observer is able to make a judgment of "width" based on the relative brightness of the intervals.

The three line localization task is performed in a similar manner. The only new wrinkle is that the difference spectra has a linear phase term (see figure 3.16). As before, the effect of the offset on the apparent brightness of the criterion interval is negligible. Positive offsets induce decrements in the brightness of the test interval; negative offsets induce increments. The Observer can make judgments as to the relative brightness of the two intervals, in effect a comparison of the summed response of the underlying filters at those locations in space.

The two line localization task is different in that there is no criterion interval simultaneously present for reference. It is not self-evident. This task requires feedback to train the Observer. If zero-crossings of the spectrum amplitude envelope generated perceptually salient activity (e.g., Marr, 1982), one might expect that the relation between two of them might be used to perform the task. But this is not the case. The alternative proposed here is that the Observer makes use of the feedback to establish an internal brightness standard against which each test stimulus is compared. Offsets in localization stimuli induce relatively large changes in perceived brightness due to the coincidence of peaks in the offset spectra and sensitive filters.

The proposed ability of the Observer to learn and maintain (with feedback) a criterion brightness raises the issue as to the extent this ability is applied in self-evident cases. A good Observer doesn't cling to a subjective standard of reality but, instead, adjusts to minimize the occurrence of the buzzer. It is rather likely that in some conditions of the relative brightness judgments, particularly in the four line interval task, the assessment is not one of equality but one based on a criterion brightness. In the four line interval task, the substrate of filters that contribute to the brightness of the center interval are different from those that contribute to the side intervals. The relation in the criterion stimulus between the brightness of the center interval and those adjacent changes both with separation and with contrast. For example, a dark striation was easily visible for a range of negative offsets and small criterion separations at the highest contrast but could not be seen at lower contrasts. In the early studies (usually without feedback or balanced staircase methods), a marked Observer bias was often obtained. The bias might be a consequence of an overt strategy to equate the interval luminances (i.e., equate the appearance of the intervals) or possibly the Observer simply latched onto the wrong brightness as the standard.

The ability of the Observer to establish an internal standard other than equality was demonstrated in a study where a stimulus with a nonzero offset (unpublished data). The criterion was presented to the Observer for 30 seconds at the start of a 500 trial session. With feedback, the Observer was able to maintain the criterion separation to within 1 second of the desired interval for criterion

offsets between ±24" arc. Thresholds for larger and smaller offsets about the criterion were all in the range of 3 to 7" arc.

The ability to establish and maintain an arbitrary criterion is only a small indication of the plasticity of the "good" Observer. The same objective task (e.g., detect of offset) places demands on the Observer that are a function of both the procedure and the stimulus set. For example, four line interval thresholds for a single staircase of larger offsets is half that of a double staircase with both larger and smaller offsets (unpublished data). Faced with only one staircase, the Observer is free to make a relative judgment as to the brightness of the center intervals in the two stimuli presented on a given trial. With two staircases, an internal standard must be maintained. The associated cost of maintaining the standard is reflected in the increased threshold. Possible changes in task demands should be considered when interpreting the effect of altered procedures on threshold. For example, the introduction of variability in the criterion separation or contrast will possibly alter the strategy of the Observer. Equivalent thresholds on the same objective task do not guarantee that the Observer is doing the same thing in both conditions. Suggestions of the employment of different strategies often appear as subjective differences in the "ease" of the task. If a practiced Observer can do one condition almost immediately but requires thousands of practice trials on a second condition, caution should be exercised in using the ultimate equality of performance to imply equality of action.

In the final analysis (or at least here in the last paragraph), the selection of a theory can be considered analogous to a beauty contest. After the data have been cleaned up, the model closely shaved with Occam's razor and the conclusions dressed in the appropriate statistics, a judgment is made on the utility of one theory relative to that of the competing theories. How do the theories based on converging featural hierarchies compare to the distributed representation proposed herein? Where are they? A functional relation between some feature (such as proximal ends) and offset threshold does not a model make, certainly not in a way that can be used to predict the responses to other stimuli and integrated into other facets of visual processing. The proposed theory, based on a distributed representation, offers not only a unified description of sensation but presents a promising interface to perception as well.

Conclusions

- The position sense of the human visual system has a resolution of several minutes of arc. Common measures of positional acuity, such as two line resolution and localization, are enhanced by the responses of contrast sensitive filters. Most experimental paradigms allow the operational definition of position to be expanded beyond the labeling of location in the visual field to include information from these intensive changes in contrast.

- Two-line resolution depends on a discriminable change of response in the high frequency filters. The decrease in amplitude of the stimulus spectrum brought on by increasing line separation induces changes in response that are compared to activity associated with the flat spectra of two superimposed lines. Although the activity induced by the criterion stimulus is above threshold levels in the high frequency filters, offsets too small to reliably activate distinct positional labels induce a large decrease in response. The changes in response in the high frequency filters for a threshold separation of the lines are sufficiently large (based on sinewave detection and discrimination data) to be discriminated against the activity induced by the two lines superimposed. In this manner, offsets of a half minute of arc may be reliably detected by a system that is able to specify absolute position only to within minutes of arc.

- Undulating spectra are characteristic of stimuli with features that are separated by a few minutes of arc, and it is at these separations that optimal localization is obtained. Localization acuity is enhanced beyond that obtained for two line resolution by the presence of spectrum nulls, regions where the broadband amplitude spectra contain a reversal in sign (180^o phase shift). Although much of the amplitude spectrum of the criterion localization stimuli is considerably suprathreshold, the sensitivity of bandpass filters in the region of the spectrum nulls is close to, or at, threshold sensitivity since amplitude components of opposite phase cancel when summed in a linear filter. In addition, spatial offsets in stimuli used for localization tasks all induce changes in the spectrum that are largest in the region of spectrum nulls. This correspondence underlies the increased sensitivity localization tasks enjoy over resolution tasks and results in acuities of seconds of arc.

- The use of one octave bandpass contrast-sensitive filters as the mechanism subserving measures of fine positional acuity not only provides an explanation of the exceptional absolute sensitivity to spatial offset, but it also accounts for the variation in sensitivity with changes in stimulus parameters. The multitude of localization phenonema (e.g., critical intervals, masking by flanking lines, length by separation interaction and the effects of blurring and contrast) can all be attributed to properties of the same array of spatial filters used to account for sinewave detection and discrimination.

- Discrimination may be modeled by the same vector magnitude formulation that simulates probability summation at detection. The major addition made to accommodate discrimination is the inclusion of a response compression that reduces the discriminability of large responses. A Weber discrimination function (slope = 1) is applied to all responses above a particular response level that is the same for all filters. In addition, it is proposed that the stored representation of the image reflects this response compression. Discrimination is based on a comparison of these stored representations, not by comparison of the responses at the linear filter stage.

- The analysis of any acuity task should consider the stimulus as a whole, and not just relations among individual features. Features that are manifest in the percept are the end product of a distribution of filter activity, and part of this activity may contribute to the representation of many features. In particular, the activity in the initial sensory interface that underlies the detection and discrimination of small positional offsets is not readily isolated as a separate feature in the final percept, distinct from the activity associated with the criterion stimulus. Such discriminations are not enhanced by attending to a subset of filters active at a given location but, instead, judgments are based on local changes in apparent brightness. Under optimal conditions for acuity, the major contribution to these changes in apparent brightness come from a relatively few filters disproportionately sensitive and disproportionately stimulated. The Observer

maintains an internal representation of these spatially local brightness levels across trials and uses this representation as a standard on which localization judgments are based.

Appendix A

LOCALIZATION PERFORMANCE

Introduction

Part of the extensive literature on human spatial vision is a collection of studies which document exceptional localization performance, performance that is much finer than the interreceptor spacing. At first examination, the diverse nature of the stimuli used in these experiments might suggest that several different mechanisms are required to explain the exceptional localization performance. However, it is a major tenet of this thesis that all of the performance presented in appendix A reflects the activity of a single process, and further, that this process is the same one that is responsible for the other, less demanding, resolution capabilities of spatial vision.

The experiments reviewed in this section are grouped according to stimulus and Observer variables (spatial extent, orientation, luminance, wavelength, contrast, duration, motion, monocular/binocular viewing and criterion). The organization is uncomplicated since most studies of localization have involved the manipulation of a single variable. This concentration within experiments avoided confounding the source of any changes in threshold. Although only one parameter was usually varied within a study, the selection of the other parameters varied widely among studies, at times altering the threshold relations being examined. An attempt is made here to establish a consensus across studies by an

analysis of the relations between each parameter, in turn, and localization performance.[1] This consensus provides a basis for the evaluation of the theories presented in appendix B.

Spatial extent

Over three hundred years ago Pierre Vernier published a description of his invention, a sliding scale placed in opposition to a fixed scale (Vernier, 1631). He found that if n divisions on the sliding scale extended over n-1 divisions of the fixed scale, then the proportion of the last interval traversed by the end of the sliding scale was indicated by the graduation on the sliding scale which was in closest alignment with a graduation on the fixed scale (figure A.1). This adjustment allowed the position of the sliding scale to be determined to 1/nth of an interval. When the scale was applied to the sextant, it greatly improved measurement accuracy. Together with the precise chronometers introduced in that period, reliable long distance navigation became a reality. The success of this invention was due in no small part to navigators' ability to detect exceedingly small offsets of two opposing lines. However, over two hundred years were to pass before this discrimination ability was investigated scientifically.

Helmholtz (1856-1866/1909-1911) considered the coincidence between the closest interreceptor spacing and the minimally resolvable line pairs (both estimated by him to be approximately one minute of arc) to account satisfactorily for maximum spatial acuity. Subsequent findings were not so easy to reconcile

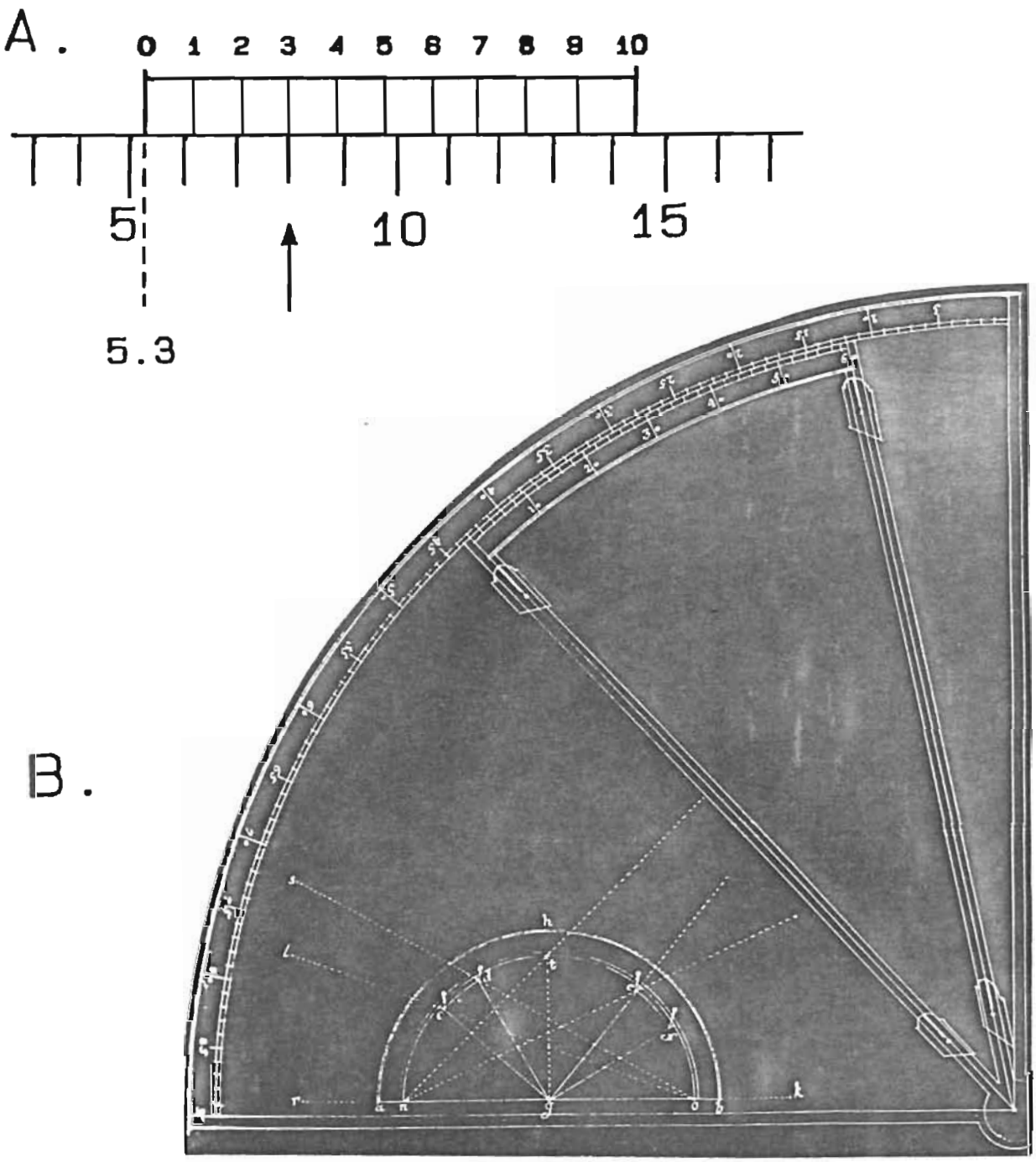

Figure A.1 Vernier measurement.

In this schematic of a vernier scale (a), the proportion of the interval on the lower (fixed) scale traversed by the zero mark on the upper sliding scale is indicated by the opposing striations in closest alignment (arrow). The vernier scale is also shown in quadrant form (b) as would be found on a sextant (from Vernier, 1631).

with the anatomy and physiology. Beginning with Volkmann (1863), positioning accuracies of from 15" arc to as low as 0.5" arc were found for a variety of spatial stimuli. The body of evidence detailing the precise positioning skills quickly grew, establishing the relation between the localization capabilities that became known as vernier acuity and the structure of the visual system as a major theoretical issue.

Unfortunately, the diversity of the stimuli, experimental conditions and even criteria for threshold make it difficult to determine what feature or features are necessary for such remarkable resolution. More than a score of different stimuli have been used to produce positional thresholds on the order of seconds of arc. Figure A.2 shows the stimulus configuration most commonly associated with the term vernier acuity. The Observers' task, which can be traced back to Pierre Vernier's original invention, requires the adjustment of the relative horizontal position of two vertical lines until they are judged collinear. The effect on offset threshold of three spatial parameters (the length (l) and width (w) of the lines and the vertical separation between the proximal ends (s)) have been extensively examined with the alignment stimulus. French (1920) was the first to manipulate the three experimentally (figure A.3). The data showed that under all his conditions threshold for vernier offset was monotonically reduced by increasing line length and that no threshold improvement was found for line lengths greater than approximately 8' arc. Decreasing the separation (s) by a factor of over 300 reduced the threshold by a factor of only three. The effect of s on offset threshold was slightly greater for thick lines (444" arc) than for thin (52" arc).

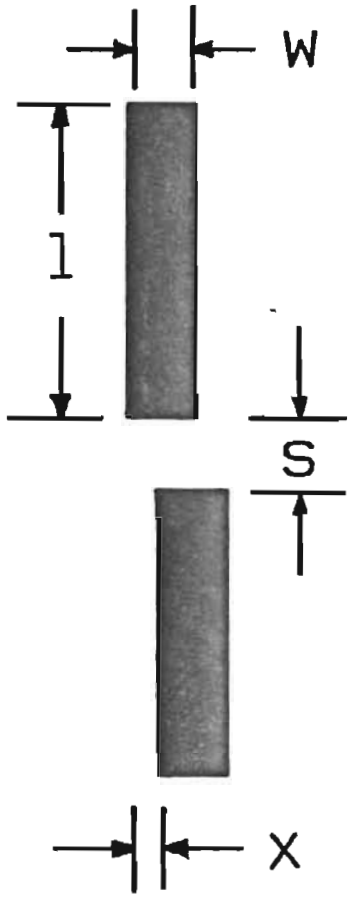

Figure A.2 Coincidence stimulus.

The alignment of two vertical bars is the most commonly investigated vernier task. The length (l), the width (w) and the separation (s) are features often studied in attempts to characterize the mechanism that is used in the detection of small positional offsets (x).

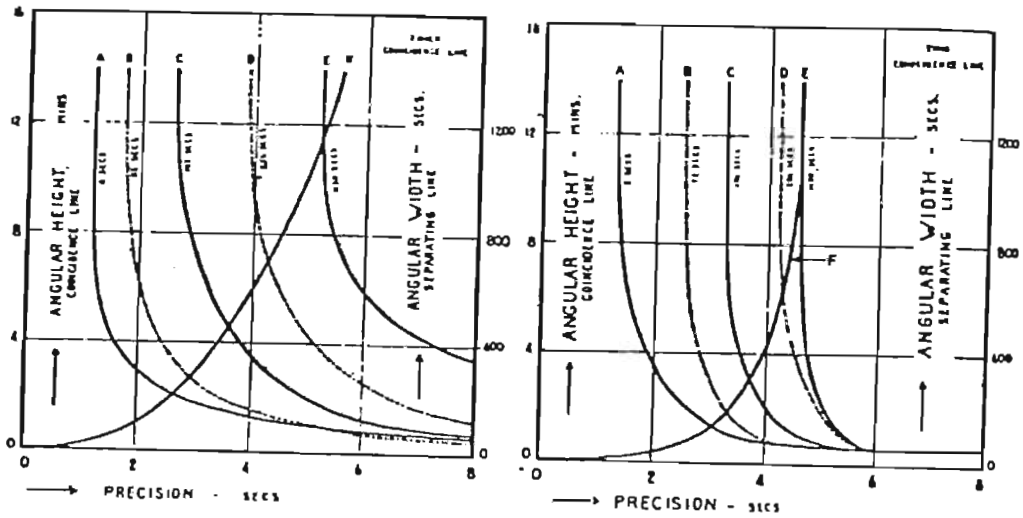

Figure A.3 Interaction of length, width and vertical separation.

In these early graphs, threshold is represented on the abscissae and angular length (l) on the ordinates. The different curves (A to E) represent a range of vertical separations (s) extending from a few seconds to about 20' arc. The graph on the left shows data obtained with a 444" arc wide bar; the other, a 52" wide bar.

(French, 1920)

Unfortunately, no measures of the variability are available for French's data. The results were based on only 5 readings for each data point and the graphs derived from these were idealized, the original data were not shown.

Pennington (1971) and Foley-Fisher (1973) each replicated French's results on the relation between line length and vernier threshold. In these studies threshold decreased, rapidly at first, with increased line length and then, much more slowly. Averill and Weymouth (1925) found that a comparable relation existed between offset threshold and the length of an edge (a coincidence task with w semi-infinite). With edges, threshold improved for lengths up to 20' arc. Although the form of the relation between contour length and offset threshold was similar in these four studies, the value beyond which there was little change in threshold varied greatly among them; 4' arc (French, 1920), 20' arc (Averill and Weymouth, 1925; Foley-Fisher, 1973) and 70' arc (Pennington, 1971). However, there may be some justification for the exclusion of Pennington's results. The coincidence thresholds reported in his study were all above 40" arc, not at a "vernier" level of performance. In addition, French's thresholds were idealizations based on scant data. Exclusion of these doubtful thresholds would eliminate much of the discrepancy among the findings.

In conflict with these studies, Sullivan, Oatley and Sutherland (1972) found no shift in vernier threshold with changes in line length. The major difference in the last study was the presence of a 90" arc vertical gap (s) between the coincidence lines (w: 80" arc). In the other four studies, the ends of the lines

abutted each other. Sullivan et al. argued that line length and separation interacted, that when the elements of the stimulus were separated sufficiently to be perceived as distinct, there was no improvement found with increasing line length. The interaction may also be seen in the idealized curves of French (figure A.3). For thin lines (w: 52" arc), threshold varied more rapidly with changes in line length at small separations than at large separations. (It should be noted that this relation was reversed for thick lines (w: 444" arc), the greater separations were associated with the more rapid change in threshold resulting from increased line length.) Although it is not possible to establish an exact correspondence between the conditions in French and those in Sullivan et al., it is possible that the latter study measured thresholds in a region corresponding to one of the straight (vertical) portions of the curves in figure A.3. In order for this region to be flat, it would require that the rapid threshold increase found for short lines to occur for values of l less than 80" arc, the smallest length examined in Sullivan et al.

The interaction between line length and separation was also demonstrated in studies that held l constant while varying s. This manipulation is equivalent to taking a horizontal slice through curves A to E (figure A.3). The result obtained from French's data is a monotonic relation between separation and threshold for any line length. Using stimuli in which the lines were reduced to dots (figure A.4, b), Ludvigh (1953) found evidence that conflicted with French's; threshold was at a minimum for separations of 5 to 10' arc, with poorer performance at larger and smaller separations. The monotonic relation between s and threshold reported by

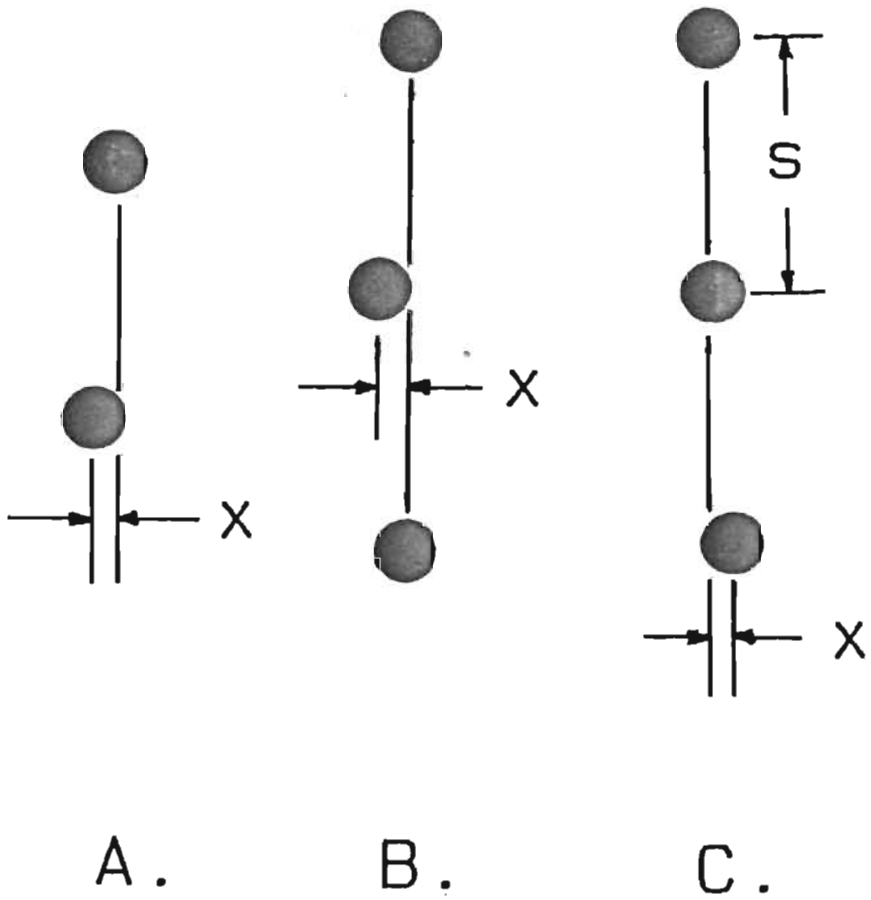

Figure A.4 Dot stimuli used in alignment tasks.

In a, the alignment of the two dots is judged relative to the perceived vertical. In b and c, the displaced dot (middle and bottom dots, respectively) is judged to be collinear (or not) with the two fixed dots.

Beck and Schwartz (1979) did not help to resolve the discrepancy since none of the separations they investigated were less than 7.5' arc, which was the value of the separation at the minimum found by Ludvigh. However, Westheimer and McKee (1977c) did examine the effect of small separations. As did Ludvigh, Westheimer and McKee found a threshold minimum at a separation of a few minutes of arc (figure A.5). Further, they discovered by increasing the line length that the threshold increase found at small separations was reduced. This trend continued until no threshold increase was found at all for small separations when line length was greater than 8' arc. The interaction between line length and separation is important and accounts for much of the disparity among the published results. It should be noted that the relations just described pertain to simple lines. The situation becomes more complex for other congruence figures (e.g., arrows) (Squillance and Bien, 1970). The multiplicity of contours found in some alignment targets can result in the establishment of spurious coincidences. The offset threshold would then depend on which facet of the stimulus is being aligned.

Lateral extent (w) is another spatial parameter that has been used to study offset thresholds obtained with simple coincidence stimuli (figure A.2). The variation of threshold for different line widths found by French (1920) was slight (figure A.3); however, the interaction between l and s for thick lines was greater than that found with thin lines. A subsequent study (Berry et al., 1950) concluded that there was no change in coincidence thresholds for widths from 26.8 to 424.0"

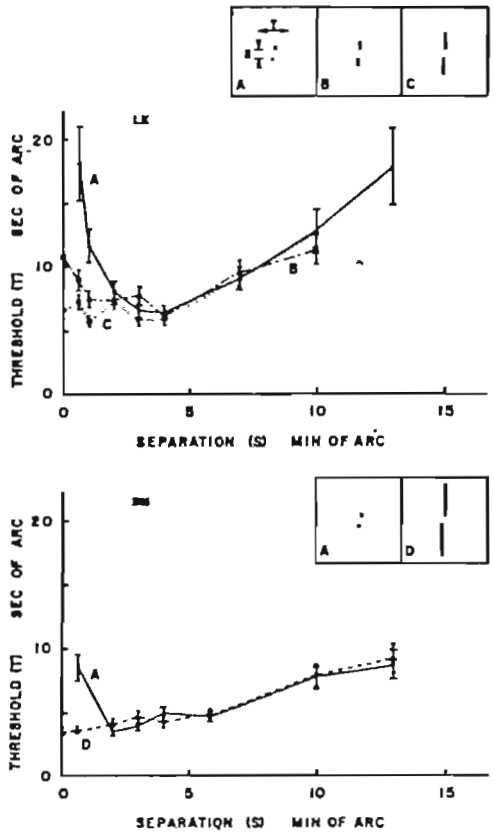

Figure A.5 Effect of vertical separation on threshold for different line lengths.

Threshold for detection of direction of vertical misalignment of two vertical lines, as a function of separation of the lower end of the top line and the upper end of the bottom line for four lengths of lines. Condition A: Lines each 30" arc (solid dots); Condition B: Lines each 2' arc (open squares); Condition C: Lines each 4' arc (open dots); Condition D: Lines each 8' arc (open triangles). Note that the data for the shortest lines (30" arc long) represent essentially the vernier capability of two dots, as a function of their separation.

(Westheimer and McKee, 1977c)

arc. With data that appeared not much different than those of Berry et al., Foley-Fisher (1977) proposed that a threshold minimum occurred when the line width was 15' arc. Unfortunately, the width that produced a threshold minimum was more than twice that examined in either of the other studies and thus this finding could not be corroborated.

Changes in vernier threshold with line width were all either close to or smaller than the confidence intervals consistent with the variability of the data. It appears that the width of the lines in a coincidence stimulus does not influence offset threshold to the same extent as line length or separation. This conclusion must be tempered by the realization that the three-space defined by the three spatial parameters (l,w,s) is only sparsely sampled in any of these studies. For example, a study by Berry (1948) with a wider (107" arc), longer (2426" arc) line produced a small, but consistent, increase in threshold at the minimum separation (3.6" arc). The apparent conflict with the data of Westheimer and McKee (figure A.5, d) may possibly be due to a difference in the width of the stimuli used in the two studies.

Westheimer and McKee (1977c) also investigated the effect of separation on a different vernier task, the spacing of two vertical bars (figure A.6). This task may be viewed as an interval judgment rather than the recognition of a specific position. Following each trial, the Observers were informed as to the correctness of their response. Repeated exposure to stimuli which bracketed the criterion separation allowed the Observer to establish an estimate of the desired interval.

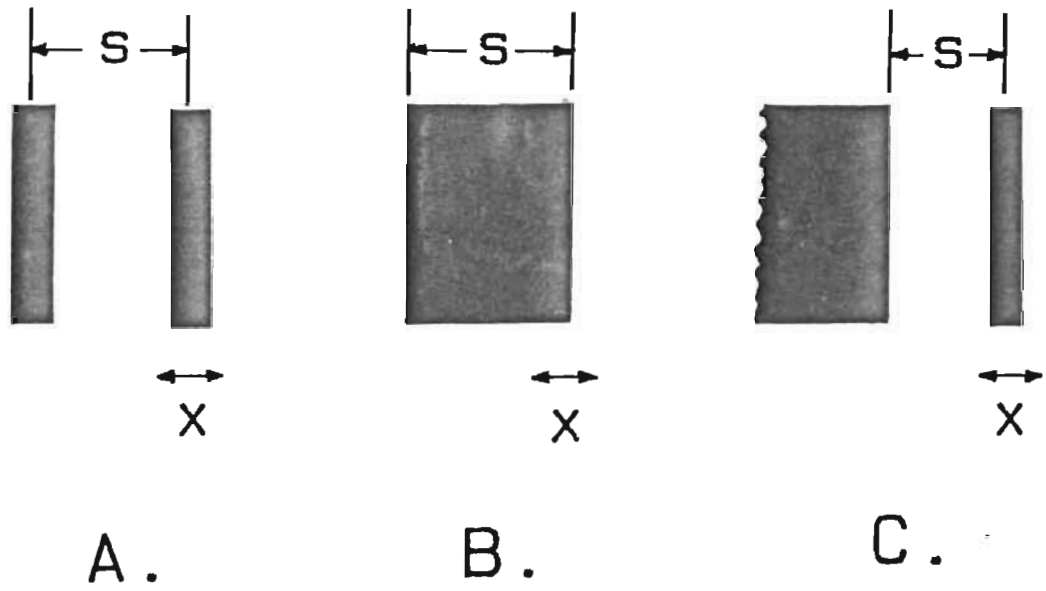

Figure A.6 Positioning tasks requiring feedback.

The separation of two bars (a), the width of a rectangle (b) and the separation of an edge and a bar (c) can be adjusted to within a few seconds of arc of an arbitrary criterion separation (s) when the subjects are given feedback as to the correctness of their responses.

(Westheimer and McKee, 1977c)

The precision of this estimate varied as a function of the criterion separation (figure A.7). Separations between 2 and 6' arc produced thresholds as low as 5" arc. Thresholds increased for separations above and below this range in a manner similar to that found by Ludvigh (1953) for the alignment of dots. Westheimer (1977) extended this analysis to the simultaneous comparison of two or of three intervals (figure A.8). Again, thresholds were a few seconds of arc for line separations of a few minutes of arc.

An interesting complication was introduced by the results obtained when flanking lines were presented on either side of a traditional vernier target (Westheimer and Hauske, 1975). This task may be viewed either as two simultaneous interval judgments, one the mirror image of the other, or, as the detection of a positional offset in the presence of two vertical reference lines (figure A.9). With either interpretation, it is highly surprising that vernier threshold was increased by the presence of flanking lines spaced 2 to 6' arc apart and is virtually unaffected when the separation is beyond these limits. Again, the pattern of interaction between separation and threshold was similar to the U-shaped curve reported by Ludvigh (1953); in this instance, only separations within the critical region interfered with the task.

Orientation

Physically similar to the detection of offset of short lines in the presence of a reference line is the judgment of parallelism (orientation discrimination). For

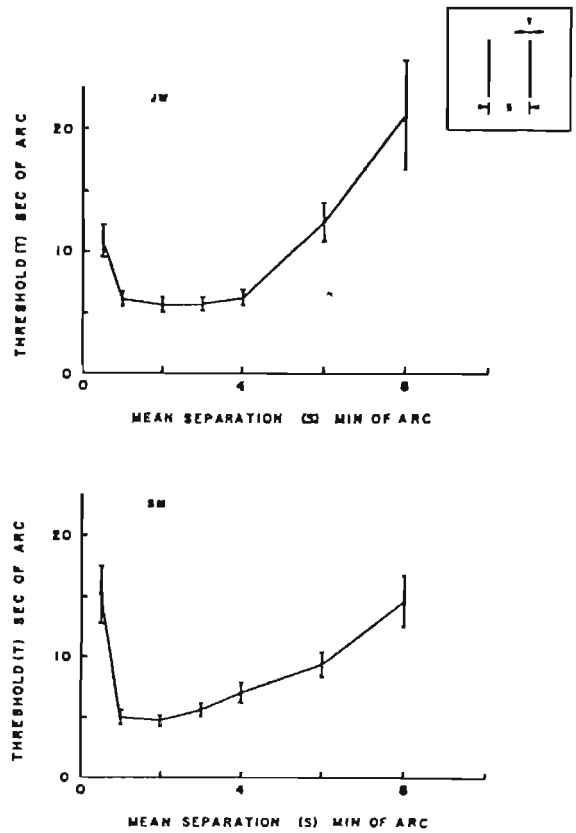

Figure A.7 Adjustment of the separation between two bars.

Sensitivity for differences in the spatial interval between two vertical lines as a function of their separation. For example, a threshold of 6" arc for a separation of 3' arc means that in a single presentation of two parallel lines, 12.8' arc long, separated by 3'6" arc, the subject will with 75% probability determine that the lines were more widely apart that the criterion distance of 3' arc, which constituted the center of the distribution of presented configurations.

(Westheimer and McKee, 1977c)

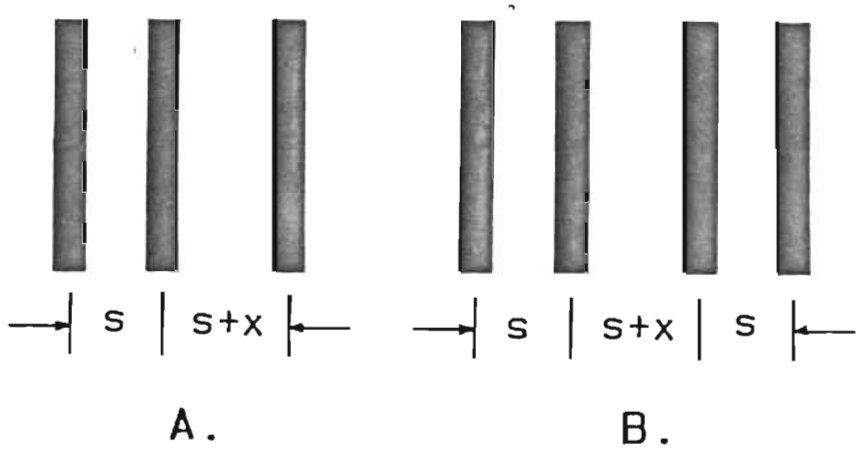

Figure A.8 Spatial interval judgments.

In this task, the observer must detect differences between the left and right intervals (a) or between the center and either of the two flanking intervals (b). One important distinction between the two tasks is that a constant line of symmetry exists for (b) but not for (a).

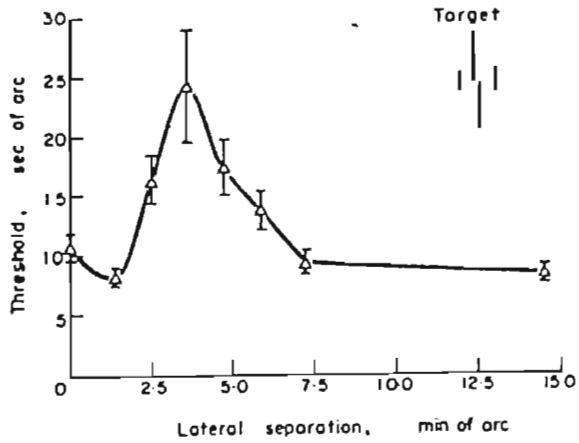

Figure A.9 The effect of flanking lines on a coincidence task.

Offset resolution for a 50-msec vertical vernier target as a function of lateral separation of a pair of vertical flanking interfering lines. The lines were presented synchronously with the main target, were of the same intensity and were half as long as each of the two making up the main target. Lateral separation in graph refers to distance between center of vernier target and position of each of the interfering lines. Target generation on display scope ensured that total amount of light reaching subject's eye was constant throughout all values of the parameter. Subject SM.

(Westheimer and Hauske, 1975)

short lines (figure A.10) between 3.5 and 9.0' arc in length Andrews (1967a, b) produced threshold angular deviations that were inversely proportional to line length cubed. For lengths greater than 9' arc, the angular threshold was only proportional to the length squared. The decrease in threshold continued for line lengths up to 69' arc. If instead, however, threshold is considered to be the positional offset from vertical of the end of the line, then a different interpretation emerges. Andrews et al. (1973) found that the minimum positional offset threshold occurred for lines 9' arc in length. This measure of orientation threshold was less than 4" arc, well into the localization range (figure A.11). When the length of a traditional vernier stimulus (figure A.2) was short, the offset threshold varied with line length as in an orientation discrimination task (figure A.12). The similarity in the two tasks between threshold and line length held for line lengths up to 15' arc. As line length increased beyond 15' arc, coincidence threshold remained constant while orientation discrimination threshold (lateral offset) increased. The Observers' subjective impression of the stimulus also changed as line length exceeded 15' arc. The impression of short lines with a vernier offset was one of a single sloping line; for longer lines, the perception of offset was of a disjunction in the center of a single line.

Other experiments also attempted to relate localization and orientation performance. Using two-dot and three-dot stimuli (figure A.4), Beck and Schwartz (1979) determined that localization threshold was linearly related to dot separation in the range between 7.5 and 44.4' arc. This relation is similar to that found for

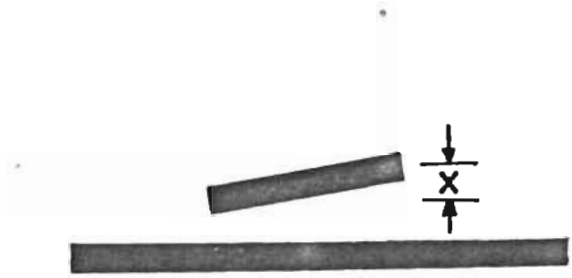

Figure A.10 Orientation discrimination stimulus.

This configuration was used by Andrews (1967a, b) to measure the effect of line length on orientation judgments. The length of the bottom (reference) line was considerably longer than the top (test) line.

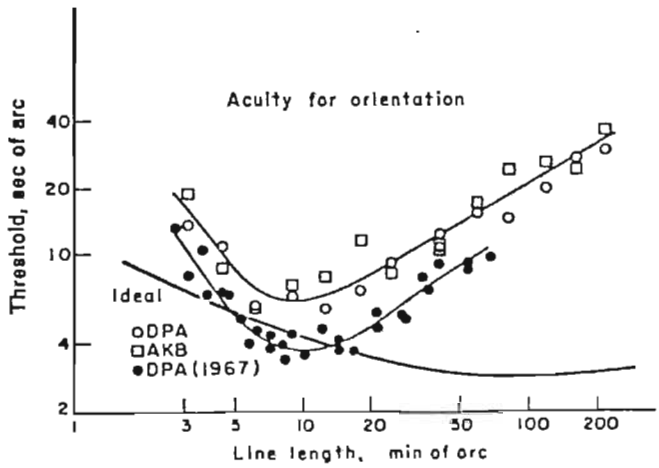

Figure A.11 Variation of orientation threshold with line length.

Human and ideal performances in detecting the slope of a line in relation to a long companion line just below it. Open and filled symbols represent different exposure durations. The ideal curve may be scaled vertically by arbitrary constants.

(Andrews et al., 1973)

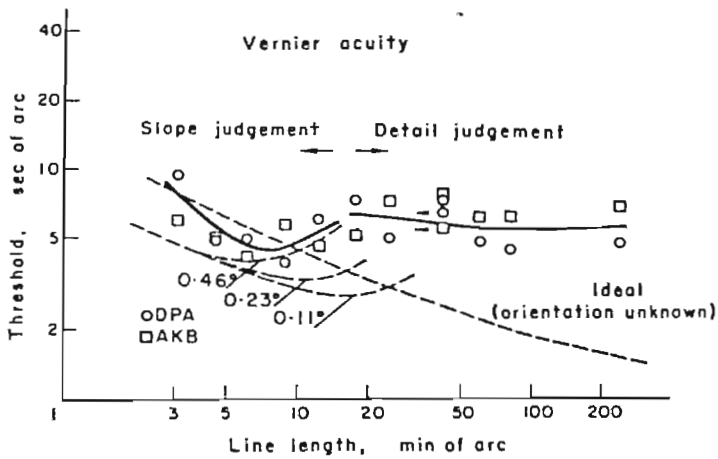

Figure A.12 Coincidence thresholds as a function of line length.

Human and ideal performance in detecting vernier offset in horizontal lines. The line length as plotted includes both lines. For lines less than 15' arc, the subjects responded according to the perceived slope of the whole array. For longer lines the discontinuity was detected more easily that the overall slope, and the subject responded accordingly. The ideal machine likewise has two modes of detection (dashed lines). When detecting slope, its performance is limited by how well it knows the true horizontal.

(Andrews et al., 1973)

orientation discrimination (as measured by lateral offset) by Andrews et al. (1973) if line length is considered to be equivalent to dot separation. Beck and Schwartz noted that the linear relation between offset threshold and dot separation results in a nonlinear relation between dot separation and orientation threshold (as measured by the angle from vertical). A nonlinear relation between dot separation (line length) and orientation threshold is what was found by Andrews (1967a, b). However, it appears that dot separation is apparently not equivalent to line length in all configurations of a coincidence task since there was no increase in vernier threshold for line lengths greater than 15' arc (figure A.12), a region where the abutting of disjoint line segments provides a cue to positional offset not available with widely separated dots.

Using an unusual localization stimulus (figure A.13, a), Tyler (1973) studied the effect of orientation on the determination of localization threshold. At low spatial frequencies, the positional oscillations of a thin line at threshold varied in amplitude in such a way that a constant angle of 20 to 30' arc was maintained between the opposing slopes. The constant slope at threshold existed in the range between 0.03 and 1.0 cpd. Maximum sensitivity to lateral displacement (5" arc) occurred for oscillations of 2 to 3 cpd. If line length is assumed to be approximately equal to a half period of the oscillation, then the optimal 10 to 15' arc equivalent line length is in good agreement with the results of Andrews et al (1973).

A.

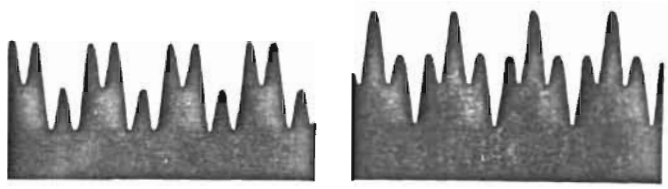

B.

Figure A.13 Periodic lateral displacement.

Tyler (1973) used the stimulus shown in (a) to determine the threshold for a sinusoidal displacement of a constant width line as a function of the spatial frequency of the displacements. This is an unusual application of the term spatial frequency since the variations are of position, not of luminance.

Hamerly and Springer (1981) avoided line width problems by varying the profile of an edge. In addition, they investigated the relative detectability of f/3f sinewave pairs in peaks-subtract (b) and peaks-add (c) configurations and found that phase (local slope) did not alter the amplitude of threshold positional modulation.

Tyler's data for high spatial frequencies were possibly distorted by an increase in the apparent thickness of his lines resulting from the finite width of the oscilloscope beam. Threshold may have determined by the detection of changes in the thickness of an otherwise perceptually straight line rather than the detection of positional modulation. Using modulated edge profiles (figure A.13, b and c), Hamerly and Springer (1981) avoided the line width artifact. As with the detection of line oscillations, the edge modulation threshold was at a minimum near 5 cpd and was well within the range of localization performance (4" arc). Beyond the minimum, threshold increased rapidly with increased spatial frequency, reaching 50" arc at 60 cpd.

Hamerly and Springer also measured the detectability of more complex edge patterns, f/3f sinewave pairs. The two components were presented in both peaks-add and peaks-subtract relative phase.[2] Detection of the compound grating occurred when each of the components was near its respective threshold. The relative phase of the gratings did not apparently alter the detectability of the compound grating. Neither the marked change in boundary profile nor the difference in peak to trough amplitude appeared to affect threshold. The experiments with complex edge patterns, therefore, appear to preclude the direct use of orientation measures to account for offset detection.

In a different experiment that supported the importance of orientation as a factor in localization while at the same time complicating its description, Findlay (1973) found that the extent to which a high contrast (60%) sinusoidal grating

interfered with vernier performance in a coincidence task depended on the orientation of the grating (figure A.14). The vernier threshold at some orientations of the grating was more than double that at other orientations. Curiously, the peak interference occurred not when the grating was oriented close to the vertical but rather when it was tilted 20° to either side. In addition, the most effective spatial frequency mask (12 cpd) was much lower in frequency than might be expected given the small positional offsets.

Further complications were presented by Westheimer, Shimamura and McKee (1976). As with vernier performance, line orientation sensitivity was reduced by flanking lines a few minutes of arc away (figure A.15). Also as before, the threshold increase peaked with separations of 2 to 6' arc and was reduced outside of the range. Since the orientation of the flanking pattern did not greatly alter threshold, Westheimer et al. concluded that it was the lateral position of the flanking bars that caused the interference. However, they could not explain the lack of interference that resulted when only one flanking line was presented.

It appears the orientation of some features affects the judgments that are an integral part of certain localization tasks. Unfortunately, as with the other spatial features discussed, its relation to localization threshold remains unclear.[3]

Luminance

As with may other visual tasks, variations in luminance have a significant effect on localization. Surprisingly, French (1920) stated that in his experiment

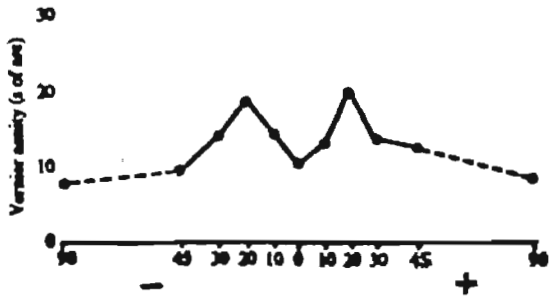

Figure A.14 Coincidence threshold as a function of the orientation of a masking grating.

The offset threshold is much greater st some orientations of a 12 cpd 60% contrast grating than at others. The peak interference occurred at $\pm 20^{o}$ from the vertical.

(Findlay, 1973)

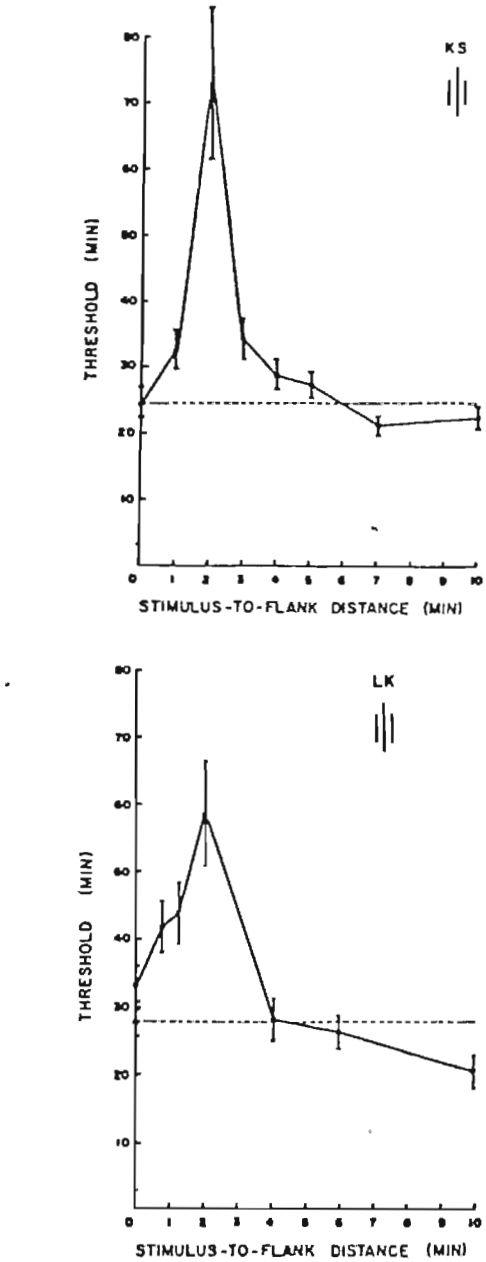

Figure A.15 Interference of orientation judgments by a flanking line.

Threshold for detection of inclination from the vertical of a line, 30' arc long, presented for 0.2 sec, in the presence of a pair of flanking vertical lines, 15' arc long (see inset), as a function of lateral separation of the flanking lines from the test line. Subjects KS and LK. Dashed horizontal line indicates threshold with test line unflanked.

(Westheimer et al., 1976)

there was no change in vernier performance with a 1000-fold change in illumination. He attributed any reduction in precision found at the lower levels of illumination to focusing problems. Using a 2.4 mm artificial pupil Baker (1949) found that vernier acuity first increased rapidly with illumination and then, flattening out, remained constant. She proposed that French's data were obtained while operating in this flat region. Leibowitz (1955), using a natural pupil, replicated Baker's results (figure A.16). Variability of the just detectable positional offsets at the lowest luminance levels was 3 to 6 times higher than at the highest luminance level (0.045 to 450.0 mL). The relation between vernier threshold and luminance remained constant above 10 mL. Nearly identical results were produced over a similar range of luminance by Berry et al. (1948). However, Aoki (1964) showed that this relation exists only in foveal vision; vernier acuity in the parafovea remains constant with changes in luminance.

Westheimer and McKee (1977a) measured the effect of stimulus duration on the relation between luminance and vernier threshold (figure A.17, a). Vernier thresholds with short flashes (11 msec) decreased rapidly as the luminance increased from 1 to 20 mL. As the duration lengthened (up to 190 msec) the threshold decrease occurred at increasingly lower luminances. The shift toward lower luminance levels is consistent with the improvement of other measures of acuity through some form of flux summation, a trade between intensity and duration.

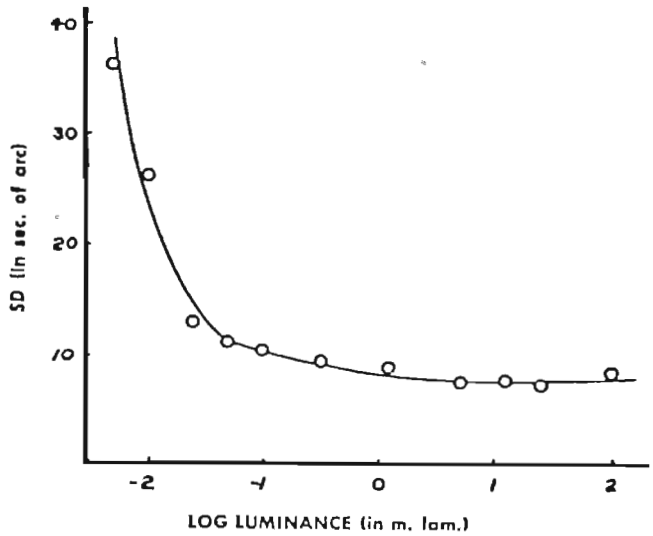

STANDARD DEVIATION OF VERNIER ADJUSTMENTS FOR DARK BARS AS A FUNCTION OF LUMINANCE

Figure A.16 The effect of luminance level on vernier threshold.

After a period of rapid improvement at low light levels, coincidence thresholds remain nearly constant for over a 1000-fold range of luminance.

(Leibowitz, 1955)

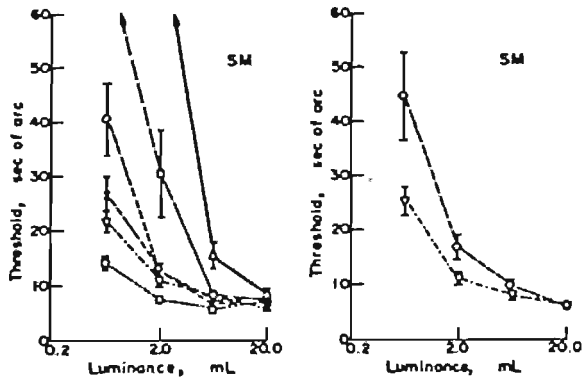

A. B.

Figure A.17 The effect of luminance level on the threshold of stationary and moving coincidence targets.

Vernier acuity thresholds for foveally seen targets at different luminances. (A) Stationary targets as seen with exposure durations 11, 22, 45, 67, 90, 190 msec from top down. (B) The targets move with horizontal velocities of 0.9 deg/sec (top) and 1.8 deg/sec (bottom) during 190 msec exposures. There is a strong resemblance over the whole range of luminance between the thresholds for the 90 msec stationary targets and the 0.9 deg/sec moving targets, and between those for the 45 msec stationary target and the 1.8 deg/sec moving targets. These results can be represented by an integration of information over a region about 4'.

(Westheimer and McKee, 1977a)

Wavelength

The wavelength of the vernier stimulus also has been reported to have an effect on threshold. Ferree and Rand (1942) found that yellow light produced the lowest vernier threshold, followed in order by white, red and blue. An experiment by Baker (1949) resulted in a different ordering: red (best), yellow, white and blue. Performance with the blue stimulus was greatly improved by the use of a -2.75 diopter lens. The lens corrected for the difference in refraction between blue and yellow light. Foley-Fisher (1968) found both types of wavelength ordering. In contrast to Baker's results, the blue threshold could not be improved in most Observers.

By analyzing the way threshold varied with line length for different distributions of wavelength Foley-Fisher (1973) concluded that there was no significant difference among the mechanisms subserving localization at different wavelengths. The lack of improvement in localization performance is consistent with an analysis of the effect of chromatic aberration on acuity measures; the proportional decrease in attenuation with white light compared with that found with monochromatic light is less at high and low than at moderate spatial frequencies (Campbell and Gubisch, 1967). The minimal effect of chromatic bandwidth on acuity (Hartridge, 1947) follows from the dependency of diffraction-limited modulation transfer on wavelength (Hopkins, 1962).

Contrast

The relation between chromatic aberration and localization threshold may be viewed as a subset of the effects of contrast: chromatic aberration lowers retinal contrast. However, retinal contrast may also be changed directly by altering stimulus contrast. In the early studies (Stratton, 1900; Bourdon, 1902) contrast was generally varied by using opaque coincidence lines and changing the background luminance, thus confounding luminance and contrast effects. Stimuli of the opposite contrast were made by cutting slits in opaque material and illuminating the openings from the rear. Variations in contrast again were confounded with changes in luminance. When similar conditions were used, the polarity of the contrast did not matter (French, 1920; Leibowitz, 1955); the shape of the functional relation between vernier acuity and the various parameters discussed above did not differ when white and black lines were interchanged.

Foley-Fisher (1977) varied contrast while maintaining a constant background luminance. Finding that vernier acuity improved with increased contrast, the edge-gradient was proposed as the major factor in the determination of vernier threshold: the steeper the slope, the higher the acuity. However, it is not clear that the interactions of contrast and line width were adequately measured in this study. In addition, the suggestion by Foley-Fisher is in conflict with data from Hartridge (1922) in which fuzzy absorption bands were aligned to within 11" arc.

With optical defocusing serving to reduce the relative contrast of high spatial frequencies, Stigmar (1971) systematically studied the effects of sharpness on

localization. Using the displacement of the interior of three vertical lines as a localization task (figure A.18), he blurred the stimuli by differing amounts. When the separations (s) between the segments were 7' arc, a 9-fold increase in half-width of the bar image (0.5 to 4.4' arc) produced no change in the 10" arc threshold (figure A.19). Reduction of the separation increased thresholds for the larger half-widths; however, even these suboptimal stimuli produced thresholds near 10" arc when blurred. Again, results obtained with unsharp stimuli conflict with Foley-Fisher's edge-gradient conclusions.

Westheimer and McKee (1977a) achieved performance similar to that of Stigmar with a different type of diffuse stimulus. They made up narrow bands of light out of nine closely spaced lines. Superimposed on these bands was a centered tenth line. The Observers were not able to detect any inhomogeneity within the band. In some trials only the tenth line was bisected and offset (figure A.20, a): in others, all ten lines were bisected and offset (figure A.20, b). In both tasks offset threshold was was found to be 4 to 5" arc; however, in the former case (figure A.20, a), the shifting "center of gravity" (i.e., the mean position) of the flux within the bar involved no change in the position of the boundary contours. As with the blurred stimuli, there were no sharp edges (high spatial frequencies) involved in the offset, yet localization performance did not suffer.

Consistent with the results suggesting that sharp edges (contours requiring high spatial frequencies) are not important in localization performance is a study by Freeman and Bradley (1980). Measures of both contrast sensitivity and vernier

Figure A.18 Double coincidence stimulus.

Stigmar (1971) used the offset of the center segment of a vertical line to study the effects of blur on coincidence thresholds.

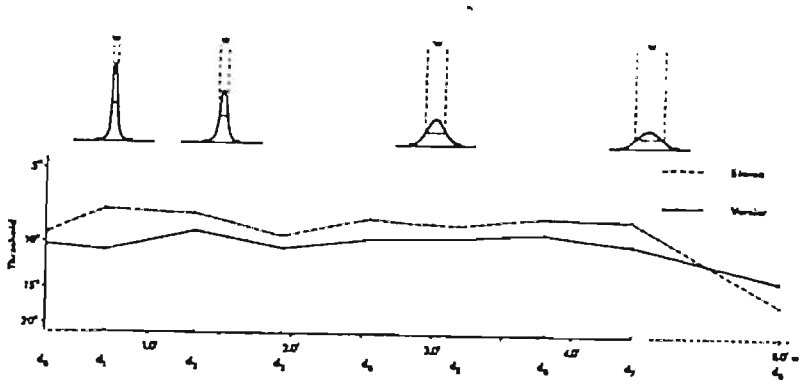

Figure A.19 The effect of blur on coincidence thresholds.

Vernier and stereo thresholds (in sec arc) obtained with increasing contour degradation (blur) of the stimulus pattern. The half-width of the light distribution of a single line is plotted on the abscissa. It should be pointed out that identical threshold values for vernier and stereo functions means that the corresponding vernier offset is, in the stereo situation, half that in the vernier situation.

(Stigmar, 1971)

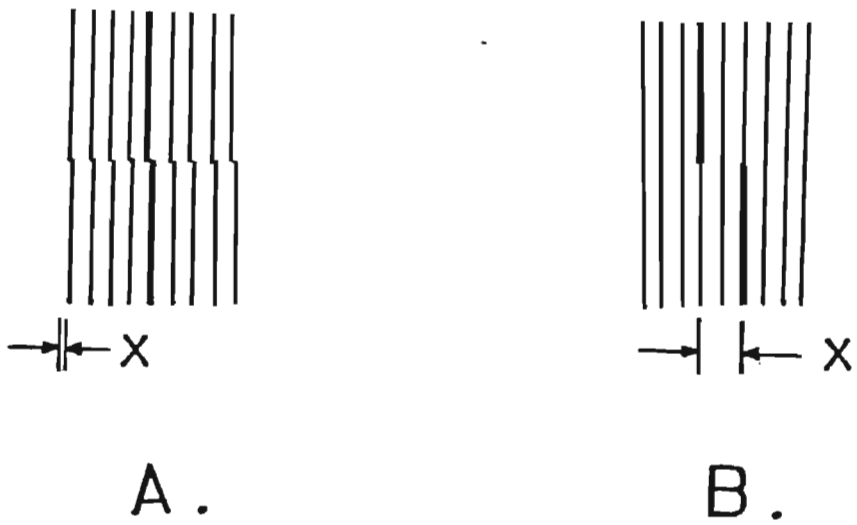

Figure A.20 "Center of gravity" stimuli.

The stimulus in (a) is composed of nine closely spaced lines with the center line brighter than the rest. Offset threshold is determined by shifting the upper half of the entire nine lines.

In (b), only the upper and lower portions of the incremental luminance of the center line are shifted in opposite directions, away from the center; the background pattern of nine equally luminant lines does not change.

(Westheimer and McKee, 1977a)

acuity in functionally monocular humans (amblyopes) were obtained. The normal eye in amblyopes displayed a capacity for higher vernier acuity than did the individual eyes of normals. Freeman and Bradley found that the magnitude of the vernier deficit in the amblyopic eye was highly correlated to that eye's deficit in contrast sensitivity at low (1 cpd) and middle (8 cpd), but not high, spatial frequencies. The sharpness of contours (supplied by high spatial frequencies) did not seem to be necessary for localization.

Marked differences in the relative transmission of high spatial frequencies can be found across the visual fields of normal Observers. As a result of increased optical aberrations and changes in the organization of the spatial detectors, most acuity measures get worse with eccentricity. The lack of sharp contours in peripheral percepts make them appear similar to those of blurred (unsharp) images presented to the fovea. However, unlike the case with foveal blur, localization performance was degraded when the image was positioned off of the fovea (Salvi and Galassi, 1978: Aoki, 1964). Weymouth (1958), using Bourdon's data (1902), calculated that vernier acuity decreased more rapidly in the periphery than did the minimum angle of resolution: however, he qualified this conclusion by stating that other data (not given) did not appear to show as rapid a degradation with increasing eccentricity as Bourdon's. A recent estimate (Villani et al., 1978) supports the view that the decline of both measures of performance occurs at nearly the same rate in the periphery (figure A.21). Westheimer (1982) corroborated the finding that vernier acuity decreased at least as fast, and possibly

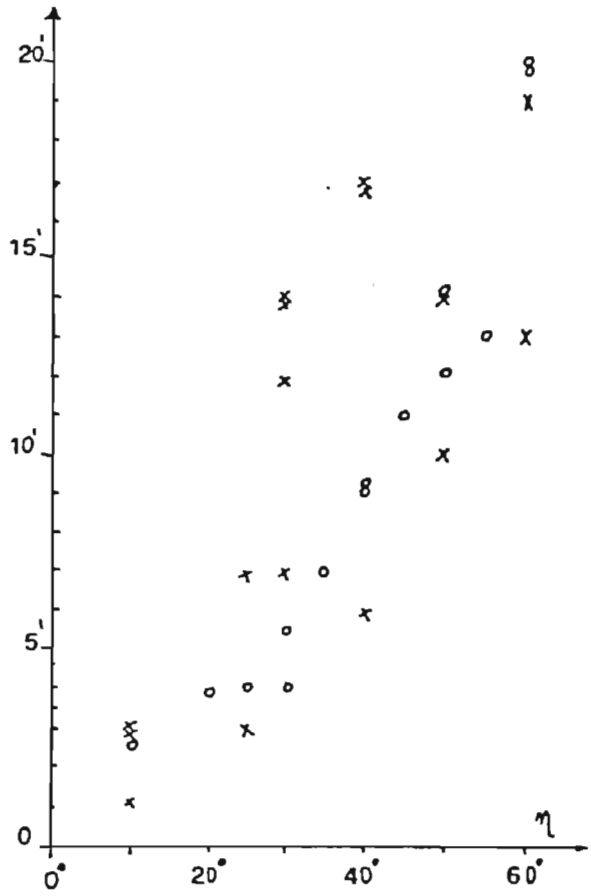

Figure A.21 Degradation of acuity measures with changes in eccentricity.

Estimates of both visual acuity and vernier acuity (open circles) change as a function of eccentricity. Data from different Observers are put together.

(Villani et al., 1978)

faster, than visual resolution in the periphery (his figure 2). In addition, the separations which produced the lowest thresholds were found to increase with eccentricity, but at a slower rate than visual resolution. The differential effect of eccentricity on the two measures of vernier performance (minimum threshold and optimal separation) could not be explained by receptor differences alone. It is possible that the reduction in vernier acuity outside the fovea results more from a difference in the sensitivity and character of the peripheral spatial detectors than solely from increased amounts of blur, spatial summation or receptor spacing.

Temporal

Another major dimension in the characterization of any vernier task is time. Baker (1949) tested vernier acuity under two temporal conditions: 19 msec and free viewing. The form of the relation between vernier threshold and luminance was the same for the two conditions. However, for the 19 msec duration, the relation shifted both toward lower acuities and higher luminances (i.e., for a short duration, threshold improved more slowly at low luminance levels and asymptoted to a lower level of vernier acuity than with free viewing). By taking into account critical duration and brightness discrimination thresholds, she was able fit the data with functions derived from the theories of Hecht (1935) and Graham (1938). Similar to Baker's results, Foley and Tyler (1976) produced lower thresholds with increases in duration (25 to 200 msec). However, differences in threshold for different durations (11 to 190 msec) disappeared at high luminance levels (figure

A.17, a: 20 mL) (Westheimer and McKee, 1977a). The convergence of curves for different durations to the same acuity asymptote is consistent with Baker's flux summation hypothesis; the curves would be expected to meet at luminances for which the critical duration was equal to or less than the stimulus duration.

Not all temporal effects may be a consequence of the summation of flux over time. Orientation discrimination of short bars (2.3 to 9.2' arc) displayed an increase in threshold for short durations (Andrews, 1967a). This configuration is similar to some of those which have been used in vernier tasks and, in fact, may itself be considered a form of localization (i.e., if the lateral offset of the end of the line is considered to be the measure of threshold). The large variability of perceived orientation associated with small deviations may have interfered with the making of reliable judgments. With longer durations or with longer lines, variability was greatly reduced. The reduced variability at longer durations may reflect the settling time required for interactions within the detectors.

One way to characterize temporal interactions, given that the detector is approximately linear, is to present the system a series of temporal sinewaves. The pattern of responses to differing temporal frequencies uniquely reflects the interactions in a linear mechanism. Using a sinusoidally flickering background, Foley-Fisher (1968) obtained equivocal temporal results. Two out of five Observers did significantly worse on a vernier task with a five Hz flickered field than with no flicker. Given the individual differences, it is not possible with only two points to tell if there are any systematic changes in sensitivity over the more

than 100-fold range of temporal frequencies to which the visual system responds. This type of temporal localization analysis remains to be done.

In contrast, the relative temporal onset of various spatial components has been extensively studied. Observers were able to discriminate the temporal order of two optimally positioned adjacent lines to within 3 to 4 msec (Westheimer and McKee, 1977b). There was no improvement of discrimination for increases in duration over the range of 10 to 100 msec. However, performance was optimal at the same spatial separation (a few minutes of arc) that optimized vernier acuity. This task displayed an insensitivity to changes in line length at the preferred spatial separation (2 to 6' arc) similar to that found for orientation discrimination (Westheimer et al., 1975) or vernier acuity (Westheimer and Hauske, 1975).

The temporal pattern of the two lines making up the traditional vernier stimulus (figure A.2) also has been varied to determine the temporal requirements of the task. If the temporal overlap of the two bars (each presented for 1 sec) was less than 100 msec, then localization performance was degraded (Westheimer and Hauske, 1975). The performance was worse than that obtained when the bars were simultaneously flashed for 100 msec. Westheimer and Hauske argued that the depressed performance resulted from "temporal flanking", a notion that is analogous to the spatial flanking regions that also were thought to reduce performance. When one of the bars was flashed for 200 msec prior to a 50 msec presentation of both bars, there was no loss in performance. However, when the 200 msec flash followed the pair, threshold increased. The effect peaked for a 50

msec stimulus onset asynchrony (SOA) and died out when the SOA was 150 msec. Performance of the pair was not degraded if their duration was 250 msec or more. Westheimer and Hauske concluded that their results were more like those of metacontrast than pattern masking since only backward interference occurs.

Breitmeyer (1978) took the interference process one step further and produced disinhibition. He combined both types of Westheimer's flanking effects. With the spatially flanking bars (figure A.9, inset) temporally asynchronous as well, vernier acuity was maximally upset with 50 msec SOAs, as before. If, in addition, those lines were flanked by lines presented synchronously with the vernier target, then the interference was reduced.

It appears, then, that the temporal characteristics of localization tasks are similar to those of a number of other spatial abilities: performance improves with duration and is degraded by short temporal asynchronies.

Motion

Fine localization is possible under free viewing conditions which allow eye movements to occur. These eye movements not only expand the retinal region over which detection may take place but also alter the temporal pattern of stimulation at each receptor. Westheimer and McKee (1975) investigated the effects of object motion on vernier acuity. Vernier coincidence targets were moved at velocities between 0 and 3.5 degrees per second for durations of 200 to 300 msec. The durations were short enough to preclude directed eye movements.

Under these conditions there were no changes in threshold over the range of velocities presented. They concluded that moderate amounts of image motion neither improved nor degraded vernier acuity.

In another study Westheimer and McKee (1977a) used a flashed sequence of vernier targets to produce the illusion of motion at 0.9 and 1.8 degrees per second (190 msec duration). The pattern of improved performance for differing rates of apparent motion over that obtained with a single 11 msec flash (the temporal duration of each position in the motion illusion) led them to propose that information relevant to localization was pooled over a region approximately 4' arc in diameter (figure A.17). With a similar experiment, Burr (1979) was able to achieve a threshold of 6.6" arc with 1.6 degree per second illusional motion. In a variation, the flashed line pairs were spatially aligned but temporally offset by 1.9 msec. The illusion of 1.6 degree per second motion of a vernier target, based on temporal cues alone, produced a threshold that was almost as good (10.3" arc) as that obtained with stationary stimuli. Given these results, localization performance appears to be robust over a wide range of translations.

Similarly, motion of a mask did not greatly reduce vernier acuity. Little interference was produced by sweeping a vertical line across an orientation target (Westheimer et al., 1976). When the motion was constrained to regions 1 to 4' arc lateral to the orientation target the threshold was increased. However, this effect may have been a consequence more of the spatial position of the motion than of the motion itself.

Motion may be a factor in localization in the form of retinal image movement. Even under conditions of steady fixation, tremors and microsaccades shift the position of the target relative to that of the receptors. When such shifts are compensated for optically and electronically the image can be maintained at a constant location on the retina. Keesey (1960) found no difference in vernier acuity between normal and stabilized viewing. Using a 22 Hz flickering field to retard image fading, Fender and Nye (1962) obtained slightly better thresholds for some, but not all, configurations of line length and separation. The two studies support the conclusion drawn from the object motion results: motion of the retinal image is not essential for, nor does it significantly degrade, localization.

However, it should be noted that there is more to eye movements than image motion. Rattle and Foley-Fisher (1968) discovered that individual differences in vernier threshold, which varied by a factor of two, were highly correlated with the Observers' mean intersaccadic interval. The result does not conflict with the stabilized image conclusions because the efferent signals associated with the saccades were still present in the visual system during conditions when retinal motion was eliminated. Under most conditions, the efferent signals were associated with a period of reduced sensitivity (saccadic suppression). In the presence of increased amounts of saccadic suppression, even a stabilized visual system would appear to be less sensitive.

Monocular/binocular viewing

The relation between binocular and monocular thresholds helps to define the mechanisms involved in a given visual task. For vernier acuity Berry (1948) reported that there was little difference among the binocular and two monocular thresholds. Stigmar (1970) found no difference between binocular and the better monocular performance; however, the monocular performance of the other eye was substantially lower (figure A.22). Intraobserver differences in monocular vernier acuity were also found in another study (Freeman and Bradley, 1980). In addition, Freeman and Bradley calculated that the ratio between binocular vernier acuity (8.7" arc) and mean monocular vernier acuity (12.1" arc) was close to the square root of two; the advantage that might be expected from the summation of the output of two noisy channels. Unfortunately, the best monocular vernier acuity was not given. It cannot be determined, therefore, whether or not the performance in this study, as in previous work, could be accounted for by the capability of the best eye alone.

The presence or absence of dichoptic interactions help determine the locus of the mechanisms that are involved in localization (although not as conclusively as has often been stated (Long, 1979)). Both line orientation sensitivity and detection of vernier offset were seriously degraded when target and flanking lines were presented to different eyes (Westheimer and Hauske, 1975; Westheimer et al., 1976). The dichoptic effect strongly implied that much of the processing was cortical, not retinal. In addition, central temporal processing is very sharp

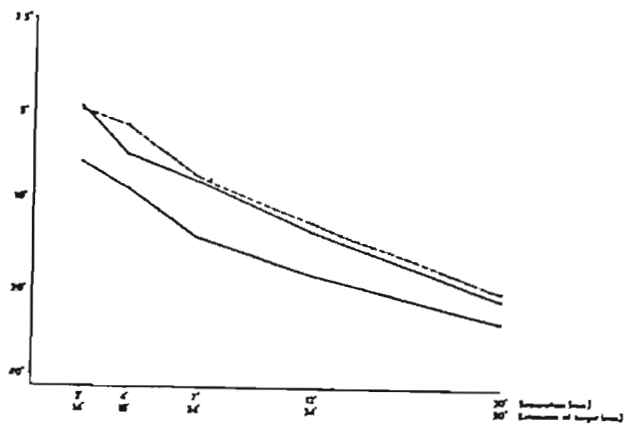

Figure A.22 Monocular and binocular vernier acuity as a function of separation.

The relation between binocular (dotted line) and monocular (continuous lines) vernier performances. The upper continuous line represents the best monocular vernier performance (right or left eye) and the lower line the result obtained with the other eye. Data averaged over three individuals.

(Stigmar, 1970)

(Westheimer and McKee, 1977b); dichoptic discrimination of temporal order was only slightly worse than monocular discrimination (10 vs. 3 msec).

Criterion

Fundamental to the establishment of the relations between stimulus parameters and threshold is the creation of the Observers' criterion. The setting of this criterion is a complex process involving the experience of the Observer, the stimulus parameters and the task demands in a given experiment.

Some vernier-like abilities exhibit exceptional plasticity. For example, two contours, placed minutes of arc apart, could be adjusted to within seconds of arc of an arbitrary criterion separation (figure A.6) (Westheimer and McKee, 1977c). The changes in performance were achieved merely by giving the Observers immediate feedback about their response; Observers were able to fine tune their criterion solely by the experienced gained from their performance on a range of stimuli around the desired separation. The extent that this plasticity plays a role in the determination of localization threshold is not certain since the criterion in most other localization tasks is self-evident; that is, the stimuli usually contain the feature(s) necessary to make the discrimination without feedback. However, the plasticity evidenced for 2-bar thresholds with feedback suggests the possibility that even with self-evident stimuli, thresholds may be influenced by the distribution of offsets presented to the Observers. The risk of this artifact may be reduced by following the convention of symmetrically distributing the stimulus offsets about

the criterion.

Other learning processes may also be at work in establishing offset thresholds. Performance on a variety of localization tasks has been found to improve markedly with experience (Leibowitz, 1955). Although the level of performance might vary with the amount of experience, the change in performance did not seem to reflect a qualitative change in the Observers' ability. The relation between offset threshold and luminance, or spatial and temporal stimulus parameters for practiced Observers tended to have the same form as those of inexperienced Observers; the curves were simply shifted along the ordinate (figure A.23). The improvement in performance seemed to occur whether or not the Observer was given trial by trial feedback or even prior instructions on how to perform the task (Volkmann, 1863; Best, 1900; McKee and Westheimer, 1978; Overbury and Bross, 1978). Naive Observers showed a decrease in threshold of 40% after just 2000 trials (figure A.24); however, there were large individual differences (improvement range: 2% to 70%) (McKee and Westheimer, 1978).

The improvement with practice in localization tasks was similar to that found with contrast sensitivity measures (figure A.25) (DeValois, 1977b). For one Observer, contrast sensitivity improved by 0.8 log units over the period of a year. In addition, this study showed that adaptation effects continued to grow in magnitude but became narrower in bandwidth. It is uncertain at this time whether the alterations in performance represent a change in sensitivity (e.g., neural reorganization, specialization), a criterion shift (e.g., increased familiarity

VERNIER VARIABILITY FOR LIGHT BARS ON A DARK FIELD

Log luminance (m. lam.)	S6 W	S6 B
−1.65	—	32.7
−1.35	14.5	19.0
−0.85	10.8	16.0
−0.35	8.6	13.3
0.65	7.0	10.3
1.65	5.8	10.8
2.65	5.7	10.8

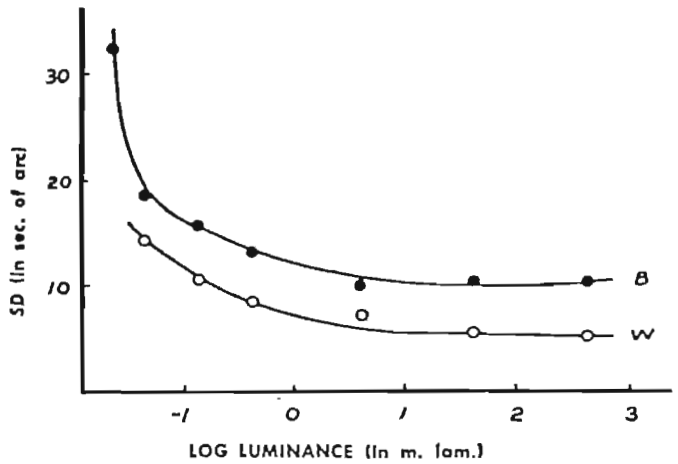

STANDARD DEVIATION OF VERNIER ADJUSTMENTS FOR LIGHT BARS AS A FUNCTION OF LUMINANCE
W, a practiced *S*; *B*, an unpracticed *S*.

Figure A.23 The effects of practice on vernier threshold.

(Leibowitz, 1955)

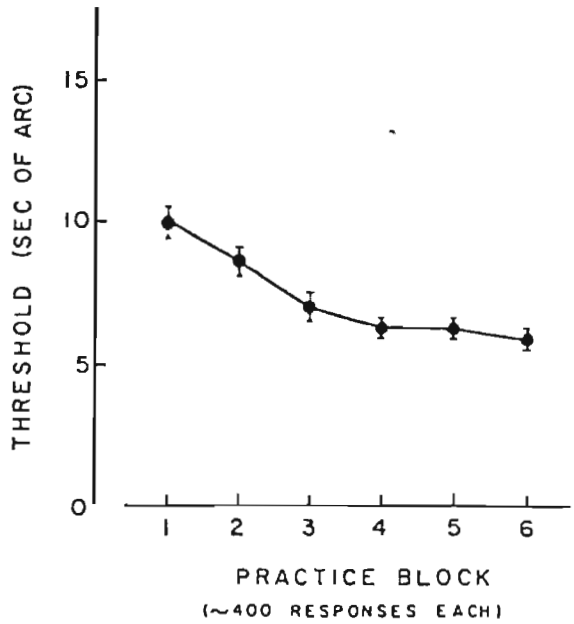

Figure A.24 Vernier threshold as a function of the number of trials.

General learning function showing the improvement found in vernier acuity with training. Each point is the average of thresholds from all subjects for all three orientations. The overall decline is about 40%.

(McKee and Westheimer, 1978)

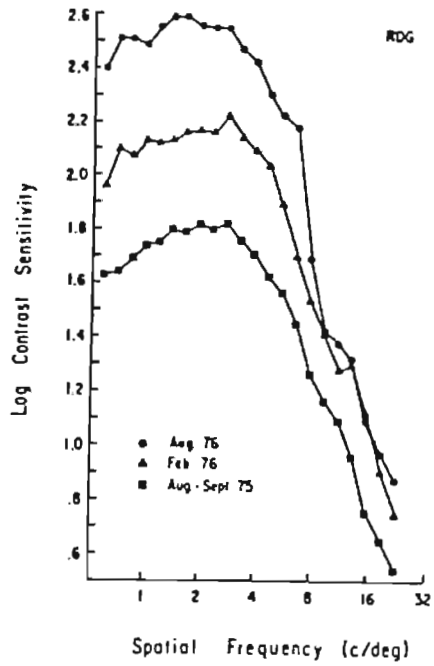

Figure A.25 Improvement in contrast sensitivity with practice.

Three unadapted contrast sensitivity functions for one subject (RDG) taken at approximately 6-month intervals. The two subsequent functions are based on four sessions each.

(DeValois, 1977b)

with the stimulus parameters) or performance not directly related to the detector (e.g., reduction in eye movements, focused attention patterns).[4]

In addition to the specification of learning effects, knowledge of an essential stimulus feature would help define how the process of setting criteria is done. It has been proposed that the resolution of two closely spaced thin bright lines is mediated by the detection of a shallow trough between their peaks (Hartridge, 1922). The corresponding feature(s) mediating localization performance have not been clearly established. Berry et al. (1950) concluded that since width does not influence threshold significantly, vernier acuity is performed by alignment of one or both pairs of edges. Sullivan et al. (1972) argued against the necessity of edge contours for fine localization performance. They were able to align two round dots to within 5" arc from vertical. Subjectively, the judgment appeared based on detecting the direction defined by the opposing ends of the two sections, across the gap. Andrews et al. (1973) found that both the perception of and thresholds for short lines in a coincidence task were similar to short line orientation discrimination. For longer lines, thresholds for the two tasks differed, as did the perception of the respective targets. The vernier target appeared to the Observers to be a line with a fuzzy knot in the middle. The possibility exists that there is not just one "vernier" task but, instead, a family of tasks, each with a different criterion. It has certainly proven difficult to find a common feature among stimuli as diverse as coincidence lines (figure A.2), two points (figure A.4, a), a wide bar (figure A.6, b) or a bar with an inhomogeneous flux distribution (figure A.20, b).

However, as will be seen from the evidence presented in the body of this thesis, a multiplicity of mechanisms is not required; it is possible to unify these divers results under a single theory.

Another area where the establishment of a criterion becomes important is the selection of an appropriate index of threshold. The choice of index depends very much on which psychophysical method is used. The usual convention is to determine the stimulus which elicits the probability of a correct response that is midway between chance and certainty. Even though the probabilities used to define threshold are mathematically equivalent, some methods (e.g., adjustment) are more susceptible to bias than others (e.g., constant stimuli). Indeed, much of the efficiency gained by determining only one point of a psychometric function is achieved at the expense of information about the bias, sensitivity and stationarity of the Observer. Even methods which determine several points along the psychometric function often require strong assumptions about the underlying distributions which shape that curve. For example, most modern investigations of localization use a form of the method of constant stimuli with a two alternative forced choice procedure. If the threshold is calculated using probit analysis (Finney, 1971) then it is implicitly assumed that the incremental contributions of the disjunction about the alignment null are linearly related to the response of the detector, that gaussian noise is linearly added to the response and that the sum must exceed a (stationary) criterion in order to be perceived. To the extent that these assumptions are false, the threshold measure will be in error.

Even more fundamental than the method of threshold calculation is the type of response required of the Observer. Different detection mechanisms and judgment processes may be required for recognition than are needed for discrimination. Stratton (1900) discussed this issue and its relation to localization and argued that spatial (positional) information is required for left/right alignment decisions. Since he felt that positional information was essential for the determination of "local sign" and that this feature was responsible for localization performance, he used a recognition task. Almost every subsequent investigator has followed his lead.[5]

In summary, it can be seen that stimulus parameters make up only one part in the establishment of a criterion. The tendency of an Observer to show a susceptibility to bias as well as a plasticity of his capabilities resulting from experience can lead to distortion of the criterion as well. The use of interleaved stimulus sequences and forced choice response techniques are required to maintain a stable, uniform criterion. It is also clear that the form of the questions that are asked may well alter the pattern of responses that are obtained. The choice of detection in place of recognition criteria could alter the nature of the relations found to exist among the many stimulus parameters.

Conclusion

This survey of performance has attempted to present localization in its many forms. Out of these, often conflicting, reports no feature stands out as essential to

the recognition of minimal spatial offset. The major influences and interactions which must be incorporated in any general theory of localization are outlined here:

Spatial extent - Separation and line length interact in their effect on coincidence thresholds. There is no substantial effect of line width. A separation of 2 to 6' arc allows dots to be aligned to within seconds of arc. Contours separated laterally by 2 to 6' arc can be positioned to within seconds of arc. Vertical flanking line pairs 2 to 6' arc away do not serve as reference aids but instead interfere with localization.

Orientation - Threshold for orientation is equivalent to vernier acuity for line lengths up to 15' arc (with no vertical separation), but degrade more rapidly thereafter. Offset thresholds for three-dot stimuli vary in a way similar to orientation discrimination thresholds, even for dot separations (line lengths) greater than 15' arc. Thresholds for sinusoidal modulations in the position of an edge or thin line are only seconds of arc and are a function of the rate of modulation; however, the detection of complex patterns of modulation does not seem to depend on either the local features of the edge profile or the peak to trough amplitude. Maximum interference with a coincidence task was produced by a 12 cpd sinusoidal grating oriented $\pm 20^{o}$ from vertical. Orientation and pattern of flanking lines does not alter the amount of interference generated, it is sufficient that the lines possess a lateral separation of between 2 to 6' arc.

However, a single flanking line does not interfere with orientation discrimination at any lateral separation.

Luminance - Localization performance increases rapidly with luminance at low luminance levels, but much less rapidly above 10 millilamberts.

Wavelength - Considering the effects of chromatic aberration in the eye and the size of the threshold positional offsets, the minimal advantage found for narrowband stimuli over those composed of white light is consistent with that found with traditional acuity measures.

Contrast - Localization is improved with increased stimulus contrast, but blurred and sharp stimuli can be aligned to the same degree of accuracy. localization performance is highly correlated with low and middle spatial frequency contrast sensitivity, but does not depend on the presence of high spatial frequencies. localization is degraded with increased retinal eccentricity of the stimulus, but at a similar rate as other measures of spatial acuity.

Temporal - Thresholds decrease with increased durations, up to 200 msec. However, spatial thresholds less than 10" arc are possible even with 11 msec flashes. Resolution of temporal order is best when the contours are spatially separated by 2 to 6' arc. Temporal asynchronies between flanking lines and the offset contours produce interference similar to metacontrast.

Motion - Localization is insensitive to a wide range of image motion (0 to 3.5 degrees per second). Illusional motion caused by temporal offsets alone do not degrade localization performance. Stabilized images neither improve nor degrade localization.

Monocular/binocular - Binocular viewing offers at best a 40% improvement in localization performance over monocular viewing. Binocular acuities may be equal to the best monocular performance. Dichoptic studies indicate a central (nonretinal) component to the processing of localization.

{1} This survey spans more than 100 years of research. Any generalization must be tempered not only by considerations of normal inter-experimental differences but also by a change in the conventions of science that occurred over that time. A good portion of the data that constituted acceptable evidence at the turn of the century would be considered today to be anecdotal at best.

{2} The expression peaks-subtract refers to a stimulus where a pair of sinewaves, one having three times the spatial frequency of the other, both are in sine phase. The peak of the lower frequency sinewave coincides with the trough of the 3f sinewave, causing the peak amplitudes to subtract. A similar opposition always occurs at each trough of the lower frequency grating. Peaks-add refers to a

stimulus where one of the sinewaves is shifted 180° with respect to the other; in this condition, the peaks of the two waveforms summate, as do the troughs.

Peaks-add and peaks-subtract stimuli are of interest because they allow changes in peak to trough contrast to occur while not altering the amplitude of any of the spatial frequency components; the f/3f pair in peaks-subtract phase are also the primary Fourier components of a squarewave; and the sinewave frequencies are more than an octave apart and may be processed by different spatial frequency channels (according to some models).

{3} Another, very different type of orientation effect should be mentioned. It concerns the orientation anisotrophy of the visual system (Appelle, 1972). Vernier threshold was found to vary slightly with changes in orientation (Leibowitz, 1955; Ludvigh and McKinnon, 1967; Westheimer and McKee, 1975; Corwin et al., 1977). However, McKee and Westheimer (1978) warned that any oblique effects should be studied with caution for both the magnitude and plasticity of the effect appear to vary widely across Observers and with practice.

{4} Given the magnitude of some of the practice effects it would seem advisable to interleave any conditions which are to be compared. A stimulus sequence which randomly mixed all conditions under study would result in an even distribution of any changes in performance across conditions and thus avoid confounding practice and stimulus effects. Also, since a data point cited in this review may be based on as few as five trials or as many as a million, the existence

of practice effects suggests that generalizations across studies should be taken with caution.

{5} Detection, as used here for localization tasks, is defined as the process of responding differentially to aligned and displaced contours. Detection threshold is the spatial offset required to produce a probability of correct response that is midway between 100% correct and chance performance.

Discrimination is the process of responding differentially to contours displaced by different amounts in the same direction. Discrimination threshold is the difference in spatial offset necessary to produce a probability of correct response that is midway between 100% and chance performance. Detection may be considered to be an instance of discrimination; the incremental difference in offset necessary to be discriminated against the noise alone.

Recognition is the process of responding differentially to contours that vary along different dimensions (a qualitative change: e.g., offsets to the left or right). It is possible that Observers may be able to detect an offset without being able to say (above chance) whether the offset is to the left or to the right. It is also possible that Observers may be able to say that two offsets are not equal and not be able to say which offset is greater.

To the extent that these task distinctions simply reflect just noticeable changes in the response of a single detector they may be considered to be an arbitrary classification. However, if some of the tasks require a qualitative change, such as a

shift in the detector population (i.e., different labeled lines) mediating the response, then the proposed taxonomy may form useful distinctions.

Appendix B

THEORIES OF LOCALIZATION

The diversity of localization performance examined over the past century resulted in an equally diverse collection of theories of localization mechanisms. The development of these theories reflected not only the range of available data but were also influenced by the improving technology and concurrent theories of other visual abilities. The rapidly increasing knowledge of visual physiology had an especially extensive influence. This section provides a chronological survey of theories of localization, the contemporary influences which shaped them and examines to what extent they explain the results outlined in appendix A.

The similarity among measures of visual resolution, cone diameter and the point spread function of the eye satisfied Helmholtz (1856-1866 /1909-1911) that the mechanisms limiting maximum visual acuity had been adequately explained. This explanation was soon challenged. In a series of experiments on spatial abilities designed to test Weber's hypothesis on just noticeable differences, Volkmann (1863) found that the threshold for some width (interval) judgments (figure A.6, b) was only 12" arc. In an attempt to explain these results, Helmholtz changed his estimates of cone diameter. He had originally cited references containing measures of cone diameters that were between 60 and 75" arc. The revised anatomical estimates were lowered to 50" and then to 21" arc. He ultimately suggested that even 9" arc was not out of the question. The last figure

was based on the narrow tips of the cones acting as the active sensory element. Eye movements would then be necessary to produce the best (most sensitive) position of the tips relative to the stimulus. Backed by these later estimates, Helmholtz did not feel forced to abandon his notion that cone diameters were the limiting factor in visual acuity.

Helmholtz notwithstanding, the results of Volkmann and, later, those of Wulfing (1892) with coincidence lines, described spatial abilities an order of magnitude finer than any reasonable estimate of intercone spacing. Wulfing argued that the performance levels obtained with laterally placed resolution targets did not reflect the true limits of localization. He felt that the spread of flux resulting from the aberrations of the optics of the eye reduced the definition of the closely spaced line pair and thus reduced the precision of spatial localization. The constraints imposed by the third of Helmholtz' factors, the point spread function, were surmounted in Wulfing's experiments by the vertical separation of the coincidence lines. The vertical separation allowed each line to be localized independently of the horizontal separation of the pair, allowing the "true" limits of spatial localization to be revealed. The mutual interference between contours was overcome in Volkman's experiments by the relatively wide criterion separation used in his interval judgments.

Earlier, the keen localization performance would have been explained as consistent with a retinal syncytium having an arbitrarily fine resolution. However, Cajal's neuron doctrine (Rodieck, 1973) eliminated that as an alternative; the

receptor as a unit, with the concomitant limitations imposed by its spatial extent, was considered to be the fundamental building block of vision.

Emphasizing the discreteness of cones, Hering (1864, 1865) assigned each a distinct "local sign", a unique correspondence between the retina and visual space. In addition, he proposed that the dense packing of cones in the fovea would lead to a regular hexagonal array, each row having a different local sign in the direction orthogonal to its length. Offsets could be detected when the displaced contour sufficiently stimulated a different row and hence were associated with its local sign (figure B.1). Although he accepted Hering's theory, Bourdon (1902) could not explain why there was no change in threshold when the lines were tilted, as would be expected with a regular hexagonal array. Hering's theory, at least in this regimented version,[1] loses credibility because of the condition wherein the ranks of foveal cones are not aligned with the contours of the stimulus. Aliasing generated by the angular difference and finite receptor spacing can't be distinguished from the response to small offsets.

Constrained by both the relatively large diameters of the cones and their irregular spacing, some theorists opted for schemes which encoded some of the positional information in another form.[2] One such trade involved replacing a binary receptor mechanism with one that had a graded response. Helmholtz, in a later part of his handbook (French, 1920) proposed just such an alternative theory for localization. He thought that there might be a neural network connecting the more numerous cones to the less numerous optic nerve fibers. If the response

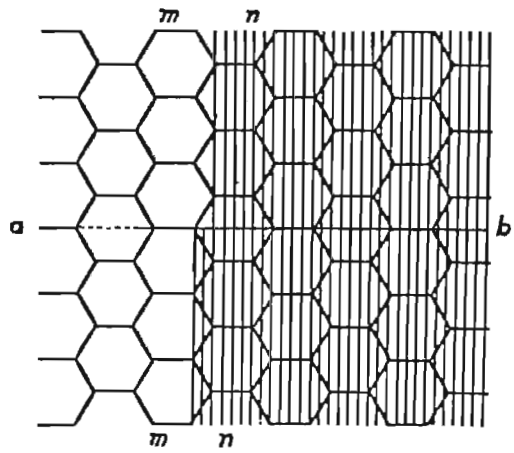

Diagram to illustrate the theory of Hering and Bourdon.

Figure B.1 Detection of vernier offset by means of local signs.

The slight offset of the lower portion of the edge sufficiently stimulates the regular column of receptors (m-m), taking on the local sign of that column, a sign different than that of the upper portion (n-n).

(from Anderson and Weymouth, 1923)

induced in a nerve by a given cone is a function of the path length between the two, then the interconnectivity could result in the response in a given nerve being proportional to position on the retina (figure B.2). This method of positional encoding would result in localization that is limited only by the incremental intensity of sensation that can be appreciated by the receiving mechanism. The proposal bears a strong resemblance to the theory used by Helmholtz to explain the trichromatic nature of color vision. Unfortunately, results from physiology could be used neither to confirm nor to dispute this hypothesis in any of its particulars for many decades.

A different mechanism was proposed by Stratton (1900). He suggested that light not only excites those receptors upon which it directly falls but that this initial activity propagates to other receptors in all directions. The magnitude of the diffusion effect on a given neighbor depends on the location of the light within the initial receptor. The net effect of the position-dependent diffusion would be to allow changes in local sign to occur with positional differences much smaller than the diameter of a single cone. Stratton argued that diffusion was also responsible for simultaneous contrast but he made no attempt to reconcile the properties of this phenomenon with those of vernier acuity. Although there is considerable physiological evidence for receptor-receptor coupling (e.g., Baylor, Fuortes and O'Bryan, 1971), there is no suggestion that the diffusion of activity is dependent on the locus of absorption within the receptor.

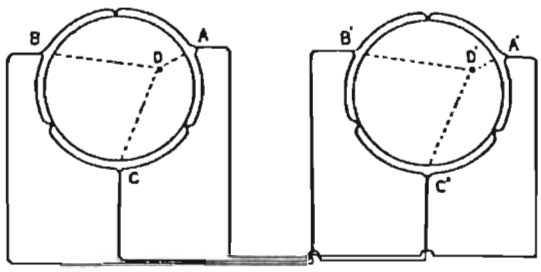

Figure B.2 Localization model of Helmholtz.

The position of the object D may be determined uniquely by the amplitude of three signals (A, B, & C). If the amplitude in each channel is proportional to the distance of D from the respective sensors, then the positional accuracy of the receiver depends only on the receiver's resolution for the graded signal within the channels.

(from French, 1920)

The optical distortion of the eye provides another mechanism for the dispersion of information across the retina. Even in the case of a narrow bright line, many receptors are stimulated along the direction normal to the orientation of the line. The distortion results from the spread of flux by diffraction at the pupil and the geometrical aberrations of the ocular media. Hartridge (1922) reasoned that when the shift of an aberration disk was large enough to be perceived there had been a perceptible change in the intensity of the light falling on a particular cone or group of cones. He found that a factor of 10 decrease in sensitivity to brightness differences occurred as stimulus size decreased from full field to that which covered a few cones and that a 10% change in intensity was required for detection of these small stimuli. He also calculated the amount of flux falling on a cone at various distances away from an edge (figure B.3). A shift of the edge of 2.6" arc caused a 16% change in the flux collected by a cone which was situated initially at the midpoint of the flux gradient. The capacity of such a mechanism to make location judgments based on the interpretation of intensive changes as positional shifts is certainly adequate to support the detection of offsets as fine or finer than those obtained by Hartridge (c. 10" arc). The fact that thresholds were not smaller was considered by him to be evidence of interference caused by eye movements.

Unfortunately, neither Hartridge nor any of the brightness discrimination theories that followed dealt with the spatial interactions that are manifest in much of the localization literature. In particular, the similarity of obtained thresholds

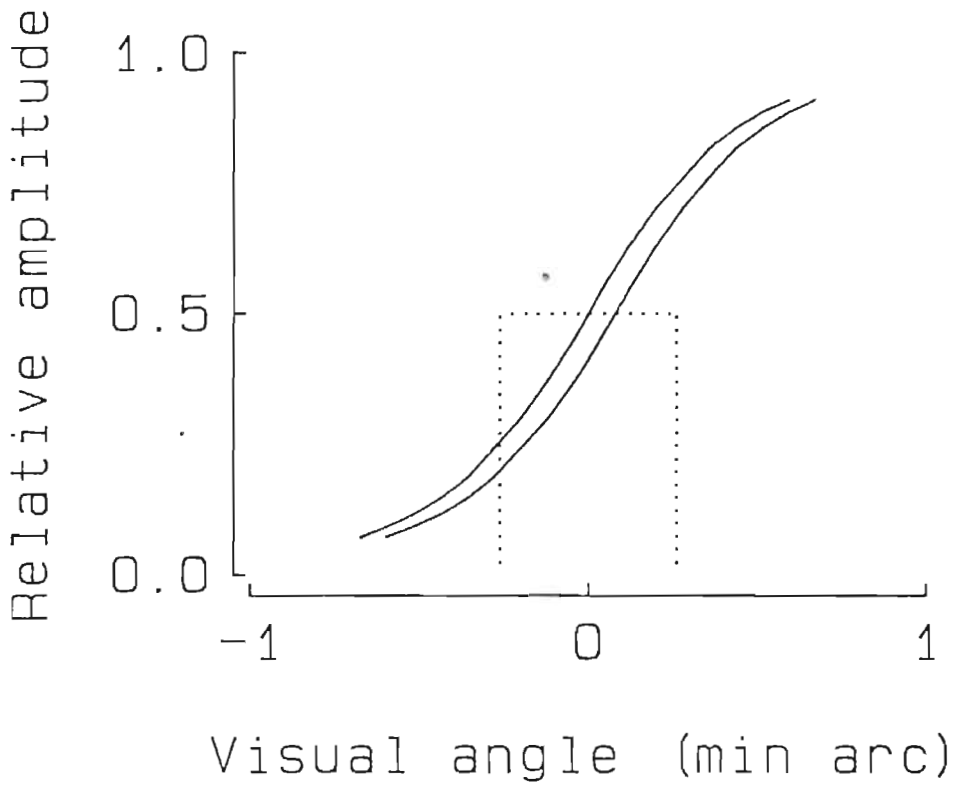

Figure B.3 Retinal flux distribution of a luminous edge.

Hartridge (1922) calculated that the relative shift in retinal location of only a few seconds of arc can result in significant changes in the flux falling on a cone positioned near the center of the edge profile. In this example from Hartridge, a 2.5" arc shift in the position of a edge results in a 16% change in the flux falling on a 32.5" arc diameter cone centered under the midpoint of the edge spread function.

with points, lines and edges must be reconciled with the disparity of flux gradients present in the point, line and edge spread functions.

A very different theory completely reversed the mechanisms of fine resolution and degradation. Weymouth (Weymouth et al., 1923; Andersen and Weymouth, 1923) proposed that the positional information (i.e., Hering's local sign) generated by individual cones was an all-or-nothing signal, incapable of graded contributions to localization. The trade-offs in this model were made possible by averaging over space as well as averaging over time. Through averaging, the calculation of spatial position takes advantage of the irregularity of the intercone spacing and of the shifting position of the contours resulting from eye movements. Weymouth proposed that when two adjacent cones are stimulated by a point of light, the local sign of each would "partake of the nature of the other". The resultant local sign would have a value intermediate to that of the sign of the two flanking cones. Extending this process along a contour overlying an irregular mosaic of receptors would assign to that edge or line the mean of all the local signs on its boundary (figure B.4). The extension of retinal mean local sign over space accounted for the obtained improvement in vernier acuity with longer lines; the increased number of cones sampled in the average reduced the variability of the localization estimate. The proposed averaging process also had a temporal component resulting from eye movements. According to this hypothesis, random eye movements altered the locus of even a fixated contour over a range that was several cone diameters wide. The weighting of a given cone's local sign in the averaging process would depend

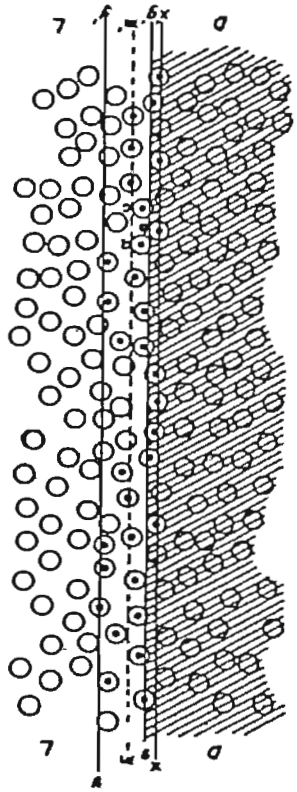

Figure B.4 Mean retinal local sign theory.

This figure illustrates Weymouth's theory of vernier and stereo-acuity (after Andersen and Weymouth). Displayed are the retinal conditions at the margin of a stimulated area. D-D is in darkness, L-L illuminated. The geometrical margin of the image is g-g'. The cones are shown as circles (x1500; traced from a photomicrograph). Cones a, b and c have local signs whose "center of gravity" lies amidst them, tending to pull b to the right. This action, among all of the cones cut by g-g', smooths the percept of the contour despite the raggedness of the line of cones concerned. Furthermore, normal nystagmus shifts g-g' back and forth between the extreme positions x-x' and y-y', so that m-m' represents the center of gravity of all the points stimulated, and is hence the local sign of the percept to which they give rise. The localization of this percept is independent of such considerations as the size of one cone.

(from Walls, 1943)

on the time it resided at the contour boundary. To Weymouth, then, the location of a contour depended on the random sampling of a large number of cones over a period of time. This mechanism allowed an irregular and irregularly moving mosaic to produce not only a precision of positioning but a uniformity in the perception of straightness not expected from such an array.[3] Andersen and Weymouth (1923) proposed that the fineness of the procedure resulted from repeated experience with straight lines. They also were the first to suggest that the assignment of local signs to a given contour did not depend on simple retinal mappings but, instead, relied on some form of complex cortical processing.

Subsequent theories often combined portions of Hartridge's static analysis and Weymouth's dynamic analysis with advancements in psychophysiology or electrophysiology. Hecht (Hecht and Mintz, 1939), building on the heritage of Hering and Hartridge, incorporated the influence of diffraction and geometrical aberrations with a detailed formulation of brightness discrimination to explain the limits of visual acuity. Hecht also incorporated portions of the dynamic theory in proposing that eye movements enhance brightness discrimination by moving many receptors in and out of the maximum flux gradient of the contour. Hecht's brightness discrimination function [B.1] closely fit the variation of vernier thresholds with changes in luminance (Baker, 1949).

$$\frac{dI}{I} = c\left\{1 + \frac{1}{(k\,I)^{\frac{1}{2}}}\right\}^2 \qquad [B.1]$$

where I is intensity and c, k are constants.

The similarity of response suggested that a brightness discrimination of some portion of the stimulus was used to make coincidence judgments. The relation was supported by the co-occurrence of maximum vernier acuity and maximum resolution acuity at about the same luminance level.

Using new anatomical and physiological evidence (e.g. Hartline, 1940), Marshall and Talbot (1941, 1942) developed a dynamic theory of the processing of retinal point images. According to their theory, position of contours depends on a statistically large number of reciprocal interactions among cells within each layer. The interactions produce a centroid of activity that may be located to a much finer spacing than the initial receptors. Repetition of the interaction process at several layers coupled with adaptation acted to enhance the sharpness of the response. Blurring of the retinal image acted to elicit greater amounts of sharpening by involving more elements at the initial stage. Between each level the multiple branching of each axon and the spatial overlap resulting from that branching tended to expand the recruitment of cells into the subset of the reciprocal network responding to the stimulus. The fineness of the cortical mosaic is maintained by at least a one hundred-fold expansion in the number of cells in the portion of primary visual cortex when compared to the equivalent receptor population (figure B.5). The representational expansion is distinct from any anatomical spread caused by multiple branching. The enhancement is further augmented by nystagmus which causes each point in the image to be swept over many receptors, increasing both the neural pool activated by a given flux discontinuity and the

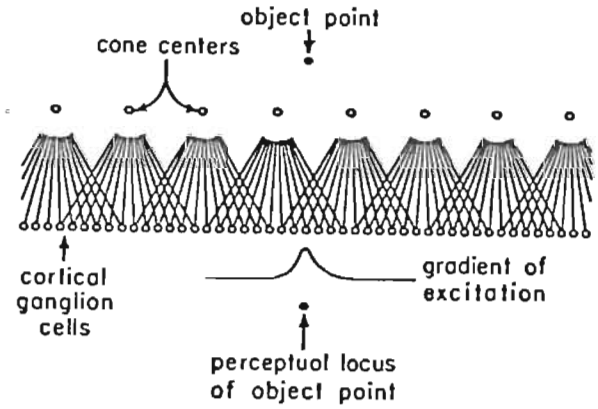

Figure B.5 Cortical local sign theory.

This figure illustrates Talbot and Marshall's explanation of the precision of spatial localization as the basis of vernier and stereoscopic acuities. Reciprocal overlap in the central visual pathway, together with neurophysiological phenomena, creates a gradient of cortical excitation whose peak is the locus of the percept of the object point. A great number of such loci can lie along the line representing the center-to-center distance between adjacent retinal cones.

(from Walls, 1943)

responses of individual neurons due to the increased sharpness of the temporal onset.

The major component of the enhancement of small discontinuities comes from the repeated processing through several cellular layers (as opposed to statistical positioning within a single layer). The net result is a differential amplification, small signals are disproportionately amplified wrt larger ones (their figure 2, p. 129). Eye movements along the length of vernier lines tend to enhance the neural response gradients where the lines are not in exact opposition creating "minute contours of activity" (their figure 5). Versions of this theory continue to the present (e.g., Barlow, 1979; Crick et al., 1980).

Advancements in technology allowed some of the necessary consequences of the various theories to be tested. Using stabilized images, Keesey (1960) found that motion neither facilitated nor degraded vernier acuity. This result is consistent with earlier data (Baker, 1949). Baker produced 12" arc thresholds with a stimulus of 19 msec duration; a duration too short to allow eye movements and the temporal averaging to occur, a critical requirement for Weymouth's theory of mean retinal local sign. Thus the two studies cast severe doubt on the dynamic theories. As Keesey concluded: "Acuity is based on the spatial pattern of retinal illumination, regardless of any temporal changes of intensity pattern on the receptor cells."

Ludvigh's (1953) experiments with three dot alignment put the spatial averaging hypotheses in jeopardy as well. The achievement of 2" arc thresholds

with points of light cannot be dependent on a statistically large number of cone inputs even if the spread of flux resulting from aberrations of the eye is considered. Although such small thresholds obtained with two-point stimuli do not preclude all forms of spatial averaging of local sign, relations such as a U-shaped function of threshold with increasing dot separation, the interaction between line length and separation and the relative insensitivity of threshold to changes of line width require a much more complex mechanism than the simple light spread/brightness discrimination models heretofore proposed.

With the temporal and spatial pooling schemes in question and the increasing difficulty in reconciling intensity difference models with the diverse set of localization stimulus configurations, a different trade-off was necessary to account for the fine spatial acuities. One possible scheme was the partitioning of spatial information by a number of detectors that were selective for different spatial features. The motivation for trade-offs of this type came from a series of single-cell studies in cat visual cortex by Hubel and Wiesel (e.g., 1962, 1965). Using points of light as stimuli, Hubel and Wiesel mapped out two-dimensional response profiles of cells in primary visual cortex. In some cells they found a regular pattern of regions of excitation and inhibition. Within each of the regions, flux was summed linearly across space. They further classified these cells by their near optimal responses to bars and edges and proposed that these cortical units formed the first level of feature processing in the increasingly complex and specific hierarchy that they thought characterized spatial vision.

The linear summation regions in the bar and edge detectors were found to be quite elongated, resulting in a selectivity for orientation. This finding led Ludvigh and Mckinnon (1967) to equate the properties of single cells in primary visual cortex with those of the detectors underlying localization and then to propose that the orientation selectivity of the detectors was responsible for vernier performance.

However, it can be argued that as one moves centrally in the visual system the pooling of receptors, each already too large to support the fineness of vernier acuity, only increases the magnitude of the task. The best orientation selectivity of cortical units found in mammals may be poorer than the orientation sensitivity in man by a factor of ten (Westheimer, 1978). Thus fine orientation judgments must be based on neural signals that result from the interaction of elements of an ensemble. The limits imposed by normal mechanisms proposed for resolution acuity may be augmented by information from other stimulus dimensions in order to account for the obtained spatial precision. Offset detection in this scheme could achieve the requisite precision by a trade-off of spatial parameters. If different superimposed feature detectors are formed by combining the input from the same cones in different ways then a given detector could be sensitive to (selective for) a small subset of all the possible patterns of cone excitation, and insensitive to the rest. A detector array with components of many orientations covering each small region of the visual field would permit a wide range of feature sensitivity while maintaining a cell's individual selectivity. The specific location information that would have been associated with the individual receptors, but was lost by the

pooling of receptor responses in the linear summation regions, was supplanted in a trade-off with increased resolution of spatial features (bars, edges, orientation). Two patterns would then be discriminable when they stimulate a different feature detector (or class of detectors) or increase the activity in a range of detectors by a sufficient increment.

Using such an array of overlapping orientation detectors to model performance, Andrews (1967a, b; Andrews et al., 1973) argued that many vernier tasks with short lines or dots are equivalent to orientation tasks. In this scheme the aberrations in the optics of the eye make the offset stimulus elements indistinct and appear as a single tilted line. He went on to show that orientation discrimination is a vernier task in that orientation differences can be perceived when the tip of a line is displaced only a few seconds of arc. Andrews proposed further that fine orientation discrimination was subserved by a mechanism similar to that suggested by Andersen and Weymouth 50 years earlier for mean retinal local sign: the output of a finite number of detectors of different orientations is combined to produce an interpolated orientation. This time, however, the proposed detectors were spatially extensive and superimposed rather than minute and disjoint.

In a further extension of the orientation hypothesis, Findlay (1973) proposed that the feature detectors that respond to orientation are sensitive to variations in size as well and that the jointly varying sensitivity results in stimuli possessing a given orientation being partitioned further according to their width. In addition,

Findlay proposed that the interaction between regions of excitation and inhibition make contrast a more appropriate measure of the stimulus than intensity. Findlay's hypothesis was that vernier performance is limited by contrast detection in an oblique detector. He proposed that the perceived kink in a coincidence task at threshold is a just visible short oblique bar (figure B.6) and that the sinusoidal masking grating of the proper orientation reduced the sensitivity of the oblique bar detector most sensitive to the offset and therefore increased vernier threshold. Consistent with this model, threshold maxima occurred when the mask was oriented 20° to either side of the vertical. Findlay proposed no explanation for the symmetry about the vertical exhibited by the masking effect of the grating (figure A.14). However well this model fit the objective and subjective data obtained in a coincidence task, Findlay found additional difficulty in applying it to Ludvigh's three dot stimulus. He saw no simple way to relate the dots to bar and edge detectors.

Sullivan et al. (1972) overcame this obstacle by considering the dots to be probes of the linear summation regions in the orientation detectors. Consistent with their formulation, they found that minimum detectable displacement of two dots increased with their separation in such a manner that a constant angle was maintained at threshold. Small separations would be expected to produce increased thresholds since errors in judgment of position of the dots would have a greater effect on the judged angle of tilt and a wider range of orientations would be stimulated. However, by similar reasoning, one might expect an increase in

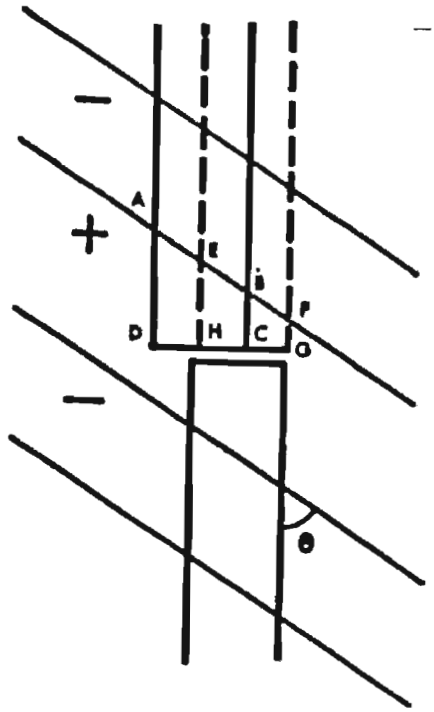

Figure B.6 Sinusoidal masking of a coincidence task.

The suggested hypothesis relates detection of misalignment to activity in a cell, the receptive field of which is oriented as shown at angle theta (Θ) to the vernier lines. There will be a change in excitation in the center of the receptive field between the offset and the aligned positions, whereas the excitation of the surround will be unaffected. With the offset shown, the change in excitation is equivalent to that produced by an area of target equal to the difference between the areas ABCD and EFGH. If the offset difference (DH) is d and the bar width (DC) is D, then this area is $d\ D\ cot(\Theta)$. This result will not be greatly altered by the transformation produced by the optics of the eye. If the receptive field width is W, the misalignment excitation change will be a function of $(\frac{d}{W})\cos(\Theta)$ of the total produced by the stimulus. This can be regarded as equivalent to a Weber fraction for the cell and, using plausible values for the variables, fractions between 1/200 and 1/30 are obtained.

(Findlay, 1973)

threshold as the dots were lengthened into lines; the strong response of the detectors tuned to the vertical orientation of the line segments would mask the response of the detectors to the orientation defined by the relative position between the line segments. This did not occur. Likewise, the model would predict an increase in threshold as width is increased and the gap size remains constant. Again, this was not the case.

While it is not necessary for a single feature, such as orientation, to constitute an essential property of all vernier tasks, it is to be hoped that generality may be established across more than a trivial subset of stimuli so that the principles of processing established with a subset of stimuli may be extended to other features in another subset of stimuli. Although some definitions of orientation are highly correlated with some localization thresholds, the particular interactions among line length, width and gap size elude all the mechanisms proposed so far.[4]

In an extensive series of experiments Westheimer and his collaborators have attempted to determine the effect that various stimulus parameters have on the feature detectors involved in vernier acuity (Westheimer, 1975, 1976, 1977, 1978, 1982; Westheimer and Hauske, 1975; Westheimer and McKee, 1975, 1977a, b, c; Westheimer et al., 1976; McKee and Westheimer, 1978). Westheimer recognized that the trade-off of one form of information for another may occur in parallel and in different ways in different detectors. Therefore, performance on two different tasks may appear to require conflicting or extraordinary resolution along a given dimension when, in fact, the requirements may be met in different neural

substrates. One example of a trade between form and position came from an analysis of the effects of moving and diffuse coincidence targets on vernier thresholds (Westheimer and McKee, 1977a). They concluded that one property of the detection mechanism was,

"retinal stimuli can be tagged with differential local signs after having been pooled over regions extending several minutes of arc. Stimuli which by themselves are devoid of contours, subthreshold, or even contrary information content, can be integrated and used for the elaboration of differential spatial localization signals precise to a fraction of a receptor diameter".

In contrast to the local sign of Hering in which averaging occurred along the length of the contours, Westheimer and McKee proposed that integration takes place in a zone lateral to the line, and in the direction of localization. Yet, with all the condensing of information, it would still be possible at the same time to resolve separate features within an integration region. Indeed, Westheimer and McKee argued that it is necessary for optimal performance that the target components be identifiable as separate, individual features (Westheimer and McKee, 1977c) and that separations less than 2' arc cause features to merge and thus set a lower bound on contour spacing (unfortunately no effort was made to reconcile the 2' arc measure and two line resolution of less than 30" arc). The fall-off of performance well within the fovea for separations greater than 5' arc indicated to Westheimer and McKee that the localization ability was a relative

process, a comparison devoid of absolute position information. Indeed, the offset threshold may result from the differencing of the local signs of well demarcated contours (Westheimer, 1982). The limit of 5' arc simply may be an indication of the upper bound on the size of the detectors subserving localization.

In contrast to the critical spacing requirements, there was a wide latitude within those regions in the allowable configurations of contours which could be used to produce localization thresholds. It may be possible that the complexities found in earlier studies were a consequence of the confounding of the effects of various stimulus parameters with relative position. Those results need to be reinterpreted in light of Westheimer's findings. Even though it is incomplete, it stands as the best analysis of the relation between features and vernier threshold to date, incorporating many of the contour interactions associated with vernier performance.

The major theories of vernier acuity, their proponents, dates and an epitome of their positions are collected for reference in Table B.1.

Table B.1 Summary of Localization Theories

Helmholtz (1860)	Receptor Resolution Theory: equality of receptor diameter, resolution and the point spread function.
Hering (1865,1899) Bourdon (1902)	Local Sign Theory: regular hexagonal array of discrete receptors each mapped to a unique location in visual space.
Stratton (1900)	Diffusion of Activation Theory: each point of light induces a spread of activity among the receptors; the activity is proportional to the location within the receptor.
Hartridge (1922)	Increment Detection Theory: light spread of contours allows graded receptor responses to signal small offsets.
Weymouth (1923)	Mean Retinal Local Sign Theory: binary receptor responses are averaged over space and time to form a composite location signal.
Hecht (1939) Baker (1949)	Brightness Discrimination Theory: vernier acuity varies in the same way as does brightness discrimination with changes in luminance.
Marshall and Talbot (1941)	Cortical Local Sign Theory: the more numerous cortical cells each with a local sign allow a finer grain to be established than is possible on the retina.
Ludvigh and McKinnon (1967) Andrews (1967) Sullivan, Oatley and Sutherland (1972) Findlay (1973)	Orientation Discrimination Theory: cortical bar detectors which are sensitive for size as well as orientation produce an ensemble response.

Westheimer and McKee (1975-1978)	Lateral Summation Theory: multiple pathways allow information to be summed over regions lateral to the contours while still allowing resolution of elements within the regions.
Barlow (1979) Crick, Marr and Poggio (1980) Morgan and Watt (1983)	Cortical Interpolation Theory: spatial phase may be reconstructed by cortical neurons by appropriate sampling of the coarse retinal mosaic. Location of features within the stimulus is marked by zero-crossings in the interpolation.

{1} The casting of the theory of local sign by Hering in terms that were "altogether too atomistic for the twentieth century" (Walls, 1943) may have been an affirmation of Cajal's neurone doctrine, a proposal that the nervous system is composed of distinct anatomical units. Whatever Hering's intent, a consequence of his choice of description was that the theory of local sign was characterized as "static" and was contrasted with the later "dynamic" theories (e.g., Weymouth et al., 1923; Andersen and Weymouth, 1923) that incorporated spatial and temporal averaging. It appears that the characterization of Hering's theory as purely static was inaccurate. In a later report Weymouth, himself, acknowledged this error: "Hering anticipated practically all of the objections urged by us against his explanation, and in a footnote clearly stated the essential features of our theory of mean local sign. Priority to this conception, therefore, belongs to Hering" (Averill and Weymouth, 1925). Weymouth apparently had developed (and extended) independently concepts very similar to those outlined by Hering 24 years earlier.

Despite this confusion of attribution, there is much utility in the comparison of the static and dynamic theories. The later literature apparently discounted Weymouth's generous account and has continued to contrast the positions of Hering and Weymouth (e.g., Walls, 1943). Support for this viewpoint may be gained by examining Hering's publications. There was no statement of dynamic processes in his early work on the subject (1864, 1865) and not much emphasis in

a later description (1899). Hering's early work certainly was the source of the static theory, intentionally or not. In addition, Weymouth's version was a more explicit description of a dynamic theory and became the standard explanation for several decades. It is considered proper, therefore, to follow the convention of the literature and ascribe the dynamic theory to Weymouth.

{2} A detector's capacity to transmit information is limited by the range of its response and the ability of subsequent mechanisms to resolve differences in that response. (The term detector is used here in the general sense, in contrast to the specific application by N. Graham in channel models.) One measure of the sensitivity of this detector/criterion organization for a given stimulus parameter is the psychometric function. It relates stimulus magnitude to the probability that the response of the detector would be perceived as different. For a range of stimuli that vary along only one dimension this description is adequate. With stimuli that vary along two or more dimensions, however, ambiguities may arise in the interpretation of the response. Although it is possible to encode more than one stimulus dimension unambiguously on a single response dimension, it is also possible that changes along different stimulus dimensions evoke the same change in detector response. This uncertainty poses a problem in interpretation for the mechanisms subsequent to the detector: Which dimension is perceived as changing, and by what amount? The consequences of this decision may be seen in the following illustration.

Consider the response of a circular disk having uniform flux sensitivity; responses are summed equally from all parts. Let the range of responses extend from zero to some maximum (R_{max}) and allow subsequent mechanisms, limited by noise and their physical makeup, to resolve changes in response equal to $1/n^{th} R_{max}$. Summing all of the flux that fell within the disk, the detector would be able to discriminate between average luminance levels that evoked a change in response of R_{max}/n or more. In addition to luminance discrimination, the position of the flux could be localized to a precision limited by the diameter of the disk. Spatial variations smaller than the diameter of the disk could not be discerned, the stimuli would appear to dim at their edges.

Consider now the same detector, but now in response to the position of an edge. The response of the detector can be interpreted as representing the position of the edge. Assuming that the dark background elicits no response, passage of the bright edge over the disk would produce a monotonic increase in response until, finally, a maximum is reached when the disk is entirely in the bright section. Position could then be determined to a precision that depended only on the sensitivity of mechanisms subsequent to the detector (R_{max}/n). The luminance response would be limited to a binary bright/dark distinction; differences in the amount of flux summed within the detector would be associated with positional changes. (Finer luminance judgments would require separate mechanisms.) The trade-off between the representations of luminance and position would be a consequence of the fixed amount of information in the response.

Complications in relating detector response to position arise when mean luminance or contrast changes. A change in luminance would result in a change in net flux (i.e., will be "perceived" by the edge detector as a change in position. A change in contrast would alter the slope of the relation between position and response; identical shifts in position by edges of different contrasts would result in different changes in response. The two edges would be "perceived" to have been displaced by different amounts. Resolution of confusions such as these require the combination of information of many detectors and some assumptions as to the way trade-offs occur in the neural representation of stimulus parameters. It was precisely this relation between response and representation that formed the core of the "local sign" theories. Each attempted to partition the available response resources in a way which would overcome the manifest insufficiency of the spatial extent of the receptors to account for vernier performance. Unfortunately, the local sign theories concentrated on the mechanism of positional encoding and did little to reconcile the consequent representational ambiguities.

{3} For an array of receptors whose response was all or nothing, offset resolution would depend both on the average interreceptor spacing and on the spacing variability. However, with a moderately long line it is very likely that two proximal receptors would be stimulated whose center locations were nearly $d/2$ away on opposite sides of the line (where d is the receptor diameter). It would not be possible, therefore, to reliably detect offsets smaller than d (and certainly

not $d/5$ or $d/10$) based on the local positional deviations of the responding receptors alone.

{4} In comparing the coincidence thresholds for the middle and bottom dots of a three-dot stimulus (figure A.4, b and c) Beck and Schwartz (1979) argued that vernier performance is based on orientation rather than alignment since the threshold for the detection of offset of the bottom dot was twice that found for the middle dot. They proposed that displacement of the middle dot could be detected by the angular offset between it and both of the other dots; displacement of the bottom dot would only produce a single angular deviation (i.e., offset relative to the middle dot). The increase in the displacement threshold when the bottom dot was moved was attributed by them to the reduced number of orientation cues available to the Observer.

If, instead, the configuration of the entire stimulus is examined it will be seen that the relative spatial position of the three dots is nearly identical in both displacement conditions at threshold. The only difference between the configurations is a small (about 20' arc) relative rotation of the entire figure. The relation between the two conditions may be seen more clearly by drawing three lines through the dots: one between the top and middle dots, one between the top and bottom dots, and one through the bottom dot normal to the first line. The resulting triangle fixes the necessary geometrical relation between the two measures of threshold at approximately two; the same ratio that Beck and

Schwartz proposed as evidence that orientation discrimination underlies vernier performance. However compelling the description of the three-dot stimuli in terms of the orientation discrimination with dot pairs, analysis of the stimuli taken as a whole exposes the similarity of the two conditions, and of the resulting displacement thresholds.

This example demonstrates that care should be exercised in the selection of the features and measures of threshold. The choice of a single feature as the basis of vernier performance without proper regard for the entire stimulus can lead to relations that are more apparent than real.

Appendix C

AGGREGATE RESPONSE MEASURES

Introduction

For sinewave detection the obtained threshold contrast is presumed to be inversely proportional to the ensemble response of the spatial filters in the visual system. Although the notion of contrast sensitivity is readily applicable to sinewaves, its extension even to the detectability of sinewave pairs is unclear. How are the individual component contrasts to be weighted when computing the ensemble sensitivity? The problem is compounded n-fold for broadband stimuli such as bars. The nonlinear multiple filter models considered in this appendix may be viewed as attempts to create a metric that relates the effectiveness of compound stimuli in activating the filters in the visual system back to the effectiveness of an appropriate basis such as single sinewaves. Generalization of such models should be done conservatively, for the metric applied internally by the Observer may not be the same for all tasks.

One direct consequence of a multiple filter model of spatial pattern vision is that the contrast sensitivity function becomes a composite of the diverse filter sensitivities. The detector array not only contains bandpass spatial filters with spatial frequency sensitivities that partially overlap, but also filters with spatial sensitivities that overlap to varying degrees. Limited spatial extent is a

characteristic of bandpass filters: spatial extent is inversely related to filter bandwidth. Even a narrowband stimulus, therefore, will produce responses in a large number of filters. The resulting threshold will depend on the way this activity is combined prior to the decision process.

The assumption of independence of linear summation within each filter greatly simplifies multiple filter models by allowing the filter responses to be individually computed. Two events are considered to be statistically independent if the occurrence of one event does not influence the probability of the other event. It follows, then, that the probability of both events occurring is simply the product of their individual probabilities. The probability that none of n independent events occurs is the product of all of the individual probabilities of non-occurrence; further, if p_j is the probability of event j, $1-p_j$ is the probability that the event will not occur. These two relations may be combined to determine the probability that at least 1 of n events occurs:

$$P = 1 - \prod_{j=1}^{n} (1 - p_j) \qquad [C.1]$$

If p_j is the probability that the activity in filter j will be sufficient to trigger an all-or-nothing detection mechanism and if there is an ORing of the detection responses across filters, then [C.1] describes the fundamental relation for probability summation among n independent filters. The sensitivity for a given stimulus depends on the magnitude of response induced in each filter and the relation between response level and the probability of triggering the all-or-nothing

detection mechanism. This latter relation, the filter's psychometric function, is nonlinear. The nonlinearity has often been modeled by the addition of gaussian noise to the filter's response following the linear spatial summation and gain stages but prior to the all-or-nothing detection mechanism (e.g., Sachs et al., 1971). The slope of the individual filter's psychometric function is proportional to the standard deviation of the noise distribution and the threshold of the filter (by convention) is defined to be the response level that trigger's a detection 50% of the time, a level that is the mean of the response distribution following the injection of the noise.

Vector magnitude model

The summation, gain, noise and detection sequence of filter stages, coupled with the assumption that the response level for detection is the same across all filters, produces a psychometric function that has a constant slope on a linear spatial frequency abscissa for different numbers and sensitivities of filters. This model is equivalent to the assumption that the noise is perfectly correlated in filters that vary in spatial position and spatial frequency sensitivity. If, however, the noise is uncorrelated, then prediction of the sensitivity of an array of bandpass spatial filters becomes computationally difficult to model since the cascading of probabilities alters the shape of the psychometric function. As the number of identical individual independent filters increases, the threshold of the ensemble decreases and the slope of the psychometric function increases (on a logarithmic

axis). The threshold nonlinearity embodied by the ORing of the filter responses prior to the detection mechanism effectively uncouples the psychometric function of the ensemble from the noise distribution within each filter. Knowledge of the spatial distribution and diversity of filter sensitivities becomes critical to the modeling of responses for even the simplest stimuli.

In an attempt to surmount the difficulty in estimating individual filter characteristics from ensemble data, Quick (1974) proposed the use of a different form of the psychometric function to model the probability of detection by a single filter (p_j) in response to a given stimulus (F) - probability summation across spatial frequency:

$$P = 1 - 2^{-R_j^B} \qquad [C.2]$$

where: B is proportional to the steepness of the psychometric function;

R_j is the absolute value of the linear sum of the stimulus spectrum weighted by the sensitivity profile of the j^{th} filter (the index j marks the ordinal sequence of increasing filter center frequencies):

$$R_j = \sum_{k=1}^{m} \left| A_k \; W_{j,k} \right| \; G_j$$

G_j is the gain of an individual filter at the j^{th} center frequency;

$W_{j,k}$ is the weight of the j^{th} filter for the k^{th} spatial frequency (normalized to one at the center frequency);

F is the stimulus, the sum of weighted (A_k) sinewaves:

$$F = \sum_{k=1}^{m} A_k \sin(2\pi kx+\varphi)$$

The form of the psychometric function in [C.2] is of interest not because it can be linked to any natural process, although the underlying noise distribution may not be very different from a gaussian (figure C.1), but because of computational advantage (Weibull, 1951). The psychometric function of a single filter, if in the form of [C.2], may also be used to characterize the response of an ensemble of such filters; the psychometric functions for the cascade of various numbers of filters are all parallel on a logarithmic axis. Psychometric functions of the form of [C.2] are in fact the only class of probability functions that are invariant in such a cascade (Green and Luce, 1975). The logic of this relation may be seen by substituting the expression for p_j in [C.2] into [C.1].

$$P = 1 - \prod_{j=1}^{n} 2^{-R_j^B} \qquad [C.3]$$

Equation [C.3] assumes that B is the same for all filters (e.g., identical uncorrelated noise distributions).

In order to make use of the computational convenience of [C.2], the relation between the response of the ensemble (S) to the stimulus and the response of an

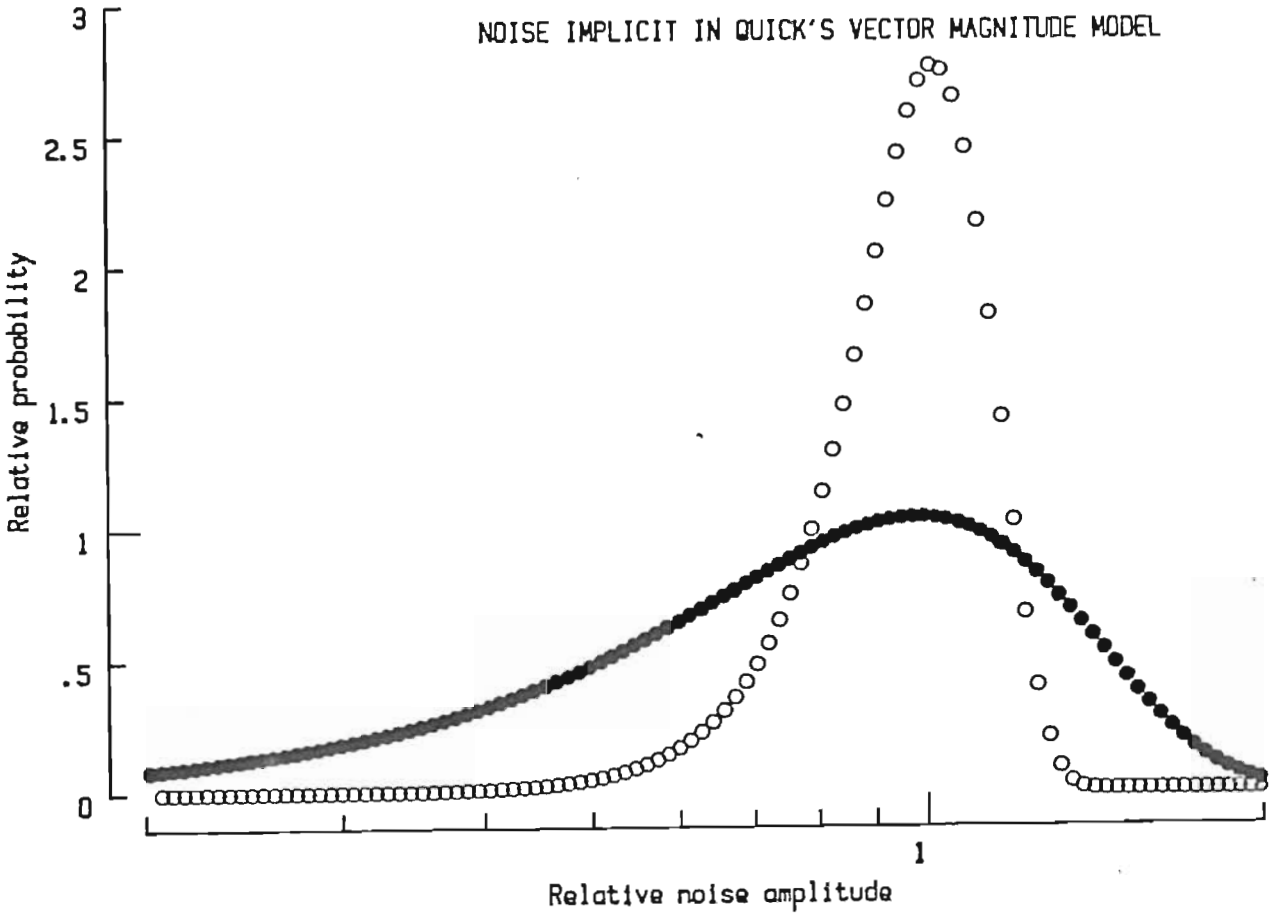

Figure C.1 Noise distribution implicit in the Weibull/Quick psychometric function.

If the psychometric function of an individual filter, j, has the form proposed by Weibull (1951) and by Quick (1974):

$$P = 1 - 2^{-R_j^{7.8}}$$

where 7.8 was the exponent that best fit the data of Sachs et al., 1971,

then the underlying noise distribution is proportional to the slope (derivative) of the psychometric function.

$$\frac{dP}{dR_j} = 7.8\ ln(2)\ \ 2^{-R_j^{7.8}}\ R_j^{6.8}$$

If the exponent of the psychometric function is in fact this large (7.8, open dots), then the effect of the skewness should be negligible in most models; however, if the exponent turns out to be closer to 3 (closed dots), then the skewness may be significant.

individual filter (R_j) must be established. Quick proposed that detection may be modeled as a form of vector addition wherein each dimension in the vector space corresponds to an individual filter.

$$S = \left\{ \sum_{j=1}^{n} R_j^{\beta} \right\}^{\frac{1}{\beta}} \qquad [C.4]$$

Measures of this kind can be traced back to the Minkowski inequality (q.v., Pearson, 1974). In the formulation used here, the assumption of a constant detection criterion is realized in the setting of S to one for all stimuli at threshold. Substituting [C.4] into [C.3] yields an expression for the ensemble response [C.5] that is of the same form as for the individual filter [C.2]:

$$P = 1 - 2^{S^{\beta}} \qquad [C.5]$$

This substitution is functionally equivalent to assuming that there is a direct relation between the way in which the magnitude of individual filter responses are weighted in the ensemble response and the shape of the noise distribution in the individual filters; both the Minkowski metric and the variance of the noise distribution are a function of B. Thus configured, Quick's vector magnitude model has been used to predict the detectability of a wide range of spatial stimuli (e.g., Wilson, 1978).

Variations in space and spatial frequency

A correlate of the bandpass nature of the filters is limited spatial extent. In order to avoid gaps in sensitivity across the visual field, therefore, an array of each filter type is required. Measurements by Robson and Graham (1981) allow estimation of the manner in which filter gain in this array changes with eccentricity. The variation of gain with eccentricity is a significant adjustment to the prediction of the relative response to spatially extensive and spatially limited stimuli. [C.2] may be expanded to include variations in sensitivity and response across the visual field - a form probability summation across space. R_j and G_j in [C.2] represent the aggregate response and gain of all filters with center frequency j. Rather than taking the magnitude of the filter response to be the activity elicited by the stimuli at the fixation point, the filter response is free to reflect variations across space.

$$R_j = \left\{ \sum_{x=-2.2^o}^{2.2^o} \sum_{y=-1.1^o}^{1.1^o} \left[r_{j,x} \; g_{j,x,y} \right]^B \right\}^{\frac{1}{B}} \qquad [C.6]$$

$$r_{j,x} = \left| H_j <*> F \right|_x$$

$$g_{j,x,y} = g_j \; 10^{-f_j (q_x^2 x^2 + q_y^2 y^2)^{1/2}}$$

H_j = the spatial profile of the filter centered at frequency f_j (includes attenuation by the optics of the eye);

q_x = the space constant for the decrease in filter sensitivity (in periods of $1/f_j$) in the horizontal dimension (q_y: vertical dimension).

The response ($r_{j,x}$) and the gain ($g_{j,x,y}$) in [C.6] represent the activity of individual spatially localized filters. The individual gains peak at the fixation point and fall off as a function of center frequency and eccentricity (Robson and Graham, 1981). The rate of decline in sensitivity is twice as fast in the vertical dimension.

An additional refinement in the determination of individual filter response is the specification of the phase of the spatial weighting function. The filter weights ($W_{j,k}$ in [C.2]) are complex values, containing both phase and amplitude terms. The response of such a filter to a stimulus may be reduced by a mismatch in phase as well as by a mismatch in spatial frequency. Since the visual system does not appear to be phase bound (subpatches of extended gratings do not appear and disappear when the grating is shifted), multiple phase spectra are applied at each filter location.

Flat phase spectra are used in the model here because they allow filters with pure odd and pure even symmetry as well as gradual transitions in between. Six phases, each 30° apart, are assumed to exist st each filter location specified by [C.6]. The response at each location is the result of probability summation among the six. When applied to sinewaves, the combined response of the six filters (with B equal to 3.5) is 28% larger than for a single filter with the optimal phase, but there is essentially no change in response (c. 0.02%) with changes in stimulus

phase.

Estimation of individual filter gain

Before using a model of this form to account for the relation between the broadband and narrowband data in this thesis, an additional adjustment was attempted. Wilson (1978) noted that the CSF falls off more rapidly in the high frequency region than does the profile of the individual filters. This relation requires that the gain of the individual filters fall off even more rapidly than the CSF. When he incorporated this adjustment, Wilson found that the theoretical curves better fit his data. For a given vector metric (B) and filter bandwidth, it should be possible to obtain an estimate of the individual filter gains. The gain estimate would be constrained by the computed filter responses for a set of stimuli and the corresponding observed sensitivities. In order to relate the ensemble response (S) to a useful metric (Michaelson contrast), the sensitivities will be obtained from single sinewave detection experiments.

The terms in [C.4] may be expanded to define the constituent stages:

$$S_i = \left\{ \sum_{j=1}^{n} R_j^B \right\}^{\frac{1}{B}} \Big|_{F_i} \qquad [C.7]$$

$$= \left\{ \sum_{j=1}^{n} \left\{ \sum_{x=-2.2^o}^{2.2^o} \sum_{y=-1.1^o}^{1.1^o} r_{j,x} \; 10^{-f_i (q_x^2 x^2 + q_y^2 y^2)^{1/2}} \right\}^B g_j^B \right\}^{\frac{1}{B}}$$

where: $S_i = 1$ at threshold contrast for F_i.

The terms in [C.7] may be rearranged to form a set of linear equations:

$$\begin{bmatrix} 1 \\ 1 \\ \cdot \\ \cdot \\ \cdot \\ 1 \end{bmatrix} = \begin{bmatrix} R^{\beta}_{1,1} & R^{\beta}_{1,2} & \cdots & R^{\beta}_{1,n} \\ R^{\beta}_{2,1} & R^{\beta}_{2,2} & \cdots & R^{\beta}_{2,n} \\ \cdot & \cdot & & \cdot \\ \cdot & \cdot & & \cdot \\ \cdot & \cdot & & \cdot \\ R^{\beta}_{n,1} & R^{\beta}_{n,2} & \cdots & R^{\beta}_{n,n} \end{bmatrix} \begin{bmatrix} g^{\beta}_{1} \\ g^{\beta}_{2} \\ \cdot \\ \cdot \\ \cdot \\ g^{\beta}_{n} \end{bmatrix} \qquad [C.8]$$

In this linear system, the unit column vector (S_i) reflects the constant detection criterion at threshold assumed for all stimuli (F_i); $R_{i,j}$ is the response (R_j in [C.7]) of the j^{th} filter to the i^{th} stimulus with the maximum individual filter gain (g_j) factored out. The stimuli are selected so as to span the range of filter sensitivities. This diversity increases the likelihood that the n stimuli and n filters can be used to construct a well-conditioned set of n independent linear equations. An inappropriate stimulus set or a narrow selection of filter parameters would likely lead to linear dependence or an ill-conditioned response matrix, M, and the concomitant lack of the M-inverse needed for a solution.

All models were approximated by 64 filters centered on frequencies between 0.5 and 32.0 cpd. Each filter had a gaussian sensitivity profile when measured on a logarithmic spatial frequency axis. A contrast sensitivity function (CSF) obtained for one Observer (BCM) was used to estimate his neural transfer function (NTF). The NTF was formed by dividing the CSF by an estimate of the optical transfer function, the Fourier transform of Campbell and Gubisch's line spread

function for a 5.8mm pupil.

Probability summation across spatial frequency

A range of filter bandwidths and exponents was examined in an attempt to determine the extent to which various models of probability summation across spatial frequency altered the pattern of isolated filter gains. The initial models were constructed without probability summation across space, all x_j's were 1. The original expectation was for the gain estimates, g_j, to decrease as the overlap in filter sensitivities increased. The major finding of the analysis was that, with the exception of exceedingly small bandwidths, no parameters could be found that yielded a set of positive gains. Bandwidth estimates derived from masking and adaptation studies universally produced solutions that oscillated wildly between huge positive and negative gains. Examination of a few solutions will make clear the extent of the incompatibility between commonly accepted filter estimates and decision criteria based on aggregate filter response measures.

In the single linear filter model ($B = 1$), the ensemble sensitivity for a given spatial frequency is based on the sum of the weights for that sinewave collected over all the filters. Even when filter bandwidth is proportional to center frequency (constant octave), the model may be reduced to a peak response decision criterion (figure C.2, a). The extremely narrow bandwidth negates all summation capability across filters. The response matrix (M) becomes essentially an identity transformation.

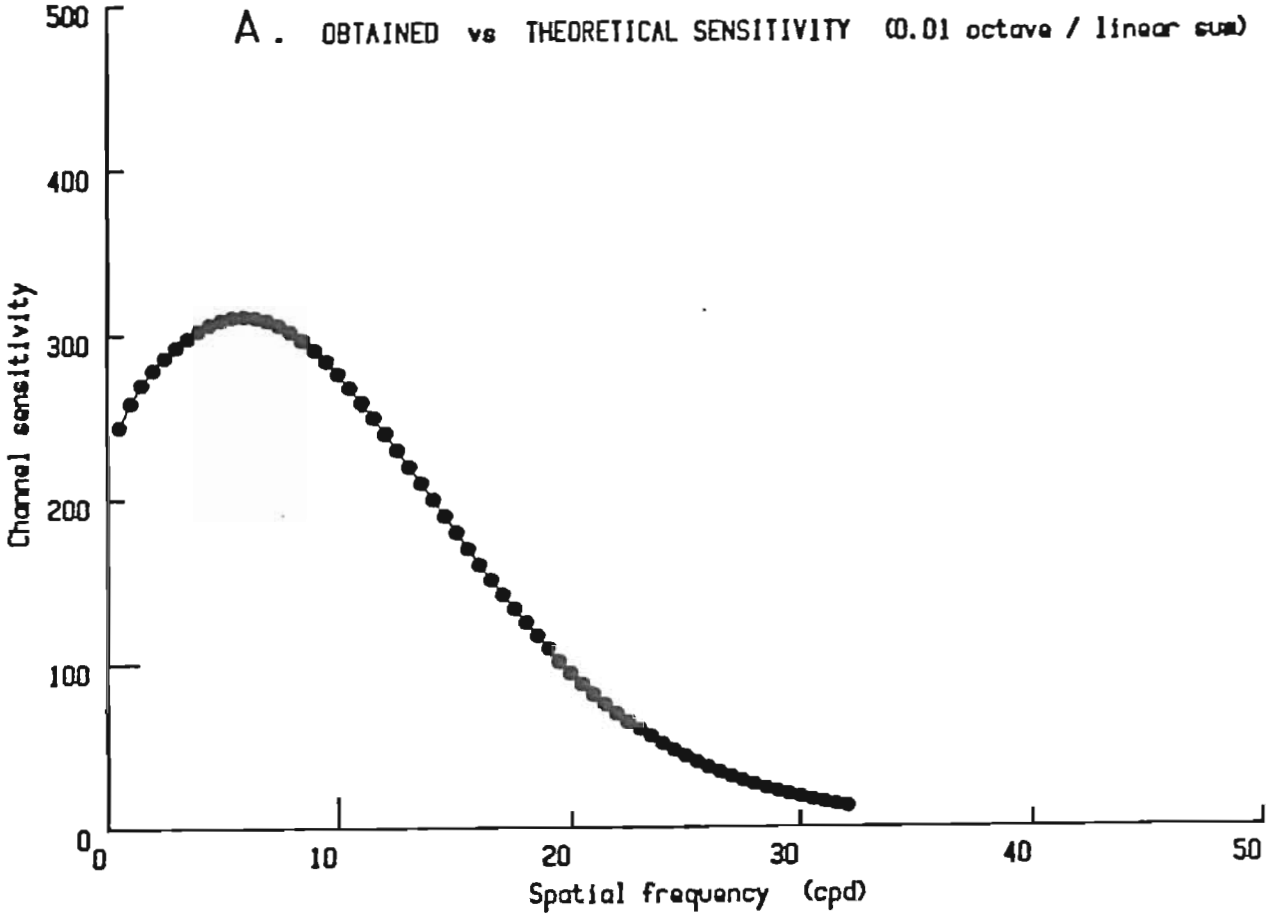

Figure C.2 Single linear filter aggregate response model (constant octave bandwidth).

A linear system in the form of [D8] was solved for a gain exponent of one and constant octave bandwidths: a, 0.01; b, 0.05; c, 0.10; d, 0.50; e, 1.00; and f, 1.50. With the exception of extremely narrow bandwidths (a, 0.01), all solutions required negative gains to match the theoretical filter model to the neural sinewave contrast sensitivities. (NTF, closed dots; model response, open dots).

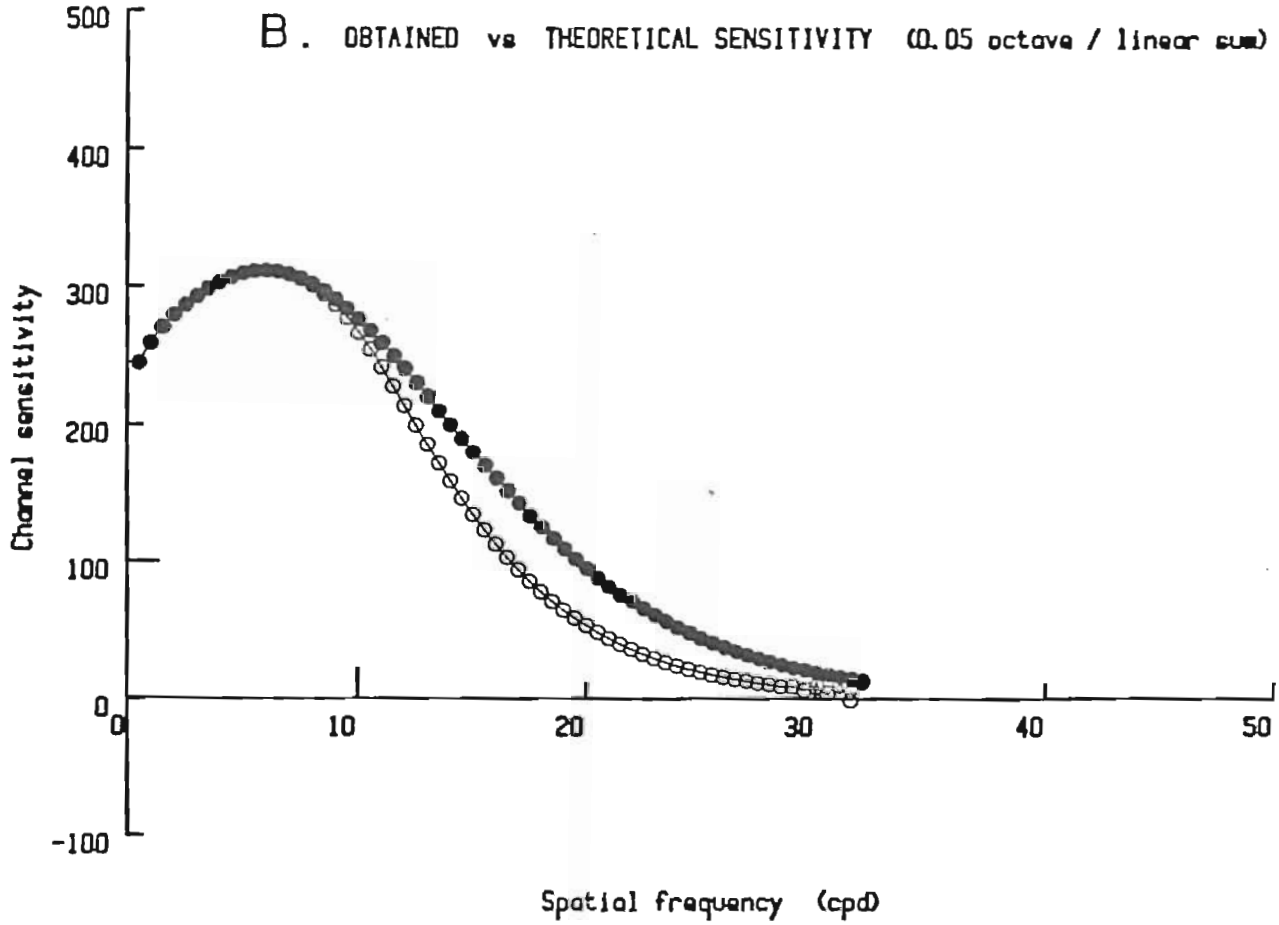
B. OBTAINED vs THEORETICAL SENSITIVITY (0.05 octave / linear sum)
Channel sensitivity
500
400
300
200
100
0
-100
0
10
20
30
40
50
Spatial frequency (cpd)

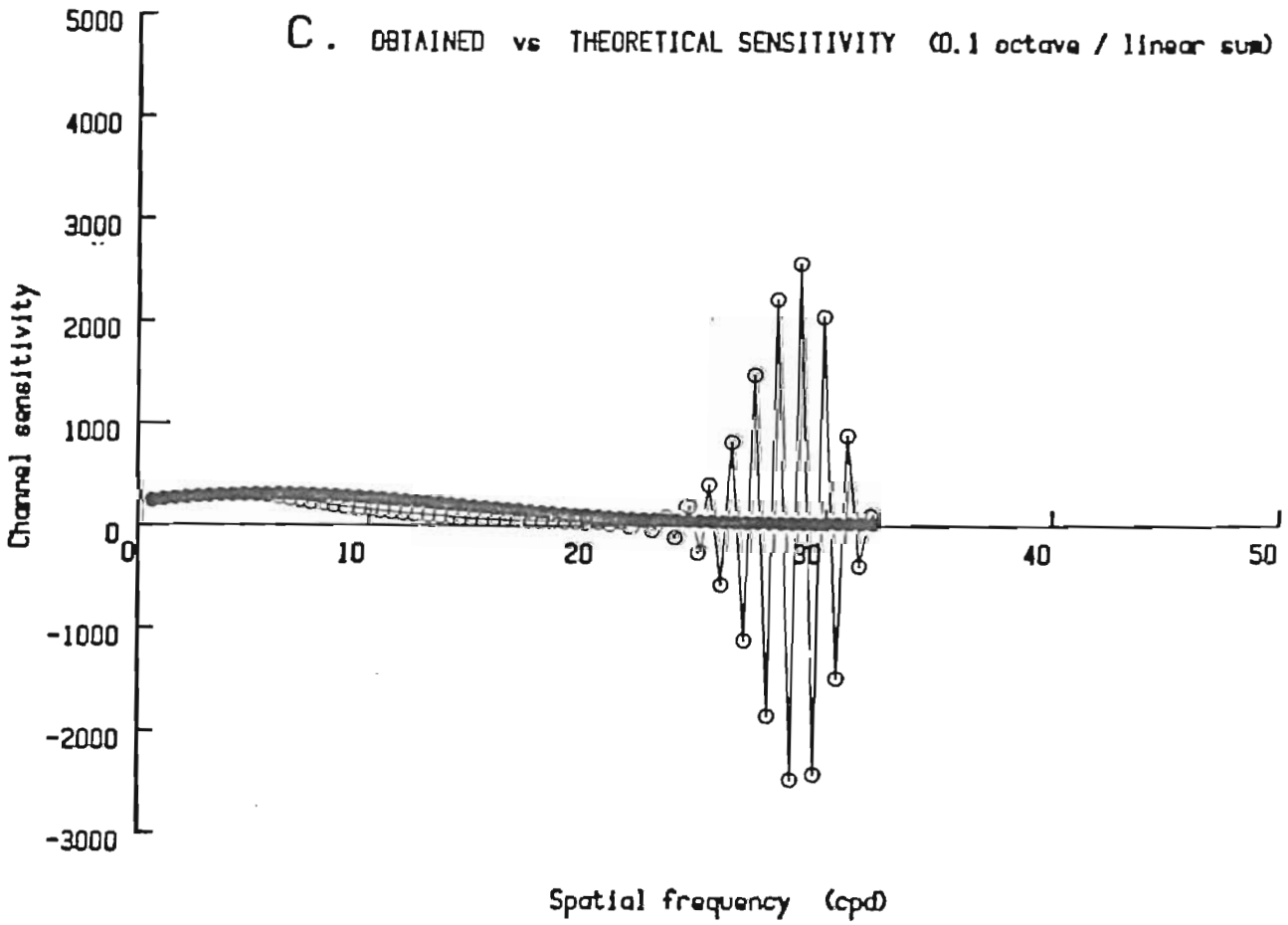
C. OBTAINED vs THEORETICAL SENSITIVITY (0.1 octave / linear sum)
Channel sensitivity
5000
4000
3000
2000
1000
0
-1000
-2000
-3000
0
10
20
30
40
50
Spatial frequency (cpd)

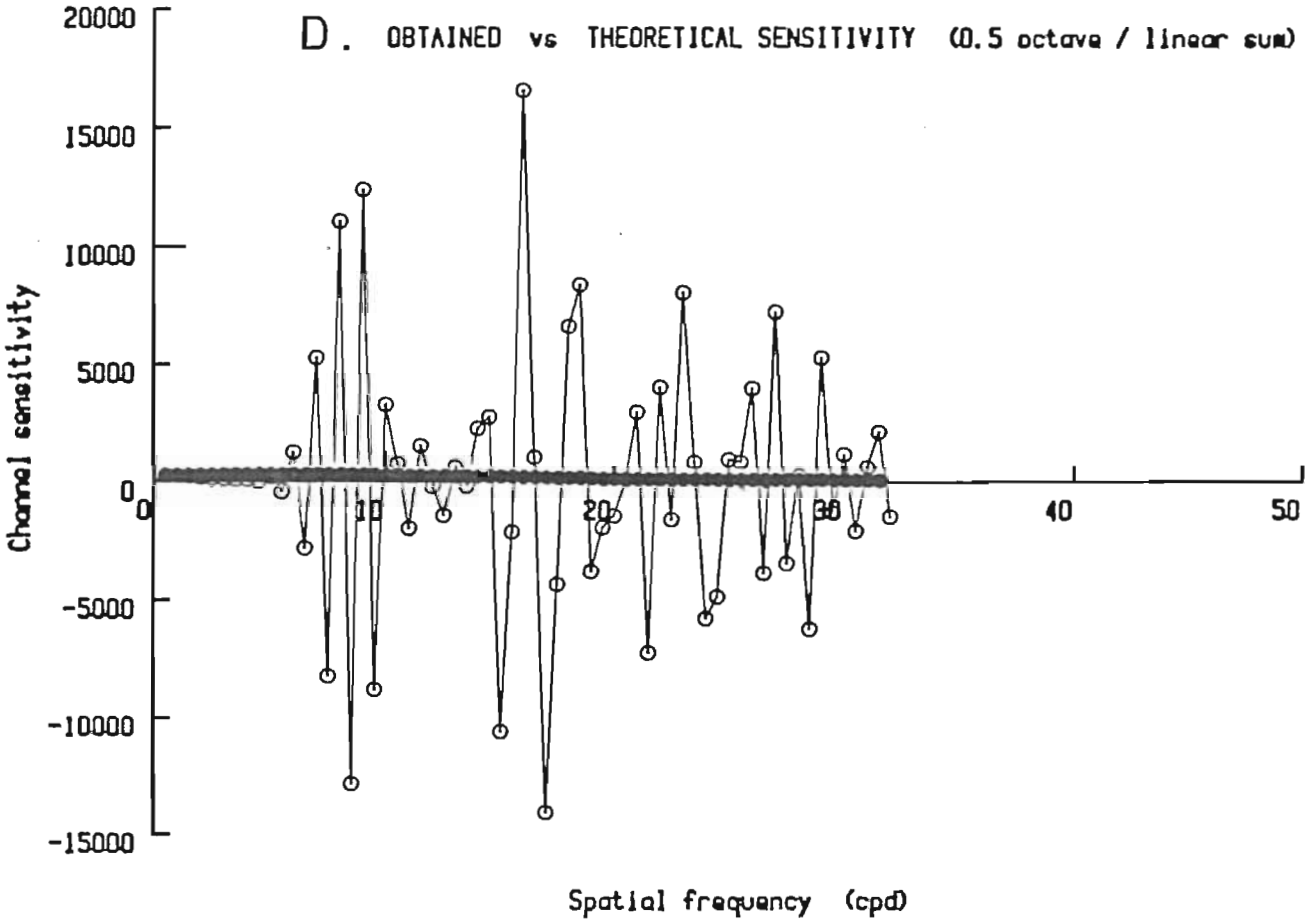
D. OBTAINED vs THEORETICAL SENSITIVITY (0.5 octave / linear sum)
Channel sensitivity
20000
15000
10000
5000
0
-5000
-10000
-15000
0
10
20
30
40
50
Spatial frequency (cpd)

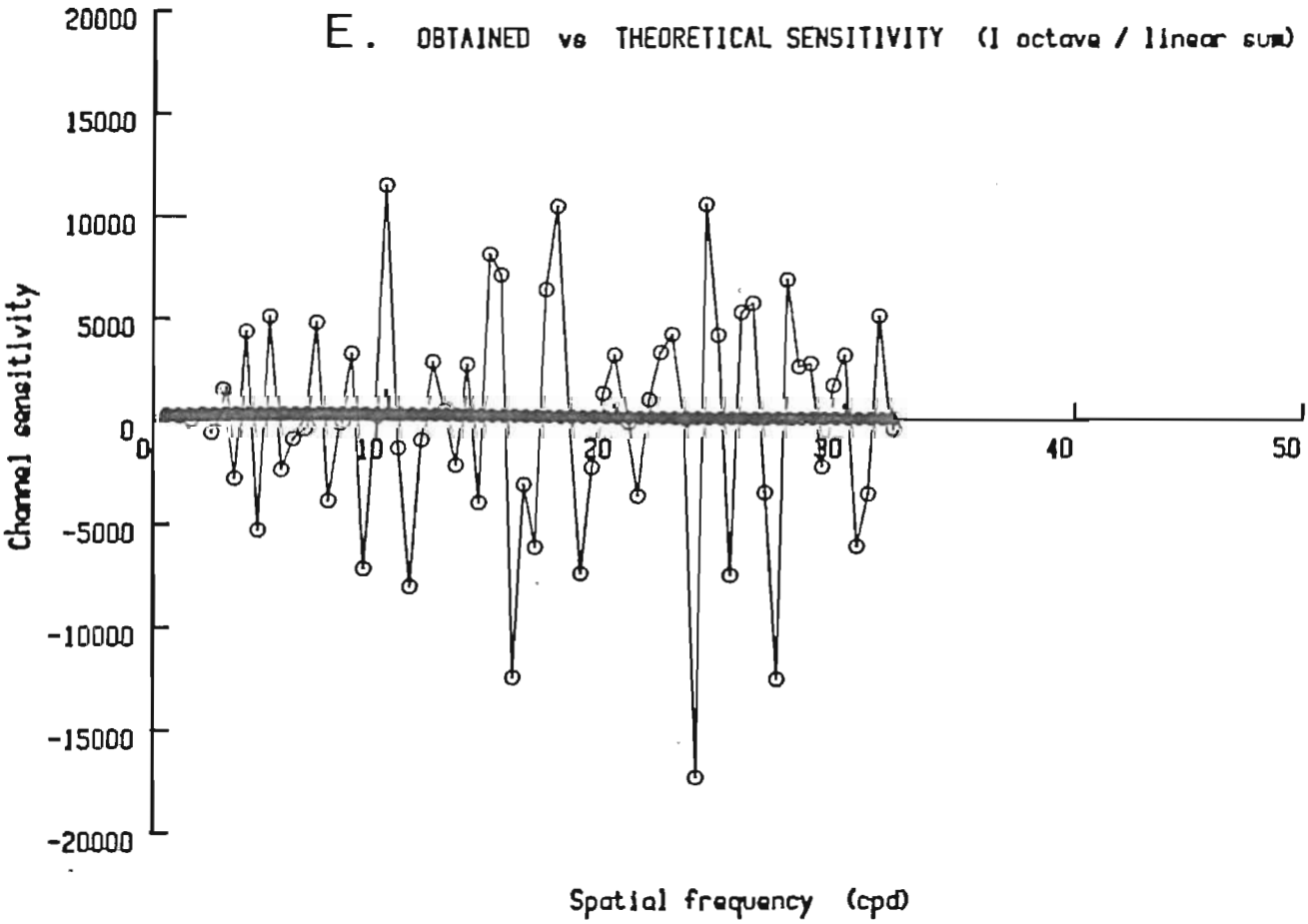
E. OBTAINED vs THEORETICAL SENSITIVITY (1 octave / linear sum)
Channel sensitivity
20000
15000
10000
5000
0
-5000
-10000
-15000
-20000
0
10
20
30
40
50
Spatial frequency (cpd)

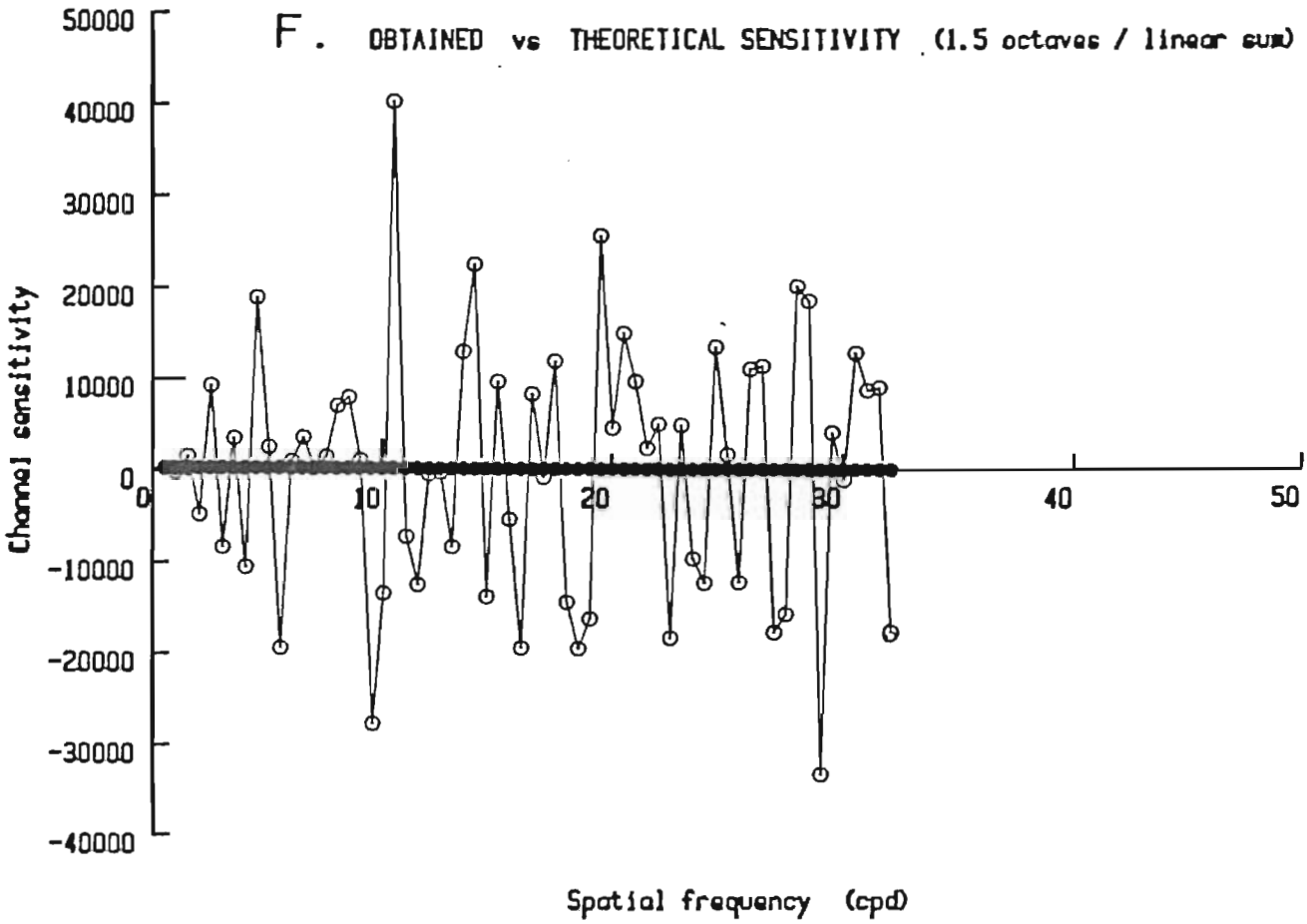
F. OBTAINED vs THEORETICAL SENSITIVITY (1.5 octaves / linear sum)
50000
40000
30000
20000
10000
0
-10000
-20000
-30000
-40000
Channel sensitivity
0
10
20
30
40
50
Spatial frequency (cpd)

The expansion of filter bandwidths to even 0.05 octave results in a significant difference between the aggregate sensitivity and the individual filter gains (figure C.2, b). As was expected, the aggregate measure overestimates the individual filter response increasingly at higher spatial frequencies where the overlap of filter sensitivities is greater; however, the magnitude of the departure is unexpectedly large for such a narrow bandwidth. More distressing is the negative estimated filter gain obtained at a center frequency of 31.5 cpd. An examination of the product of M-inverse and S suggests that neural sinewave contrast sensitivity decreases at too rapid a rate for a monotonically decreasing attenuation function to counteract the increasing response summation obtained with even 0.05 octave bandwidths. Ultimately, the filter response must be weighted negatively in order to reduce the aggregate response sufficiently. With slightly larger bandwidths (figure C.2, c), the negative gains alternate with positive ones in an region of unrealistically large amplification that coincides with the greatest filter overlap. As bandwidths approached commonly assumed values, the exaggerated oscillations spread until they spanned the entire range of filters (figure C.2, d, e and f).

Constant bandwidths

An attempt was made using fixed bandwidths to find a set of reasonable filter parameters that would produce positive individual filter estimates. This attempt also failed, but it confirmed the relation between increasing filter overlap and decreasing contrast sensitivity as the source of instability in gain estimates. The

aggregate response measure was the linear sum ($B = 1$), as in the constant octave linear model. A given filter template was formed by selecting a center frequency about which a one octave gaussian weighting function was created. That template was then replicated about each of the 64 filter center frequencies used to approximate the model. The narrowest template produced a set of individual filter gains which were approximately 50% the magnitude of the corresponding NTF measure (figure C.3, a). Even with this template, incipient oscillations may be seen in the low frequency region. For fixed bandwidth filters, the the overlap is greatest at low frequencies. As the center frequency of the template is increased, the oscillations increase dramatically and spread toward higher spatial frequencies (figure C.3, b, c, and d).

When the exponent, B, is equal to two, the model is equivalent to an rms measure. Both constant octave and fixed bandwidth filter responses were examined (figure C.4, a and b). Oscillation patterns similar to the linear model were observed.

Exponents from 3 to 8 were tested on the constant one octave bandwidth model. The oscillations remained (figure C.5). Ultimately, B can be made large enough to reduce the effective bandwidth of even one octave filters to be much less than the 0.5 cpd filter spacing (essentially a peak response model); however, the required value may be huge (figure C.6).

In the analysis of compound sinewave or broadband stimuli the effect of larger exponents is more complex; however, in octave bandwidth models the net

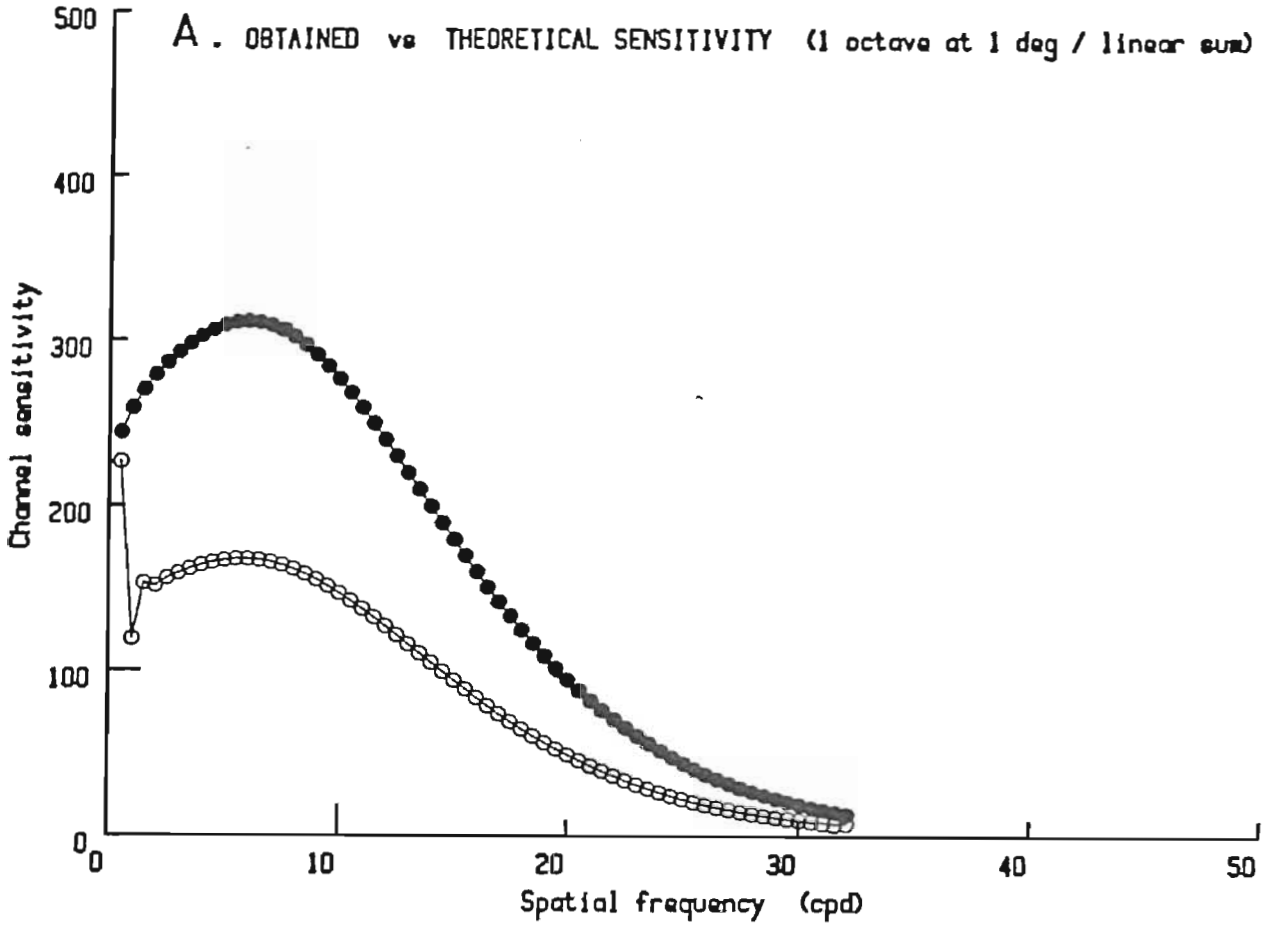

Figure C.3 Single linear filter aggregate response model (fixed bandwidth).

A linear system in the form of [D8] was solved for a gain exponent of one and fixed octave bandwidths. Solutions were obtained for one octave gaussian templates at: a, 1 cpd (0.707 cpd bandwidth); b, 2 cpd (1.414 cpd); c, 4 cpd (2.828 cpd); and d, 16 cpd (11.312 cpd). As with the constant octave filters, negative gains were obtained for all but the narrowest bandwidths. The oscillations first appeared in the low frequency region, the region of greatest filter overlap, and spread to the higher frequencies as bandwidth increased. (NTF, closed dots; model response, open dots).

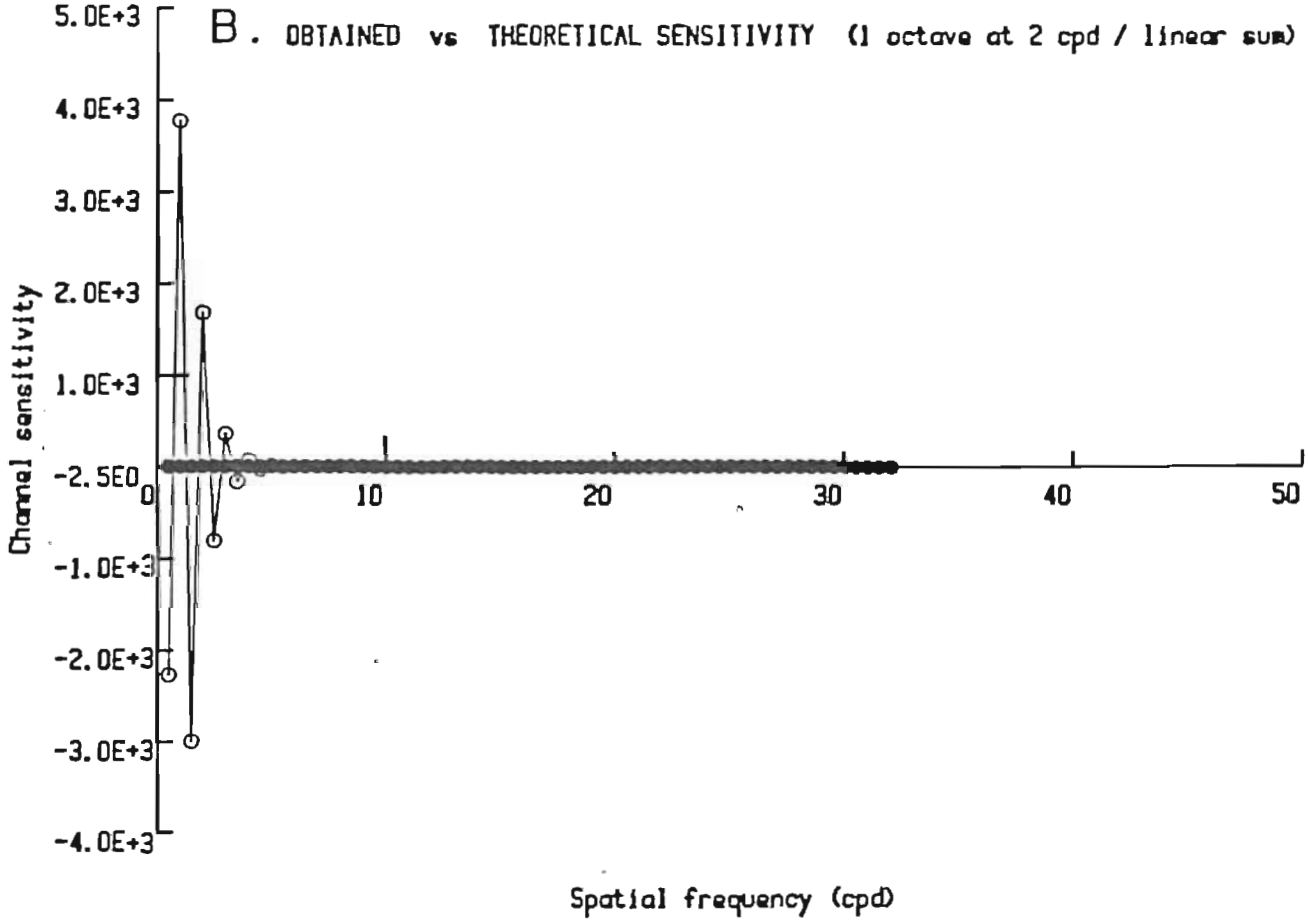
B. OBTAINED vs THEORETICAL SENSITIVITY (1 octave at 2 cpd / linear sum)
5.0E+3
4.0E+3
3.0E+3
2.0E+3
1.0E+3
-2.5E0
-1.0E+3
-2.0E+3
-3.0E+3
-4.0E+3
Channel sensitivity
0
10
20
30
40
50
Spatial frequency (cpd)

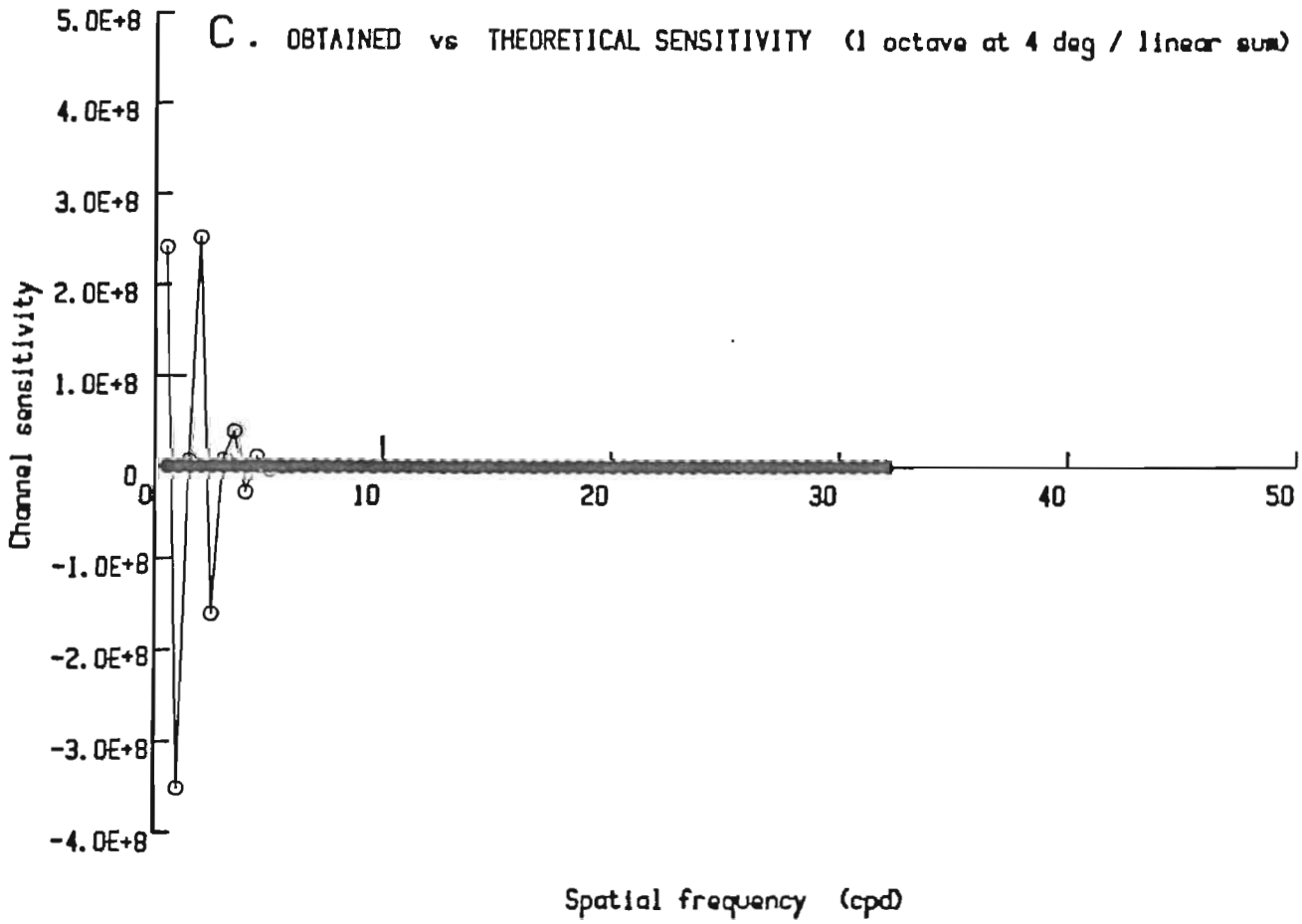
C. OBTAINED vs THEORETICAL SENSITIVITY (1 octave at 4 deg / linear sum)
5.0E+8
4.0E+8
3.0E+8
2.0E+8
1.0E+8
0
-1.0E+8
-2.0E+8
-3.0E+8
-4.0E+8
Channel sensitivity
0
10
20
30
40
50
Spatial frequency (cpd)

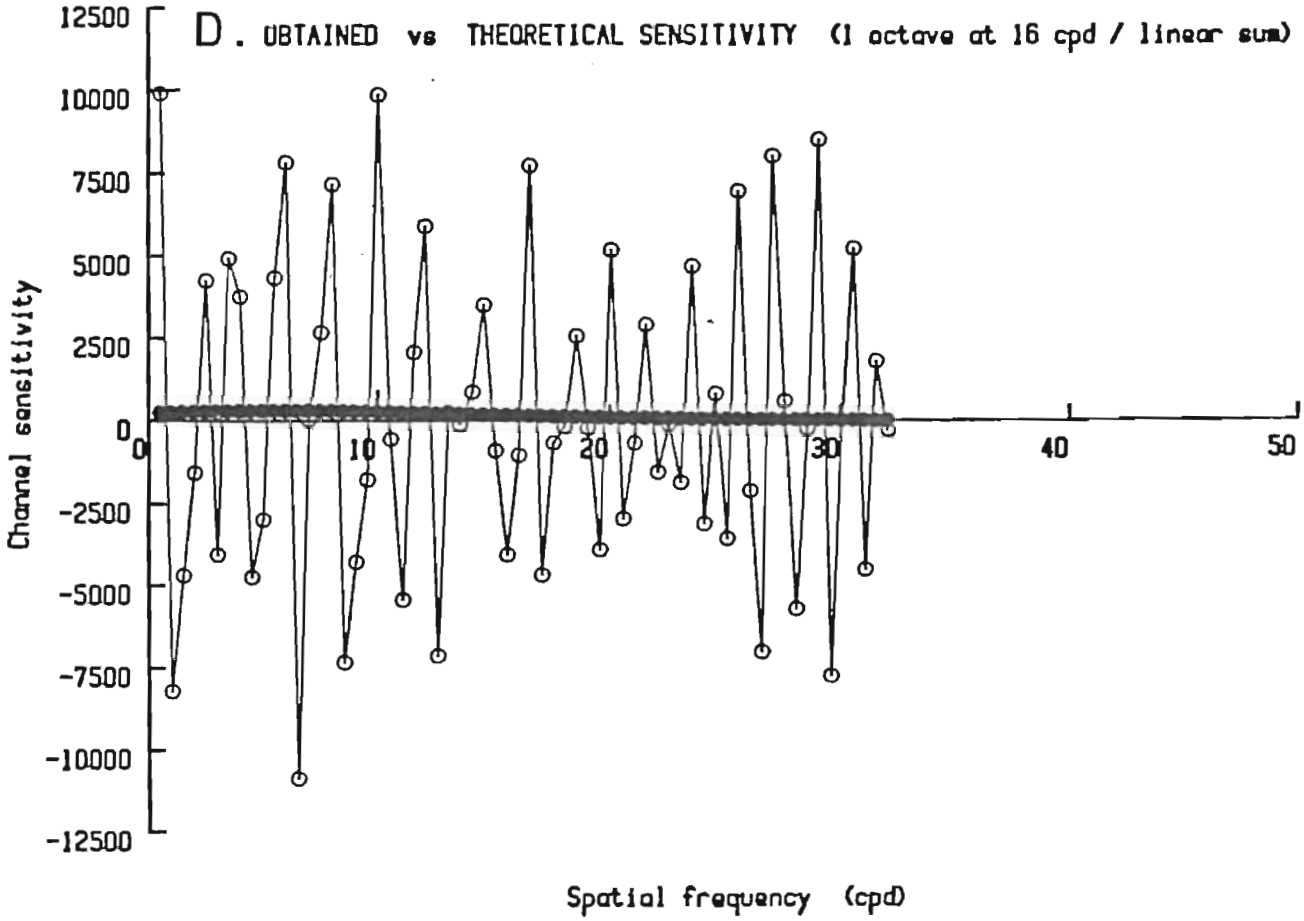
D. OBTAINED vs THEORETICAL SENSITIVITY (1 octave at 16 cpd / linear sum)
12500
10000
7500
5000
2500
0
-2500
-5000
-7500
-10000
-12500
Channel sensitivity
0
10
20
30
40
50
Spatial frequency (cpd)

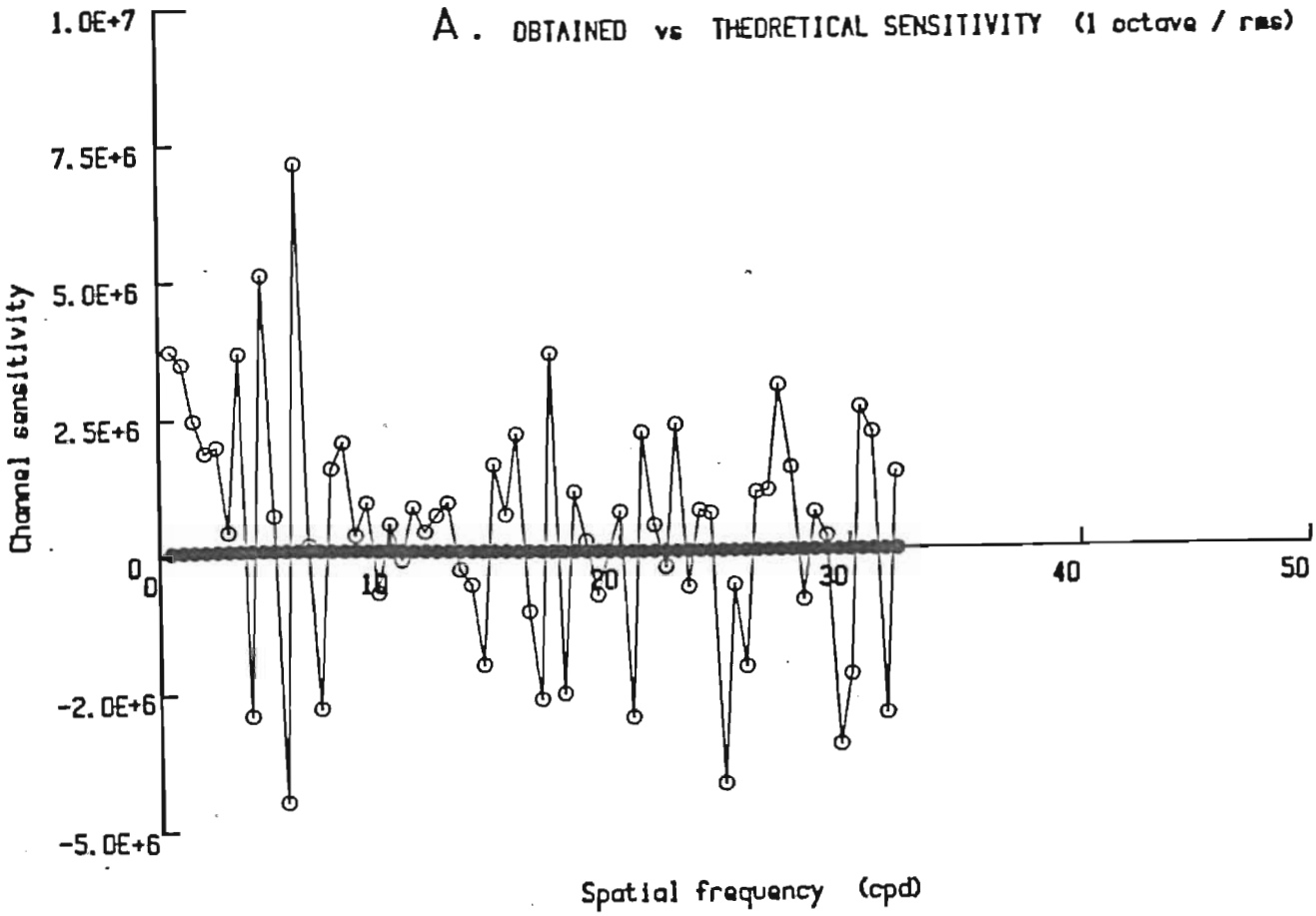

Figure C.4 Rms aggregate response model.

A linear system in the form of [D8] was solved for a gain exponent of two over a range of constant octave and fixed bandwidth models. The pattern of exaggerated oscillations continued to preclude an acceptable solution: a, constant one octave bandwidth; b, fixed one octave bandwidth at 4 cpd. (NTF^2, closed dots; $(\text{model response})^2$, open dots).

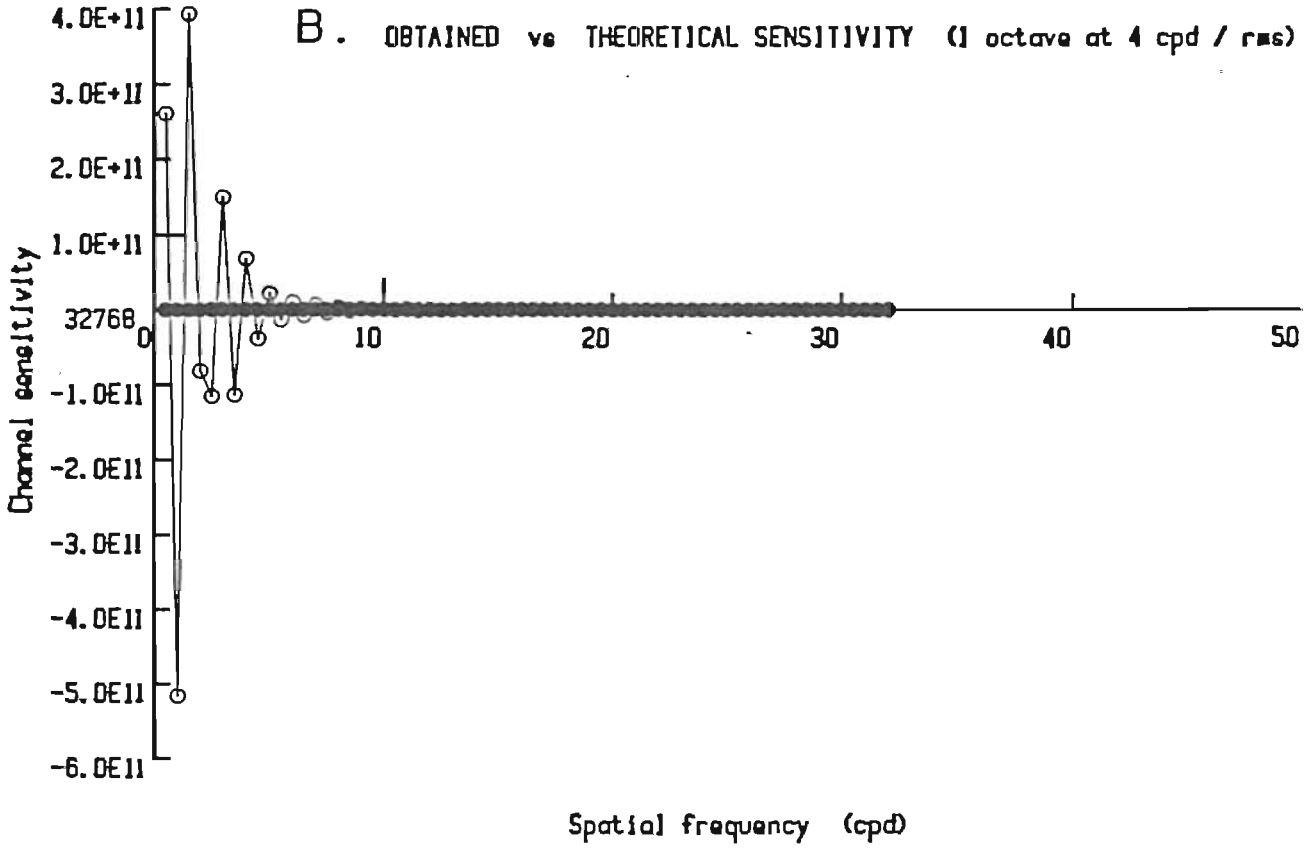
B. OBTAINED vs THEORETICAL SENSITIVITY (1 octave at 4 cpd / rms)
4.0E+11
3.0E+11
2.0E+11
1.0E+11
32768
-1.0E11
-2.0E11
-3.0E11
-4.0E11
-5.0E11
-6.0E11
Channel sensitivity
0
10
20
30
40
50
Spatial frequency (cpd)

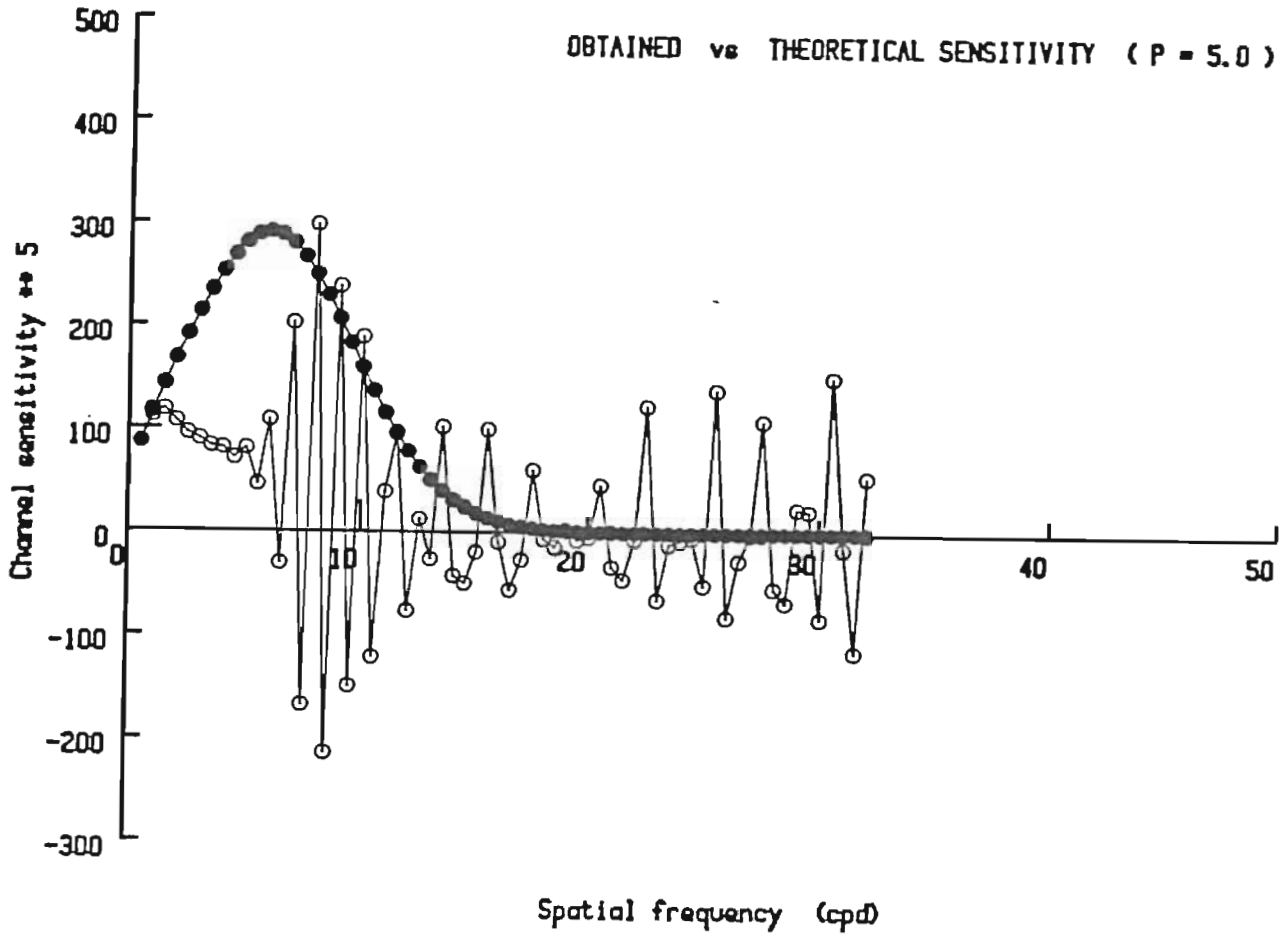

Figure C.5 Higher power aggregate response models.

Individual filter response exponents from 3 to 8 were applied to constant one octave gaussian filters. Solutions of the individual filter gains displayed the exaggerations characteristic of the lower order systems. The theoretical sensitivities diverged from the obtained sensitivities in the low spatial frequency region and broke into oscillation on the negative slope. (NTF^5, closed dots; $(\text{model response})^5$, open dots).

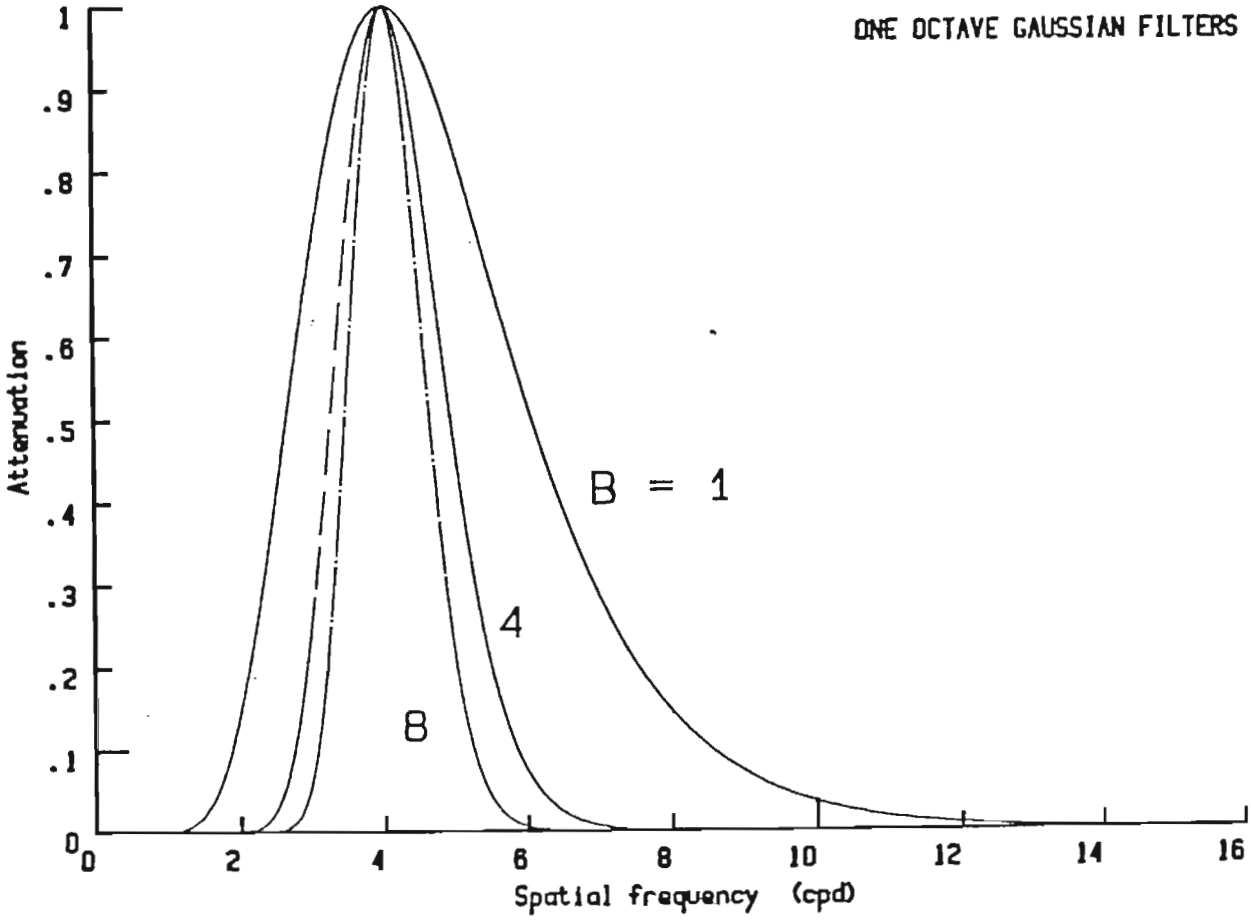

Figure C.6 Effect of exponent (B) on filter sensitivity.

In the analysis of single sinewave sensitivity, exponents greater than one cause a reduction in the effective bandwidth of the filters. As the exponents increase, the relative sensitivity of filters to non-optimal spatial frequencies is reduced. Bandwidth as a function of exponent is a decelerating relation. To achieve the narrow bandwidths necessary to eliminate the oscillations, huge exponents would be required.

effect is to increase the relative response contribution of filters with larger bandwidths. The increased sensitivity would exacerbate a situation that is already unstable with no differential in spatial frequency summation.

Probability summation across space

Probability summation across space is a mechanism that has been used to model the response of medium bandwidth filters to narrow and broadband stimuli (e.g., Graham and Rogowitz, 1976). The motivation for this addition comes from the inverse relation between absolute bandwidth and spatial extent. To span a fixed aperture with constant octave bandwidth filters while maintaining an equivalent percentage of total active filter width would require a filter population of each type that was proportional to filter center frequency. The effect of a population differential is a increase in relative sensitivity for the portion of the frequency spectrum covered by the greater number of filters over that afforded by an individual filter. Two version of probability summation across space were tested in the framework of Quick's vector magnitude model.

The first version included no channeling, no special affinity among any subset of filter types. In the linear system [C.8], the filter count for the lowest spatial frequency (x_1, 0.5 cpd) is set to 1 and the values are increased in proportion to center frequency up to 64 (x_{64}, 32 cpd). For apertures larger than the width of the lowest frequency filter, all filter counts are scaled by the same factor and the relative magnitude of the individual filter gains (g_j) does not change. Solutions

for the linear system [C.8] were obtained for a range of exponents. As before, gain estimates for one octave bandwidths displayed large positive and negative excursions as the CSF decreased toward the high spatial frequencies (figure C.7). A new effect appeared at low spatial frequencies. As the filter center frequency decreased, and with it the number of filters per center frequency, the individual gain estimates increased exponentially. Apparently, the increase in sensitivity resulting from probability summation across space occurs at a much faster rate than does the observed contrast sensitivity. In the solution, the disparity in rates is compensated for by excessively large gain estimates at the lowest spatial frequencies. At high spatial frequencies, however, the increase in sensitivity from probability summation across space aggravates the imbalance that already exists between filter bandwidth and the roll-off of observed contrast sensitivity.

The second attempt at incorporating probability summation across space in the vector magnitude model involved channels. Filters with the same center frequency were all mapped onto the same dimension of the vector space and were linearly summed prior to the vector magnitude calculation. In the linear system [C.8], the linear summation is equivalent to raising the x_j's to the B^{th} power. The distortions and instabilities in the gain estimates were amplified (figure C.7, b).

This simple model of the numerical distribution of filters as a function of center frequency contains several approximations. The distribution of filters over the central four degrees is significantly inhomogeneous and the gain of filters with the same center frequency may vary markedly, being most sensitive in the fovea

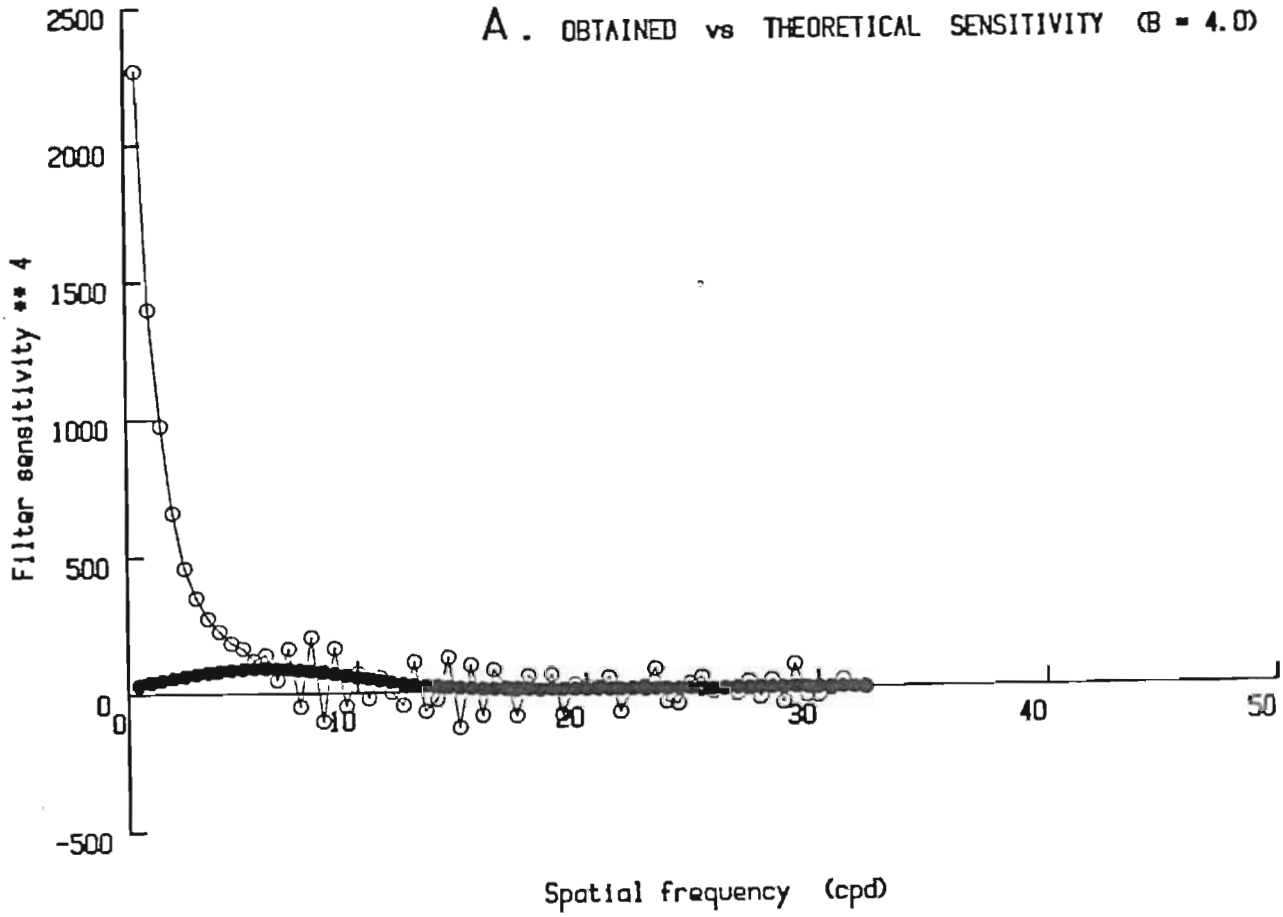

Figure C.7 Aggregate response model with probability summation across space.

The filter count is increased in proportion to the filters' center frequency. This model maintains coverage of a constant percentage of the stimulus aperture. The model in (a) uses no channeling. For one octave gaussian filters, the estimated individual gains greatly exceed the obtained CSF at low spatial frequencies and oscillated between positive and negative gains at high spatial frequencies. In (b), filter responses were linearly pooled across space for filters with the same center frequency. The adjustment increased the distortions. (NTF^4, closed dots; $(\text{model response})^4$, open dots).

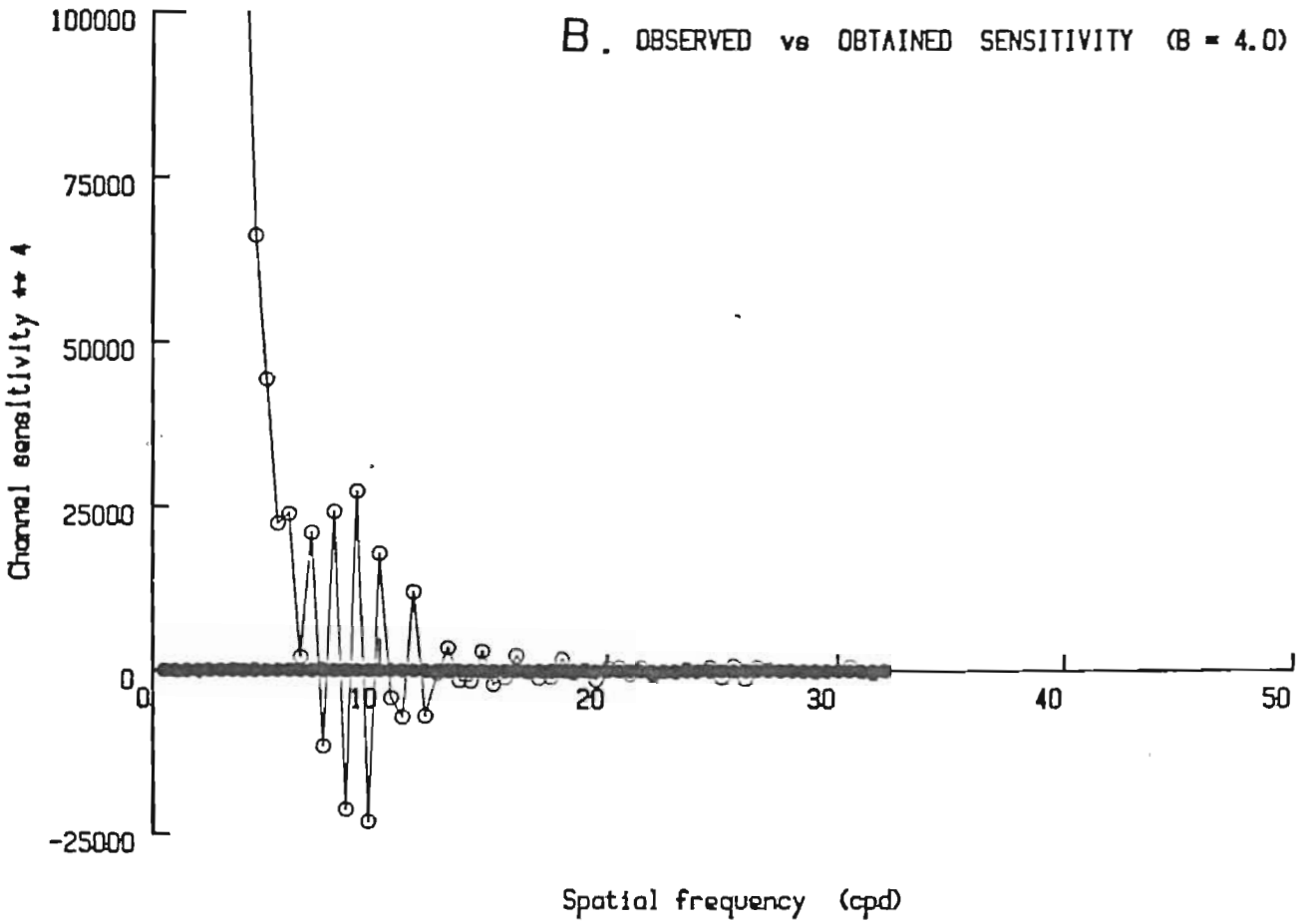
B. OBSERVED vs OBTAINED SENSITIVITY (B = 4.0)
100000
75000
50000
25000
0
-25000
Channel sensitivity ** 4
0
10
20
30
40
50
Spatial frequency (cpd)

(Hilz and Cavonious, 1974; Wilson and Giese, 1977; Graham et al., 1978; Robson and Graham, 1981). A two-dimensional model in which filters were limited in both vertical and horizontal extent also failed to produce positive gain estimates (figure C.8). Given the range of spacings for which oscillations occur, it is unlikely that the errors in the density estimates are sufficient to be the dominant source of the gain distortions.

Logarithmic filter spacing

The analysis underlying the various models presented here has presumed that the center frequency of the filters is a random variable. The 64 filters sampled this continuum with sufficient density to avoid scalloping of the predicted sinewave contrast sensitivity function when the effective filter bandwidth was moderately large and the power of the nonlinearity moderately small. An acceptable model with minimal scalloping and a solution set of individual filter gains that is both positive and smooth could not be found. Implicit in the sampling of the random filter center frequency distribution was the additional assumption that any changes in the density of filters could be incorporated in the model by changes in the gains of filters representing small regions of the continuum. If the combination of filter responses is indeed nonlinear, the assimilation of different filter densities across spatial frequency through gain changes may not be appropriate or accurate. For filters that symmetric weightings on a logarithmic spatial frequency axis, scalloping is minimized (for a fixed

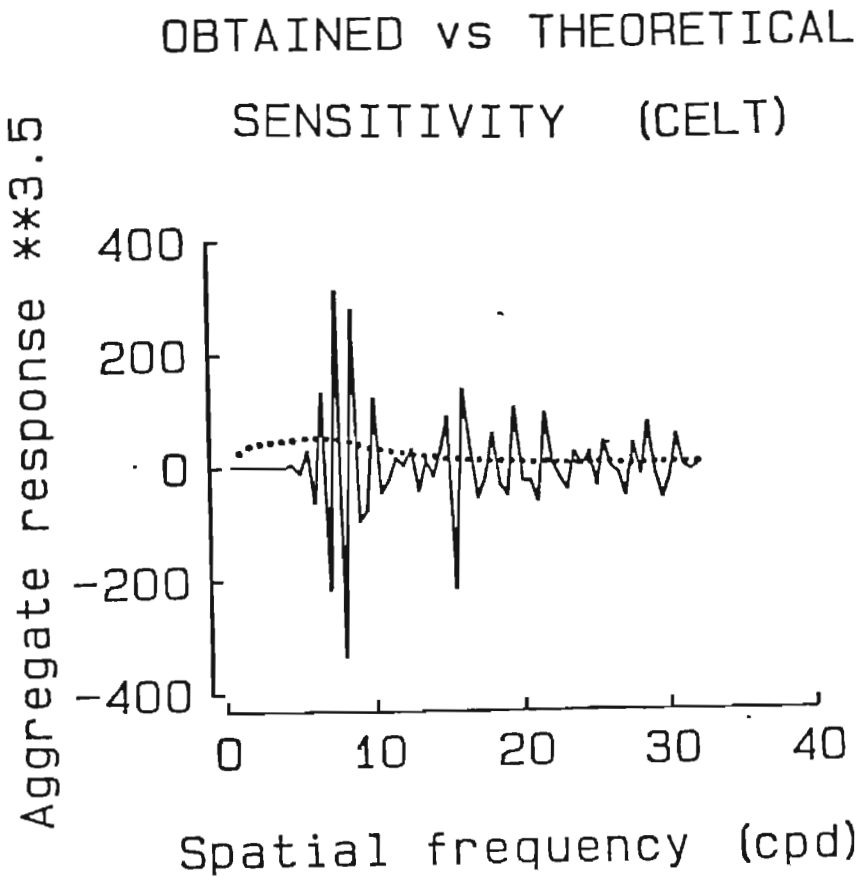

Figure C.8 Linear systems solution for CELT.

An exact solution for the filter approximations in CELT also contain oscillating positive and negative gain estimates (gain estimates, dotted line; NTF, solid line). The model is composed of one octave gaussian filters with probability summation across space and spatial frequency. Compare these gain estimates with those in figure 2.10.

number of filters over a fixed range of spatial frequencies) by separating the center frequencies in constant ratios. For narrowband stimuli, such are being used to assess gains in this appendix, a logarithmic separation rule disproportionately weights the lower frequencies in the aggregate measure. Several models of this form were examined.

Negative solutions were obtained for individual gains with filter bandwidths of one octave and exponents from one to eight (figure C.9, a, b). When bandwidth was decreased to 0.5 octave ($B = 4.0$), some oscillation and negative gain remained in the low spatial frequency range, the region of greatest filter overlap (figure C.10, a). A bandwidth of 0.1 octave ($B = 4.0$) produced a solution that was virtually identical to the Observer's sensitivity (figure C.10, b); however, large notches in contrast sensitivity existed across the entire spatial frequency range for sinewaves lying between filter center frequencies.

In summary, the principal result of this analysis is the manifest failure of aggregate response measures that incorporate probability summation across spatial frequency and across space. Models that increase filter overlap toward either end of the Observer's spatial frequency contrast sensitivity cannot match observed decreases in contrast sensitivity without incorporating negative and oscillating individual filter gains. It is concluded that for the case of single sinewaves the nonlinear vector magnitude models that use exponents upwards of 8 do so to reduce effective filter bandwidth and approximate peak response mechanisms.

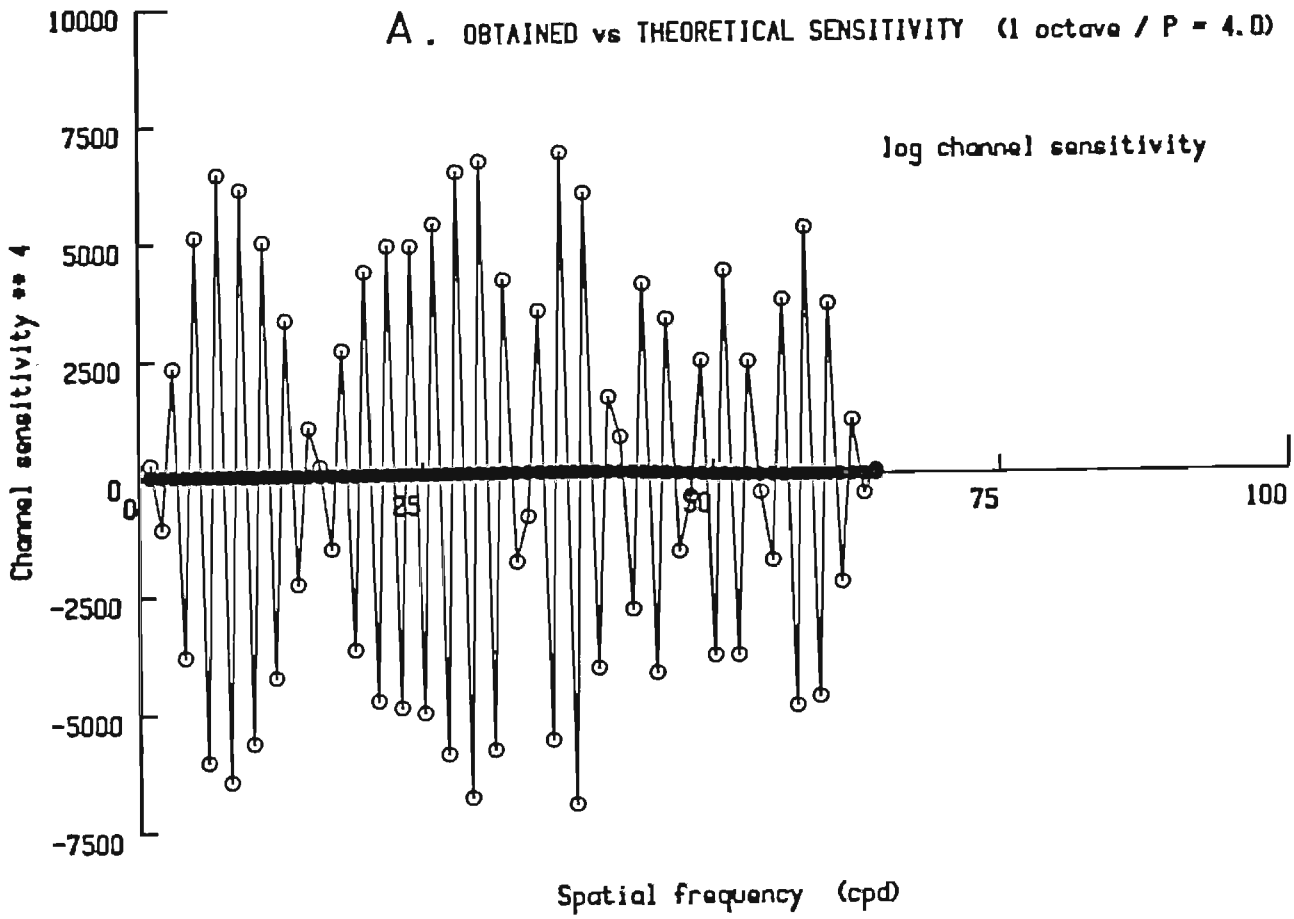

Figure C.9 Logarithmic separation of medium bandwidth filters.

Sixty-four one octave raised cosine filters were logarithmically distributed between 0.5 and 32.0 cpd. With a moderate exponent (a) extreme oscillations and negative gains occurred over the entire range of center frequencies. With a larger exponent (b) the oscillations were diminished and restricted to the region of greatest filter concentration. (NTF^B, closed dots; (model response)^B P, open dots).

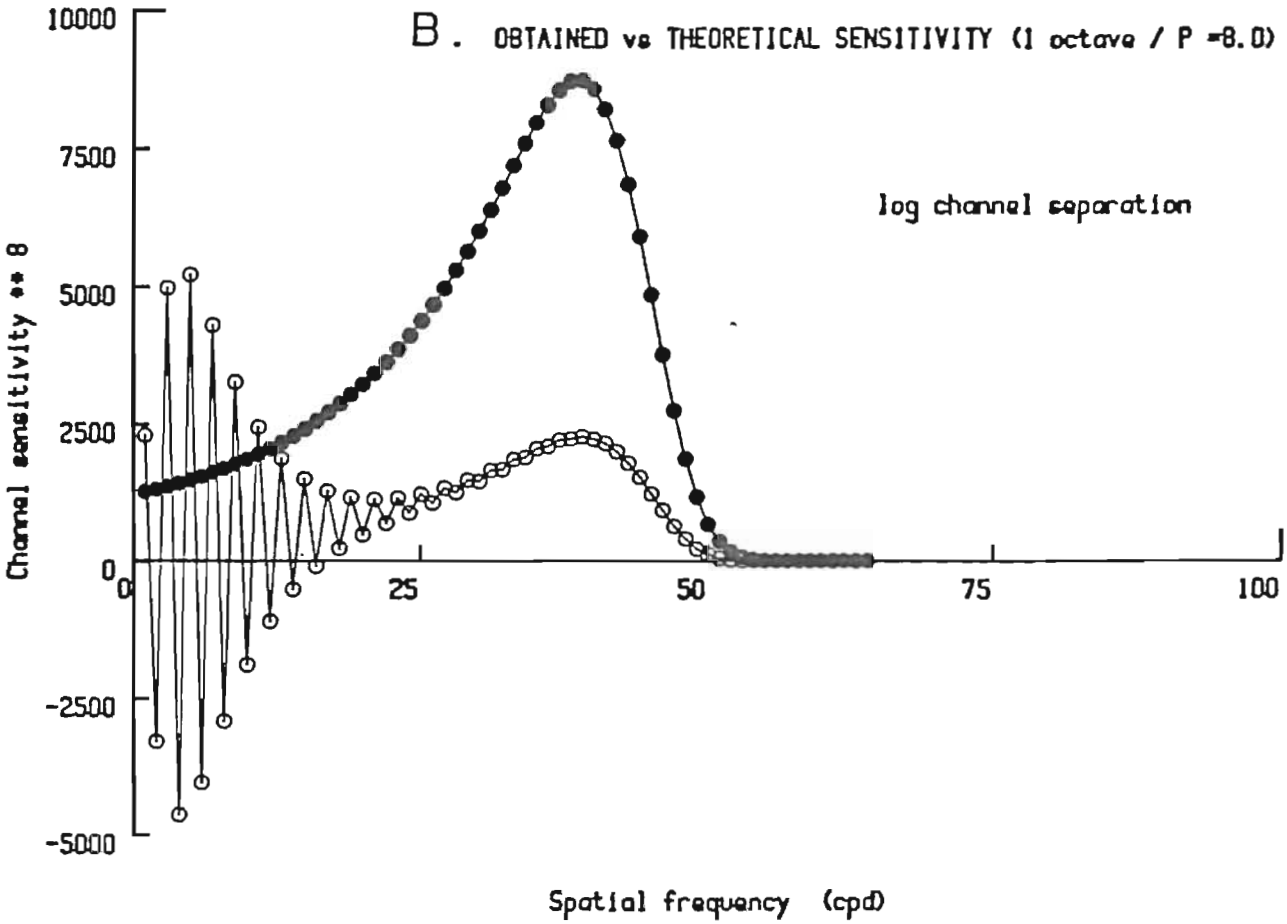
B . OBTAINED vs THEORETICAL SENSITIVITY (1 octave / P =8.0)
log channel separation
Channel sensitivity ** 8
10000
7500
5000
2500
0
-2500
-5000
0
25
50
75
100
Spatial frequency (cpd)

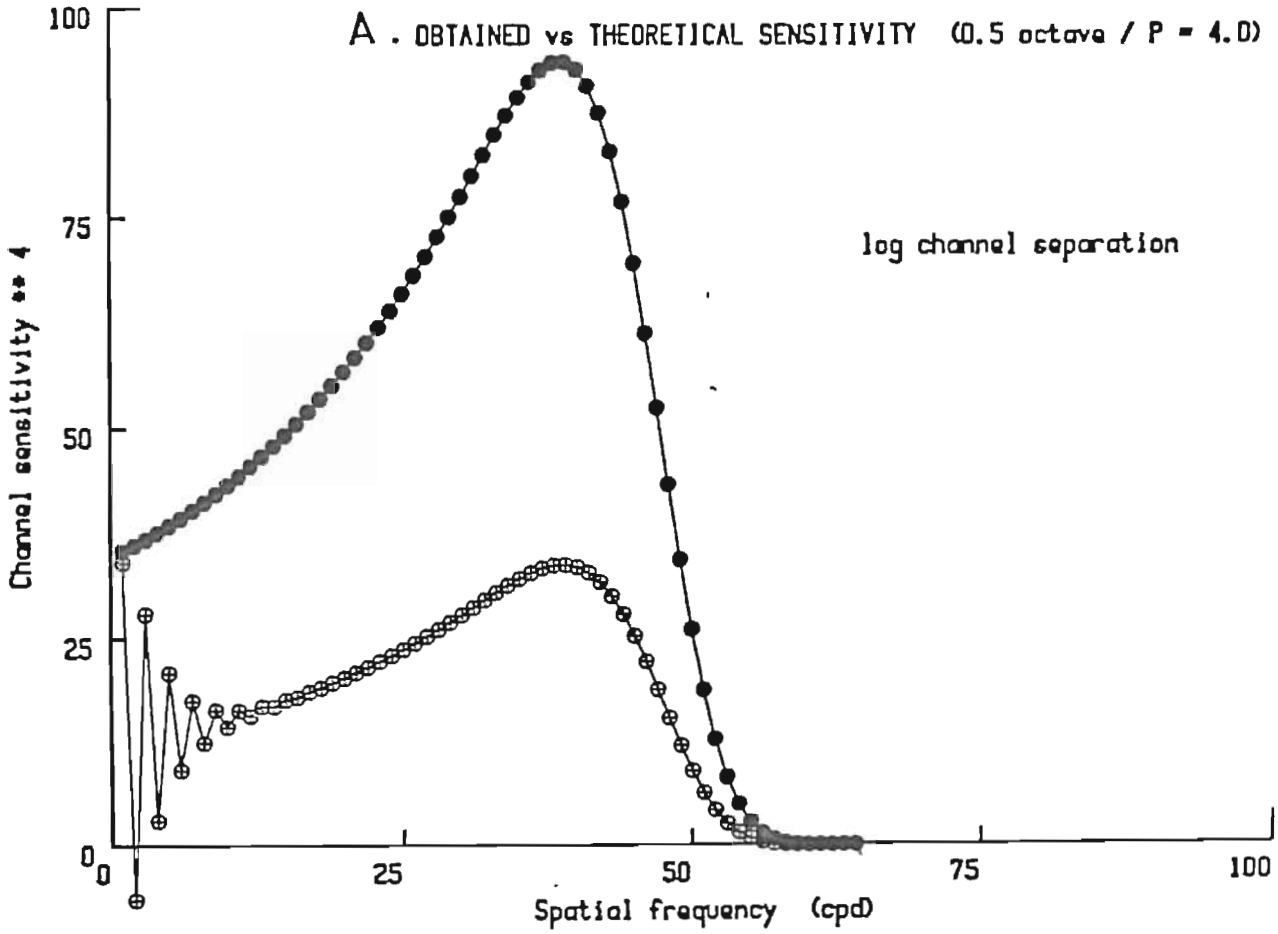

Figure C.10 Logarithmic separation of narrow bandwidth filters.

Gain oscillations were greatly reduced for 0.5 octave filters ($B = 4.0$) logarithmically distributed in proportion to their center frequencies (a). When the bandwidth was reduced further to 0.1 octave (b), the model virtually became an identity transformation for the sinewave sensitivities tested. (NTF^4, closed dots; $(\text{model response})^4$, open dots).

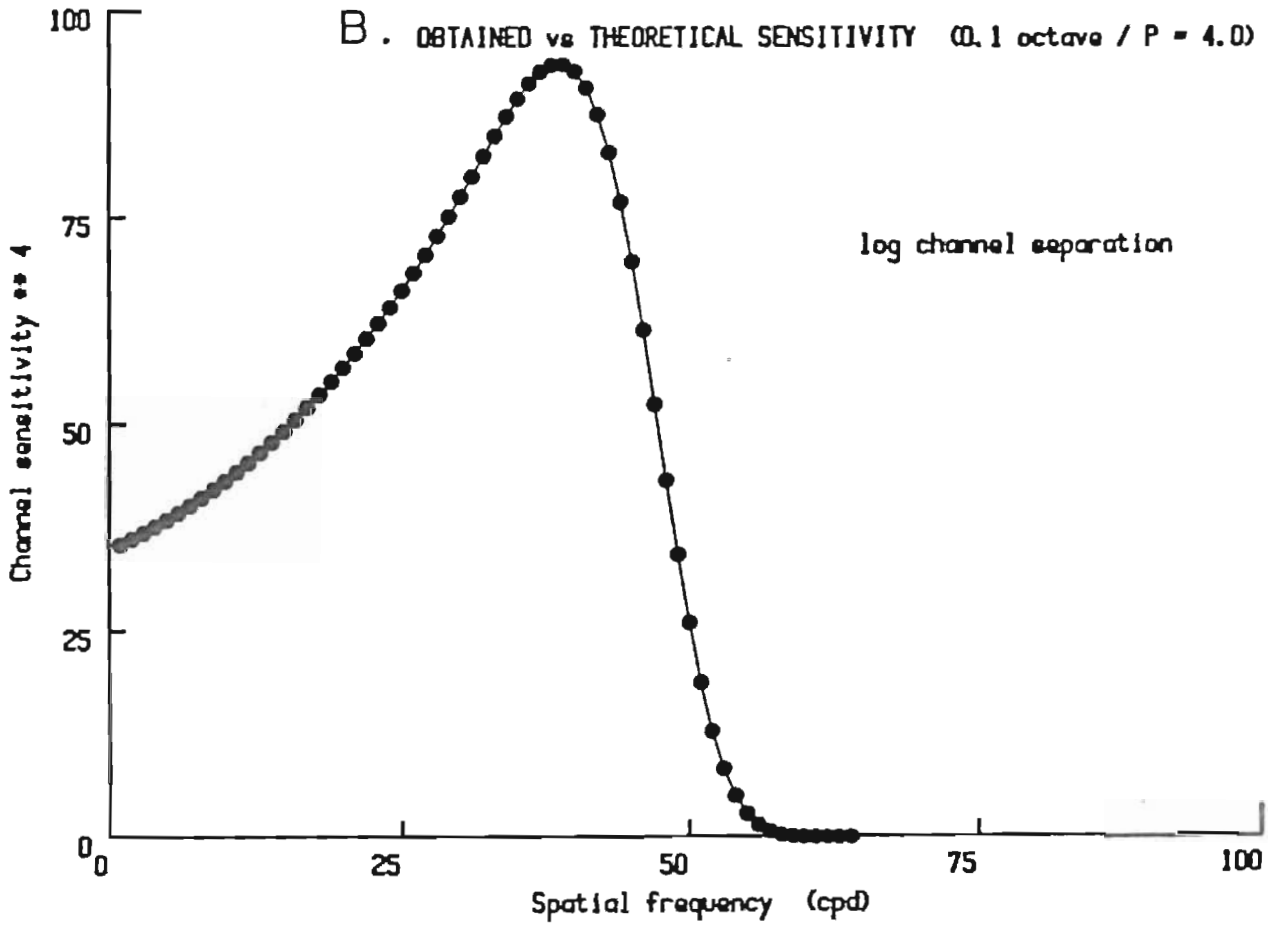
B . OBTAINED vs THEORETICAL SENSITIVITY (0.1 octave / P = 4.0)
log channel separation
Channel sensitivity ** 4
100
75
50
25
0
0
25
50
75
100
Spatial frequency (cpd)

For the case of multiple sinewaves, it is proposed that in detection tasks filter thresholds or signal to noise limitations disproportionately reduce the contributions of individual stimulus frequency components that are away from the center frequency of the filter. The failure to achieve uniformly positive gains could stem either from insufficiently accurate estimates of the filter parameters (e.g., the shape of the filter weighting profile) or possibly from a fundamental limitation in the ability of the vector magnitude model to approximate closely the threshold or signal to noise limitations.

The technique of finding an exact solution to the system of linear equations appears to be extremely sensitive to the shape of the filter profile in regions where sensitivity is low and overlap among filters is high. As a result of this property the technique may be useful as a metric to discriminate among candidate filter profiles. Other methods, such as those that use iteration, appear to be more tolerant of errors in the filter estimates and should be used to obtain gain approximations.

REFERENCES

Abadi, R. V. and Kulikowski, J. J. (1973) Linear summation of spatial harmonics in human vision. *Vision Res.* **13**, 1625-1628.

Airy, G. B. (1834) *Cambridge Phil. Soc. Trans.*, p. 283.

Andersen, E. E. and Weymouth, F. W. (1923) Visual perception and the retinal mosaic. I. Retinal mean local sign - an explanation of the fineness of binocular perception of distance. *Am. J. Physiol.* **64**, 561-594.

Andrews, D. P. (1965) Perception of contours in the central fovea. *Nature* **205**, 1218-1220.

Andrews, D. P. (1967a) Perception of contour orientation in the central fovea. Part I: Short lines. *Vision Res.* 7, 975-997.

Andrews, D. P. (1967b) Perception of contour orientation in the central fovea. Part II: Spatial integration. *Vision Res.* 7, 999-1013.

Andrews, D. P., Butcher, A. K. and Buckley, B. R. (1973) Acuities for spatial arrangement in line figures: Human and ideal observers compared. *Vision Res.* **13**, 599-620.

Andrews, D. P. and Miller, D. T. (1978) Acuity for spatial separation as a function of stimulus size. *Vision Res.* **18**, 615-619.

Aoki, M. (1964) Studies on amblyopia - vernier acuity of macular region. *Acta Soc. Ophthal. Jap.* **68**, 1367-1376.

Appelle, S. (1972) Perception and discrimination as a function of stimulus orientation: The "oblique effect" in man and animals. *Psych. Bull.* **78**, 266-278.

Arend, L. E. and Lange, R. V. (1979) Phase-independent interaction of widely separated spatial frequencies in pattern discrimination. *Vision Res.* **19**, 1089-1092.

Atkinson, J. and Campbell, F. W. (1974) The effect of phase on the perception of compound gratings. *Vision Res.* **14**, 159-162.

Aubert, H. (1865) *Physiologie der Netzhaut.* Morgenstern, Breslau.

Baker, K. E. (1949) Some variables influencing vernier acuity. *J. opt. Soc. Am.* **39**, 567-576.

Baker T. Y. and Bryan, G. B. (1912) Errors of observation. *Proc. opt Convention.* **Vol. 2.** Hodder and Stoughton, London.

Barlow, H. B. (1972) Single units and sensation: A neuron doctrine for perceptual psychology? *Perception.* **1**, 371-394.

Barlow, H. B. (1979) Reconstructing the visual image in space and time. *Nature.* **279**, 189-190.

Baylor, D. A., Fuortes, M. G. F. and O'Bryan, P. M. (1971) Receptive fields of cones in the retina of the turtle. *J. Physiol. (Lond.)* **214**, 265-294.

Beck, J. and Schwartz, T. (1979) Vernier acuity with dot test objects. *Vision Res.* **19**, 313-319.

Berry, R. N. (1948) Quantitative relations among vernier, real depth, and stereoscopic depth acuities. *J. exp. Psych.* **38**, 708-721.

Berry, R. N., Riggs, L. A. and Duncan, C. P. (1948) The relation of vernier and depth discriminations to field brightness. *J. Exp. Psych.* **40**, 349-354.

Berry, R. N., Riggs, L. A. and Richards, W. (1950) The relation of vernier and depth discrimination to width of test rod. *J. Exp. Psych.* **40**, 520-522.

Best, F. (1900) Uber die Grenze der Erkennbarkeit von Lagenunterschieden. *Albrecht v. Graefes Arch. Ophthal.* **51**, 453-460.

Blakemore, C. and Campbell, F. (1968) Adaptation to spatial stimuli. *J. Physiol. (Lond.)* **200**, 11-13P.

Blakemore, C. and Campbell, F. W. (1969) On the existence of neurons in the human visual system selectively sensitive to the orientation and size of retinal images. *J. Physiol. (Lond.)* **203**, 237-260.

Blakemore, C., Muncey, J. P. J. and Ridley, R. M. (1971) Perceptual fading of a stabilized cortical image. *Nature* **233**, 204-205.

Blakemore, C., Muncey, J. P. J. and Ridley, R. M. (1973) Stimulus specificity in

the human visual system. *Vision Res.* **13**, 1915-1931.

Blakemore, C. and Sutton, P. (1969) Size adaptation: a new aftereffect. *Science* **166**, 245-247.

Bodis-Wollner, I., Hendley, C. D. and Kulikowski, J. J. (1972) Electrophysiological and psychological responses to modulation of contrast of a grating pattern. *Perception* **1**, 341-349.

Bodis-Wollner, I., Hendley, C. D. and Tajfel, M. (1973) Contrast-modulation thresholds as a function of spatial frequency. *J. opt. Soc. Am.* **63**, 1297 (A).

Boring, E. G. (1935) The relation of the attributes of sensation to the dimensions of the stimulus. *Philos. Sci.***2**, 236-245.

Bourdon, B. (1902) *La perception visuelle de l'espace.* Schleicher, Paris.

Braddick, O., Campbell, F. W. and Atkinson, J. (1978) Channels in vision: Basic aspects. In *Handbook of sensory physiology, vol.* **VIII** *Perception.* R. Held, H. W. Leibowitz and H-L. Teuber (eds.), Springer-Verlag, Berlin.

Breitmeyer, B.G. (1978) Disinhibition in metacontrast masking of vernier acuity targets: Sustained channels inhibit transient channels. *Vision Res.* **18**, 1401-1405.

Brindley, G. S. (1960) *Physiology of the retina and the visual pathway.* Edward Arnold Ltd. London.

Bryngdahl, O. (1964) Characteristics of the visual system: psychophysical measurements of the response to spatial sine wave stimuli in the photopic region. *J. opt. Soc. Am.* **54**, 811-821.

Burgess, P. R., Tuckett, R. P. and Horch, K. W. (1984) Topographic and non-topographic mapping of spatial sensory information. Predictions from Boring's formulation. In *Comparative Physiology of Sensory Systems*, L. Bolis, R. D. Kenes and S. H. P. Maddrell (eds.) Cambridge University Press.

Burr, D. C. (1979) Acuity for apparent vernier offset. *Vision Res.* **19**, 835-837.

Burr, D. C. (1980) Sensitivity to spatial phase. *Vision Res.* **20**, 391-396.

Burton, G. J. (1973) Evidence for nonlinear response processes in the human visual system from measurements on the thresholds of spatial beat frequencies.

Vision Res. **13**, 1211-1225.

Burton, G. J. (1981) Contrast discrimination in the human visual system. *Biol. Cybern.* **40**, 27.38.

Campbell, F. W. (1979) Recent attempts to link psychophyics with neurophysiology in vision research. *Proc. Austral. Physiol. Pharmacol. Soc.* **10**, 1-8.

Campbell, F. W., Carpenter, R. H. S. and Levinson, J. Z. (1969) Visibility of aperiodic patterns compared to that of sinusoidal gratings. *J. Physiol. (Lond.)* **204**, 283-298.

Campbell, F. W. and Green, D. G. (1965) Optical and retinal factors affecting visual resolution. *J. Physiol. (Lond.)* **181**, 576-593.

Campbell, F. W. and Gubisch, R. W. (1966) Optical quality of the human eye. *J. Physiol. (Lond.)* **186**, 558-578.

Campbell, F. W. and Gubisch, R. W. (1967) The effect of chromatic aberration on visual acuity. *J. Physiol. (Lond.)* **192**, 345-358.

Campbell, F. W. and Kulilowski, J. J. (1966) Orientation selectivity of the human visual system. *J. Physiol. (Lond.)* **187**, 437-445.

Campbell, F. W. and Robson, J. G. (1968) Application of Fourier analysis to the visibility of gratings. *J. Physiol. (Lond.)* **197**, 551-556.

Cannon, M. Y. (1979) Contrast sensation: a linear function of stimulus contrast. *Vision Res.* **19**, 1045-1052.

Carlson, C. R., Cohen, R. W. and Gorog, I. (1977) Visual processing of simple two-dimensional sine-wave luminance gratings. *Vision Res.* **17**, 351-358.

Carlson, C. R. and Pica, A. (1979) Invariance in sine wave contrast discrimination. *Invest. Ophthal. visual Sci. Suppl.* **18**, 61.

Carter, B. E. and Henning, G. B. (1971) The detection of gratings in narrow-band visual noise. *J. Physiol. (Lond.)* **219**, 355-365.

Cobb, P. W. and Moss, F. K. (1925) The effect of brightness on the precision of visually controlled operations. *J. Franklin Institute.* **199**, 507-512.

Coleman, H. S. and Coleman, M. F. (1947) Theoretical resolution angles for point and line test objects in the presence of a luminous background. *J. opt. Soc. Am.* **37**, 572-576.

Collins, J. B. (1959) Visual fatigue and its measurement. *Ann. Occup. Hyg.* **1**, 228-236.

Cornsweet, T. N. (1970) /f2Visual Perception. Academic Press. New York.

Corwin, T. R., Moskowitz-Cook, A. and Green, M. A. (1977) The oblique effect in a vernier acuity situation. *Percep. and Psychophys.* **21**. 445-449.

Cowey, A. and Rolls, E. T. (1974) Human cortical magnification factor and its relation to visual acuity. *Exp. Brain Res.* **21**, 447-454.

Crick, H. C., Marr, D. C. and Poggio, T. (1980) An information processing approach to understanding the visual cortex. *A. I. Memo No.* **557**, M.I.T.

Daugman, J. G. (1980) Two-dimensional spectral analysis of cortical receptive field profiles. *Vision Res.* **20**, 847-856.

Davidson, M. (1968) Perturbation approach to spatial brightness interaction in human vision. *J. opt. Soc. Am.* **58**, 1300-1308.

Dealy, R. S. and Tolhurst, D. J. (1974) Is spatial adaptation an aftereffect of prolonged inhibition? *J. Physiol. (Lond.)* **241**, 261-270.

de Jongste-Breeman, K. K. and van Balen, A. T. M. (1979) The determination of the maximum angular visual acuity and of the vernier acuity. *Klin. Mbl. Augenheilk.* **175**, 185-190.

DeValois, K. (1977a) Independence of black and white: phase-specific adaptation. *Vision Res.* **17**, 209-215.

DeValois, K. (1977b) Spatial frequency adaptation can enhance contrast sensitivity. *Vision Res.* **17**, 1057-1065.

DeValois, R. L., Albrecht, D. G. and Thorell, L. G. (1982) Spatial frequency selsctivity of cells in macaque visual cortex. *Vision Res.* **22**, 545-559.

Enroth-Cugell, C. and Shapley, R. M. (1973) Flux, not retinal illumination, is what cat retinal ganglion cells realy care about. *J. Physiol.* **187**, 311-326.

Erickson, R. P. (1968) Stimulus coding in topographic and non-topographic afferent modalities. *Psych. Rev.* **75**, 447-465.

Fender, D. H. and Nye, P. W. (1962) The effects of retinal image motion in a simple pattern recognition task. *Kybernetik*. **1**, 192-199.

Ferree, E. and Rand, G. (1942) Colour and composition of light in relation to the blackout. *J. Aviat. Med.* **13**, 193-215.

Findlay, J. M. (1973) Feature detectors and vernier acuity. *Nature* **241**, 135-137.

Finney, D. J. (1971) *Probit analysis (3rd ed.)* Cambridge University Press, Cambridge.

Foley, J. M. and Legge, G. E. (1981) Contrast detection and near-threshold discrimination in human vision. *Vision Res.* **21**, 1041-1053.

Foley, J. M. and Tyler, C. W. (1976) Effect of stimulus duration on stereo and vernier displacement thresholds. *Percep. and Psychophys.*, **20**, 125-128.

Foley-Fisher, J. A. (1968) Measurements of vernier acuity in white and coloured light. *Vision Res.* **8**, 1055-1065.

Foley-Fisher, J. A. (1972) The information content of a vernier judgment. *Kybernetik*. **11**, 175-177.

Foley-Fisher, J. A. (1973) The effect of target line length on vernier acuity in white and blue light. *Vision Res.* **13**, 1447-1454.

Foley-Fisher, J. A. (1977) Contrast, edge-gradient, and target line width as factors in vernier acuity. *Optica Acta.* **24**, 179-186.

Franzen, O. and Berkley, M. A. (1975) Apparent contrast as a function of modulation depth and spatial frequency. *Vision Res.* **15**, 655-660.

Freeman, R. D. and Bradley, A. (1980) Monocularly deprived humans: Nondeprived eye has supernormal vernier acuity. *J. Neurophysiol.* **43**, 1645-1653.

French, J. W. (1920) The unaided eye, Part III. *Trans. opt. Soc.* **21**, 127-156.

Fritsch, G. (1908) *Uber Bau und Bedeutung der Area Centralis der Menchen.* Berlin.

Fry, and Cobb, (1935) *Am. Acad. Ophthalmol.* **1**.

Furchner, C. S. and Ginsburg, A. P. (1978) "Monocular rivalry" of a complex waveform. *Vision Res.* **18**, 1641-1648.

Furchner, C. S., Thomas, J. P. and Campbell, F. W. (1977) Detection and discrimination of simple and complex patterns at low spatial frequencies. *Vision Res.* **17**, 827-836.

Gambardella, G. (1971) A contribution to the theory of short-time spectral analysis with nonuniform bandwidth filters. *IEEE Trans.* **CT-18**, 455-460.

Gambardella, G. (1975) Representation of the spatial-frequency analysis performed by the visual system. *J. opt. Soc. Am.* **65**, 99-100.

Gambardella, G. (1979) The Mellin transforms and constant-Q spectral analysis. *J. acous. Soc. Am.* **66**, 913-915.

Geisler, W. S. (1984) The physical limits of acuity and hyperacuity. (In press.)

Georgeson, M. A. and Sullivan, G. D. (1975) Contrast constancy: deblurring in human vision by spatial frequency. *J. Physiol. (Lond.)* **252**, 627-656.

Gilinsky, A. S. (1968) Orientation-specific effects of patterns of adapting light on visual acuity. *J. opt. Soc. Am.* **58**, 13-18.

Ginsburg, A. P., Cannon, M. Y. and Nelson, M. A. (1980) Suprathreshold processing of complex visual stimuli: evidence for linearity in contrast perception. *Science* **208**, 619-621.

Glezer, V. D., Kostelyanets, N. B. and Cooperman, A. M. (1977) Composite stimuli are detected by grating detectors rather than by line detectors. *Vision Res.* **17**, 1067-1070.

Gottesman, J., Rubin, G. S. and Legge, G. E. (1981) A power law for perceived contrast in human vision. *Vision Res.* **21**, 791-799.

Green, D. M. and Luce, R. D. (1975) Parallel psychometric functions from a set of independent detectors. *Psych. Rev.* **82**, 483-86.

Graham, C. H. and Kemp, E. H. (1938) Brightness discrimination as a function of the duration of the increment of intensity. *J. Gen. Physiol.* **21**, 635-650.

Graham, N. (1975) Explaining the detection of aperiodic visual stimuli as probability summation among channels. (Unpublished manuscript).

Graham, N. (1977) Visual detection of aperiodic spatial stimuli by probability summation among narrowband channels. *Vision Res.* **17**, 637-652.

Graham, N. (1980) Spatial frequency channels in human vision: Detecting edges without edge detectors. In *Visual Coding and Adaptability*. (C. S. Harris, ed.). Lawrence Erlbaum Assoc., Hillsdale, N. J.

Graham, N. and Nachmias, J. (1971) Detection of grating patterns containing two spatial frequencies: A comparison of single channel and multichannel models. *Vision Res.* **11**, 251-259.

Graham, N., Robson, J. G. and Nachmias, J. (1978) Grating summation in fovea and periphery. *Vision Res.* **18**, 815-825.

Graham, N. and Rogowitz, B. (1976) Spatial pooling properties deduced from the detectability of FM and quasi-AM gratings: a reanalysis. *Vision Res.* **16**, 1021-1026.

Guzman, A. (1968) Computer recognition of three-dimensional objects in a visual scene. MAC **TR-59**, Project MAC, M.I.T.

Hadani, I., Gur, M., Meiri, A. Z. and Fender, D. H. (1980) Hyperacuity in the detection of absolute and differential displacements of random dot patterns. *Vision Res.* **20**, 947-951.

Hallett, P. E. (1969) The variations in visual threshold measurement. *J. Physiol. (Lond.)* **202**, 403-419.

Hamerly, J. R. (1975) Grating contrast perception at low suprathreshold contrasts: the combination of responses of frequency-selective channels. PhD. dissertation, Carnegie-Mellon U.

Hamerly, J. R., Quick, R. F. and Reichert, T. A. (1977) A study of grating contrast judgement. *Vision Res.* **17**, 201-207.

Hamerly, J. R. and Springer, R. M. (1981) Raggedness of edges. *J. opt. Soc. Am.* **71**, 285-288.

Harburn, G., Taylor, C. A. and Welberry, T. R. (1975) *Atlas of Optical Transforms*. Cornell University Press, Ithaca, N. Y.

Hartline, H. K. (1938) The response of single optic nerve fibers of the vertebrate eye to illumination of the retina. *Am. J. Physiol.* **121**, 400-415.

Hartridge, H. (1922) Visual acuity and the resolving power of the eye. *J. Physiol. (Lond.)* **57**, 52-67.

Hartridge, H. (1947) The visual perception of fine detail. *Phil. Trans. R. Soc.* **B232**, 519-671.

Hecht, S. (1935) A theory of visual intensity discrimination. *J. Gen. Physiol.* **18**, 767-789.

Hecht, S. and Mintz, E. U. (1939) The visibility of single lines at various retinal illuminations and the retinal basis of visual resolution. *J. gen. Psych.* **22**, 593-612.

Helmholtz, H. (1856-1866/1909-1911) *Handbuch der physiologischen Optik (3rd ed.).* Voss, Hamburg and Leipzig (English trans. by J. P. C. Southall, Opt. Soc. Am., Rochester, N. Y.).

Henning, G. B., Hertz, B. G. and Broadbent, D. E. (1975) Some experiments bearing on the hypothesis that the visual system analyzes spatial patterns in independent bands of spatial frequency. *Vision Res.* **15**, 887-898.

Henning, G. B., Hertz, B. G. and Hinton, J. L. (1981) Effects of different hypothetical detection mechanisms on the shape of spatial-frequency filters inferred from masking experiments. I. Noise masks. *J. opt. Soc. Am.* **71**, 574-581.

Hering, E. (1864) *Beitr. z. Physiol.*

Hering, E. (1865) *Arch. f. Anat. Physiol. und Wissensch. Med.*, p. 152.

Hering, E. (1899) *Bericht d. math.-phys. Klasse d. Konigl. Sachs Gesellsch. Wissenschaftend Leipzig.* **51(3)**, 16-24.

Hilz, R. and Cavonius, C. R. (1974) Functional organization of the peripheral retina: sensitivity to periodic stimuli. *Vision Res.* **14**, 1333-1337.

Hirsch, J. and Hylton, R. (1982) Limits of spatial-frequency discrimination as evidence of neural interpolation. *J. opt. Soc. Am.* **72**, 1367-1374.

Hirsch, J., Hylton, R. and Graham, N. (1982) Simultaneous recognition of two

spatial-frequency components. *Vision Res.* **22**, 365-375.

Hoekstra, J., Goot, D. P. J. van der, Brink, G. van den and Bilsen, F. A. (1974) The influence of the number of cycles upon the visual contrast threshold for spatial sinewave patterns. *Vision Res.* **14**, 365-368.

Holt, J. J. and Ross, J. (1980) Phase perception in the high spatial frequency range. *Vision Res.* **20**, 933-935.

Hopkins, H. H. (1962) 21st Thomas Young Oration. The application of frequency response techniques in optics. *Proc. phys. Soc.* **79**, 889-919.

Hubel, D. H. and Wiesel, T. N. (1962) Receptive fields, binocular interaction, and functional architecture in the cats visual cortex. *J. Physiol. (Lond.)* **160**, 106-154.

Hubel, D. H. and Wiesel, T. N. (1965) Receptive fields and functional architecture in two non-striate visual areas (18 and 19) of the cat. *J. Neurophysiol.* **28**, 229-289.

Jastrow, J. (1893) On the judgment of angles and positions of lines. *Am. J. Psych.* **5**, 214-223.

Jones, R. M. and Tulunay-Keesey, U. (1980) Phase selectivity of spatial frequency channels. *J. opt. Soc. Am.* **70**, 66-70.

Keesey, U. T. (1960) Effects of involuntary eye movements on visual acuity. *J. opt. Soc. Am.* **50**, 769-774.

Keesey, U. T. (1972) Flicker and pattern detection: A comparison of thresholds. *J. opt. Soc. Am.* **62**, 446-448.

Kelly, D. H. (1971) Theory of flicker and transient responses, II. Counterphase gratings. *J. opt. Soc. Am.* **61**, 632-640.

Kelly, D. H. and Burbeck, C. A. (1980) Spatiotemporal characteristics of visual mechanisms: Excitatory-inhibitory model. *J. opt. Soc. Am.* **70**, 1121-1126.

Kelly, D. H. and Magnuski, H. S. (1975) Pattern detection and the two-dimensional Fourier transform: circular targets. *Vision Res.* **15**, 911-915.

King-Smith, P. E. and Kulikowski, J. J. (1975) The detection of gratings by independent activation of line detectors. *J. Physiol. (Lond.)* **247**, 237-271.

King-Smith, P. E. and Kulikowski, J. J. (1975) Pattern and flicker detection analysed by subthreshold summation. *J. Physiol. (Lond.)* **249**, 519-548.

King-Smith, P. E. and Kulikowski, J. J. (1981) The detection and recognition of two lines. *Vision Res.* **21**, 235-250.

Klein, S., Stromeyer, C. F. and Ganz, L. (1974) The simultaneous spatial-frequency shift: A dissociation between the detection and perception of gratings. *Vision Res.* **14**, 1421-1432.

Krakau, C. E. T. (1967) An automatic apparatus for time series analysis of visual acuity. *Vision Res.* 7, 99-105.

Kulikowski, J. J. (1976) Effective contrast constancy and linearity of contrast sensation. *Vision Res.* **16**, 1419-1432.

Kulikowski, J. J., Abadi, R., and King-Smith, P. E. (1973) Orientational selectivity of grating and line detectors. *Vision Res.* **13**, 1479-1486.

Kulikowski, J. J. and Gorea, A. (1978) Complete adaptation to pattern stimuli: a necessary and sufficient condition for Weber's law for contrast. *Vision Res.* **18**, 1223-1227.

Kulikowski, J. J. and King-Smith, P. E. (1973) Spatial arrangement of line, edge and grating detectors revealed by subthreshold summation. *Vision Res.* **13**, 1455-1478.

Kulikowski, J. J. and Tolhurst, D. J. (1973) Psychophysical evidence for sustained and transient detectors in human vision. *J. Physiol. (Lond.)* **232**, 149-162.

Lange, R. V., Sigel, C. and Stecher, S. (1973) Adapted and unadapted frequency channels in human vision. *Vision Res.* **13**, 2139-2143.

Lathi, B. P. (1968) *Communications systems.* John Wiley and Sons, Inc., New York.

Laurance, L. (1926) *Visual optics and sight testing, third ed.* School of optics, London.

Legge, G. E. (1978) Space domain properties of a spatial frequency channel in human vision. *Vision Res.* **18**, 959-969.

Legge, G. E. (1979) Spatial frequency masking in human vision: binocular

interactions. *J. opt. Soc. Am.* **69**, 838-847.

Legge, G. E. (1981) A power law for contrast discrimination. *Vision Res.* **21**, 457-467.

Legge, G. E. and Foley, J. M. (1980) Contrast masking in human vision. *J. opt. Soc. Am.* **70**, 1458-1470.

Le Grand, Y. (1967) *Form and space vision.* (M. Millodot and G. G. Heath, trans.) Indiana U. Press, Bloomington.

Leibowitz, H. W. (1955) Some factors influencing the variability of vernier adjustments. *Am. J. Psych.* **68**, 266-273.

Leibowitz, H. W., Meyers, N. A. and Grant, D. A. (1955) Radial localization of a single stimulus as a function of luminance and duration of exposure. *J. opt. Soc. Am.* **45**, 76-78.

Leibowitz, H. W., Meyers, N. A. and Grant, D. A. (1955b) Frequency of seeing and radial localization of single and multiple visual stimuli. *J. exp. Psych.* **50**, 369-373.

Levi, D. M. and Klein, S. A. (1983) Spatial localization in normal and amblyopic vision. *Vision Res.* **23**, 1005-1017.

Long, G. M. (1979) The dichoptic viewing paradigm: Do the eyes have it?. *Psych. Bull.* **86**, 391-403.

Luckliesch, M. and Moss, F. K. (1931) *Seeing.* Williams and Wilkins Co., Baltimore.

Ludvigh, E. (1953) Direction sense of the eye. *A. J. Ophthal.* **36**, 139-142.

Ludvigh, E. and McKinnon, P. (1967) The effect of orientation on the three-dot alignment test. *Am. J. Ophthal.* **64**, 261-265.

Madden, B. C. and Mancini, M. (1980) Separation of temporal and spatial linearity in cat visual cortex. Optical Society Topical Meeting on Recent Advances in Vision. April 30 - May 3, 1980. Sarasota, Florida.

Mansfield, R. J. W. (1976) Visual adaptation: retinal transduction, brightness and sensitivity. *Vision Res.* **16**, 679-690.

Marr, D. (1982) *Vision.* W. H. Freeman. San Francisco.

Marr, D., Poggio, T. and Hildreth, E. (1980) Smallest channel in early human vision. *J. opt. Soc. Am.* **70**, 868-870.

Marshall, W. H. and Talbot, S. A. (1942) Recent evidence for neural mechanisms in vision leading to a general theory of sensory acuity. In *Biological Symposia, vol. 7 (Visual mechanisms)*, pp. 117-164, The Jaques Cattell Press, Lancaster.

Martin , Day. and Kaniowski (1950) *Brit. J. Ophthalmol.* **34**, 89.

McFadden, D. (1970) Three computational versions of proportion correct for use in forced-choice experiments. *Percep. and Psychophys.* **8**, 336-342.

McKee, S. P. and Westheimer, G. (1978) Improvement in vernier acuity with practice. *Percep. and Psychophys.* **24**, 258-262.

Morgan, M. J. and Watt, R. J. (1983) On the failure of spatiotemporal interpolation: a filtering model. *Vision Res.* **23**, 997-1004.

Mostafavi, H. and Sakrison, D. J. (1976) Structure and properties of a single channel in the human visual system. *Vision Res.* **16**, 957-968.

Mueller, C. G. and Lloyd, V. V. (1948) Stereoscopic acuity for various levels of illumination. *Proc. Nat. Acad. Sci.* **34**, 223-227.

Nachmias, J. (1981) On the psychometric function for contrast detection. *Vision Res.* **21**, 215-223.

Nachmias, J. and Kocher, E. C. (1970) Visual detection and discrimination of luminance increments. *J. opt. Soc. Am.* **60**, 382-389.

Nachmias, J. and Sansbury, R. (1974) Grating contrast: Discrimination may be better than detection. *Vision Res.* **14**, 1039-1042.

Nachmias, J. and Weber, A. (1975) Discrimination of simple and complex gratings. *Vision Res.* **15**, 217-224.

Nes, F. L. van, Koenderick, J. J., Nas, H. and Bouman, M. A. (1967) Spatiotemporal modulation transfer function in the human eye. *J. opt. Soc. Am.* **57**, 1082-1088.

Overbury, O. and Bross, M. (1978) Improvement of visual acuity in partially and

fully sighted subjects as a function of practice, feedback, and instructional techniques. *Perceptual and Motor Skills* **46**, 815-822.

Pantle, A. and Sekuler, R. (1968) Size detecting mechanisms in human vision. *Science* **162**, 1146-1148.

Pearson, C. E. (1974) *Handbook of applied mathematics.* Van Nostrand Reinhold Company, New York.

Pelli, D. G. (1979) The effects of noise masking and contrast adaptation on contrast detection, contrast discrimination and apparent contrast. *Invest. Ophth. and visual Sci. Suppl.* **18**, 59.

Pennington, J. (1971) Physiological relationship between stereothreshold and vernier acuity. *Am. J. Optom.* **48**, 759-762.

Pollehn, H. and Roehrig, H. (1970) Effect of noise on the modulation transfer function of the visual channel. *J. opt. Soc. Am.* **60**, 842-848.

Pollen, D. A., Lee, J. R. (1971) How does the striate cortex begin the reconstruction of the visual world? *Science* **173**, 74-77.

Pollen, D. A. and Ronner, S. F. (1982) Spatial computation performed by simple and complex cells in the visual cortex of the cat. *Vision Res.* **22**, 101-118.

Quick, R. F. Jr. (1973) Spatial-frequency selectivity in human vision: the frequency response of contrast detection channels. Doctoral dissertation, Carnegie-Mellon University, Pittsburg, Pennsylvania.

Quick, R. F. (1974) A vector magnitude model of contrast detection. *Kybernetik* **16**, 65-67.

Quick, R. F. Jr., Mullins, W. W. and Reichert, T. A. (1978) Spatial summation effects on two-component grating thresholds. *J. opt. Soc. Am.* **68**, 116-121.

Quick, R. F. Jr. and Reichert, T. A. (1975) Spatial frequency selectivity in contrast detection. *Vision Res.* **15**, 637-643.

Rattle, J. D. and Foley-Fisher, J. A. (1968) A relationship between vernier acuity and intersaccadic interval. *Optica Acta.* **15**, 617-620.

Regan, D., Bartol, S., Murray, T. J. and Beverley, K. I. (1982) Spatial frequency discrimination in normal vision and patients with multiple sclerosis. *Brain.* **105**,

735-754.

Regan, D. and Beverley, K. I. (1983) Spatial-frequency discrimination and detection: comparison of postadaptation thresholds. *J. opt. Soc. Am.* 73, 1684-1690.

Rentschler, I., Hilz, R. and Grimm, W. (1975) Processing of positional information in the human visual system. *Nature* **253**, 444-445.

Riggs, L. A. (1965) Visual acuity. In Graham, C. H. (ed.) *Vision and visual perception.* Wiley and Sons, New York.

Riggs, L. A., Armington, J. C. and Ratliff, F. (1954) Motions of the retinal image during fixation. *J. opt. Soc. Am.* **44**, 315-321.

Robson, J. G. (1966) Spatial and temporal contrast-sensitivity of the visual system. *J. opt. Soc. Am.* **56**, 1141-1142.

Robson, J. G. and Graham, N. (1981) Probability summation and regional variation in contrast sensitivity across the visual field. *Vision Res.* **21**, 409-418.

Rodieck, R. W. (1973) *The Vertebrate Retina.* W. H. Freeman and Co., San Francisco.

Roelofs. (1918) *Arch. Neerl. Physiol.* **2**, 199.

Ronchi, L. and Frosini, R. (1975) On a possible counter-part of vernier acuity. *Atti Fonz. G. Ronchi.* **80**, 1021-1025.

Sachs, M., Nachmias, J. and Robson, J. G. (1971) Spatial frequency channels in human vision. *J. opt. Soc. Am.* **61**, 1176-1186.

Salvi, G. and Galassi, F. (1978) Vernier acuity and apparent depth for targets of different hues, in extrafoveal vision. *Atti Fonz. G. Ronchi.* 33, 514-520.

Sansbury, R. V., Distelhorst, J. and Moore, S. (1978) A phase-specific adaptation effect of the square-wave grating. *Invest. Ophthal. visual Sci.* **17**, 442-448.

Schade, O. H. (1956) Optical and photoelectric analog of the eye. *J. opt. Soc. Am.* **46**, 721-739.

Shapley, R. M. and Enroth-Cugell, C. (1984) Visual adaptation and retinal gain controls. *Progress in Retinal Res.* 3, 263-246.

Shapley, R. M. and Tolhurst, D. J. (1973) Edge detectors in human vision. *J. Physiol. (Lond.)* **229**, 165-183.

Shlaer, (1937) *J. Gen. Physiol.* **21:165**.

Smith, W. J. (1978) Image formation: geometrical and physical optics. In: W. G. Driscoll and W. Vaughan (eds.), *Handbook of Optics*. McGraw-Hill, New York.

Sparrow, (1916) *Astrophys. J.* **44**, 76.

Springer, R. M. (1978) Suprathreshold information transfer in the visual system: brightness match profile of high contrast gratings. *Vision Res.* **18**, 291-300.

Squillace, A. S. and Bien, A. R. (1970) The functional relation between alignment accuracy and vertical separation of alignment marks. *Human Factors.* **12**, 599-604.

Stigmar, G. (1970) Observations on vernier and stereo acuity with special reference to their relationship. *Acta Ophthal.* **48**, 979-998.

Stigmar, G. (1971) Blurred visual stimuli II. The effect of blurred visual stimuli on vernier and stereo acuity. *Acta Ophthal.* **49**, 364-379.

Stratton, G. M. (1900) A new determination of the minimum visible and its bearing on localization and binocular depth. *Psych. Rev.* 7, 429-435.

Stromeyer, C. F. and Julesz, B. (1972) Spatial-frequency masking in vision: Critical bands and spread of masking. *J. opt. Soc Am.* **62**, 1221-1232.

Stromeyer, C. F. and Klein, S. (1974) Spatial frequency channels in human vision as asymmetric (edge) mechanisms. *Vision Res.* **14**, 1409-1420.

Stromeyer, C. F. and Klein, S. (1975) Evidence against narrow-band spatial frequency channels in vision: the detectability of frequency modulated gratings. *Vision Res.* **15**, 899-910.

Stromeyer, C. F., Lange, A. F. and Ganz, L. (1973) Spatial frequency phase effects in human vision. *Vision Res.* **13**, 2345-2360.

Sullivan, G. D., Oatley, K. and Sutherland, N. S. (1972) Vernier acuity as affected by target length as separation. *Percep. and Psychophys.* **12**, 438-444.

Talbot, S. A. and Marshall, W. H. (1941) Physiological studies on neural mechanisms of visual localization and discrimination. *Am. J. Ophthal.* **24**, 1255-1264.

Thomas, G. B. (1965) *Calculus and analytic geometry (3rd Ed.).* Addison-Wesley Publishing Company, Inc. Reading, Massachusetts.

Tolhurst, D. J. (1972) Adaptation to square wave gratings: Inhibition between spatial frequency channels in human visual system. *J. Physiol. (Lond.)* **226**, 231-248.

Tolhurst, D. J. (1973) Separate channels for the analysis of the shape and the movement of a moving visual stimulus. *J. Physiol. (Lond.)* **231**, 385-402.

Tolhurst, D. J. (1975) The detection and identification of lines and edges. *Vision Res.* **15**, 1367-1372.

Tolhurst, D. J. and Thompson, I. D. (1981) On the variety of spatial frequency selectivity shown by neurons in area 17 of the cat. *Proc. Roy. Soc. (London).* **B213**, 183-199.

Tolhurst, D. J. and Barfield, L. P. (1978) Interactions between spatial frequency channels. *Vision Res.* **18**, 951-958.

Tolhurst, D. J. and Thomson, P. G. (1975) Orientation illusions and after-effects: Inhibition between channels. *Vision Res.* **15**, 967-972.

Tyler, C. W. (1973) Periodic vernier acuity. *J. Physiol. (Lond.)* **228**, 637-647.

Tyler, C. W. and Mitchell, D. E. (1977) Orientation differences for perception of sinusoidal line stimuli. *Vision Res.* **17**, 83-88.

Vernier, P. (1631) *The construction, uses, and properties of a new mathematical quadrant.*

Villani, S., Del Dotto, P. and De Napoli, P. A. (1978) Some remarks on the lack of extrafoveal hyperacuity. *Atti Fonz. G. Ronchi.* **33**, 717-722.

Volkmann, A. W. (1863) *Physiologische Untersuchungen im Gebiete der Optik.* Breitkoph und Hartel, Leipzig.

Walls, G. L. (1943) Factors in human visual resolution. *J. opt. Soc. Am.* **33**, 487-505.

Watanabe, A., Mori, T., Nagata, S. and Hiwatashi, K. (1968) Spatial sine wave responses of the human visual system. *Vision Res.* **8**, 1245-1263.

Watson, A. B. and Robson, J. G. (1981) Discrimination at threshold: Labelled detectors in human vision. *Vision Res.* **21**, 1115-1122.

Watt, R. J., Morgan, M. J. and Ward, R. M. (1983) The use of different cues in vernier acuity. *Vision Res.* **23**, 997-1004.

Weber, E. H. (1846) *Wagner Handworterbuch. d. Physiol., vol.* 3.

Weibull, W. (1951) A statistical distribution function of wide applicability. *J. appl. Mech.* **18**, 292-297.

Westheimer, G. (1975) Visual acuity and hyperacuity. *Inv. Ophthal. visual Sci.* **14**, 570-572.

Westheimer, G. (1976) Diffraction theory and visual hyperacuity. *Am. J. Optom. physiol. Opt.* **53**, 362-364.

Westheimer, G. (1977) Spatial frequency and light-spread descriptions of visual acuity and hyperacuity. *J. opt. Soc. Am.* **67**, 207-212.

Westheimer, G. (1978) The optics of the eye and visual acuity. *Int. Ophthal. Clin. (Summer).* **18**, 9-19.

Westheimer, G. (1982) The spatial grain of the perifoveal visual field. *Vision Res.* **22**, 157-162.

Westheimer, G. and Hauske, G. (1975) Temporal and spatial interference with vernier acuity. *Vision Res.* **15**, 1137-1141.

Westheimer, G. and McKee, S. P. (1975) Visual acuity in the presence of retinal-image motion. *J. opt. Soc. Am.* **65**, 847-850.

Westheimer, G. and McKee, S. P. (1977a) Integration regions for visual hyperacuity. *Vision Res.* **17**, 89-93.

Westheimer, G. and McKee, S. P. (1977b) Perception of temporal order in adjacent visual stimuli. *Vision Res.* **17**, 887-892.

Westheimer, G. and McKee, S. P. (1977c) Spatial configurations for visual hyperacuity. *Vision Res.* **17**, 941-947.

Westheimer, G., Shimamura, K. and McKee, S. P. (1976) Interference with line-orientation sensitivity. *J. opt. Soc. Am.* **66**, 332-338.

Weymouth, F. W. (1958) Visual sensory units and the minimum angle resolution. *Am. J. Ophthal.* **46(1, part II)**, 102-113.

Weymouth, F. W., Andersen, E. E. and Averill, H. L. (1923) Retinal mean local sign: A new view of the relation of the retinal mosaic to visual perception. *Am. J. Physiol.* **63**, 410-411.

Wilcox, W. W. and Purdy, D. M. (1933) Visual acuity and its physiological basis. *Brit. J. Psychol.* **23**, 233-261.

Wilson, H. R. (1978) Quantitative prediction of line spread function measurements: implications for channel bandwidths. *Vision Res.* **18** 483-496.

Wilson, H. R. (1978) Quantitative characterization of two types of line- spread function near the fovea. *Vision Res.* **18**, 971-981.

Wilson, H. R. and Giese, S. C. (1977) Threshold visibility of frequency gradient patterns. *Vision Res.* **17**, 1177-1190.

Wilson, H. R., Phillips, G., Rentschler, I. and Hilz, R. (1979) Spatial probability summation and disinhibition in psychophysically measured line-spread functions. *Vision Res.* **19**, 593-598.

Woodhouse, M. (1975) Unpublished Ph.D. thesis. Cambridge University, Cambridge, England.

Wright, W. D. (1942) The functions and performance of the eye. *J. Sci. Instr.* **19**, 161-165.

Wulfing, E. A. (1882) Ueber den kleinsten Gesichtswinkel. *Z. Biol.* **29**, 199-202.

Zoethout, W. D. (1947) *Physiological Optics.* The Professional Press, Chicago.